



COLLEGE OF ENGINEERING, MATHEMATICS AND PHYSICAL SCIENCES

A Risk-Based Decision Support System for Failure Management in Water Distribution Networks

*Submitted by Josef Bicik to the University of Exeter
as a thesis for the degree of
Doctor of Philosophy in Engineering
in June 2010*

This thesis is available for library use on the understanding that it is copyright material and that no quotation from the thesis may be published without proper acknowledgement.

I certify that all material in this thesis which is not my own work has been identified and that no material has previously been submitted and approved for the award of a degree by this or any other University.

Signature:

ABSTRACT

The operational management of Water Distribution Systems (WDS), particularly under failure conditions when the behaviour of a WDS is not well understood, is a challenging problem. The research presented in this thesis describes the development of a methodology for risk-based diagnostics of failures in WDS and its application in a near real-time Decision Support System (DSS) for WDS' operation.

In this thesis, the use of evidential reasoning to estimate the likely location of a burst pipe within a WDS by combining outputs of several models is investigated. A novel Dempster-Shafer model is developed, which fuses evidence provided by a pipe burst prediction model, a customer contact model and a hydraulic model to increase confidence in correctly locating a burst pipe.

A new impact model, based on a pressure driven hydraulic solver coupled with a Geographic Information System (GIS) to capture the adverse effects of failures from an operational perspective, is created. A set of Key Performance Indicators used to quantify impact, are aggregated according to the preferences of a Decision Maker (DM) using the Multi-Attribute Value Theory. The potential of distributed computing to deliver a near real-time performance of computationally expensive impact assessment is explored.

A novel methodology to prioritise alarms (i.e., detected abnormal flow events) in a WDS is proposed. The relative significance of an alarm is expressed using a measure of an overall risk represented by a set of all potential incidents (e.g., pipe bursts), which might have caused it. The DM's attitude towards risk is taken into account during the aggregation process.

The implementation of the main constituents of the proposed risk-based pipe burst diagnostics methodology, which forms a key component of the aforementioned DSS prototype, are tested on a number of real life and semi-real case studies. The methodology has the potential to enable more informed decisions to be made in the near real-time failure management in WDS.

ACKNOWLEDGEMENTS

Firstly, I would like to express the deepest gratitude to my first supervisor Professor Dragan Savić, who gave me this life-changing opportunity, to do my PhD in the Centre for Water Systems. I am very grateful for all the support, guidance and encouragement I received from him as well as from my second supervisor Professor Zoran Kapelan throughout the period of my studies.

My further thanks go to Dr. Christos Makropoulos for his supervision during the first year of my PhD. The stimulating discussions we held helped shape this PhD into its current form.

I would like to acknowledge the financial support received through the NEPTUNE project (grant EP/E003192/1) funded by the U.K. Science and Engineering Research Council, and Industrial Collaborators. The additional funding provided by Yorkshire Water after the end of the NEPTUNE project, which contributed towards successful completion of this PhD thesis, is also gratefully acknowledged.

The kind assistance and support of academic as well as industrial partners of the NEPTUNE project is much appreciated. In particular I would like to thank Mr Ridwan Patel from Yorkshire Water Services, Mr Derek Clucas from United Utilities, and Drs. Steve Mounce and John Machel from the Pennine Water Group.

I would like to thank all the current and past members of the Centre for Water Systems, with whom I had the pleasure of working, for creating an inspiring research environment. I am particularly thankful for the help and support received from Drs. Mark Morley, Gianluca Dorini, Darko Joksimović and Haytham Awad. Grateful acknowledgements for proofreading this thesis and correcting the English also go to Mrs. Alexandra Slater.

Finally, I would like to thank my family and my fiancé Kristyna for their love, support, patience and understanding during these years. This thesis is dedicated to them.

TABLE OF CONTENTS

ABSTRACT	2
ACKNOWLEDGEMENTS	3
TABLE OF CONTENTS	4
LIST OF FIGURES.....	8
LIST OF TABLES.....	11
LIST OF ABBREVIATIONS.....	12
CHAPTER 1 INTRODUCTION	15
1.1 Motivation and Background.....	15
1.2 Aims and Objectives.....	17
1.3 Thesis Structure	18
CHAPTER 2 REVIEW OF LITERATURE	20
2.1 Introduction	20
2.2 Decision-Making & Decision Support	20
2.2.1 Real-Time Decision Support	22
2.3 The Concept of Risk and Its Applications.....	23
2.3.1 WDS Reliability Studies.....	24
2.3.2 Applications of Risk	24
2.4 Burst Detection and Diagnostics	29
2.4.1 Data and Model Driven Anomaly Detection.....	30
2.4.2 Anomaly Diagnostics	31
2.5 Failure Impact in WDS.....	34
2.5.1 WDS Modelling Under Failure Conditions.....	38
2.5.2 Pipe Burst Modelling.....	40
2.6 Information Fusion	43
2.7 Summary & Conclusions.....	44
CHAPTER 3 RISK-BASED PIPE BURST DIAGNOSTICS	48
3.1 Introduction	48
3.2 Risk-Based Decision-Making.....	49

3.3	Likelihood Component of Risk	55
3.3.1	Dempster-Shafer Theory of Evidence	56
3.3.2	Information Sources	59
3.3.3	Information Fusion	63
3.3.4	Independence Assumption.....	68
3.3.5	Dempster-Shafer Model Calibration	69
3.4	Impact Component of Risk.....	73
3.4.1	Customer Categories	74
3.4.2	Failure Modelling	75
3.4.3	Impact Aggregation	77
3.4.4	Key Performance Indicators	79
3.5	Abnormal Event Prioritisation.....	90
3.5.1	Alarm Ranking	92
3.5.2	Diagnostics and Risk Assessment	93
3.5.3	Pipe Burst Risk Aggregation	93
3.5.4	Overall Risk Aggregation.....	95
3.5.5	Anomaly Ordering.....	98
3.6	Summary.....	100
CHAPTER 4 DSS IMPLEMENTATION.....		102
4.1	Introduction	102
4.2	Architecture Overview	102
4.3	Database Management System.....	104
4.4	The Back-End	106
4.4.1	Alarm Monitor	107
4.4.2	Likelihood Evaluator	109
4.4.3	Impact Evaluator.....	111
4.4.4	Alarm Ranking	117
4.5	The Front-End	119
4.5.1	System Overview User Interface.....	119
4.6	External Modules.....	123
4.7	Summary.....	124
CHAPTER 5 CASE STUDIES		126

5.1	Introduction	126
5.2	Hydraulic Model Evidence.....	127
5.2.1	Large Burst Flow Simulations (EE1)	128
5.2.2	Medium Burst Flow Simulations (EE2)	137
5.2.3	Engineered Events in a Typical DMA (EE3)	140
5.3	Dempster-Shafer Model: Semi-Real Case Study	144
5.3.1	Individual Model Screening	146
5.3.2	Dempster-Shafer Model Calibration	149
5.3.3	Results and Discussion	156
5.3.4	Sensitivity Analysis	163
5.3.5	Comparison with Other Methods	165
5.4	Impact Model.....	165
5.4.1	Impact Importance Survey.....	166
5.4.2	Questionnaire Survey Analysis Methodology.....	169
5.4.3	Questionnaire Survey Results.....	172
5.5	Alarm Prioritisation Case Study	176
5.5.1	Main Results	177
5.5.2	Detailed Alarm Prioritisation Results.....	180
5.5.3	Sensitivity Analysis	187
5.5.4	Discussion.....	189
5.6	Summary.....	189
CHAPTER 6 CONCLUSIONS.....		192
6.1	Summary.....	192
6.1.1	Summary of the Contributions	193
6.2	Main Conclusions	194
6.2.1	Risk-Based Pipe Burst Diagnostics	194
6.2.2	Dempster-Shafer Model	195
6.2.3	Impact Model.....	197
6.2.4	Alarm Prioritisation & Ranking	199
6.3	Future Research	200
6.3.1	Dempster-Shafer Model	200
6.3.2	Impact Model.....	201

6.3.3	Alarm Prioritisation & Ranking	202
APPENDIX A	EVIDENCE THEORY	204
APPENDIX B	FAILURE IMPACT SURVEY	214
APPENDIX C	HYDRAULIC MODEL RESULTS	218
APPENDIX D	D-S MODEL PERFORMANCE	228
GLOSSARY		237
BIBLIOGRAPHY		239
	Papers Presented by the Candidate	239
	List of References	240

LIST OF FIGURES

Figure 3.1 Structure of the risk-based pipe burst diagnostics methodology	49
Figure 3.2 A conceptual diagram of the alarm generation process	50
Figure 3.3 A high level overview of the risk-based diagnostics methodology	51
Figure 3.4 An example risk map of a real pipe burst	52
Figure 3.5 A scatter plot showing distribution of risk of two alarms.....	54
Figure 3.6 An example of spatial distribution of Belief and Plausibility	56
Figure 3.7 A graphical representation of Belief and Plausibility	57
Figure 3.8 Sources of evidence used in the information fusion	60
Figure 3.9 Weighed distance from customer contacts to a pipe.....	62
Figure 3.10 Transformation of measurement criteria into BPAs based on Beynon (2005)	64
Figure 3.11 A data flow diagram of the information fusion process.....	66
Figure 3.12 An example of a mapping curve	69
Figure 3.13 An example of the Rank of the TBL (Link Id 0004G2MM)	72
Figure 3.14 An example of a Pareto front	72
Figure 3.15 A relationship between pressure and demand of node j	76
Figure 3.16 A sample outflow profile from a pressure sensitive burst.....	77
Figure 3.17 A tree of objectives	78
Figure 3.18 Measurement of duration of supply interruption and low pressure impact	82
Figure 3.19 A map showing the DISCM KPI after a pipe burst	85
Figure 3.20 An example output from the third party damage model	90
Figure 3.21 A hierarchical representation of alarms and potential incidents	93
Figure 3.22 Distance metric used to represent aggregated risk of a pipe burst.....	95
Figure 3.23 The effect of DM's attitude towards risk α on maximum entropy OWA weights.....	98
Figure 3.24 An alarm state diagram	99
Figure 4.1 A simplified overview of DSS architecture	103
Figure 4.2 An entity-relationship diagram capturing the main tables used by the DSS	105
Figure 4.3 The interaction of processes involved in anomaly diagnostics.....	107
Figure 4.4 An activity diagram describing the Alarm Monitor module.....	108
Figure 4.5 An activity diagram describing the Likelihood Evaluator module	110

Figure 4.6 An activity diagram describing the Impact Evaluator module.....	112
Figure 4.7 A database-centric architecture for distributed impact evaluation.....	114
Figure 4.8 Speedup achieved using distributed computing.....	115
Figure 4.9 Speedup achieved using distributed computing on 1 node vs. N nodes	116
Figure 4.10 An activity diagram describing the Alarm Ranking module	118
Figure 4.11 Table structure of the cache used to store maximum entropy weights	119
Figure 4.12 A screen capture of GIS layers projected on top of a background map....	120
Figure 4.13 Online generation of GIS layers from a spatial DB	121
Figure 4.14 An example of an alarm list	122
Figure 4.15 An interactive trend display	123
Figure 5.1 Location of the case study area in the UK	127
Figure 5.2 An overview of the case study area for EE1 and EE2	129
Figure 5.3 Erroneous data from sensors 3583 and 3587	130
Figure 5.4 Pressure data of a selected logger for event detection on 6 and 7 August 2008	133
Figure 5.5 Comparison of flow data on 7 August 2008 with an average demand	134
Figure 5.6 Corrupt flow data of logger 3276.....	138
Figure 5.7 An overview of the case study area for EE3	141
Figure 5.8 A map showing the most likely location of hydrant opening of EE3	143
Figure 5.9 An overview of DMA E022.....	145
Figure 5.10 A histogram of an average distance of customer contact from a burst location	148
Figure 5.11 Illustration of the Proximity function.....	150
Figure 5.12 A 2D View of the 3D Pareto front showing the chosen solution.....	153
Figure 5.13 Mapping functions of the PBPM	153
Figure 5.14 Mapping functions of the HM.....	154
Figure 5.15 Mapping functions of the CCM	154
Figure 5.16 An example output from the a) PBPM, b) HM, c) CCM and d) the D-S model: $BetP(\{Burst\})$	159
Figure 5.17 Belief and Plausibility maps produced by the D-S model	160
Figure 5.18 Distribution of respondents depending on their role within a company ...	169
Figure 5.19 The relative importance of various types of customers	174
Figure 5.20 The relative importance of different types of impact.....	174

Figure 5.21 The relative importance of different types of Economic impact.....	175
Figure 5.22 An objective tree used in impact aggregation with determined weights ..	175
Figure 5.23 Case study area overview with locations of inlet flow meters and alarms	177
Figure 5.24 An example of ranking based on histogram and an average.....	178
Figure 5.25 A risk map of alarm 8777	180
Figure 5.26 A risk map of alarm 8966	182
Figure 5.27 A risk map of alarm 9030	182
Figure 5.28 A scatter plot of alarms 8966 and 9030	183
Figure 5.29 A risk map of alarm 8802	184
Figure 5.30 A risk map of alarm 8660	185
Figure 5.31 An original (un-filtered) scatter plot of alarms 8854 and 8563	186
Figure 5.32 A filtered scatter plot of alarms 8854 and 8563.....	186
Figure 5.33 Influence of parameter values on distance from a reference solution.....	188
Figure A.1 A relationship between <i>Bel</i> and <i>Pl</i> functions (Agarwal <i>et al.</i> 2004).....	205
Figure A.2 Combination of N independent bodies of evidence	207
Figure A.3 A hierarchical structure of evidence.....	207
Figure C.1 The most likely location of hydrant opening for EE1-1.....	219
Figure C.2 The most likely location of hydrant opening for EE1-2.....	220
Figure C.3 The most likely location of hydrant opening for EE1-3.....	221
Figure C.4 The most likely location of hydrant opening for EE1-4.....	222
Figure C.5 The most likely location of hydrant opening for EE1-5.....	223
Figure C.6 The most likely location of hydrant opening for EE2-5.....	224
Figure C.7 The most likely location of hydrant opening for EE2-4.....	225
Figure C.8 The most likely location of hydrant opening for EE2-1.....	226
Figure C.9 The most likely location of hydrant opening for EE2-2.....	227
Figure D.1 a) PBPM, b) HM, c) CCM and d) D-S Model results for case #7080348 .	229
Figure D.2 a) Belief and b) Plausibility of the D-S Model for case #7080348.....	230
Figure D.3 a) PBPM, b) HM, c) CCM and d) D-S Model results for case #8905881 .	231
Figure D.4 a) Belief and b) Plausibility of the D-S Model for case #8905881	232
Figure D.5 a) PBPM, b) HM, c) CCM and d) D-S Model results for case #9315021 .	233
Figure D.6 a) Belief and b) Plausibility of the D-S Model for case #9315021	234
Figure D.7 a) PBPM, b) HM and c) D-S Model results for case #4639990.....	235
Figure D.8 a) Belief and b) Plausibility of the D-S Model for case #4639990.....	236

LIST OF TABLES

Table 3.1 Structure of a vector of decision variables \mathbf{z}	71
Table 3.2 Available types of surfaces, their reclassification and category.....	89
Table 3.3 Types of roads and their sub-category.....	89
Table 4.1 Results of profiling of the distributed Impact Evaluator	117
Table 5.1 Difference between pressure measurements and the HM in m of head	131
Table 5.2 Detected and actual hydrant opening times of EE1	133
Table 5.3 Summary of times and abnormal flows used by the HM	135
Table 5.4 HM hydrant opening results for EE1.....	136
Table 5.5 Time schedule and hydrant flow rate of EE2	138
Table 5.6 HM hydrant opening results for EE2.....	139
Table 5.7 Alarm information provided by a pipe burst detection module	142
Table 5.8 Pressure measurement corrections for EE3.....	142
Table 5.9 An average distance of CCs from a burst pipe	147
Table 5.10 A histogram showing frequency of CCs per pipe burst	147
Table 5.11 Detailed results of the performance of the D-S model.....	156
Table 5.12 An overview of the performance of the D-S model	161
Table 5.13 Performance of the D-S model compared with PBPM, HM and CCM based on spatial distribution of the likelihood of potential incidents	163
Table 5.14 Results of a global sensitivity analysis (case 9315021)	164
Table 5.15 Comparison of the performance of the D-S theory with other combination functions	165
Table 5.16 A summary of questions included in the online survey	167
Table 5.17 Arithmetic scale used in AHP (adapted from (Saaty (1980)).....	168
Table 5.18 A pairwise comparison matrix \mathbf{A} for Customer importance (Company 1).....	171
Table 5.19 Values of Random Index for a given number of criteria.....	172
Table 5.20 An overview of consistency of the responses.....	173
Table 5.21 A list of 50 alarms considered in this case study.....	178

LIST OF ABBREVIATIONS

AHP	Analytic Hierarchy Process
AIJ	Aggregation of Individual Judgements
AIP	Aggregation of Individual Priorities
ANN	Artificial Neural Network
API	Application Programming Interface
AVG	Average
BFOD	Binary Frame Of Discernment
BPA	Basic Probability Assignment
BPBM	Pipe Burst Prediction Model
BST	British Summer Time
CC	Customer Contact
CCM	Customer Contacts Model
CPU	Central Processing Unit
CR	Consistency Ratio
DB	Database
DBMS	Database Management System
DM	Decision Maker
DMA	District Metered Area
DRM	Discolouration Risk Model
D-S	Dempster-Shafer
DSS	Decision Support System
EE	Engineered Event
EM	Eigenvector Method
EPS	Extended Period Simulation

ES	Expert System
FDD	Fraction of Delivered Demand
FIS	Fuzzy Inference System
FMEA	Failure Mode and Effects Analysis
FMECA	Failure Mode, Effects, and Criticality Analysis
FTP	File Transfer Protocol
GA	Genetic Algorithm
GIS	Geographic Information System
GM	Geometric Mean
GMT	Greenwich Mean Time
HACCP	Hazard Analysis and Critical Control Point
HDA	Head Driven Analysis
HM	Hydraulic Model
HTTP	HyperText Transfer Protocol
KPI	Key Performance Indicator
MAUT	Multi-Attribute Utility Theory
MAVT	Multi-Attribute Value Theory
MCDA	Multi-Criteria Decision Analysis
NP	Non-deterministic Polynomial time
NSGA	Non-dominated Sorting Genetic Algorithm
ODBC	Open Database Connectivity
OFWAT	The Office of Water Services
OGC	Open Geospatial Consortium, Inc.®
OODBMS	Object-Oriented Database Management System
ORDBMS	Object-Relational Database Management System

OWA	Ordered Weighted Averaging
PCR	Proportional Conflict Redistribution
PDD	Pressure Dependent Demand
PHP	Personal Home Page
PNG	Portable Network Graphics
PRV	Pressure Reducing Valve
PVC	Polyvinyl Chloride
RDBMS	Relational Database Management System
RI	Random Index
R-T	Real-Time
SBX	Simulated Binary Crossover
SCADA	Supervisory Control And Data Acquisition
SCEM-UA	Shuffled Complex Evolution Metropolis
SSE	Sum of Squared Errors
TBL	True Burst Location
TBM	Transferable Belief Model
TPD	Third Party Damage
UI	User Interface
UML	Unified Modelling Language
WA	Weighted Average
WDS	Water Distribution System
WFS	Web Feature Service
WMS	Web Map Service
WMSY	Work Management System
WSS	Water Supply System

CHAPTER 1 INTRODUCTION

1.1 Motivation and Background

Water utilities all over the world face serious problems with satisfying increasing water demands. The number of sources of clean and fresh water is becoming scarce while the population of the Earth grows. Furthermore, year by year the required standards of service of the delivery of potable water increase in terms of water quality, reducing the number of supply interruptions and providing adequate pressure at consumers' taps. Apart from this, water utilities are also required to deliver water more efficiently than ever before in order to cut down their carbon footprint (e.g., due to climate change). Effective and efficient operational management of Water Distribution Systems (WDS) has thus become a vital, however, difficult task faced by water utilities nowadays.

In the UK water utilities have to deal with an increasing number of problems (e.g., pipe bursts) due to ageing infrastructure. Some of the underground assets (e.g., pipes) were laid more than 100 years ago. Although, significant effort is put into their ongoing rehabilitation and maintenance programmes the number of incidents caused by pipe bursts and other equipment failures is still significant. Control room operators are not only tasked with operating WDS optimally to meet required standards, but also to deal with contingency situations when failures of various types occur in day-to-day operation. Due to the stochastic nature of failures it is impossible to predict and completely eliminate them.

Risk analysis has started to be applied by water utilities in their strategic rehabilitation plans to maximise benefits of investment by replacing or repairing those elements, which represent the highest risk. However, applications of risk analysis in operational management of WDS in near Real-Time (R-T) are currently lacking, despite the consistent approach towards failure management they offer. Possible reasons for the shortage of near R-T risk applications could be in the difficulties imposed by a usually dynamically changing environment and severe time constraints.

Early detection and location of failures in WDS is of paramount importance to all water utilities. Whilst, early warning failure detection systems have started to be applied in real life WDS (Mounce *et al.* 2010), locating failures represents a major challenge,

which has not yet been satisfactorily resolved. Diagnostics of failures in WDS still usually relies on time intensive and expensive field investigations carried out by field technicians. Their work is, however, becoming more and more difficult, particularly when dealing with burst pipes, which are harder to locate due to pressure management programmes and the installation of Polyvinyl Chloride (PVC) pipes. This represents an opportunity for the application of data and model driven burst diagnostics methods, which at the same time have to cope with a limited number of field measurements and imperfect knowledge of failure behaviour as well as inaccurate data. The challenges of such an uncertain environment and the lack of knowledge are addressed in this thesis using a risk-based decision-making methodology. The early location of failures, which could be achieved using the proposed approach, can facilitate their timely repair and safeguard the continuity of water supply for customers.

Expert Systems (ES) have for a long time dominated the field of R-T applications. Such systems have been successfully deployed to solve well defined structured problems, however, their adoption in fields requiring solutions to complex unstructured problems has been limited. On the other hand, Decision Support Systems (DSS), which aim to provide human Decision Makers (DM) with relevant information in order to reach better informed decisions, have enjoyed a growing popularity in the past few decades. They have been successfully applied to support complex decision-making situations, however, their application in near R-T environments has been challenging. Nevertheless, tasks such as a near R-T pipe burst diagnostics can benefit from the synergetic effect of combining the expertise of an experienced operator and a DSS capable of reducing the information load, which will be explored in this work.

Some of the above mentioned issues were investigated in a three-year research project NEPTUNE (Savić *et al.* 2008) funded by the EPSRC, which started in April 2007. The project was a joint effort of seven major academic institutions (Imperial College London, University of Sheffield, University of Exeter, Leicester University, De Montfort University, Cambridge University and Lancaster University) and three industrial partners (Yorkshire Water, United Utilities and ABB). The project aimed to develop a number of methodologies to improve the operational management of WDS in terms of energy efficiency and level of service of delivery of potable water. This thesis discusses the development, implementation and application of a risk-based decision-

making methodology for failure diagnostics in WDS, which forms a significant part of a near R-T DSS prototype, one of the project's key deliverables. The work presented in this thesis is, therefore, relevant for the water industry and has the potential to improve current practices of operational management of WDS.

1.2 Aims and Objectives

The main aim of this work is to develop and implement a risk-based methodology for near R-T diagnostics of failures (i.e., pipe bursts) in a WDS. More specifically, this aim is achieved through the following objectives:

1. To investigate the potential of applying information fusion in diagnostics of pipe bursts. Information from a number of sources and models currently available to water utilities worldwide will be combined in the effort to locate a burst pipe within a District Metered Area (DMA). The Dempster-Shafer theory of Evidence will be used to fuse outputs of a Pipe Burst Prediction Model (PBPM), a Customer Contacts Model (CCM) and a Hydraulic Model (HM) to increase the confidence in locating a burst pipe, given the frequently imperfect and conflicting outputs of the individual models and underlying data sources.
2. To design an impact model capable of capturing various adverse effects of a burst pipe on the principal stakeholders (i.e., the water utility and its customers). The impact assessment will be approached from an operational, rather than strategic perspective to enable R-T decision-making. A suitable aggregation technique will be developed, which reflects preferences of a water utility in terms of significance of specific types of impact. The integrated impact model will thus be able to return a single measure representing an impact of a burst pipe over a specific risk horizon.
3. To explore the potential of risk-based pipe burst diagnostics, which will enable WDS operators to focus their investigation of burst pipes within a DMA not only based on the information about the most likely location of the burst but also the likely impact. A risk metric comprising likelihood and impact of potential failure will be formed based on the outcomes of the above two objectives. The non-aggregated risk of a pipe burst will be presented in the form of a risk-map

and will enable WDS operators to make better informed decisions on where to dispatch field technicians for further investigation.

4. To develop a methodology to prioritise amongst multiple abnormal events (i.e., increased inflow into a DMA indicating a possible pipe burst) occurring in a similar time horizon in different parts of a WDS. A suitable ranking technique will be applied, incorporating attitude towards risk of a human DM, in order to calculate the criticality of a particular abnormal event. This will allow better utilisation of resources in situations when investigating multiple failures, ensuring that the most significant events are dealt with first according to the overall level of aggregated risk they represent.

1.3 Thesis Structure

This thesis is divided into six chapters including this introduction.

In Chapter 2 a review of relevant literature is provided. The review covers key areas of research addressed in this thesis including decision-making and decision support, application of risk-based methodologies in water systems, techniques for locating burst pipes within WDS, modelling of the impact of failures in WDS and information fusion methods.

In Chapter 3 first the overall methodology for risk-based pipe burst diagnostics is introduced and its individual constituents are described. Suitable models to quantify the likelihood and impact components of risk are then presented. A novel methodology, based on evidential reasoning and information fusion, to estimate the likely location of a burst pipe in a WDS is described. Next, an operational impact model, utilising the Multi-Attribute Value Theory (MAVT) to incorporate preferences of a water utility regarding various aspects of failure impact, is proposed. Finally, a possible application of the risk metric formed by outputs of the aforementioned likelihood and impact models to prioritise abnormal events in a WDS is discussed.

In Chapter 4 an implementation of the proposed risk-based pipe burst diagnostics methodology in the context of an integrated DSS is presented. The structure of a spatial database, which forms the core of a near R-T DSS, is proposed there. The functionality and mutual interaction of a number of background modules, which contain the actual

implementation of individual constituents of the risk-based pipe burst diagnostics methodology, are described. Special attention is paid to parallel computing, which is explored as one of the possibilities to improve the performance of the DSS to reach the requirements of a near R-T environment. Efficient ways of storage and visualisation of underlying spatial and non-spatial data used by the DSS are also discussed.

In Chapter 5, a number of case studies to illustrate the proposed methodologies are presented. First, the possibility of locating a burst pipe within a DMA using an HM and R-T data collected from the field is illustrated on a set of engineered events conducted in a real life WDS. Next, the proposed evidential reasoning methodology (i.e., information fusion) is applied on a number of semi-real case studies, based on historical events, to demonstrate its full potential if sufficient data were available over a long period of time. Consequently, results of a quantitative questionnaire survey, used to determine preferences of a water utility with respect to different aspects of failure impacts, are presented. Finally, a risk-based prioritisation of abnormal events detected in a real life WDS over a period of two years is shown to portray the possible advantages of this approach.

In Chapter 6 the key findings of this thesis are summarised and relevant conclusions are drawn. The novel aspects introduced in this thesis are highlighted, followed by possible directions of future research to enhance and extend the methodologies presented.

CHAPTER 2 REVIEW OF LITERATURE

2.1 Introduction

This chapter provides a review of literature relevant to near Real-Time (R-T) risk-based decision support for the operation of WDS under abnormal conditions, when failures such as pipe bursts occur. First, the literature dealing with decision-making and decision support, with an emphasis on near R-T Decision Support Systems (DSS), is reviewed to establish a context for the methodology presented in this thesis. Secondly the concept of risk, which forms the foundation of the proposed methodology, is introduced and its applications related to water systems are reviewed. Currently available burst detection and diagnostics methods are then examined as a means to provide an indication of a likely location of a burst pipe within a WDS to represent the likelihood of pipe failure. Literature dealing with quantification of impact of failures is reviewed to establish grounds for development of an integrated impact model, which complements the aforementioned risk metric. WDS modelling methods are then presented with a focus on their simulation under abnormal conditions, when failures occur. Finally, a brief overview of information fusion techniques is given because of its importance to the methodologies presented in this thesis. The chapter concludes with a summary identifying gaps in the current research.

2.2 Decision-Making & Decision Support

Decision-making is a cognitive process of choosing amongst several alternatives which results in only one of the alternatives being selected in the end according to the preferences of a Decision Maker (DM) (Turban 1995). Making decisions is one of the daily activities each human being has to perform. Some decisions are made almost automatically thanks to intuition and instincts without deeply analysing the problem, other more complex decisions require thorough analysis and understanding of various options, risks and consequences inherently linked to them. The ongoing research in several fields including Mathematics, Psychology and also the rapid development of computers help improve our problem solving capabilities. (Holloway 1979; Gass 1985)

The foundations of decision-making and decision support can be traced back to the early work of Herbert A. Simon in the 1960s. Simon (1977) studied decision-making by management executives and looked at how the decision-making of organisations is

influenced by new technologies. He was awarded the Nobel Prize in Economics in 1978 for his work on decision-making processes. He classified decision-making processes as: (1) *structured* processes that are routine or repetitive for which standard solutions exist, and (2) *unstructured* decision processes that are the exact opposite and are defined as complex “fuzzy” processes for which there are no routine solutions.

There exists no exact definition of a DSS. The meaning of DSS has been evolving together with the wider application of such systems. DSS developed from early Management Information Systems. The term DSS was first defined by Scott-Morton in 1971 as “an interactive computer-based system, which helps DMs utilise data and models to solve unstructured problems”. This differentiates DSS substantially from Expert Systems (ES).

An ES is according to Turban (1995) defined as “a decision-making and/or problem solving package of computer hardware and software that can reach a level of performance comparable to - or even exceeding that of - a human expert in some specialised and usually narrow problem area.” DSS have gained increasing popularity over ES that focused on solving structured problems (Simon 1977). On the other hand DSS exploit the synergetic effect of combining modern techniques of artificial intelligence with human judgement to tackle complex semi-structured and unstructured problems. Eom *et al.* (1998) conducted a large survey of over 270 DSS developed over a period from 1988-1994 and concluded that their number has increased compared to the previous period and highlighted artificial intelligence as an emerging area of decision support.

Recently, Kapelan *et al.* (2005a) reviewed a number of DSS in urban water planning and suggested the following future research to improve the DSS currently in place: (1) Better integration of DSS into existing systems as well as improved integration of various models that form part of a DSS. The issues with insufficient integration have been partially addressed using OpenMI (Moore and Tindall 2005), an open standard for model interfacing; (2) Modelling of risk and uncertainty should be part of DSS; (3) Further development of comprehensive impact assessment models and their integration within DSS is important, together with better support for group decision-making tools;

(4) More systematic calibration and validation of models used by DSS should be put in place.

2.2.1 Real-Time Decision Support

Given the focus of this thesis extra attention is paid to supporting DMs in dynamically changing environments in near R-T. This section outlines some of the challenges imposed by the R-T environment. In the past, computerised support of decision-making was typically in the area of strategic decisions. However, with the growing performance of today's computers, decision support in R-T applications is becoming more and more frequent. Typical areas where decisions must be made in R-T include: scheduling, dynamic vehicle routing and dispatching, air traffic control, military applications, process control systems, etc. The operational management of WDS is a field that could certainly benefit from near R-T decision support as well.

As discussed by Turner (1986) the main use of R-T ES is to reduce the cognitive load on users or to enable them to increase their productivity without increasing the load. In situations requiring making decisions in R-T, humans tend to overlook relevant information, respond inconsistently, respond too slowly or panic when the rate of information flow is too great (Laffey *et al.* 1987; Musliner *et al.* 1995). The concept of R-T is perceived differently in various disciplines. Laffey *et al.* (1987) defined the R-T applications as: (1) fast, (2) faster than a human can do it, or (3) fast enough. According to the third definition a "fast enough" R-T system is able to respond to incoming data at a rate as fast or faster than it is arriving. Musliner *et al.* (1995) also defined "hard R-T" domain as an environment where decisions must be produced within the available time frame otherwise catastrophic events occur.

Jamieson *et al.* (2007) developed a DSS for R-T near-optimal control of WDS. They emphasised the importance of feed-forward control systems using forecasts of future demands. The size, complexity and varying pattern of water demand of WDS was identified as one of the main difficulties in the application of R-T control. A single-objective Genetic Algorithm (GA) was applied to minimise operating costs. The computational burden of running a hydraulic solver was eliminated using a surrogate model based on an Artificial Neural Network (ANN) (see e.g., Haykin 1999). The proposed R-T DSS was verified on a number of case studies to propose optimal

alternatives to an operator who could manually override the suggested solution at any time.

2.3 The Concept of Risk and Its Applications

Every individual is exposed to various risks and has to deal with them every day throughout their whole life. The early works dealing with risk date back to the beginning of the 20th century when risk generated interest particularly in the insurance industry (Rowe 1977). One of the first formal definitions of risk can be found in the work by Willet (1901) who defined risk as “the objectified uncertainty as to the occurrence of an undesired event”. Since then a number of other definitions have emerged and no common definition has been established. Lowrance (1976) defined risk as a measure of the probability and severity of adverse effects. On the other hand Rowe (1977) suggested the following risk definition: “the potential for realization of unwanted, negative consequences of an event”. Mathematically risk can also be formulated according to Kaplan and Garrick (1981) as an ensemble comprising risk scenarios associated with the likelihood of their occurrence and a damage vector of resulting consequences. Frequently, risk is also referred to as a function of likelihood, severity and vulnerability, where likelihood and severity represent the characteristics of a hazard or threat while vulnerability represents the property of an asset that is influenced by the hazard or threat. In this definition, both hazards/threats and assets are explicitly considered. Risk was also defined in the IEC 60300-3-9 standard as a “combination of the frequency, or probability, of occurrence and the consequence of a hazardous event” (Tuhovcak *et al.* 2006).

Knight (1921) stressed the importance of distinguishing between risk and uncertainty. The fundamental difference between these two lies in the fact that risk is a situation where mathematical probabilities can be assigned either through a priori knowledge or from the statistics of past experience. On the other hand, uncertainty refers to randomness, which cannot be explained. It was argued by Haines (2004) that the need for risk assessment becomes more imperative with less knowledge of a system. Such needs have become increasingly important with the emergence of complex man-made engineering systems, such as WDS, which affect our daily lives.

2.3.1 WDS Reliability Studies

Reliability can be defined as the probability that a system is operational for a given period of time (Haines 2004). WDS reliability has received significant attention in literature over the past few decades. In the field of WDS the research has been concerned with their ability to supply water of adequate quality and quantity under normal and abnormal conditions (Xu and Goulter 1999). As discussed by Gupta and Bhave (1994) there exists no common definition of reliability of a WDS.

Reliability studies can be seen as the first step to a complete risk analysis, providing not only the likelihood part (i.e., indicating if the network is able to supply water), but also including the consequence component that quantifies the impact in case of a failure (Kapelán *et al.* 2007). Only several applications related to WDS will be discussed here since reliability studies fall beyond the scope and focus of this thesis. Ostfeld (2001) classified WDS reliability studies as: topological (e.g., Wagner *et al.* 1988a) and hydraulic (e.g., Gupta and Bhave 1994; Todini 2000). Lansey (2006) in his overview of optimisation techniques applied to WDS highlighted the importance of taking reliability of newly designed or rehabilitated WDS into account as one of the design objectives. Farmani *et al.* (2005a) developed a single-objective reliability based optimization model for rehabilitation of WDS using fuzzy rules. Duan *et al.* (1990) presented a methodology for reliability-based design of WDS with a focus on number, location, and size of pumps and tanks. Farmani *et al.* (2005b) used multi-objective optimisation to obtain a trade-off between cost and reliability of a WDS.

2.3.2 Applications of Risk

The concept of risk has been successfully applied in various disciplines including military (Dillon *et al.* 2009) and business applications (Li and Liao 2007), the aircraft industry, food processing, software engineering (Lee 1996), etc. According to Egerton (1996) risk analysis and management were not commonly applied in the water utility sector until recently. She suggested that water companies in the UK were increasingly interested in risk analysis since it could help ensure maximum value for invested money. She also pointed out that with improved quality of data sources, risk analysis would be more frequently applied to optimise maintenance and operational processes. Consequently, Egerton (1999) reviewed a number of risk assessment techniques used in the water industry, particularly in water treatment works. She was then followed by

Pollard *et al.* (2004) and MacGillivray *et al.* (2006) who provided a comprehensive review of applications of risk analysis and management in the water utility sector from strategic, program and operational perspectives. Their works focused on a broad range of risks faced by water utilities worldwide rather than on specific applications of risk-based methodologies, as presented below.

Applications of risk in the water industry, reviewed below, can be broadly classified into quantitative, qualitative and quantitative-qualitative studies. Quantitative studies express risk in purely numerical terms, whereas in case of qualitative risk analysis linguistic terms and fuzzy logic (Zadeh 1975) were used. Hybrid studies typically utilise and combine both of these methods.

Risk analysis techniques have received significant attention from the investigators dealing with water treatment and water quality issues (e.g., Sadiq *et al.* 2007; Francisque *et al.* 2009), primarily due to health and safety implications caused by failures. Recent studies have also emerged from several other fields including design and rehabilitation of WDS (e.g., Kapelan *et al.* 2006). Nevertheless, applications of risk analysis in near R-T WDS operation and failure diagnostics are currently lacking.

Zongxue *et al.* (1998) applied quantitative risk analysis to evaluate the performance of a Water Supply System (WSS) during drought periods. They proposed an integrated drought risk index, defined as a weighted function of reliability, resiliency and vulnerability of the system studied. The consequences of drought were captured using a ratio of water deficit and water demand over a specific period of time.

Cooper *et al.* (2000) built a trunk mains burst risk model using a Geographic Information System (GIS) for optimisation of a WDS maintenance program. Their consequence model was based on the cost of damage caused by major pipe breaks and included damage of properties combined with a flooding model evaluated using a GIS. They suggested that for low probability and high consequence pipe breaks a valve exercising program could be adjusted to ensure timely isolation in case of their failure.

Dey (2001) developed a strategic risk-based DSS for inspection and maintenance of cross-country petroleum pipelines. Analytic Hierarchy Process (AHP) (Saaty 1980) was

used to identify factors that most influence the risk of failure of a specific segment of the pipeline.

Rajani and Kleiner (2002) proposed a holistic methodology for pro-active renewal of water mains based on the level of risk associated with their failure. The authors discussed possible ways to quantify the probability and impact components of risk, however, they did not provide any specific details or models to do so.

Sadiq *et al.* (2004a) presented a quantitative-qualitative framework for aggregative risk analysis of water quality failures in WDS using fuzzy logic. AHP was applied to aggregate individual risk factors in a hierarchical structure. Their approach, however, lacked an application on a real life case study.

Sadiq *et al.* (2004b) used Monte Carlo simulations to perform quantitative risk analysis of corrosion associated failures of iron water mains. They suggested that the high degree of uncertainty in attributes that contribute to pipe failure requires a probabilistic analysis. The consequences of pipe failure were only quantified as a reduction of a Factor of Safety (FOS), which reflected a relationship between structural capacity of a pipe and its actual loads.

Dewis and Randall-Smith (2005) presented a methodology to assess discolouration risk based on risk trees developed by a panel of experts. Their model considered the likelihood of pipe failure based on properties of an asset (e.g., a pipe). A demand driven Hydraulic Model (HM) was used to estimate changes in velocity in a WDS caused by pipe failure (i.e., burst). Simulation results together with additional input data were then combined using the aforementioned risk tree. As discussed by Vreeburg and Boxall (2007) other more advanced techniques to model discolouration exist (e.g., the Resuspension potential method or Cohesive transport model).

Almoussawi and Christian (2005) used quantitative risk analysis to evaluate the performance of several designs of water distribution networks. They used a simple consequence model based on the amount of undelivered water due to isolation of a network segment and did not report on using a hydraulic solver to evaluate impact.

Merrifield (2005) stressed the importance of risk analysis for effective asset management (i.e., a strategic application) and outlined key features of software to

enable it. No details of models to quantify likelihood and impact components of risk were provided.

Michaud and Apostolakis (2006) presented a methodology for the ranking of elements of WDS based on quantitative risk analysis. They developed an impact model based on a value tree, considered different types of consumers and impact categories, however, only used graph theory to evaluate the impact of segment isolations.

Tuhovcak *et al.* (2006) provided an overview of the most commonly used techniques of WSS risk analysis and described the implementation of Hazard Analysis and Critical Control Points (HACCP) methodology. They concluded that performance risk analysis of WSS was not very common in the Czech Republic and that methodologies from other industries are easily applicable. Later on, Tuhovcak and Rucka (2007) proposed a methodology for risk analysis of drinking WSS using the Failure Mode, Effects and Criticality Analysis (FMECA) (Department of Defense 1980). Application of such approaches from an operational perspective is not seen as suitable.

Kapelan *et al.* (2006) compared the robustness and risk-based solution of multiple-objective rehabilitation of WDS and concluded that the risk-based approach was superior since it considered the impact of hydraulic failures. Only a simple measure based on a fraction of assumed undelivered demand, evaluated using a demand driven hydraulic solver, was used to represent the consequences.

Kapelan *et al.* (2007) developed a methodology to assess the risk of supply interruption due to mechanical failures. They used a pressure driven hydraulic solver to evaluate consequences of burst pipes, however, only based the impact metric on the amount of undelivered water irrespective of the type of consumers and other aspects of the failure impact.

Filion *et al.* (2007) proposed a stochastic design of WDS considering the impact of low- and high-pressure failures in WDS. They quantified the consequences of a failure using expected annual damages sustained by residential, commercial, and industrial users.

Liserra *et al.* (2007) assessed the vulnerability of a WDS by combining a demand driven HM with a GIS and argued that due to scarce data it was not possible to apply a

complex risk based approach like Failure Mode and Effects Analysis (FMEA). Failure to use a pressure driven hydraulic model in their study can be seen as a significant drawback.

Beuken *et al.* (2008) used quantitative risk analysis to identify the most critical pipes (i.e., in terms of likelihood of burst and impact) within a WDS. In their study they applied an HM and a GIS in the impact evaluation. A set of impact factors reflecting the potential damage caused by a pipe burst was developed including surrogate models for water quality problems and public image of a water utility.

Meoli *et al.* (2008) used an aggregated risk measure to prioritise replacement of water mains. They coupled a pressure driven HM with a GIS to evaluate the impact of supply interruption on two types of customers (i.e., key customers and others). However, due to performance implications they only evaluated the impact during morning peak demand and did not use extended period simulation.

Thorne and Fenner (2009) developed a risk-based methodology to assess impacts of climate change on reservoir water quality. They argued that it was not only necessary to present the system operators with possible impacts of climate change, but also with the probability of their occurrence so that better informed decisions could be made. The authors represented risk as a product of probability and consequences, which might not be suitable for all decision-making situations as shown later in this thesis.

Sadiq *et al.* (2007) used fuzzy logic and evidential reasoning to evaluate the risk of accidental water quality failures in WDS. Sadiq *et al.* (2008) and Lee *et al.* (2009) used fuzzy fault tree analysis to predict risk of water quality failures in distribution networks. None of the above water quality studies attempted to use an HM to model the consequences of the actual contaminant intrusion.

Li (2007) used fuzzy fault trees in a hierarchical object-oriented risk assessment of components of WSS. The adopted qualitative approach might suit high level strategic decision-making, however, operational decisions would benefit from a quantitative approach and use of hydraulic modelling to better estimate consequences of a failure.

Christodoulou *et al.* (2009) developed a neuro-fuzzy DSS for risk-based asset management of water piping networks. Their work was mostly concerned with the relative probability of failure of a particular pipe, expressed in linguistic terms, and lacked the impact component of risk. A GIS was used to present the outputs of the risk analysis to a DM.

Francisque *et al.* (2009) proposed a fuzzy-risk methodology to prioritise water quality monitoring locations within a WDS. The proposed method considered vulnerability of a particular area in the WDS to water quality problems depending on the hydraulics, structural integrity of pipes and various water quality parameters as well as sensitivity of the customers in that area (e.g., hospitals, day care centres, small children and old people).

2.4 Burst Detection and Diagnostics

This section reviews relevant literature dealing with the detection of abnormal events (e.g., pipe bursts and leakage) in WDS and their location (i.e., diagnostics) using data driven and model based techniques. The focus of the review is on methods for diagnostics (i.e., model-based location of bursts) and only key publications dealing with burst detection methods will be discussed here since the contribution of this thesis lies in the combination of multiple imperfect models.

Detection of leaks and bursts has been vital for many other industries. The majority of failure detection methods for pipelines originated from the gas, oil and chemical industries where leakages can cause severe environmental impacts or represent health and safety hazards. Misiunas (2005) in his PhD thesis provided a review of burst detection and location techniques in both, pipelines and pipe networks. Methods based on steady and unsteady (i.e., transient) network conditions were discussed. A more recent review of leakage detection, location and management methods can be found in Puust *et al.* (2010). A broad range of methods was considered by the authors, including traditional techniques for leak detection and location, such as acoustic logging, step-testing, ground motion sensors, ground penetrating radars, etc. Methods requiring field inspection, will not be considered here since they are beyond the scope of this thesis.

2.4.1 Data and Model Driven Anomaly Detection

With recent advances in sensor technologies and Supervisory Control And Data Acquisition (SCADA) systems, “intelligent”, wireless pressure and flow sensors have been widely deployed to monitor the state of WDS in R-T (Mounce *et al.* 2010). Their data was used in combination with data and model-based methodologies in an attempt to detect and locate leakage or pipe bursts within a WDS.

Verde (2001) presented a methodology, based on transient analysis, for detection and location of multiple-leaks in fluid pipelines based on a set of pressure and flow measurements taken at the ends of a duct. Given the focus of the methodology on pipelines only, its application in a WDS would be problematic.

Khan *et al.* (2002) designed a low-cost turbidity sensor and tested its functionality in a real life WDS. Changes in water flow regime, such as sudden increases in flow caused by pipe bursts or flushing affect opacity of water flow (e.g., due to disturbance of sediments in the pipe).

The use of ANNs to detect anomalies, such as pipe bursts, in a WDS has been explored by a number of researchers (e.g., Mounce *et al.* 2002; Romano *et al.* 2009). Mounce *et al.* (2003) coupled an ANN burst detection system with a rule based classifier to fuse outputs of several ANNs to identify the state (i.e., burst or no-burst) of multiple DMAs. They demonstrated the methodology on a hydrant flushing case study and also suggested that pressure gradients within a DMA might provide a more precise location of the burst pipe. Mounce and Machell (2006) compared the capabilities of several types of ANNs to detect bursts and leakage in DMA flow patterns and concluded that time delay neural networks performed better for leak detection than static networks. In Mounce *et al.* (2006) a Fuzzy Inference System (FIS) was used to classify discrepancies between DMA inflow predictions produced by an ANN and field observations. Alarms signalling an anomaly were then generated using fuzzy rules. Mounce *et al.* (2007) further improved their burst detection methodology to provide accurate estimates of average burst flow. Later on, Mounce *et al.* (2008; 2010) presented an application of their methodology in a near R-T environment and demonstrated its performance on real life case studies. The time window (i.e., 12h or 24h) used in their work for burst detection was in all cases rather wide, which can be seen as a significant drawback to

their approach. Late detection of the burst not only reduces the response time a water utility might gain to locate and fix the burst but it also makes further diagnostics (e.g., model based burst location) more difficult.

On the other hand, Romano *et al.* (2009) worked with only a 30 minute time window in their Bayesian-based burst detection methodology. They utilised both pressure and flow measurement data from multiple sensors within a DMA to increase the accuracy of correct detection. The performance of the new methodology was demonstrated by an analysis of historical burst events. Its application in a near R-T environment, which represents significant challenges in terms of automatic re-training of the burst detection system, was not demonstrated by the authors.

Buchberger and Nadimpalli (2004) proposed a statistical leak detection method for well defined residential DMAs. Their method required high frequency flow measurements taken during a minimum night flow period and was never tested in a real life WDS. The method provided certain advantages over traditional water audits, however, was unsuitable for R-T burst detection and location.

Ragot and Maquin (2006) proposed a model-based methodology for detection of measurement faults (e.g., sensor failures) in water supply networks. A number of redundant models were first developed based on physical relationships between sensor measurements (e.g., flow mass balance relations, pressure-flow relationships, etc.). Residuals of sensor measurements and model expectations were generated and analysed using fuzzy logic to identify sensor failures. The method was tested on data obtained from a real life system.

2.4.2 Anomaly Diagnostics

A number of techniques for burst diagnostics (i.e., determining location of a burst pipe) based on the behaviour of pipe networks in unsteady (i.e., transient) state were developed. Colombo *et al.* (2009) and Puust *et al.* (2010) provided a comprehensive review of these methods. Only key publications from this field will be mentioned here since such methods typically rely on more expensive transient loggers, which are not commonly available. Moreover, most of the applications of transient techniques were only done in laboratory conditions or in pipelines and there has been very little evidence that they can be successfully applied in real WDS (Wu *et al.* 2010). The higher costs of

collection, processing and storage of high frequency data produced by transient loggers could be also seen as another disadvantage of such approaches.

Wiggert (1968) was amongst the first to investigate unsteady flows in pipelines experiencing leakage. He concluded that the lateral outflow attenuated the pressure transient wave. The transient-based methods can be generally classified into: leak reflection methods (Brunone 1999), inverse transient analysis (Vitkovsky *et al.* 2000; Kapelan *et al.* 2003), impulse response analysis (Liou 1998), transient damping method (Wang *et al.* 2002) and frequency domain response analysis (Stoianov *et al.* 2001).

A more promising approach to help locate leaks and bursts in a WDS is seen in various model-based methodologies that can be applied under steady conditions and do not require the collection of data at high frequencies. Pudar and Liggett (1992) were amongst the first to solve the inverse problem to locate leaks in a WDS using pressure and flow measurements under steady conditions. They argued that measurements should be taken at locations of maximum sensitivity and that the more over determined (i.e., the higher was the number of pressure measurements compared to the number of leaks in a WDS) the inverse problem, the better the results. It was suggested that the success of leak detection further depended on a particular configuration of a WDS, accuracy of pressure measurements, and accuracy of system characteristics such as pipe roughnesses and known demands.

Evolutionary optimisation techniques were used by several researchers to solve the inverse problem of locating a leak. Puust *et al.* (2006) used the Shuffled Complex Evolution Metropolis (SCEM-UA) (Vrugt *et al.* 2003) optimisation algorithm to estimate the posterior probability density functions of leakage areas and demonstrated their approach on a synthetic case study with uncertain measurements. Wu and Sage (2006) used a Genetic Algorithm (GA) combined with a steady-state HM calibration to locate leakage hotspots within DMAs. Despite its pressure sensitive character, leakage was modelled as constant demand. Deagle *et al.* (2007) presented the results of leakage hotspot identification using an HM on 3 real life DMAs. They used a GA to calibrate their HMs and incorporated leakage allocation into the calibration procedure. Wu *et al.* (2008) used GAs to optimise the pressure-dependent emitter locations and coefficients as possible leakage areas and illustrated the methodology on a real life network. Wu

(2009; 2010) proposed a unified parameter optimisation approach, combining identification of leakage hotspots with Extended Period Simulation (EPS) HM calibration using a GA and demonstrated the methodology on a real life DMA in the UK.

Misiunas *et al.* (2006) presented a methodology for detection and location of bursts in residential DMAs. They used a change detection test based on Cumulative Sum (CUSUM) to detect the burst and estimate its size. Consequently, the EPANET (Rossman 2000) hydraulic solver was applied to find the burst location by comparing the fit between modelled and measured changes in pressures in a DMA. The methodology was only demonstrated on a small synthetic case study, assuming real-time pressure measurements at 3 locations within a DMA.

Sterling and Bargiela (1984) presented a WDS state estimation algorithm and solved the problem of minimisation of measurement inconsistencies using linear programming. Gabrys and Bargiela (1999) examined the patterns of state estimates of a WDS using an ANN and developed a fault detection system capable of locating leakage. Andersen & Powell (2000) presented an implicit state estimation technique to locate a burst and demonstrated the methodology on a simple looped network without explicitly taking into account uncertainty and measurement errors. Izquierdo *et al.* (2007) developed a neuro-fuzzy approach to perform diagnostics of leaks and other failures and anomalies in a WDS based on network state estimation and data driven modelling. Their methodology has only been applied to a synthetic case study.

Poulakis *et al.* (2003) developed a Bayesian probabilistic framework for pipe burst detection and showed the capability of the methodology to identify the most likely burst location on a synthetic case study based on a simple network. Uniformly distributed demands were assumed across the WDS studied. Furthermore, an unrealistic sensor density of 7 sensors per 30 demand nodes in this WDS was considered by the authors. It was concluded that measurement accuracy as well as sensor locations played an important role in successful burst location.

Shinozuka *et al.* (2005) used a data driven technique to analyse pressure measurements collected from a WDS in order to determine the location and extent of damage of a burst caused by an earthquake. An ANN was trained to provide Euclidean distance from a

suspected burst location to a pressure monitoring station. The method was demonstrated on the same simple case study as used by Poulakis *et al.* (2003). The use of Euclidean distance might have been suitable for the WDS being studied, which was shaped as a rectangular grid with only two different pipe lengths, but could be inappropriate in other situations.

Holnicki-Szulc *et al.* (2005) applied the Virtual Distortion Method to solve the inverse problem of locating leakages in a WDS. The method assumed a reliable numerical model of the WDS and continuous observation of pressure heads in the WDS. Measurement uncertainty was not accounted for by the authors and availability of pressure measurements at every node in the network was assumed. The application of the methodology was not demonstrated on real life data and the unrealistic assumptions stated above seriously restrict its applicability to real life WDS.

Mashford *et al.* (2009) attempted to use Support Vector Machines (SVM), which act as pattern recognisers, to detect and locate leakage in a WDS. They trained two SVMs on synthetically generated noise-free data to predict leak size and leak location. The assumption of complete knowledge of a WDS without any uncertainties and availability of unrealistically accurate pressure measurements to detect small leakages makes the study infeasible for practical use.

Recently, Borovik *et al.* (2009) presented an active burst identification procedure based on altering DMA inlet pressure during the minimum night flow period to obtain a gradient of pressure line. An HM was used to simulate bursts at different nodes of the network and the modelled gradient of pressure line was then compared with the measured one using chi-square test. The requirement to alter the DMA inlet pressure typically involves manual intervention (at least in the UK where the number of remotely controlled devices is generally low) and is, therefore, not suitable for R-T burst diagnostics.

2.5 Failure Impact in WDS

Failures in WDS occur on a daily basis, primarily due to ageing infrastructure or equipment failure, but often also due to damage caused by third parties. The magnitude and scale of their impact typically depends on a number of factors amongst which the

geographic location and topology of the WDS play an important role. Generally, three types of failures in WDS can be recognised: mechanic, hydraulic and water quality failures (Filion *et al.* 2007). Many researchers over the years tried to estimate the impact of failures in a WDS on its stakeholders and a number of Key Performance Indicators (KPIs) were developed. An exact quantification of failure impact is a highly subjective and complex problem, particularly because of differing social situations.

The work done so far has focused primarily on impacts caused by pipe bursts, as part of strategic management and long term asset management plans (e.g., Skipworth *et al.* 2002). With very few exceptions (e.g., Burrows *et al.* 2000) operational impact assessment has been mostly lacking.

In the UK, the high standard of delivery of potable water is monitored by the Water Services Regulation Authority (OFWAT) using several KPIs, which amongst other aspects focus on long term pressure adequacy (i.e., Pressure of water mains – the DG2 indicator) and continuity of water supply (i.e., Supply interruptions – the DG3 indicator) (OFWAT 2008). Such indicators provide only a long term overview of performance of a water utility and do not sufficiently reflect the impact of a failure on customers from an operational perspective.

Most of the research dealing with failures in WDS (e.g., Gupta and Bhawe 1994; Ostfeld *et al.* 2002; Kapelan *et al.* 2006) used the Fraction of Delivered Demand (FDD) and its similar forms as a KPI to assess the level of service. Although being an effective measure on large scale, FDD does not consider the sensitivity of individual customers to a reduced level of service and additional impacts, such as increased discolouration risk, lost water, etc.

Rajani and Kleiner (2002) outlined direct, indirect and social costs associated with pipe failure but did not suggest how these should be quantified. Consequently, Rahman *et al.* (2005) developed a framework to estimate social costs related to infrastructure works, such as pipe burst repairs, which incorporated a number of aspects such as, property damage, traffic disruptions, environmental impacts and health and safety issues. They argued that failure to account for social costs might lead to poor decisions. Studying past projects was suggested as means for data collection to better quantify costs

associated with social impacts. Their framework is best suited to strategic applications due to the medium and long term character of some of the impacts considered.

Mansoor *et al.* (2005) analysed the performance of WDS under failure conditions and proposed a number of operational and strategic performance indicators. They used an ANN to simulate the effect of pressure on nodal demands and improved the commonly used performance indicator based on the fraction of undelivered demand to incorporate different types of customers. The customers were divided into 4 classes (i.e., low income, medium income, high income) and their sensitivity was, therefore, primarily determined by their financial situation. Although such classification might be appropriate for less developed countries, its application in the UK could be questionable.

Beuken *et al.* (2006) studied external effects of pipe bursts, such as damage and injuries in the proximity of the burst pipe. They performed a strategic risk analysis using a GIS to identify high risk pipes depending on their proximity to important structures (e.g., railway, main roads, bridges, etc.). Beuken *et al.* (2008) further extended their consequence model to account for the following impacts: supply interruption, low pressure, water quality, public image and direct costs. They suggested suitable measures to quantify these impacts from a strategic perspective and used a GIS and an HM to identify critical valve sections in a WDS. Furthermore, a rule based system was applied to aggregate the above listed impacts.

Trietsch and Mesman (2006) performed a strategic analysis of the reliability of valves in a WDS to isolate a burst pipe. They only considered complete interruption of water supply and did not use an HM to evaluate potential secondary low pressure problems. Walski (1993) was one the first who pointed out the importance of considering the location of valves in WDS reliability studies. He argued that often not only one pipe is taken out of service to carry out burst repairs but rather a segment of pipes is disconnected depending on the location and functionality of isolation valves. Jun *et al.* (2007; 2008) presented an efficient algorithm to identify segments in a WDS and evaluated the system wide impact of valve failures from a strategic perspective. Low pressure problems or other types of impacts, such as water utility's financial losses were not considered by the authors.

Recently, Giustolisi *et al.* (2008a) evaluated the impact of segment isolations in a WDS over an EPS using a pressure-driven HM. They proposed several operational KPIs based on the amount of undelivered demand, however, they did not capture the effects of the burst before it was isolated and also did not take into account the sensitivity of customers.

Michaud and Apostolakis (2006) analysed the criticality of network elements in a WDS using graph theory. They proposed a hierarchical value tree to aggregate impacts (i.e., health & safety, company image, financial and environmental) of pipe isolation using the Multi-Attribute Utility Theory (MAUT). Several types of customers were considered by the authors. Their strategic assessment did not take into account locations of isolation valves and neither used an HM to evaluate the full effect of segment isolation (e.g., low pressure problems).

Vamvakeridou-Lyroudia *et al.* (2009) proposed a hierarchical structure to aggregate multiple KPIs calculated using a pressure driven HM. The factors considered included supply interruption, low pressure, discolouration, and economic impacts to assess the effectiveness of interventions (e.g., valve manipulation) to mitigate the impact of unintended isolation. The proposed hierarchical structure seemed too rigid to provide a DM with sufficient flexibility to express his/her preferences.

Water quality problems, such as discolouration or contaminant intrusion, caused by pressure and flow disturbances triggered by a pipe burst or consequently repair works, have been mentioned by many (Rajani and Kleiner 2002; Sadiq *et al.* 2005; Sadiq *et al.* 2006; Beuken *et al.* 2008). However, quantification of such impacts has been difficult and often only surrogate measures were used. Dewis and Randall-Smith (2005) developed a discolouration model based on risk trees developed by a panel of experts and applied it to estimate the increase in discolouration potential of all pipes in the WDS after a failure. As Vreeburg and Boxall (2007) pointed out using a discolouration model based on shear stress (Boxall and Saul 2005) would be more appropriate than the adopted approach.

Burrows *et al.* (2000) developed a near R-T WDS performance evaluation system, based on EPANET and a GIS. They used demand driven EPANET to develop a specific regression formula for every node in the network. Pressure at a node was a function of

boundary conditions of the HM (i.e., inlet pressure and flow, export flows and pressure measurements in a DMA). Their approach, which considered also dynamic model recalibration thus enabled a truly near R-T impact assessment. The impact model, based only on a demand driven solver, simply considered low pressure impacts on customers linked with an HM through an integrated information system.

2.5.1 WDS Modelling Under Failure Conditions

Modelling of WDS has become a widely applied practice amongst academics and practitioners of water utilities. It is most frequently applied to simulate the operational behaviour of a WDS, for planning, design (Savić and Walters 1997; Kapelan *et al.* 2005b), rehabilitation purposes, etc. Hardy Cross (1936) developed the first numerical method to solve looped WDS in the 1930s and established the foundations for future use of this technique on computers. Adams (1961) used a computer to model the hydraulics of a WDS using Cross' method in 1960s. He was shortly after followed by Shamir and Howard (1968) who used a more powerful Newton-Raphson method. Since then various methods (Todini and Pilati 1988) have been developed to solve the mass and energy conservation equations used to describe the behaviour of a WDS (Walski *et al.* 2003; Kapelan *et al.* 2005b).

Traditionally, WDS were modelled under the assumption that demands are always delivered. Such an approach is also referred to as demand driven analysis, however, under pressure deficient conditions the assumption of fixed demands at nodes does not hold. When insufficient pressures are available in a WDS the nodal demands cannot be completely satisfied. Bhave (1981) was one of the first who studied the behaviour of WDS under pressure deficient conditions and reformulated the mass and energy conservation equations to include Pressure Dependent Demands (PDD), sometimes also referred to as Head Driven Analysis (HDA) or Pressure Driven Analysis. Since then a number of different formulations describing the dependence of nodal demand on available pressure have emerged (Germanopoulos 1985; Wagner *et al.* 1988b; Reddy and Elango 1989; Gupta and Bhave 1996; Fujiwara and Li 1998; Tucciarelli *et al.* 1999; Tanyimboh *et al.* 2001; Wu *et al.* 2006).

As suggested by Gupta and Bhave (1996) the approach of Wagner *et al.* (1988b) has yielded the best results. This fact has been further proven by its application by many

other researchers (e.g., Cheung *et al.* 2005; Giustolisi and Doglioni 2005; Morley and Tricarico 2008). Cheung *et al.* (2005) implemented Wagner's formula in the EPANET (Rossman 2000) hydraulic solver. They concluded that pressure driven formulations by Fujiwara and Li (1998) and Tucciarelli *et al.* (1999) produced similar results and that testing on larger networks was necessary.

Hayuti and Burrows extensively studied HDA and have extended the EPANET solver to support such analysis (Hayuti and Burrows 2004; Hayuti and Burrows 2005; Hayuti *et al.* 2006; Hayuti *et al.* 2007). They called their approach Simple Sequential HDA Solution Seeking (SSS) demand driven approach. They iteratively called the EPANET solver to identify all pressure deficient nodes and modified their outflows according to Wagner *et al.* (1988b). Their approach was computationally extremely inefficient and PDD should be directly implemented in the hydraulic solver as done by, e.g., Giustolisi and Doglioni (2007).

Todini (2003), Ozger and Mays (2003), and Ang and Jowitt (2006) proposed very similar approaches, which instead of modifying nodal demands according to available pressure, connected / disconnected an artificial reservoir to pressure deficient nodes. Water was allowed to flow only from the node to the reservoir (i.e., the reservoir was disconnected if the outflow was negative and started to drain water from the reservoir into the system). The major benefit of their approach was that no calibration parameters (i.e., describing the pressure-demand relationship) were required unlike in the case of all the other previously mentioned methods. The only reasonable assumption made was that customers experiencing pressure deficient conditions drew as much water as possible (i.e., up to the requested demand).

Rossman (2007) commented that the approaches described above were also computationally demanding since every iteration consisted of running a full hydraulic simulation of EPANET and the addition or removal of artificial reservoirs as needed until convergence was achieved. Another argument against this technique was made by Wu (2007) who pointed out that implementation of EPS, was in such a technique, difficult if at all possible. However, Rossman (2007) showed that the above mentioned algorithm (SSS) could be efficiently implemented in EPANET using emitters by introducing an extra status array which controlled their state and activated them only in

pressure deficient situations when system pressures were above 0 m. Recently, Morley and Tricarico (2008) extended the pressure driven implementation of EPANET proposed by Rossman (2007) to allow for any pressure - demand relationships and used Wagner's representation as the default one.

Giustolisi *et al.* (2008c) developed a steady-state network simulation model, which integrated PDD and leakage at pipe level into hydraulic representation. The authors stressed the importance of a more realistic simulation model allowing for leakage analysis, verified its convergence and concluded that the proposed algorithm was robust, which was not the case in most of the PDD modifications discussed above. It was further noted that PDD simulation generally resulted in higher pressures in a WDS. Consequently, Giustolisi *et al.* (2008b) extended the robust pressure driven simulation model discussed above and incorporated an algorithm for an automatic detection of topological changes in pipe networks due to interruptions. Nodes and pipes that were not linked to any source were removed from the set of hydraulic equations. The newly developed algorithm was demonstrated on a real life pipe network. It was concluded that the newly proposed algorithm was robust in terms of numerical accuracy and convergence rate but was computationally demanding.

2.5.2 Pipe Burst Modelling

Modelling of pipe bursts has received significant attention in the literature, primarily due to its significance in reliability studies and risk assessment. This section provides details about modelling of pipe bursts in the EPANET (Rossman 2000) hydraulic solver, which has *de facto* become a standard software package used by the academic community. Depending on the purpose of the simulation (e.g., reliability analysis, etc.) as well as the capabilities of the hydraulic solver used, the methods of modelling pipe bursts can be broadly divided into two classes depending on the type of analysis: (1) Strategic decision-making or (2) Operational decision-making.

2.5.2.1 Strategic Applications

In strategic applications, the time over which a pipe needs to be isolated for repairs is dominant and, therefore, the outflow from a burst before the isolation takes place is neglected. The simplest technique applied by several researchers (e.g. Farmani *et al.*

2005b) was to disconnect the failed pipe. In EPANET a single pipe can be disconnected in the following ways:

- set its status to CLOSED
- set its diameter to a very small number (e.g., 0.0001)
- physically remove the pipe from the network

The physical removal of the failed pipe, although being the most difficult one to implement, can be considered as the best option since it effectively reduces the complexity of the governing nonlinear equations and thus speeds up the convergence of the gradient algorithm (Todini and Pilati 1988) used in EPANET. It also eliminates potential convergence problems caused by the first two approaches, which introduce abnormally high resistance coefficients in the hydraulic equations.

Furthermore, as noted by Walski (1987; 1993) and Jun *et al.* (2007; 2007; 2008) another limitation of such an approach is that it does not respect the location of isolation valves in the real network (note that isolation valves are not typically included in HMs). This is vital since it is often necessary to isolate a segment of pipes due to the location of the valves or because of the inability to shut a valve which has not been exercised regularly. As an example Jun *et al.* (2008) reported that there were approx. 4.3% of inoperable valves in a studied WDS. An unintended isolation of additional segments can occur downstream when pipes are isolated for repairs.

2.5.2.2 Operational Applications

From an operational view, typically the outflow from the burst is modelled to observe the effects of an abnormal demand (e.g., drops in pressures) on the rest of a WDS. Hayuti and Burrows (2005), and Mansoor and Vairavamoorthy (2003) modelled pipe bursts in EPANET by inserting an artificial reservoir in the middle of a pipe and setting its water surface level to correspond to the elevation of the pipe. The outflow through the pipe was then controlled by changing its properties (i.e., diameter, length and roughness). Placing the burst into the centre of a pipe is an approximation which is reasonable for relatively short pipes, however, might become less applicable in rural areas where pipe lengths tend to be significantly longer than in urban areas.

More frequently, pressure sensitive outflows are modelled using emitters, which are devices used typically to model sprinklers or irrigation networks governed by the equation for orifice flow (Walski *et al.* 2003):

$$Q = C_d A \sqrt{2gh} \quad (2.1)$$

where: Q is the outflow (discharge), C_d is a discharge coefficient, A is the area of an orifice, g is the gravitational acceleration constant (9.81 ms^{-2}), and h is the head loss across orifice (m).

The orifice equation can be generalised and written as:

$$Q = C_d P^\gamma \quad (2.2)$$

where: Q is the flow rate, P is pressure at junction, C_d is a discharge coefficient and γ is a pressure exponent.

The generalised orifice equation is used in EPANET to model pressure sensitive outflow, such as leakage or pipe bursts.

Studying the behaviour of bursts and leakage has attracted the attention of many researchers. Van Zyl and Clayton (2005; 2007) investigated factors affecting magnitude of pipe a burst. They identified four primary factors: (1) leak hydraulics, (2) pipe material behaviour, (3) soil hydraulics and (4) water demand. Van Zyl and Clayton (2007) further noted that specific types of failures are likely to develop depending on pipe material. Results of their experimental study related pipe material and type of the opening to the pressure exponent γ which had the most significant effect on the flow through a burst. The value of γ typically ranged from 0.52 to 1.85 for round holes and longitudinal cracks, respectively. Lambert (2002) reported that values of γ typically ranged from 0.5 to 1.5 and occasionally also between 2.0 and 2.5 during field tests conducted in the UK. Lately, Cassa *et al.* (2010) conducted a numerical study into the effects of pressure on holes and cracks and concluded that values of $\gamma > 1.5$ did not have theoretical justification. The above reported findings could be exploited to produce a more realistic model of leakage and bursts in a WDS by assigning the most likely values of pressure exponent to bursts in pipes according to their material and additional properties.

2.6 Information Fusion

With the increasing availability of sensors and measurements, information fusion has become a popular approach in order to infer maximum information from collected data. Amongst other available techniques, the Dempster-Shafer theory (D-S) of Evidence (Shafer 1976) represents a suitable mathematical framework to combine uncertain information. Sentz & Ferson (2002) provided a review of applications of D-S theory in various disciplines including classification and recognition (Polikar 2006; Oukhellou *et al.* 2010), decision-making (Tanaka and Klir 1999), engineering and optimization (Agarwal *et al.* 2004), fault detection (Chen and Aickelin 2006), failure diagnostics (Rakar *et al.* 1999; Basir and Yuan 2007), target tracking (Dezert *et al.* 2006), etc.

A limited number of applications of evidence theory can also be found in the water industry. Most frequently, it has been employed in water quality problems or strategic applications. However, its use on operational problems has been limited, unlike in other fields, including, e.g., military applications (Dezert *et al.* 2006).

Demotier *et al.* (2003) applied the Transferable Belief Model (TBM), which is an extension of D-S theory proposed by Smets and Kennes (1994) to risk analysis of water treatment processes. No application of the methodology on a real life case study was reported by the authors.

Sadiq and Rodriguez (2005) and Sadiq *et al.* (2006) used D-S theory to interpret water quality data. They explored the potential of four combination rules (i.e., Dempster's, Yager's, Dubois-Prade's and Dezert-Smarandache's rules) and discussed their limitations, particularly with respect to combining conflicting evidence. The authors did not attempt to determine the most suitable combination rule for their particular decision-making context.

Li (2007) used D-S theory and fuzzy logic to aggregate risk levels in a hierarchical risk assessment of components, subsystems, and the overall WSS. The proposed methodology lacked the calibration of fuzzy membership functions representing hazards in a WDS, however, it was suggested that they could be determined from analysis of historical data.

Bai *et al.* (2008) used Dempster's combination rule in a hierarchical aggregation of evidence to assess the condition of buried pipes. Only Dempster's combination rule was used by the authors, despite evidence in the literature that the selection of a particular combination rule is problem specific.

2.7 Summary & Conclusions

This chapter provided a review of literature related to risk-based operation of WDS under failure conditions, particularly when pipe bursts occur. Given the multi-disciplinary character of this research a number of areas were covered, including decision-making and decision support, risk-based methodologies, pipe burst diagnostics, WDS failure impact assessment including pressure driven WDS modelling and information fusion.

In section 2.2 the key publications dealing with decision-making and decision support, with an emphasis on applications of DSS in R-T were reviewed. The key conclusions that can be drawn from the current research are summarised as follows:

- Decision support systems have gained popularity in a number of industries and recently also in the water sector.
- Optimisation algorithms and artificial intelligence methods are commonly becoming part of modern DSS.
- The number of applications of R-T DSS in the literature is scarce compared to R-T ES used to solve structured problems. This can be explained by difficulties with the presentation of R-T data to DMs and insufficient performance of conventional computers in the past.
- It can be expected that the number of R-T DSS will be increasing because the current trend is to support expert judgement rather than trying to replace it completely by AI (Koutsoyiannis *et al.* 2003).
- High efficiency of DSS in terms of their performance is crucial for any kind of R-T application and, therefore, off-line pre-computing of results and the use of surrogate models have been frequently applied.

From the review of applications of risk presented in section 2.3 it can be concluded that:

- Risk assessment of WDS has primarily focused on strategic applications. It can be argued that until recently the computing power available prevented operational applications requiring near R-T performance.
- The number of applications of risk to water quality problems clearly dominates other research areas.
- The lack of research in the field of risk analysis applied to the failure management of WDS is apparent, which creates the grounds for the work addressed in this thesis.
- Frequently, the measure of risk, comprising the probability and consequence components (Kaplan and Garrick 1981), has been presented to DMs in an aggregated form. As shown in this work, this can be often avoided and can lead towards better informed decisions.

Section 2.4 provided a review of model based pipe burst diagnostics methods.

- It can be seen that despite the progress achieved in the field of pipe burst diagnostics there is little evidence that the methods reviewed, when used on their own, are ready to be applied in real life conditions for operational decisions.
- The application of transient techniques is seen as problematic since the published results are typically not based on real water distribution networks that exhibit much higher noise levels than pipelines studied under laboratory conditions.
- The R-T environment considered in this work also presents a significant obstacle for a number of methods presented in this section.
- Up to now none of the proposed techniques attempted to combine the outputs of several models in order to determine the location of a burst pipe within a DMA.

In section 2.5 a review of commonly used performance indicators to capture the impact of failures in WDS was provided. The following can be observed:

- The performance indicators currently used by researchers and practitioners do not fully satisfy the requirements of operational impact assessment. The majority of them suit best strategic applications, concerned with whole-life cost of assets and frequently they are unable to capture the wide range of adverse effects caused by failures, such as pipe bursts.
- HMs have been frequently coupled with a GIS in order to include customer information and land use data from the proximity of a failure to quantify its impact on the principal stakeholders.
- As pointed out by many (Wagner *et al.* 1988b; Gupta and Bhawe 1994) the use of pressure driven HMs is imperative when studying WDS under pressure deficient conditions, which has not always been the case in previous research.
- The use of complex impact models (e.g., Beuken *et al.* 2008), capturing a wide range of effects of a failure on stakeholders has been limited and such models have not been applied to operational impact assessment. Furthermore, studies investigating the preferences of water companies in terms of significance of various types of impacts (e.g., supply interruption, inadequate pressure, discolouration, etc.) are lacking.
- As stated by many (e.g., Gupta and Bhawe 1996; Tanyimboh and Tabesh 1997, etc.), the behaviour of a WDS under pressure deficient conditions is a complex phenomena which is not well understood. A particular difficulty is caused by an uneasy collection of sample data from real WDS because simulation of such conditions can affect customers.
- The inclusion of HDA has only minimum impact on computational efficiency but on the other hand models the behaviour of a WDS under pressure deficient conditions more realistically (Germanopoulos 1985).
- From an operational perspective, bursts should be modelled as pressure sensitive outflows from a WDS, using emitters. Information about the properties of a burst pipe, such as its material could be used to set the most likely value of pressure exponent to more accurately capture the behaviour of a failure.

Finally section 2.6 provided a brief overview of the application of information fusion, with an emphasis on D-S theory, from a number of fields, including the water industry.

It can be concluded that:

- D-S theory has become a popular mathematical tool for information fusion across many industries, however, its application in the water sector has been so far limited.
- The choice of the most suitable combination rule in information fusion is problem specific and no single rule can perform well in all situations. Selection of a combination rule should, therefore, be carefully determined as part of the development of an information fusion model.
- D-S theory has been applied in R-T applications in other industries, predominantly in military applications and pattern recognition problems, however, its operational use in the field of WDS has been so far limited.

CHAPTER 3 RISK-BASED PIPE BURST DIAGNOSTICS

3.1 Introduction

Dealing with failure conditions in a WDS is one of the primary functions of control room operators. The process of discovering that a WDS is not functioning normally, investigating potential incidents and deciding on how to deal with them is still challenging, even with recent progress in monitoring and communication technologies. Data coming from sensors and notifications from customers in the form of phone calls are the two main indicators that a problem that warrants further investigation and possibly repairs has occurred in a WDS. The operator then typically has to check and process information coming from various systems in order to assess whether the perceived incident in the network is real, rather than a consequence of malfunctioning monitoring and communication devices. The investigation depends strongly on the internal business processes of a particular water utility but frequently requires a field technician to be sent out to visually inspect the situation at a particular location and confirm (or not) the potential incident. Furthermore, in situations when several alarms (i.e., detected abnormal events, such as pipe bursts) occur simultaneously in the same time horizon, the operator usually has to prioritise both investigative and intervention actions with dynamically changing information about the potential incidents. Most decisions are currently made on an ad-hoc basis, primarily based on the experience of skilled operators.

This chapter presents a methodology to enhance the decision-making of WDS operators when dealing with abnormal situations (e.g., increased DMA inflows) in a WDS caused by pipe bursts. The chapter is organised as shown in Figure 3.1, which also indicates the mutual relationships between constituents of the proposed methodology. First, in section 3.2 the conceptual development of a risk-based decision-making methodology to support near R-T diagnostics of burst pipes within a DMA is discussed. Then the components of a risk metric (i.e., the likelihood and impact) used in this work are described in detail in the following sections. A novel method to estimate the likely location of a burst pipe within a DMA in near R-T is proposed in section 3.3. The method is based on the fusion of evidence provided by a number of models. The

combined results, generated using a Dempster-Shafer (D-S) model, form the likelihood component of the above mentioned risk metric. An impact model able to capture various operational aspects of adverse effects caused by a pipe burst is described in section 3.4. The impact model, based on the Multi-Attribute Value Theory (MAVT), completes the risk metric and provides control room personnel with an insight about the expected consequences of a burst in different parts of a DMA, if left unattended. Often, multiple failures can occur in a similar time horizon (e.g., during 24 hours) in different parts of a large WDS. Such situations require operators to prioritise their actions due to limited resources. A novel ranking methodology is introduced in section 3.5, which is able to prioritise alarms based on an overall aggregated level of risk they represent, to help control room operators deal with the most severe failures first.

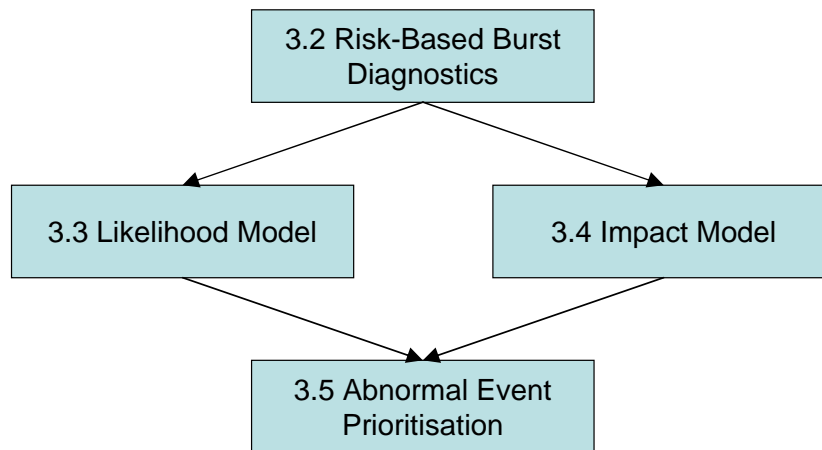


Figure 3.1 Structure of the risk-based pipe burst diagnostics methodology

3.2 Risk-Based Decision-Making

Nowadays, WDS are typically divided into DMAs to better account for and reduce leakage. Within a DMA all water inputs and outputs are measured to allow monitoring of consumption trends of water consumers. The number of properties supplied by a DMA is usually between 1,000 to 5,000 (Burrows *et al.* 2000), however, this may vary depending on topographic and demographic characteristics of an area. Thanks to technological advances, the cost of pressure and flow monitoring devices has reached the level that enables their large scale deployment at strategic locations in DMAs (Kapelan *et al.* 2005c). The wide availability of pressure and flow data has triggered research into early warning systems (Mounce *et al.* 2002; Mounce *et al.* 2003; Buchberger and Nadimpalli 2004; Romano *et al.* 2009) and lead towards their

application in real life WDS to detect leaks and bursts (Mounce and Boxall 2010; Mounce *et al.* 2010).

Currently, the online early warning systems (i.e., pipe burst detection systems) typically do not go beyond generating an alarm (see Figure 3.2) to notify control room personnel of possible problems in a particular DMA that exhibits abnormal flow and/or pressure patterns.

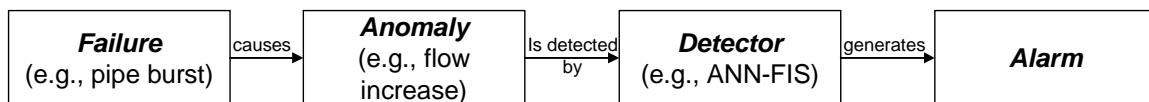


Figure 3.2 A conceptual diagram of the alarm generation process

Such an alarm, which carries information about the likely timing of a burst, its size and ID of the DMA where it occurred (without providing information about the exact location of the burst within a DMA) is a starting point for the risk-based pipe burst diagnostics methodology presented in this thesis. It was assumed here that the detected flow anomalies are the result of a single failure (i.e., a pipe burst within a DMA). This assumption might not hold every time and it is possible that multiple pipe bursts could occur within a DMA. Given the typical size of DMAs discussed above (i.e., 1,000 – 5,000 properties) such situations are not very common. Analysis of main pipe repair data of Yorkshire Water in the UK, over a period of eight years, has shown that multiple main pipe repairs were carried out in the same DMA during the same day in 10.2% of cases (i.e., in total there were 55,641 main repairs carried out). This analysis was based on main pipe repair data and not directly on detected burst times and dates. It is possible that main repair records could contain some follow up actions (e.g., another burst occurred as a result of the repair work) and the number of simultaneous bursts that occurred in one DMA during one day might be significantly lower. This, however, does not prevent the simultaneous occurrence of failures in multiple DMAs, which is not uncommon given the size of WDS (e.g., more than 2,100 DMAs in case of Yorkshire Water in the UK). Multiple failures are likely to occur particularly under severe weather conditions (e.g., extended periods of air frost). According to the above mentioned dataset 89.7% of main repairs were carried out in different DMAs during the same day.

A burst detection system monitoring only flow measurements is typically unable to distinguish between a pipe burst and an abnormal demand (e.g., caused by a fire flow, etc.). If the increased demand is not localised (as in the case of a burst) the risk analysis presented here could provide incorrect results since both, the likelihood component of risk (i.e., the likely location of a burst pipe) as well as the impact component would be based on an erroneous assumption.

Following the above assumptions a one-level (i.e., only one failure at a time) fault tree analysis (Vesely *et al.* 1981) of every detected anomaly (i.e., an alarm) is performed as suggested in Figure 3.3. The outcome of the analysis is a set of potential incidents, which typically comprises every pipe segment in the affected DMA. Additional types of failures, such as pump or valve failures could be included in the analysis as well. The focus of this thesis is an investigation of pipe bursts only and other failure types will not be discussed here.

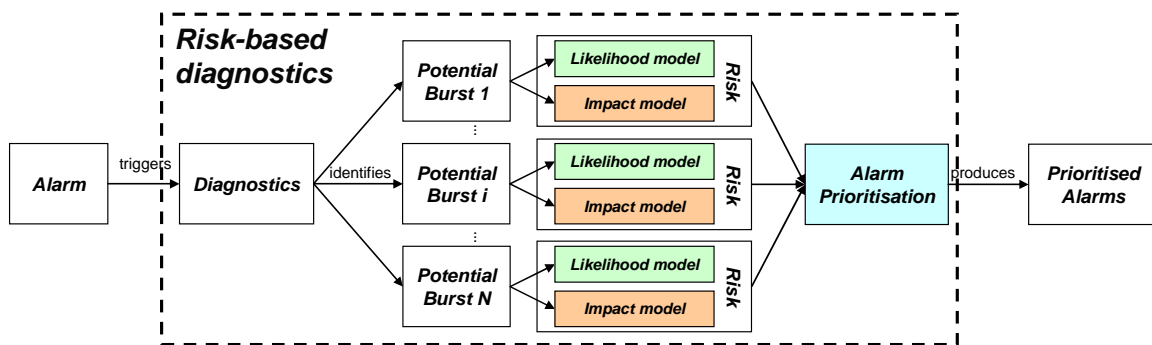


Figure 3.3 A high level overview of the risk-based diagnostics methodology

The diagram in Figure 3.3 provides an overview of the risk-based pipe burst diagnostics methodology. Moreover, it also highlights the key components of the whole methodology (using different colours). These are mainly the models to estimate the likely location of a burst pipe and its impact as well as the alarm prioritisation model, which ranks alarms in the order of their significance based on the overall level of risk they represent.

Each potential incident identified during the preliminary diagnostics phase can be characterised with a certain level of risk as indicated in Figure 3.3. The definition of risk used in this work was adopted from Lowrance (1976), as a measure of likelihood and impact of adverse effects. The risk metric can thus be defined as $R=f(L,I)$ where R

stands for the risk, L represents the likelihood of burst occurrence and I represents its impact. The above adopted definition implies that risk of potential incidents is not aggregated before it is presented to a Decision Maker (DM).

Presenting the risk to a DM in a non-aggregated form using risk maps (see, e.g., Figure 3.4) brings a number of advantages. First of all the spatial distribution of risk can be fully revealed. Because risk was not aggregated, no assumptions about the DM's preferences between impact and likelihood were made. Risk-based pipe burst diagnostics thus leads towards better informed decisions compared to the state of the art methods, based primarily on ad-hoc investigations and experience of WDS operators.

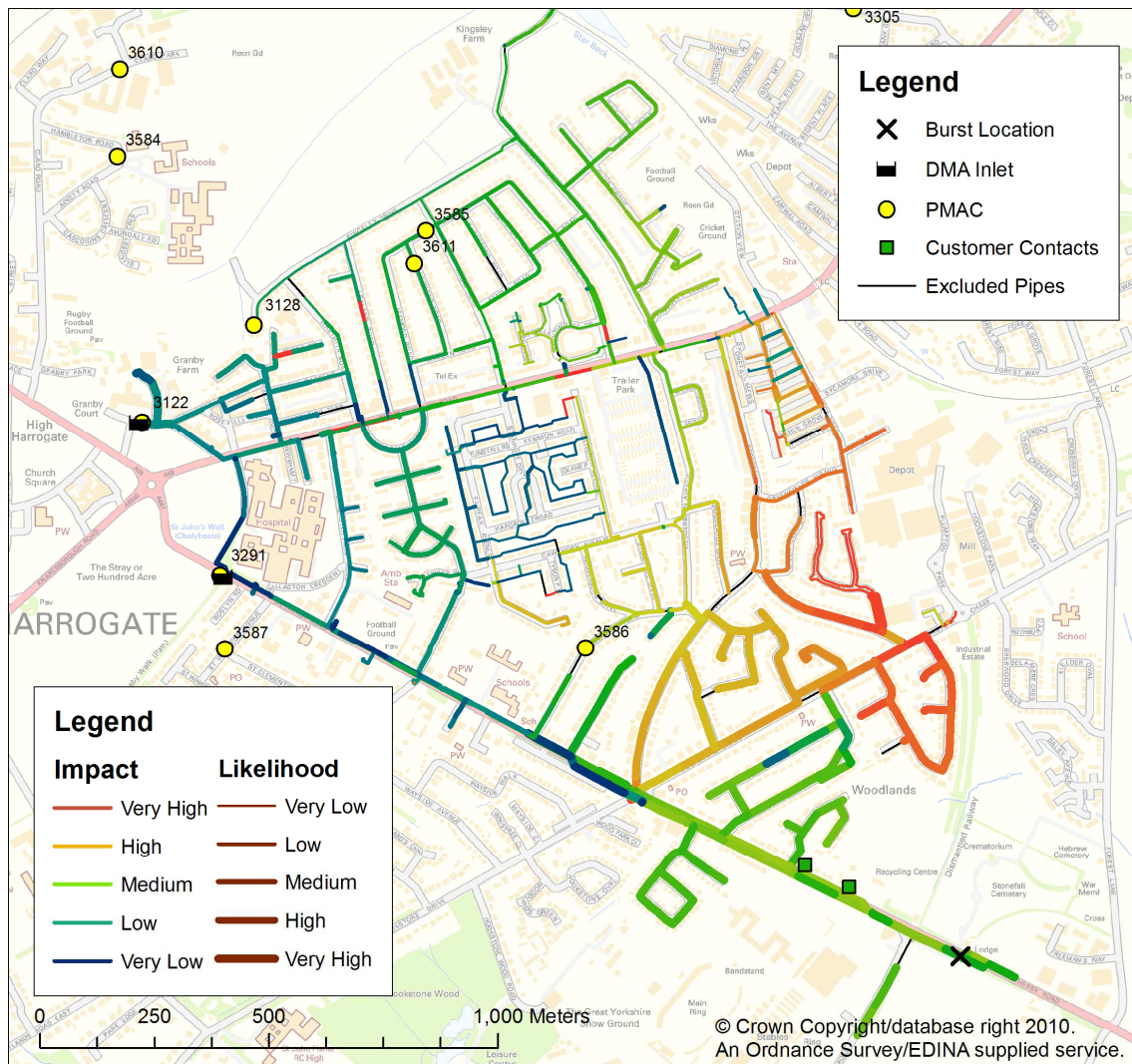


Figure 3.4 An example risk map of a real pipe burst

One of the advantages of the use of risk maps is that they allow an easy identification of important potential incidents, requiring the attention of a DM. Such potential incidents have typically low likelihood of occurrence, but on the other hand, very high impact in comparison to other cases. If the likelihood and impact components of risk are aggregated prior to the visualisation it is impossible to immediately differentiate between potential incidents with high impact and low likelihood of occurrence and their counterparts having low impact and high likelihood of occurrence.

During the risk-based diagnostics all elements within the set of potential incidents (see Figure 3.3) undergo a full risk assessment. The real incident (i.e., cause) which triggered the alarm and the consequent diagnostics should (ideally) be a member of this set and have a higher likelihood of occurrence than other potential incidents. To visualise the risks of individual potential incidents, the risk maps can be also rendered in the form of scatter plots (see e.g., Figure 3.5). The scatter plot displaying the non-aggregated risk of potential incidents (i.e., likelihood and impact) provides a more intuitive means to compare overall risk of alarms in order to distinguish their mutual significance. This will be investigated further in section 3.5, where an alarm ranking methodology is presented.

The likelihood of occurrence will probably be the primary criteria to drive the field investigations. The operator, however, may also choose to investigate pipe bursts with lower likelihood but higher impact. This could be the case in situations when the impact of a burst in elevated parts of a DMA would cause low pressures, ultimately leading to a full interruption of water supply. Even if the likelihood of pipe burst occurrence in such parts of the system was lower, the risk might still be unacceptable for the water utility. To clearly identify such pipes (i.e., low likelihood of occurrence and high impact), it is vital that the risk of each potential pipe burst is presented in a non-aggregated form. The key advantage of the proposed approach is that the DM can make a risk-aware decision when it is possible to consider the trade-off between the likelihood of burst occurrence and the impact of the failure at a given location.

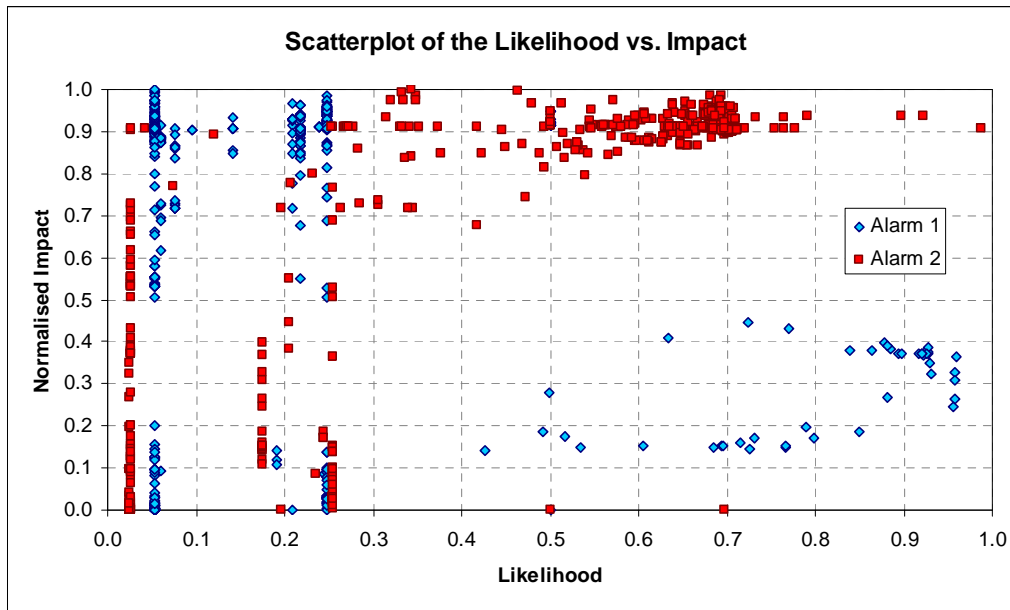


Figure 3.5 A scatter plot showing distribution of risk of two alarms

In most applications of strategic risk analysis, the risk of a failure can be managed by reducing the probability of its occurrence or mitigating its consequences. In the context of operational risk analysis presented here, the likelihood component of risk does not refer to the traditional understanding of probability as the frequency of occurrence of a failure (e.g., return period of a flood, etc.) but instead suggests the fact that the occurrence of a failure on one element is more likely than on another. Unlike in strategic applications, the likelihood component of risk, therefore, cannot be reduced by the replacement or rehabilitation of assets in the short term operational horizon, since the failure has already occurred and only its exact nature is unknown. Moreover, the risk metric considered here can be dynamic and evolve with time, depending on new evidence available (e.g., field measurements or investigations). On the other hand the consequence component of risk of a failure could be reduced by a fast intervention (e.g., temporary valve manipulation). The possible ways to mitigate the impact, however, fall beyond the scope of this thesis and will not be discussed here.

Following the general description of the risk-based decision-making approach individual models to quantify the likelihood and impact components of risk are described in the next two sections.

3.3 Likelihood Component of Risk

As discussed in the literature review in section 2.4, locating a burst within an affected DMA using data and model-based methods is a challenging task. A number of emerging methodologies are available (e.g., Misiunas *et al.* 2006; Wu *et al.* 2010), however, none of them seems to be entirely fit for the purpose of a near R-T pipe burst diagnostics required in this work. In situations of great importance, one frequently seeks an opinion of others before making a final judgement. Consulting a number of experts in order to reach a better informed decision seems to be natural in decision-making by humans. However, similar approaches have only recently started to be applied in automated decision-making (Polikar 2006). Given the severe time constraints, highly uncertain environment and limited availability of measurements in the field, it is argued here that such conditions can benefit from utilising information fusion (Nilsson and Ziemke 2007) to combine available evidence from multiple sources providing an indication of the likely/unlikely location of a burst pipe.

A methodology for combining outputs of several models, including a Pipe Burst Prediction Model (PBPM), a Hydraulic Model (HM) and a Customer Contacts Model (CCM) is proposed here to improve the potential for reliable and rapid identification of the possible location of a pipe burst. This is essential to water companies, reflecting a proactive approach that attempts to detect and fix failures in a WDS before they start affecting customers. Proactive response to failures (i.e., their detection, location and repair) is not always possible (e.g., due to the time required to receive and process data from the field or dispatch a leakage team) and in some situations the water utility can only react after a problem is first reported by customers.

In the proposed methodology, information provided by individual models is fused together, using D-S theory of Evidence (Shafer 1976). The combined output, which encapsulates the varying credibility of the individual models, provides spatial distribution of *Belief* and *Plausibility* (see e.g., Figure 3.6) of failure of any pipe in the WDS being studied to support the decision-making process by an operator in a control room. This evidential reasoning approach further reduces the information load faced by operators and increases confidence in the results that are supported by several models.



Figure 3.6 An example of spatial distribution of Belief and Plausibility

The rest of this section is organised as follows. First the theoretical concepts of D-S theory necessary to understand the information fusion process proposed here are introduced. Then the individual information sources (i.e., models) whose outputs are combined are described. Finally, the process of information fusion, including a novel calibration methodology based on multi-objective optimisation, are explained.

3.3.1 Dempster-Shafer Theory of Evidence

This sub-section provides a brief introduction to the underlying mathematical Theory of Evidence applied here to combine outputs from multiple information sources. The reader is referred to Appendix A of this thesis for a more detailed explanation.

The D-S theory, also known as Evidence Theory, was first formulated in the late 1970's by Dempster (1967) and later on extended and formalised by Shafer (1976). D-S theory can be used for inference in the presence of incomplete and uncertain information, provided by different, independent, sources. A significant advantage of D-S theory is its ability to deal with missing information (i.e., epistemic uncertainty) and to estimate the imprecision and conflict between different information sources.

The D-S theory operates on a “frame of discernment” Θ , which is a finite set of mutually exclusive and exhaustive propositions. Unlike traditional Bayesian models (Bayes 1763), probability mass can be assigned to subsets of the frame of discernment Θ using a Basic Probability Assignment (BPA), typically denoted $m(A)$, where A is a

non-empty subset of Θ . D-S theory defines two fundamental functions: *Belief* (Bel) and *Plausibility* (Pl):

$$Bel : 2^\Theta \rightarrow [0,1] \quad \text{and} \quad Bel(A) = \sum_{B \subseteq A} m(B) \quad (3.1)$$

$$Pl : 2^\Theta \rightarrow [0,1] \quad \text{and} \quad Pl(A) = \sum_{B \cap A \neq \emptyset} m(B) \quad (3.2)$$

Where: B is a non-empty subset of Θ .

Bel corresponds to the total mass of evidence, which supports a proposition and all of its subsets, whereas Pl corresponds to the total mass of evidence, which is not in contradiction with a proposition (Shafer 1976). The mutual relationship between Bel and Pl is shown in Figure 3.7.

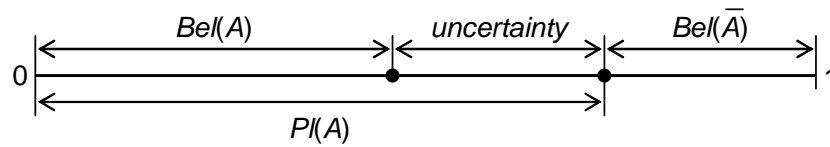


Figure 3.7 A graphical representation of Belief and Plausibility

In this study, a Binary Frame of Discernment (BFOD) Θ (Safranek *et al.* 1990), is used, comprising two propositions (“*Burst*” and “*NoBurst*”) representing the likelihood of occurrence / non-occurrence of a burst in a particular pipe. The power set 2^Θ is thus formed by the following subsets: (\emptyset , $\{Burst\}$, $\{NoBurst\}$, $\{Burst, NoBurst\}$), where the subset $\{Burst, NoBurst\}$ represents the whole frame of discernment Θ and any probability mass assigned to this subset corresponds to a lack of knowledge (i.e., ignorance). The chosen definition of the BFOD implies that the process of identifying the location of a burst pipe is similar to a classification problem where value of belief is calculated for every pipe in the WDS indicating the likelihood of that pipe being the true (i.e., $\{Burst\}$) or false (i.e., $\{NoBurst\}$) burst location. As suggested by Polikar (2006) combining outputs of several classifiers (i.e., ensemble classifiers) has been shown to be an effective approach, to obtain better and more reliable classification results, in a number of real-world problems. Other representations of the frame of discernment Θ are possible (e.g., containing multiple hypotheses), however, these are likely to have negative effect on computational complexity of algorithms implementing the D-S theory (see Appendix A.4 for more details).

Dempster's rule of combination (Shafer 1976) forms an inherent part of D-S theory, which allows information from different, independent sources of evidence to be combined. It is defined as follows:

$$m_{1,2}(A) = \frac{\sum_{B \cap C = A} m_1(B)m_2(C)}{1 - K} \text{ when } A \neq \emptyset \quad (3.3)$$

$$K = \sum_{B \cap C = \emptyset} m_1(B)m_2(C) \quad (3.4)$$

$$m_{1,2}(\emptyset) = 0 \quad (3.5)$$

Where: $m_{1,2}$ is the combined BPA, m_1 , m_2 are the BPAs of independent sources of evidence, K represents the level of conflict amongst the evidence and A , B and C are non-empty subsets of Θ .

Since the introduction of Dempster's rule various other combination rules have been developed. Sentz and Ferson (2002) discussed foundations of D-S theory and provided a review of a number of the available combination rules available. As argued by many (Hall and Garga 1999; Polikar 2006) there is no universal combination rule that would perform well in all situations. In this work, Yager's combination rule (Yager 1987) and the PCR5 combination rule (Smarandache and Dezert 2006) were used, in addition to Dempster's rule, to observe their different behaviour and performance in the process of information fusion. These rules differ in the way they distribute conflicting probability mass K (Eq. (3.4)) amongst the propositions of Θ . Dempster's rule distributes the conflicting mass equally amongst all propositions of Θ (e.g., $\{A\}$ and $\{B\}$), while Yager's rule (see Eq. (A.13)) attributes conflicting mass to Θ (e.g., $\{A, B\}$) and the PCR5 rule (see Eq. (A.17)) proportionally redistributes partial conflicting masses amongst propositions involved in the partial conflict. Further details about the additional combination rules, including their definition and a numerical example demonstrating combination of conflicting evidence, can be found in Appendix A.2.

3.3.1.1 Decision-Making Using Belief Structures

Although decision-making using Beliefs and Plausibilities as suggested in Figure 3.6 brings certain advantages, it can be challenging for DMs. On the one hand, a DM has the opportunity to fully explore the evidence directly supporting a particular hypothesis (e.g., that a pipe burst is located in some part of a WDS) represented by Belief and also the evidence, which does not contradict a hypothesis (i.e., Plausibility). On the other

hand, particularly in situations when one operates with complex frames of discernment (i.e., comprising a higher number of hypotheses) the additional complexity of operating with Beliefs and Plausibilities might be overwhelming. To make decisions based on belief functions, Smets & Kennes (1994), proposed a model of transformation, based on the assumption that “*beliefs manifest themselves at two mental levels: the ‘credal’ level where beliefs are entertained and the ‘pignistic’ level where beliefs are used to make decisions*”. Based on the principle of insufficient reason, Smets & Kennes (1994) defined the pignistic probability function $BetP$, which performs the transformation from the credal level, as follows:

$$BetP(B) = \sum_{A \in 2^{\Theta}} m(A) \frac{|B \cap A|}{|A|} \quad (3.6)$$

The pignistic probability function ($BetP$) is a measure that can be used to present the outputs of the information fusion process to DMs and will be later utilised in calibration of the D-S model (section 3.3.5) and performance evaluation of the information fusion methodology (section 5.3.3.2).

On a simple BFOD used in this work, the pignistic probability function reduces to:

$$BetP(\{Burst\}) = m(\{Burst\}) + \frac{1}{2} m(\{Burst, NoBurst\}) \quad (3.7)$$

This effectively distributes the uncertainty, represented by the probability mass $m(\{Burst, NoBurst\})$, equally between the $\{Burst\}$ and $\{NoBurst\}$ hypotheses.

3.3.2 Information Sources

Due to the flexibility of D-S theory, any kind of information providing an indication of the likelihood of a burst in a particular pipe in a WDS can be combined to reduce the lack of knowledge about the location of the failed pipe and increase the confidence in its correct identification. Without any loss of generality this research utilises three information sources depicted in Figure 3.8 that are considered to be independent: (a) a PBPM output, (b) a CCM output and (c) an HM output. This particular set of information sources was chosen because of its general availability to many water utilities worldwide and does not prevent other information sources from being used (e.g., information from a work management system or perhaps transient-based burst location models). The first source of information (i.e., based on the PBPM output) is

treated as a static indicator of pipe burst occurrence whereas the other two remaining sources can be dynamic and provide new information as it becomes available (e.g., when another customer complaint is received or when the HM is updated with new R-T measurements obtained from field sensors).

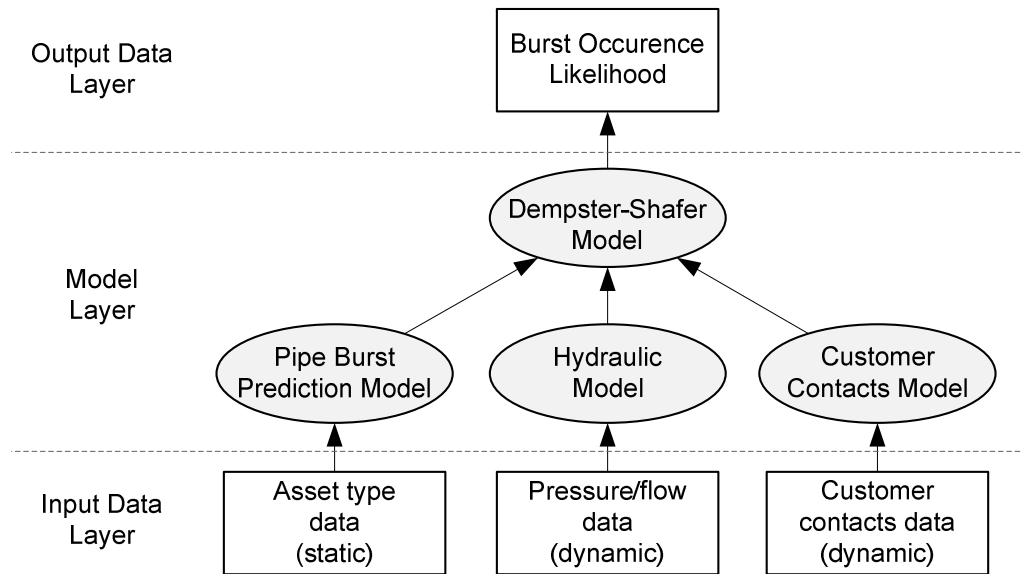


Figure 3.8 Sources of evidence used in the information fusion

The focus of this thesis is not on the development of the individual models but instead to demonstrate that by combining their outputs, certain benefits can be gained as illustrated later on a case study (section 5.2.3.1). Some of the models (e.g., the PBPM) have been extensively studied in the literature and will not be discussed here in detail.

3.3.2.1 Pipe Burst Prediction Model

A PBPM is used to obtain expected burst frequencies for every pipe in the WDS. The particular choice of the PBPM depends on the availability of data and is not important for the methodology shown here as long as the independence of the model outputs used in the information fusion holds (Bai *et al.* 2008; Marashi *et al.* 2008).

More specifically, a regression-based PBPM was used here to obtain expected burst frequencies for every pipe in the WDS being studied during the current month. The burst frequency of a pipe was expressed as a function of its material, diameter, age, soil type, land use, and weather conditions. The specific expression and the related coefficients used in this work can be found in Tynemarch Systems Engineering Ltd. (2007) and will not be reported here as it falls outside the scope of this thesis.

3.3.2.2 Customer Contacts Model

The current methods of detection and location of pipe bursts aim to notify control room personnel of any abnormal conditions before a failure starts affecting customers. However, frequently, large pipe bursts are first reported by customers (i.e., when leaked water emerges on the surface). In situations where no explicit pipe burst detection mechanisms are in place, customers reporting locations of bursts are the only means of (reactive) response to control leakage. Despite being a very strong indicator of a burst location, Customer Contacts (CC) are imperfect and cannot be entirely trusted. A CCM was developed under the assumption that a burst pipe is located in the proximity of the location reported by a customer. The coordinates of the geocoded location of a burst (i.e., easting and northing) provided by a customer were used in this work. Furthermore, the CCM used a weighted distance to reduce the influence of misleading CCs (i.e., outliers) in situations when multiple CCs were received. The fact of whether a CC is genuine and originated from the proximity of a burst can only be verified retrospectively. Analysis of CC data of a large number of DMAs confirmed the existence of misleading contacts. The mathematical formulation of the model is as follows:

$$CCM_i = \min_j (\text{dist}(i, CC_j) \times w_j) \quad (3.8)$$

$$w_j = \frac{\text{dist}(CC_j, C)}{\sum_{k=1}^{N_{CC}} \text{dist}(CC_k, C)} \quad (3.9)$$

where: i is the index of a pipe, dist is the shortest Euclidean distance between the customer location and the pipe, CC_j is a customer contact j , w_j corresponds to a relative distance and is a weight reflecting the significance of a particular CC (i.e., the lower the value of w_j the more significant a given customer contact is), N_{CC} is the total number of CCs associated with a particular pipe burst and C is the centroid of all CCs related to the pipe burst.

The CCM is illustrated in Figure 3.9, which depicts an example of three CCs associated with a pipe burst. Two CCs (i.e., CC_1 and CC_3) form a cluster and the customer contact no. 2 (i.e., CC_2) was incorrectly assigned to this particular pipe burst or was misleading.

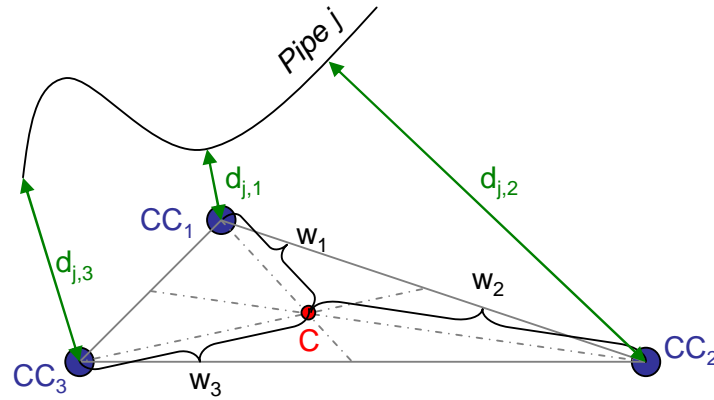


Figure 3.9 Weighed distance from customer contacts to a pipe

The CC_1 and CC_3 , therefore, receive lower values of w_1 and w_3 compared to w_2 received by CC_2 and so will be treated as more important.

3.3.2.3 Hydraulic Model

A HM was used to locate a burst in a WDS by simulating its effects (i.e., an increase in flow and drops of pressure) and compare them with values obtained from pressure and flow sensors deployed in the field. An estimated magnitude of the burst flow is first provided by an early warning pipe burst detection system able to discover abnormally high inflows into a DMA (e.g., Mounce and Machell 2006; Romano *et al.* 2009). An extra demand, equal to the estimated burst flow, is then added to the centre of every pipe to model the effects of a burst in that location. The pressure boundary conditions of the HM are set according to the data obtained from inlet pressure sensors at the time when the burst was first detected. The customer demands are proportionally scaled so that they add up to the measured inflow into the DMA obtained from the DMA inlet flow meters data and all measured exports (i.e., $Customer\ Demands = DMA\ inflow - exports - burst\ flow$). The likelihood of any pipe bursting in the system is then indicated by a Sum of Squared Errors (SSE) between observed and modelled pressures calculated as follows:

$$HM_i = \sum_{s=1}^{N_s} \sum_{t=1}^T (P_{1,s}(t) - P_{2,s}(t))^2 \quad (3.10)$$

where: i is an index of the burst pipe in the HM, s is an index of a node where a pressure sensor is located, N_s is the total number of pressure sensors in the network, T is the

number of pressure measurements available (i.e., different times), $P_{1,s}(t)$ is the modelled pressure at time t at node s and $P_{2,s}(t)$ is the measured pressure at time t at node s .

Flow measurements inside a DMA have not been utilised since these are not typically available in real life systems (at least not in the UK) due to the higher cost of flow meters in comparison to pressure sensors. Multi-inlet DMAs could also be easily exploited since depending on the location of the burst different amounts of water would be drawn from each of the DMA inlets.

Only one set of pressure measurements taken at the time of burst detection was used here to allow for fast identification of the location of the burst. Clearly a trade-off exists between the response time and quality of the location. The method could be further improved to better utilise multiple measurements over time, e.g., by modelling the burst as pressure sensitive outflow using an emitter (Pudar and Liggett 1992; Wu *et al.* 2010).

A pressure driven modification of EPANET (Morley and Tricarico 2008) was used here instead of a conventional demand driven hydraulic solver to obtain more realistic results. The burst flow added to the network at the time of its detection was considered to be pressure insensitive, unlike the nodal demands, which could be reduced when pressures in the system dropped below 15 m of head. The assumption of pressure insensitive burst flow in this situation can be justified since the amount of water escaping from the WDS was estimated by an ANN. The estimated burst flow, however, represents an average outflow over a given time window, which could be seen as a limitation to the adopted approach. Better results could be achieved if the ANN was able to provide estimated flow for every time step from the burst detection time.

3.3.3 Information Fusion

This section describes the information fusion process, which forms the core of the newly proposed D-S Model. Each of the information sources described above provides a single output (i.e., criterion measurement) for each potential incident associated with an alarm, reflecting the likelihood (i.e., a normalised value of the criterion measurement) of occurrence of a burst in that pipe. The criterion measurement is the expected burst frequency, weighted distance from a CC or SSE for the PBPM, CCM and HM, respectively. The individual information sources used are not considered to be fully reliable and each may be associated with a different level of credibility (i.e.,

trustworthiness of the model, which is reflected through its mapping curves). In order to improve the combined confidence in the location of a burst pipe, the information from all available sources is fused using the D-S theory by applying a suitable combination rule (i.e., Eq. (3.3), Eq. (A.13) or Eq. (A.17)).

Before the outputs of individual models can be combined, the criterion measurements (i.e., model outputs) need to be transformed into BPAs, each representing the exact belief in the given proposition (i.e., $m(\{Burst\})$, $m(\{NoBurst\})$) as well as the degree of ignorance (i.e., $m(\{Burst, NoBurst\})$). For this purpose a two-step procedure has been adapted from Beynon (2005). The criterion measurement values are first converted to confidence factors using a suitable normalisation function and then transformed into BPAs as shown in Figure 3.10.

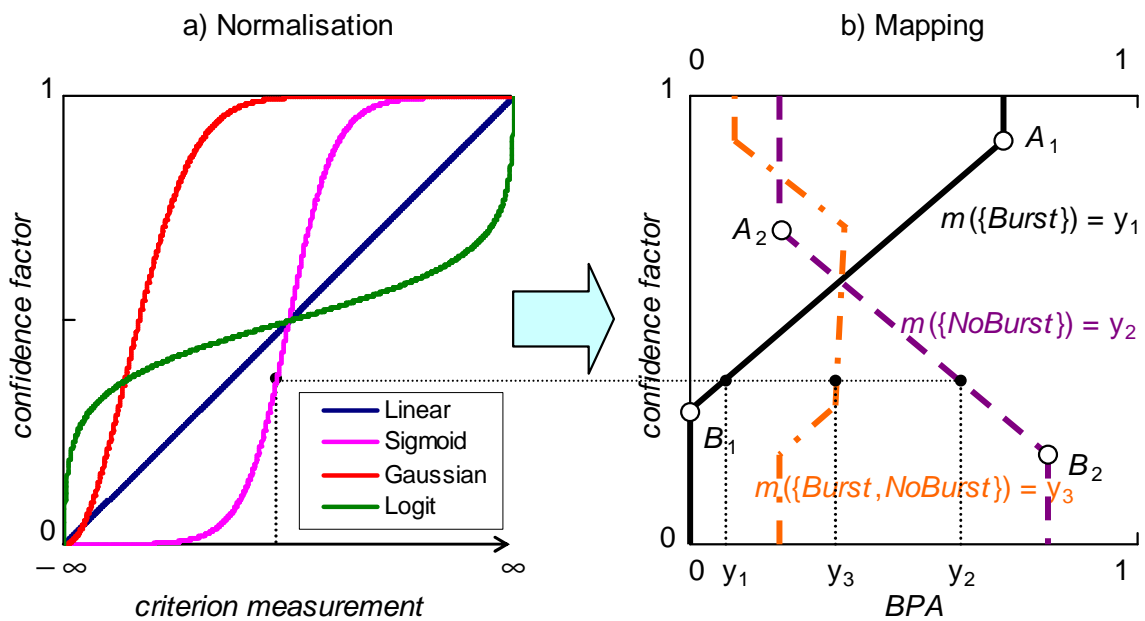


Figure 3.10 Transformation of measurement criteria into BPAs based on Beynon (2005)

Beynon (2005) used a sigmoid normalisation function to transform criterion measurements into confidence factors that were mapped to corresponding BPAs. In accordance to Safranek *et al.* (1990), Beynon (2005) applied simple symmetric functions defined by two parameters A and B to map confidence factors to BPAs. On the other hand, Sadiq *et al.* (2006) used trapezoids, typical for fuzzy sets, to obtain BPAs directly from criterion measurements. In this work, however, the type of normalisation functions (i.e., linear, sigmoid, one-sided Gaussian and logit function) as well as the

shape of the mapping functions (defined by 8 parameters, i.e., 4 points A_1 , B_1 , A_2 and B_2 as shown in Figure 3.10) were determined for each of the input models based on its performance (i.e., credibility) on a number of historical cases during calibration. The mapping function describing $m(\{Burst\})$ is a non-decreasing function whereas the function describing $m(\{NoBurst\})$ is a non-increasing function. Once the evidence for every pipe in the network is transformed to BPAs the individual pieces can be combined using a combination rule (e.g., Eq. (3.3)). The actual rule used (i.e., Dempster's rule, Yager's rule or the PCR5 rule) was determined as part of a calibration procedure (described in section 3.3.5) so that the ensemble of the combination rule, the normalisation and mapping functions gained the maximum benefit according to calibration objectives described in section 3.3.5.

The information fusion procedure described above can be summarised in the following steps:

1. Run each of the considered input models (e.g., PBPM, CCM and HM) to **obtain criterion measurement** of every potential incident.
2. Based on the range of criterion measurements of a particular model obtained for every potential incident, **perform normalisation** (using appropriate normalisation function) as shown in Figure 3.10 to obtain value of confidence factor.
3. For every potential incident compute its BPAs (i.e., $m(\{Burst\})$, $m(\{NoBurst\})$ and $m(\{Burst, NoBurst\})$) based on the value of its confidence factor by **applying mapping functions** corresponding to a particular model as suggested in Figure 3.10.
4. Once BPAs for every potential incident and every considered input model (i.e., source of evidence) are obtained, **apply a suitable combination rule** (e.g., Eq. (3.3)) to obtain the combined BPAs, representing the level of Belief and Plausibility as well as BetP of every potential incident as being or not being the True Burst Location (TBL).

A data flow diagram of the information fusion methodology, described in the four steps above, is given in Figure 3.11.

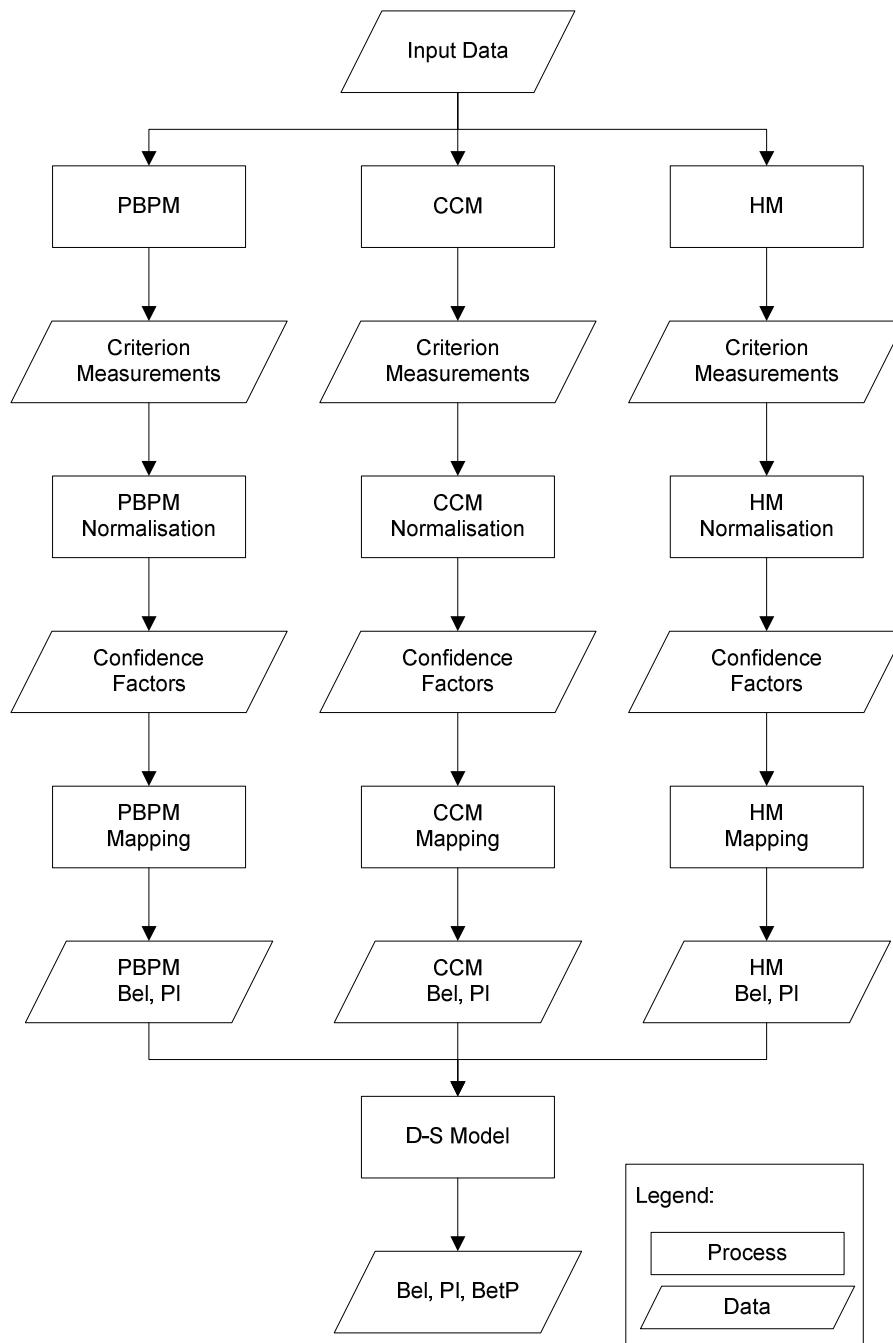


Figure 3.11 A data flow diagram of the information fusion process

3.3.3.1 Information Fusion Example

To illustrate the actual process of information fusion as described above a simplified example of one potential incident (i.e., pipe segment ID “0EJ9LL9L”) and 2 sources of evidence (i.e., the PBPM and HM only) is presented here.

1. PBMP and HM are run for every considered potential incident in a DMA and for the selected potential incident (“0EJ9LL9L”) return the following result:

$$\begin{aligned} \text{CriterionMeasurement}_{\text{PBPM}}(\text{“0EJ9LL9L”}) &= 481 \text{ bursts/1000 km/year (burst rate)} \\ \text{CriterionMeasurement}_{\text{HM}}(\text{“0EJ9LL9L”}) &= 5.42 \text{ m}^2 \text{ (SSE)} \end{aligned}$$

2. Confidence factor is then obtained after normalising Criterion Measurement of every considered model using a suitable normalisation function (i.e., sigmoid function for PBPM and logit function for HM):

$$\begin{aligned} \text{ConfidenceFactor}_{\text{PBPM}}(\text{“0EJ9LL9L”}) &= 0.998 \\ \text{ConfidenceFactor}_{\text{HM}}(\text{“0EJ9LL9L”}) &= 0.635 \end{aligned}$$

3. From the value of confidence factor the BPAs are obtained using mapping functions corresponding to each of the considered models (see, e.g., Figure 3.12). The actual mapping curves used in the case of the PBPM can be found in Figure 5.13.

$$\begin{aligned} m_{\text{PBPM}}(\{Burst\}) &= 0.357 \\ m_{\text{PBPM}}(\{NoBurst\}) &= 0.014 \\ m_{\text{PBPM}}(\{Burst\}, \{NoBurst\}) &= 0.629 \end{aligned}$$

According to Eqs. (3.1), (3.2) and (3.6) the *Bel*, *Pl* and *BetP* structures can be calculated:

$$\begin{aligned} Bel_{\text{PBPM}}(\{Burst\}) &= m_{\text{PBPM}}(\{Burst\}) = 0.357 \\ Pl_{\text{PBPM}}(\{Burst\}) &= m_{\text{PBPM}}(\{Burst\}) + m_{\text{PBPM}}(\{Burst\}, \{NoBurst\}) = 0.357 + \\ &0.629 = 1 - 0.014 = 0.986 \\ BetP_{\text{PBPM}}(\{Burst\}) &= [Pl_{\text{PBPM}}(\{Burst\}) + Bel_{\text{PBPM}}(\{Burst\})] / 2 = [0.986 + 0.357] \\ &/ 2 = 0.672 \end{aligned}$$

The actual mapping curves used in the case of the HM can be found in Figure 5.14.

$$\begin{aligned} m_{\text{HM}}(\{Burst\}) &= 0.000 \\ m_{\text{HM}}(\{NoBurst\}) &= 0.130 \\ m_{\text{HM}}(\{Burst\}, \{NoBurst\}) &= 0.870 \end{aligned}$$

According to Eqs. (3.1), (3.2) and (3.6) the *Bel*, *Pl* and *BetP* structures can be calculated:

$$\begin{aligned} Bel_{\text{HM}}(\{Burst\}) &= 0.000 \\ Pl_{\text{HM}}(\{Burst\}) &= 0.000 + 0.870 = 1 - 0.130 = 0.870 \\ BetP_{\text{HM}}(\{Burst\}) &= [Pl_{\text{HM}}(\{Burst\}) + Bel_{\text{HM}}(\{Burst\})] / 2 = 0.435 \end{aligned}$$

Steps 1-3 are graphically illustrated in Figure 3.10

4. Once the BPAs are obtained Dempster's combination rule Eqs. (3.3)-(3.5) can be applied:

$$K = m_{\text{PBPM}}(\{Burst\}) \times m_{\text{HM}}(\{NoBurst\}) + m_{\text{HM}}(\{Burst\}) \times m_{\text{PBPM}}(\{NoBurst\}) = 0.357 \times 0.130 + 0.000 \times 0.014 = 0.046$$

$$m_{\text{PBPM,HM}}(\{Burst\}) = [m_{\text{HM}}(\{Burst\}) \times m_{\text{PBPM}}(\{Burst\}) + m_{\text{HM}}(\{Burst\}) \times m_{\text{PBPM}}(\{Burst\}, \{NoBurst\}) + m_{\text{PBPM}}(\{Burst\}) \times m_{\text{HM}}(\{Burst\}, \{NoBurst\})] / (1 - K) = [0.000 \times 0.014 + 0.000 \times 0.629 + 0.357 \times 0.870] / [1 - 0.046] = 0.326$$

$$m_{\text{PBPM,HM}}(\{NoBurst\}) = [m_{\text{HM}}(\{NoBurst\}) \times m_{\text{PBPM}}(\{NoBurst\}) + m_{\text{HM}}(\{NoBurst\}) \times m_{\text{PBPM}}(\{Burst\}, \{NoBurst\}) + m_{\text{PBPM}}(\{NoBurst\}) \times m_{\text{HM}}(\{Burst\}, \{NoBurst\})] / (1 - K) = [0.130 \times 0.014 + 0.130 \times 0.629 + 0.014 \times 0.870] / [1 - 0.046] = 0.1$$

$$m_{\text{PBPM,HM}}(\{Burst\}, \{NoBurst\}) = 1 - m_{\text{PBPM,HM}}(\{Burst\}) - m_{\text{PBPM,HM}}(\{NoBurst\}) = 0.574$$

The corresponding belief structures *Bel*, *Pl* and *BetP* could then be easily calculated using Eqs. (3.1), (3.2) and (3.6), respectively. Given the associativity of Dempster's rule the combined results obtained above could be again combined with evidence from the CCM. If other combination rules (e.g., Yager's or PCR5 rules) were applied, their quasi-associative versions would have to be used since the fusion results should be independent of the order in which evidence is combined.

3.3.4 Independence Assumption

One of the conditions of using the Dempster's combination rule (as well as the other combination rules introduced here), applied in this work, is that the evidence coming from different sources is independent (Dempster 1967). Marashi *et al.* (2008) explained the concept of independence as “*a situation when the knowledge of the particular value taken by a piece of evidence does not change our belief about the value that the second could take*”. They further noted that the assumption of independence may suit domains such as sensor information fusion but is less realistic in the case of human subjective judgements. Bi *et al.* (2008) discussed the independence of outputs of ensemble classifiers and concluded that the assumption of their independence was sensible.

In this work, the evidence considered comes from three different models (i.e., PBPM, HM and the CCM), which accept different inputs and employ completely different methodologies. For example, the PBPM is based on the physical properties of the assets, the HM solves a series of continuity and energy equations to calculate pressures and flows in a WDS and the CCM calculates distances from CCs. The assumption of their independence is hence seen as realistic. However, if subjective human judgements also need to be considered as evidence (e.g., operator's judgement), different families of combination rules may need to be adopted (Marashi *et al.* 2008).

3.3.5 Dempster-Shafer Model Calibration

The D-S model, like any other model, needs to be calibrated before it can be used. As suggested before, the credibility of the input models used in the information fusion process can vary significantly. The calibration procedure explicitly incorporates the varying credibility of the input models across their entire output range (i.e., the range of criterion measurements). The D-S theory is equipped with a mechanism to discount evidence (see Appendix A.3), to reflect the credibility of a particular information source and avoid situations of absolute conflict between two information sources. Discounting was not used in this work and the credibility of a particular information source was instead indirectly reflected through its mapping curves (see e.g., Figure 3.12).

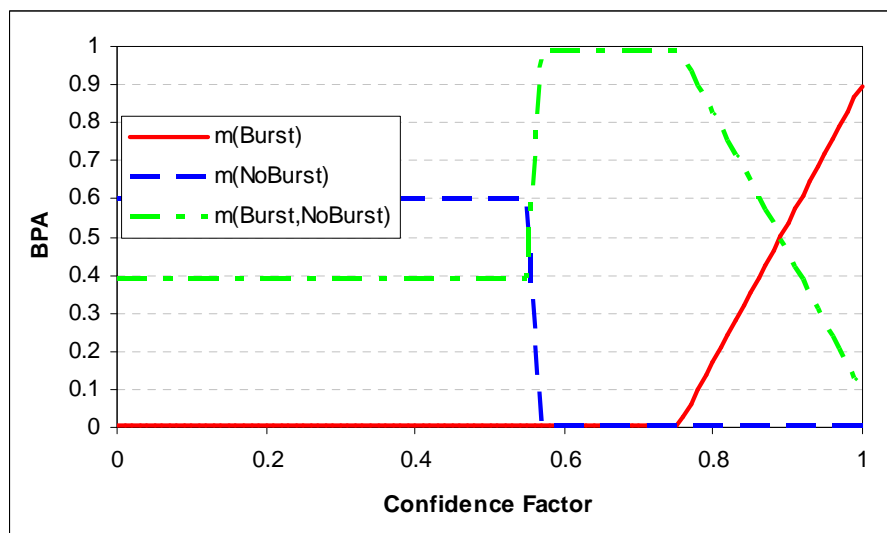


Figure 3.12 An example of a mapping curve

The maximum value of probability mass that can be attributed either to the $\{Burst\}$ or $\{NoBurst\}$ hypothesis using a mapping curve reflects the credibility of a particular

information source. The higher the probability mass attributed to either the $\{Burst\}$ or the $\{NoBurst\}$ hypothesis, the more trustworthy a particular source of evidence is and the better is its capability to determine if a particular potential incident is the cause of the observed anomaly. On the other hand the higher the probability mass attributed to the $\{Burst, NoBurst\}$ hypothesis the less specific and credible the given information source is.

The calibration aims to determine the optimal values of the parameters defining the mapping functions (i.e., their coordinates) as well as to select the optimal normalisation function and the most suitable combination rule. Historical cases, where the TBL of an alarm was known were used to find the optimal set of parameter values that yield maximum benefit during the information fusion process in terms of identifying the true cause of a failure (using the three individual models). The calibration problem was formulated as a multi-objective optimisation problem as follows: Find vector $\mathbf{z}^* = [z_1^*, z_2^*, \dots, z_n^*]$ such that:

$$f(\mathbf{z}^*) = \min f(\mathbf{z}) = \min[f_1(\mathbf{z}), f_2(\mathbf{z}), \dots, f_n(\mathbf{z})] \quad (3.11)$$

Without any loss of generality only minimisation is assumed here, however, any maximisation problem can be easily re-formulated as a minimisation problem.

The structure of the vector \mathbf{z} is given in Table 3.1, which shows all its elements. The meaning of individual components of the vector is described as follows. Three information sources (i.e., the PBPM, the HM and the CCM) were considered here, each requiring two mapping functions (i.e., $m(\{Burst\})$, $m(\{NoBurst\})$) and each of the functions comprising 2 points (i.e., four x and y coordinates). This in total accounted for 24 floating-point variables. The x coordinates were in the range $[0, 1]$, however, the y coordinates were in the range $[0, 0.9]$ (to avoid problems with saturation, when one of the information sources reaches absolute certainty (Safranek *et al.* 1990)). There were also 4 additional integer variables, 3 of them (i.e., N1, N2 and N3) were used to select a normalisation function (i.e., $a \in \{0,1,2,3\}$) for each of the three information sources (models) and the fourth variable (i.e., R) was used to choose the combination rule (i.e., $b \in \{0,1,2\}$). Each of the integer values of parameters a and b corresponded to one type of normalisation function or a combination rule, respectively.

Table 3.1 Structure of a vector of decision variables \mathbf{z}

Mapping curve 1								Mapping curve 2								Mapping curve 3								N1	N2	N3	R
x	y	x	y	x	y	x	y	x	y	x	y	x	y	x	y	x	y	x	y	x	y	x	y	a	a	a	b

Based on Eq. (3.11), a three objective optimisation problem was formulated, minimising functions $f_1(\mathbf{x})$, $f_2(\mathbf{x})$ and $f_3(\mathbf{x})$ defined as follows:

$$f_1(\mathbf{x}) = \sum_{i=1}^N Rank_i(BetP_{TBL_i}(\{Burst\})) \quad (3.12)$$

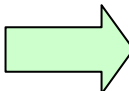
$$f_2(\mathbf{x}) = -\sum_{i=1}^N \sum_{j \in Proximity(TBL_i)} w_j Bel_j(\{Burst\}) \quad (3.13)$$

$$f_3(\mathbf{x}) = -\sum_{i=1}^N \sum_{j \in PI_i \setminus \{TBL_i\}} Pl_j(\{NoBurst\}) \quad (3.14)$$

where:

- N is the number of historical calibration cases,
- TBL_i is the known True Burst Location (i.e., an index of a pipe where the burst was found) of historical case i ,
- $BetP_x(\{Burst\})$ is the pignistic probability (see Eq. (3.6)) that pipe x burst, $Rank_i(BetP_{TBL_i}(\{Burst\}))$ is a function which returns the rank (see Figure 3.13 for illustration) of the TBL within the set of potential incidents associated with case i when sorted in descending order of their value of $BetP(\{Burst\})$,
- $Proximity(TBL_i)$ is a function that returns a set of 10 pipes that are topologically nearest to the TBL of case i . The topological distance is determined by tracing the network, w_j is a weighting factor proportional to the distance of a pipe from the TBL (i.e., the closer a pipe from the TBL, the higher the weight),
- $Pl_j(\{NoBurst\})$ is the Plausibility (see Eq. (3.2)) that pipe j did not burst, and
- $Bel_j(\{Burst\})$ is the Belief (see Eq. (3.1)) that pipe j is the burst location. PI_i is a set of potential incidents (i.e., possible burst locations) associated with historical case i .

Link Id	BetP
0004G38E	0.962
0004G370	0.945
0004G2MM	0.986
0EIII5H	0.826
0EJ9KAGM	0.869
0004E1IL	0.909
0004G2F0	0.820



Link Id	BetP	Rank
0004G2MM	0.986	0
0004G38E	0.962	1
0004G370	0.945	2
0004E1IL	0.909	3
0EJ9KAGM	0.869	4
0EIII5H	0.826	5
0004G2F0	0.820	6

Figure 3.13 An example of the Rank of the TBL (Link Id 0004G2MM)

Note that the minus sign in Eq. (3.13) and Eq. (3.14) effectively changes the minimisation problem into a maximisation problem. The optimisation produces a Pareto-front comprising non-dominated (i.e., equally good) solutions. The concept of dominance is graphically illustrated in Figure 3.14 on an example of a two-objective minimisation problem, where the non-dominated solutions are displayed in green.

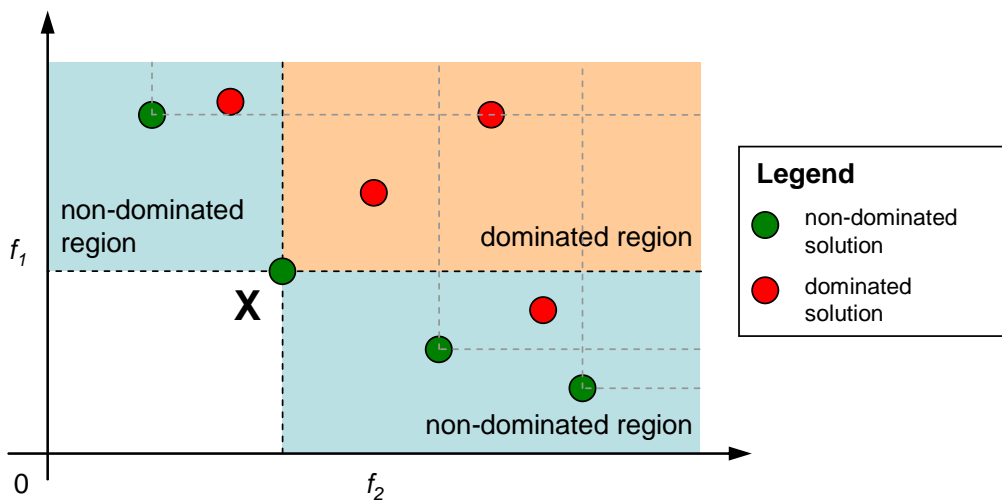


Figure 3.14 An example of a Pareto front

In the case of a two-objective problem, the non-dominated solutions are points on a Pareto curve. In the case of a three-objective problem as defined in this work, the non-dominated solutions are points on a Pareto surface. Clearly, the objective functions presented in Eqs. (3.12), (3.13) and (3.14) are conflicting and the optimisation produces a trade-off surface. A single solution from the trade-off surface then has to be selected based on the DM's preferences. The objective function $f_1(\mathbf{x})$ plays the most significant role in terms of the overall performance of the information fusion. The remaining two objective functions $f_2(\mathbf{x})$ and $f_3(\mathbf{x})$ are equally important and reaching a balance between those two objectives is desirable.

3.4 Impact Component of Risk

As discussed in the literature review impact of various failures (e.g., pipe bursts, segment isolations, pump failures, etc.) in a WDS has been studied by a number of researchers. The adopted approach so far was primarily from a strategic perspective, to support rehabilitation of existing networks, and was not suitable to fully meet the requirements of operational decisions. Furthermore, only in very few cases (e.g., Michaud and Apostolakis 2006; Beuken *et al.* 2008; Vamvakeridou-Lyroudia *et al.* 2009) was the impact model based on a complex metric, comprising a number of KPIs.

This section describes an impact model, developed specifically to capture various adverse effects of pipe bursts (e.g., supply interruption, low pressure problems, discolouration, etc.) in a short term risk horizon (e.g., 24 hours) before they are located and repaired. The impact model presented here attempts to utilise data and models typically available to water utilities and does not try to cover all aspects associated with an impact of a failure, which would be beyond the scope of this thesis. The impacts are evaluated from the perspective of a water utility, rather than of its customers. Nevertheless, a strong focus on quality of service for various water consumers is incorporated in the impact model. The core of the proposed model is formed by a pressure-driven hydraulic solver (Morley and Tricarico 2008) coupled with a GIS. This ensemble is used to calculate basic performance measures (e.g., system pressures) that are later utilised by a number of additional models (e.g., a discolouration model and a third party damage surrogate model). The outputs of the models serve two main purposes.

- 1) To provide a DM with a detailed breakdown of various aspects of the impact of a failure and its development throughout a given risk horizon.
- 2) As inputs for calculation of an aggregated impact measure of a failure allowing comparison of mutual significance of the impacts in different parts of a WDS.

The impact model was developed as follows:

- 1) First major types of customers were identified,

- 2) A suitable way of failure modelling was established,
- 3) An objective tree using MAVT, based on the requirements of a water utility and data availability, was constructed,
- 4) A set of KPIs, which serve as suitable surrogate measures to quantify the severity of various types of impacts considered in the objective tree, was formed.

3.4.1 Customer Categories

The KPIs proposed by OFWAT (2008) focusing on continuity of water supply (i.e., the DG3 indicator) and pressure adequacy (i.e., the DG2 indicator) treat all customers as equal. A number of publications (Michaud and Apostolakis 2006; Liserra *et al.* 2007; Beuken *et al.* 2008) suggested that it was important to take into account the type of customers when assessing impact of a failure. The results of a questionnaire survey shown later in this thesis (section 5.4.1) also confirmed that water companies consider the type of a customer when making operational decisions. Without any loss of generality, this research closely follows the customer classification suggested by Michaud and Apostolakis (2006) and operates with the following customer categories:

- **residential** (houses, flats, etc.),
- **commercial** (shops, businesses, etc.),
- **industrial** (factories, mills, etc.), and
- **critical** (hospitals, schools and other vulnerable customers)

Michaud and Apostolakis (2006) further considered sub-zones, which are typically modelled as demand nodes in an HM representing a high number of accumulated customers of the four types above. Sub-zones were not considered in this work since estimating the effects of a failure beyond the boundaries of a WDS (i.e., its HM) is difficult. It is suggested here that the impact on sub-zones should only be considered when a full interruption of water supply occurs because of the physical disconnection of an export node. Even in such a case it is unknown whether or not the sub-zone is supplied from another source. Given the focus of this work on the impact of pipe bursts before they are repaired, no demand nodes can be completely disconnected and

therefore the exclusion of sub-zones does not represent any limitation to the methodology.

3.4.2 Failure Modelling

A pressure driven extension of EPANET (Morley and Tricarico 2008) was used in this work to model the effects of a pipe burst in a WDS. The pressure-demand relationship of all demand nodes was considered to be identical and described according to Wagner *et al.* (1988b) using following equations:

$$Q_j = \begin{cases} 0 & \text{if } P_j < P_j^{\min} \\ Q_j^{req} \left(\frac{P_j - P_j^{\min}}{P_j^{des} - P_j^{\min}} \right)^{1/n} & \text{if } P_j^{\min} \leq P_j \leq P_j^{des} \\ Q_j^{req} & \text{if } P_j > P_j^{des} \end{cases} \quad (3.15)$$

where:

- Q_j is the real demand supplied at node j
- P_j is the actual pressure head at node j
- P_j^{\min} is the minimum required pressure to supply any demand
- Q_j^{req} is the required demand at node j
- P_j^{des} is pressure required to fully satisfy the requested demand
- n is a parameter, which takes value of 2 according to (Wagner *et al.* 1988b)

The values of P_j^{\min} and P_j^{des} should be ideally obtained from field tests during model calibration and are likely to differ amongst demand nodes (e.g., because of different type of customers, property height, etc.). It was assumed here that the minimum pressure P_j^{\min} was 0 m of head at the water main (although this assumption might not be entirely realistic). The value of pressure P_j^{des} required to deliver all requested demand was considered to be 15 m of head following the minimum level of service requirements issued by OFWAT (2008). A typical shape of the pressure-demand curve, described by Eq. (3.15), is shown in Figure 3.15. Other pressure-demand relationships as suggested in the literature review in section 2.5.1 could be used, without any loss of generality.

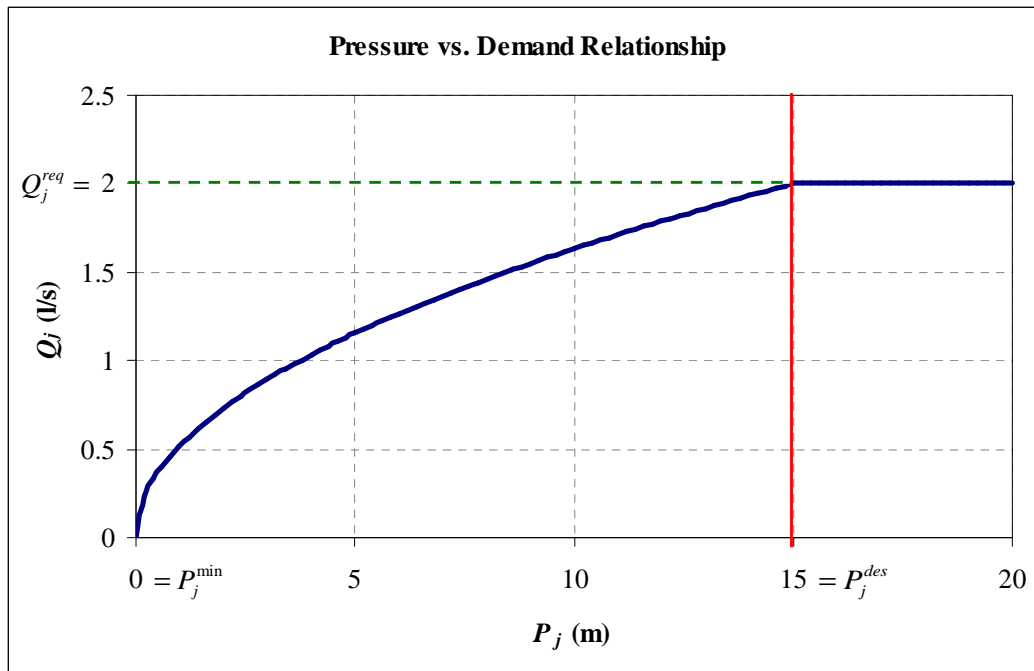


Figure 3.15 A relationship between pressure and demand of node j

Pipe bursts can be modelled in a number of ways as discussed in the literature review in section 2.5.2. The most realistic way chosen in this work models bursts using EPANET's emitters as pressure dependent outflows (see Figure 3.16) with the simplifying assumption that their pressure exponent γ was equal to 0.5, regardless of pipe material or other factors.

The value of the exponent can vary from 0.5 to 2.5, however, as suggested by Cassa *et al.* (2010) values higher than 1.5 estimated during field trials do not have ground theoretical foundations. The chosen value of the emitter exponent of 0.5 agrees with Lambert (2002) who suggested that detectable leaks and bursts in metal pipes typically have values of exponent close to 0.5. In this case the emitter coefficient is calculated based on the estimated burst flow and actual pressure at the burst location. This approach provides more realistic results, however, it requires an extra steady state simulation to obtain pressure at the beginning of the impact simulation to calculate the value of the discharge coefficient C_d using Eq. (2.2).

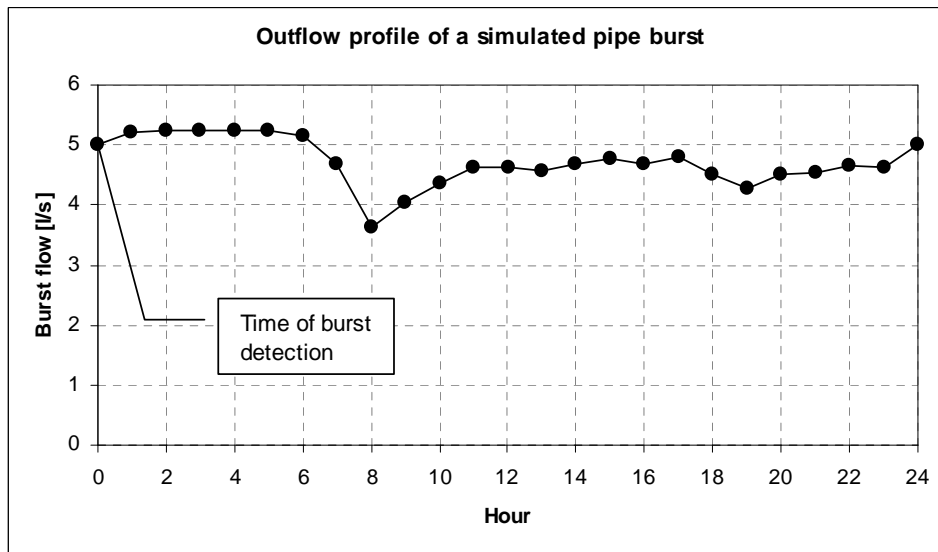


Figure 3.16 A sample outflow profile from a pressure sensitive burst

3.4.3 Impact Aggregation

A simplified tree of objectives (see Figure 3.17), sometimes also referred to as a “value tree” (Michaud and Apostolakis 2006) was established. The tree in Figure 3.17 contains four main impact categories: Supply Interruption, Low Pressure, Discolouration and Economic impact. These are discussed in more detail in section 3.4.3, where KPIs corresponding to the leaves in the objective tree are defined in Eqs. (3.18) - (3.28). Every branch in the objective tree has a weighting factor associated with it, which reflects the importance of a particular type of impact to a water utility. The way specific values of the weighting factors can be obtained is explained later in section 5.4.1.

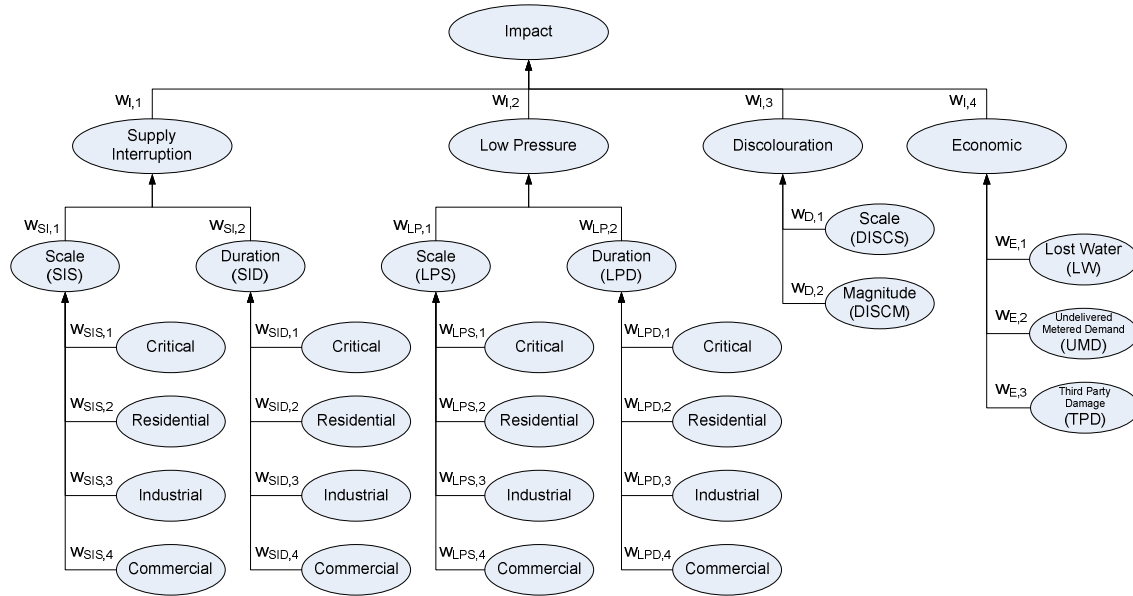


Figure 3.17 A tree of objectives

Evaluation of the overall impact represented by the objective tree shown in Figure 3.17 falls into the field of Multi-Criteria Decision Analysis (MCDA). MCDA provides a number of techniques that can be used to aid DMs to solve complex multi-objective problems. Following Løken (2007) the available methods can be broadly classified into 3 categories: (1) value measurement models, (2) goal, aspiration and reference models and (3) outranking models. None of the above techniques is suitable for every application and selection of a particular technique depends on a particular decision-making context. In this work, the MAVT (Keeney and Raiffa 1976), and the AHP (Saaty 1980) were used. The MAVT is one of the simplest methods available and is appropriate for the quantitative objectives used here. Its simplicity can be seen as an advantage since it can be easily understood and accepted by DMs, as opposed to more complex methods, such as the Multi-Attribute Utility Theory (MAUT). The principle behind MAVT is to associate a real number $V(a)$ (see Eq. (3.16)) with every considered alternative (i.e., impact of a potential incident). The value $V(a)$ is then used to rank alternatives. An alternative a is preferred (i.e., will have higher impact) to alternative b if and only if $V(a) > V(b)$ (Løken 2007):

$$V(a) = \sum_{i=1}^m w_i v_i(a) \quad (3.16)$$

where: w_i is a weighting factor associated with criterion i (i.e., a leaf in the objective tree shown in Figure 3.17), v_i is a function defining the performance of alternative a on criterion i (i.e., how severe the impact was).

If the scale of each of the criteria is different (which was the case in this work) then normalisation has to take place so that the range of outputs of function $v_i(a)$ is identical for every criterion. The weights w_i need to be elicited from a DM, which was achieved here using the AHP as shown later on a case study presented in section 5.4.2. The requirement to normalise criteria might, however, affect their scale significantly when outliers are present in the set of alternatives. Mavrotas and Trifillis (2006) suggested using the fifth and the ninety-fifth percentile in the normalisation procedure instead of the minimum and maximum to alleviate this problem. The use of percentiles was not applied in this work, despite outliers being occasionally encountered within the set of potential incidents.

The criteria in this work correspond to the leaves of the objective tree in Figure 3.17 (e.g., Duration of Supply Interruption of Residential customers). The weighting factor w_i of criterion i is obtained by multiplying all the weights on the path from the root of the tree towards a particular leaf as suggested on an example in the following formula:

$$w_{SDR} = w_{I,1} \times w_{SI,1} \times w_{SID,2} \quad (3.17)$$

The above Eq. (3.17) represents the weighting factor of the duration of supply interruption of residential customers and was expressed as a product of three weights from the objective tree in Figure 3.17. Other MCDA techniques (e.g., MAUT) could be used to aggregate the KPIs presented in section 3.4.4 into a single impact measure, without affecting the whole risk-based pipe burst diagnostics methodology.

3.4.4 Key Performance Indicators

This section describes KPIs to capture the adverse effects caused by a failure in a WDS. The KPIs introduced by OFWAT (2008) were extended and refined to better suit the needs of a near R-T impact assessment required by current customer-oriented water utilities.

In the UK the minimum level of acceptable service is set by OFWAT (2008) as follows: "For two properties, a flow of 18 l/min at a pressure of 10 m head on the customers' side

of the main stop tap is appropriate”. Generally water companies use a surrogate measure of 15 m head in the adjacent main due to the fact that measuring the pressure on customers’ side would be difficult. This implies that the minimum required pressure in the mains has to be higher in order to achieve an acceptable level of service. Typically, water utilities try to maintain the pressure of at least 20 m at the water main in the street throughout the day to allow sufficient room for fluctuations. However, it is not desirable to keep the pressures in a WDS high, due to increased levels of leakage and higher burst rates.

Following the objective-tree presented in Figure 3.17 the KPIs were classified into four main categories (i.e., supply interruption, low pressure, discolouration and economic impact), which will be discussed in detail in the following sections.

3.4.4.1 Supply Interruption

Supply interruption is treated as the disconnection from the water supply or a situation when no water is available at the consumers’ tap (i.e., the pressure is below the minimum acceptable pressure P_{int}). For the sake of simplicity, the value of P_{int} was assumed constant throughout the whole network, however, in reality it is node specific. To accommodate the height of properties, the minimum pressure P_{int} was taken as 7 m of head at the water main. The chosen value of P_{int} (7 m) might seem to be in contrast with P^{min} (0 m) used in Eq. (3.15). Although, the customers are already considered as being affected by a complete supply interruption, the pressure driven HM assumes that some water consumption still occurs at demand nodes as long as the pressure is greater than 0 m.

The major impact of the supply interruption for the water utility is in the form of penalties imposed by OFWAT as part of the DG3 performance indicator. Secondary losses are also represented by the decreased revenue due to no water consumption by disconnected metered customers and the costs of dealing with an increased number of CCs. Furthermore, significant drops of pressure (i.e., when pressure reaches 0 m of head) can lead to intrusion of contaminants into a WDS (Sadiq *et al.* 2006) and cause water quality problems that might affect the health and safety of water consumers.

OFWAT (2008) describes the DG3 indicator as follows: “*The aim of this indicator is to identify the number of properties affected by planned and unplanned supply interruptions lasting longer than 3 hours, 6 hours, 12 hours and 24 hours.*”

For the scope of this work, supply interruption will be restricted to only unplanned interruptions caused by failures in a WDS. It is proposed here to extend the existing supply interruption KPIs (Mansoor *et al.* 2005; Michaud and Apostolakis 2006; OFWAT 2008) and express the impact of supply interruption in a more customer focused way, using the Supply interruption Scale (SIS) and Supply Interruption Duration (SID) KPIs, as follows:

$$SIS_{CustType} = \sum_{i=1}^{N_N} \begin{cases} Cust_{i,CustType} & \text{if } \exists t \in \{1, 2, \dots, T\}: P_i(t) < P_{int} \\ 0 & \text{otherwise} \end{cases} \quad (3.18)$$

$$SID_{CustType}[h] = \frac{\sum_{i=1}^{N_N} ID_i \times Cust_{i,CustType}}{SIS_{CustType}} \quad (3.19)$$

where:

- $SIS_{CustType}$ is the Supply Interruption Scale quantified per customer type
- N_N is the number of demand nodes in the network
- T is the total simulation time (with assumed time step of 1 hour)
- $Cust_{i,CustType}$ is the number of customers of a particular type supplied from node i
- $P_i(t)$ is the pressure at demand node i at time step t
- P_{int} is the minimum required pressure in m of head below which a node is considered as being without water supply (in this case 7 m)
- $SID_{CustType}$ is the weighted average Supply Interruption Duration evaluated per customer type
- ID_i is the duration of supply interruption measured from the first time when pressure at demand node i dropped below P_{min} until the time when the supply was fully restored (i.e., excluding any gaps) as illustrated in Figure 3.18

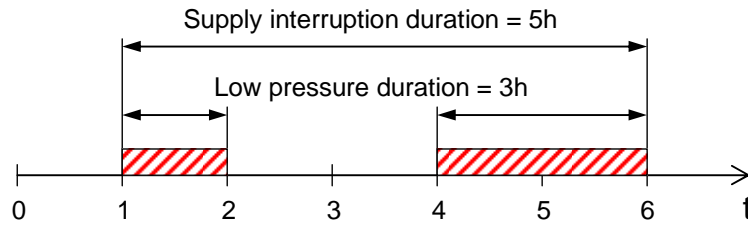


Figure 3.18 Measurement of duration of supply interruption and low pressure impact

3.4.4.2 Low Pressure

Low pressure problems cause a wide range of direct and indirect impacts affecting the water utility and its customers. The economic regulator OFWAT requires low pressure incidents (i.e., drops of pressure below 15 m of head at the water main) to be reported as part of the DG2 performance indicator by a water utility. Short term failures such as those caused by pipe bursts are excluded from the DG2 register. Although short term pressure problems caused by burst mains are excluded from the DG2 register, all properties receiving substandard pressure for more than 1 hour have to be listed together with the reason for their exclusion. Low pressure problems caused by pipe bursts thus should not represent a direct economical impact on the water utility in terms of financial penalties imposed by OFWAT.

Low pressure causes inconvenience to customers and affects pressure sensitive water consumption thus reducing the revenue of a water utility in the case of metered customers. From a strategic perspective, inadequate pressure problems occurring in the case of fire might even lead to loss of life and property (Filion *et al.* 2007).

OFWAT (2008) describes the DG2 indicator as follows: “*The register must clearly identify those properties reported under DG2 and distinguish them from those that receive low pressure but are excluded from DG2, and provide a verifiable reason for the exclusion (e.g., as abnormal demand or short duration of low pressure).*”

The DG2 index is calculated as the total number of properties receiving substandard pressure for more than 1 hour throughout the whole day. Here an extended version, which explicitly considers type of customers, was used:

$$LPS_{CustType} = \sum_{i=1}^{N_N} \begin{cases} Cust_{i,CustType} & \text{if } \exists t \in \{1, 2, \dots, T\}: P_{min} \leq P_i(t) < P_{req,i}(t) \\ 0 & \text{otherwise} \end{cases} \quad (3.20)$$

where:

- $LPS_{CustType}$ is the Scale of the Low Pressure impact expressed as the number of properties of given type experiencing low pressure problems
- $P_{req,i}(t)$ is the minimum required pressure at node i at time t (i.e., 15 m of head)
- $Cust_{CustType,i}$ is the number of customers of a particular type supplied from node i

To take into account the duration (see Figure 3.18) of the low pressure impact Eq. (3.21) defines the weighted average Low Pressure Duration (LPD) for a given type of customer.

$$LPD_{CustType}[h] = \frac{\sum_{t=1}^T \sum_{i=1}^{N_N} \left\{ \begin{array}{ll} Cust_{i,CustType} & \text{if } P_{\min} \leq P_i(t) < P_{req,i}(t) \\ 0 & \text{otherwise} \end{array} \right\}}{LPS_{CustType}} \quad (3.21)$$

Indirectly, the water utility also has to deal with an increased number of customer phone calls caused by low pressure problems (this, however, was not incorporated due to insufficient data available).

Similarly to low pressures, high pressure failures could also cause significant impact in a WDS. These could be caused by a malfunction of Pressure Reducing Valves (PRV), which could lead to an increased burst rate in the affected area. High pressure impacts were not considered in this work.

3.4.4.3 Discolouration

As reported by Vreeburg and Boxall (2007) discolouration can account for approximately 34% of CCs for a typical UK water company. It is, therefore, in the interest of water companies to be able to quantify its effects. The impact of discolouration caused by a burst pipe (i.e., increased flows and velocities and low pressures) is a complex phenomenon. A simplified Discolouration Risk Model (DRM) developed by Dewis and Randall-Smith (2005) based on risk-trees created by a panel of experts was used in this work. The development of the DRM is not a contribution presented in this thesis. The model provides a risk score for every pipe, which reflects a relative susceptibility of the pipe to generate discolouration. The magnitude (i.e., how severe the discolouration impact will be) was expressed here as a sum of the increase in discolouration risk between normal and failure operating conditions:

$$DISCM = \sum_{j=1}^{N_p} \begin{cases} Disc_{j,failure} - Disc_{j,norm} & \text{if } Disc_{j,failure} > Disc_{j,norm} \\ 0 & \text{otherwise} \end{cases} \quad (3.22)$$

where:

- N_p is the number of pipes in the network
- $Disc_{i,norm}$ is discolouration risk score of pipe i under normal conditions
- $Disc_{i,failure}$ is discolouration risk score of pipe i under failure conditions

(Note that the discolouration risk score of the burst pipe was excluded from the analysis)

Furthermore, the scale of discolouration impact (i.e., how large an area will be affected) was expressed as the total length of pipes experiencing an increase in the discolouration risk score over a given risk horizon (i.e., 24 hours).

$$DISCS = \sum_{j=1}^{N_p} \begin{cases} Length(j) & \text{if } Disc_{j,failure} > Disc_{j,norm} \\ 0 & \text{otherwise} \end{cases} \quad (3.23)$$

where:

- $Length(j)$ is a function which returns the length of pipe j

An example of a map showing the discolouration impact (based on the increase of discolouration risk score) caused by a large pipe burst (denoted by X) is shown in Figure 3.19. The figure enables WDS operators to estimate abnormal flow pathways that experience an increase in flow or possibly flow reversals and provides them with an insight into their discolouration risk.

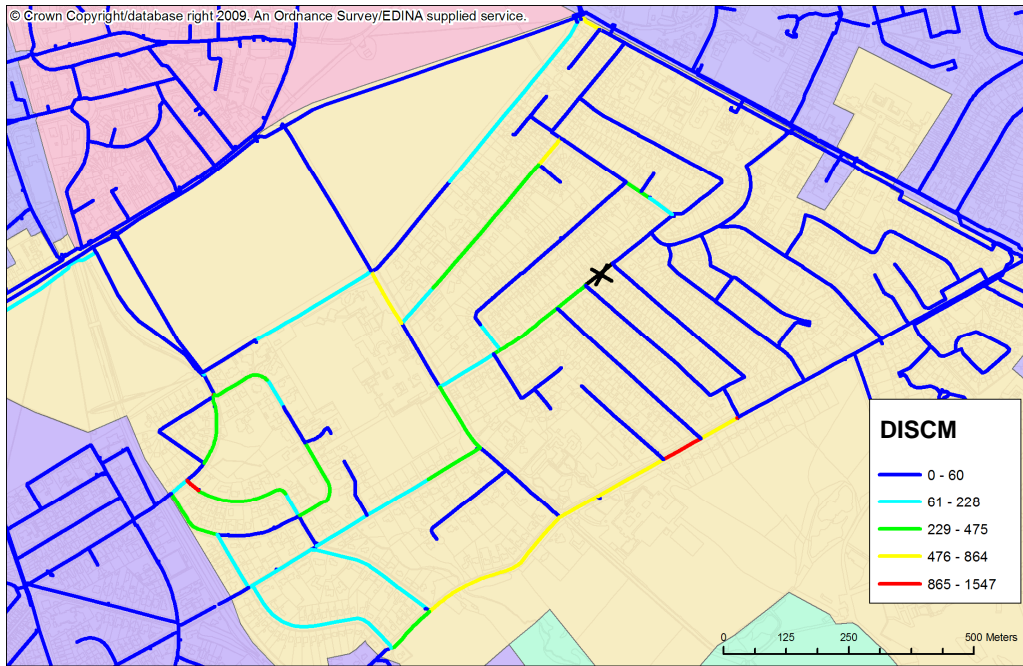


Figure 3.19 A map showing the DISCM KPI after a pipe burst

The methodology used in the discolouration model might not be the most suitable one to apply in WDS operation. Other more advanced techniques to model discolouration are available (e.g., the Resuspension potential method or Cohesive transport model) as suggested by Vreeburg and Boxall (2007).

3.4.4.4 Economic Impact

The following category of impacts represents direct and indirect costs that could affect a water utility because of a failure in a WDS.

Lost Water

In case of a pipe burst, the water losses are estimated by summing up the outflow from a burst modelled using an emitter over the whole risk horizon (e.g., 24 hours).

$$LW[m^3] = \frac{3600 \times \sum_{t=1}^T \text{BurstFlow}(t)}{1000} \quad (3.24)$$

where:

- *BurstFlow*(*t*) is the simulated pressure sensitive burst flow in l/s at time *t*

Lost Revenue Due to Undelivered Demand

Low pressures in a WDS could represent a direct loss for a water utility since customers might not be able to receive all the water that would be consumed under normal

conditions. The amount of undelivered water can be quantified thanks to the use of a pressure driven hydraulic solver described in section 3.4.2. In the UK where only 37.3% of customers were metered in the year 2009/2010 (OFWAT 2009) the incurred losses come only from those customers who have a meter installed.

The loss of revenue due to undelivered water (because of low pressure or complete supply interruption) assuming equal distribution of demand between metered and unmetered customers can be defined as follows:

$$UMD[m^3] = \frac{3600}{1000} \times \sum_{t=1}^T \sum_{i=1}^{N_N} \begin{cases} \frac{(D_{i,req}(t) - D_i(t)) \times Cust_{i,M}}{Cust_{i,M} + Cust_{i,UM}} & \text{if } P_i(t) < P_{req,i}(t) \\ 0 & \text{otherwise} \end{cases} \quad (3.25)$$

where:

- $D_{i,req}(t)$ is the requested demand of node i in l/s
- $D_i(t)$ is the delivered demand of node i in l/s
- $Cust_{i,M}$ is the number of metered customers supplied from node i
- $Cust_{i,UM}$ is the number of unmetered customers supplied from node i

Third Party Damage

Failure in a WDS, such as a burst pipe, can lead towards traffic disruption and a number of indirect impacts affecting the water utility and its customers. The focus of this KPI is to estimate the likely damage to roads and railways and the social impact associated with their repairs. The model could be further extended to account for possible damage to properties (i.e., buildings), however, these were not considered here.

Land use data and the flow in a pipe were used in this work to develop a surrogate measure for third party damage caused by a pipe burst. The model considers the length of the intersection of a pipe with various types of surfaces (of defined importance) above the pipe as well as the flow in the pipe in order to calculate the potential damage and inconvenience caused by a burst. The output of this model can be to a large extent pre-computed offline (e.g., the spatial analysis of the land above a pipe) and applied online by including information about the actual flow through the pipe. By assuming a

linear relationship between the criticality of the surface above a pipe (referred to here as the “Priority”) and the flow in the pipe, the model can be defined as follows:

$$TPD(i) = \lambda NormPriority(i) + (1 - \lambda) \frac{\sum_{t=1}^T Q_i(t)}{\max_{j \in 1 \dots N_p} \left(\sum_{t=1}^T Q_j(t) \right)} \quad (3.26)$$

where:

- $TPD(i)$ is the model output reflecting the damage caused to third parties by burst of pipe i
- $NormPriority(i)$ is a normalized measure indicating the importance of the surface(s) above pipe i
- λ is a coefficient of relative importance of the flow in a pipe compared to the type of the land above
- $Q_i(t)$ is the flow in pipe i at time step t

The “Priority” of the surface above a pipe was obtained as follows. A vector dataset with all surface elements (e.g., roads, railways, buildings, etc.) represented as polygons was utilised. In particular, the Ordnance Survey MasterMap (Ordnance Survey 2010) dataset was used. The dataset was reclassified according to Table 3.2 and corresponding Category was assigned to its elements. The most critical surface type (i.e., Category 4) was identified as a railway since a pipe burst in its proximity might potentially cause damage to the rails and lead to reduced safety. The second most critical Category comprised roads and roadsides (i.e., Category 3) since these might be damaged by a pipe burst underneath them. The polygons falling into the road or roadside category were further split into 9 sub-categories as indicated in Table 3.3, to reflect the importance of a particular type of road. The percentage of the pipe length intersecting a particular polygon was calculated and used as a weighting factor. The priority class of a pipe was calculated according to the following formula:

$$Priority(i) = \sum_{s: s \cap i \neq \emptyset} (10 \times Category(s) + SubCategory(s)) \times Weight(s, i) \quad (3.27)$$

where:

- $Priority$ is a measure of importance of the surface above a pipe

- s is the index of a surface on the land
- $Category(s)$ is a lookup function which returns a value from Table 3.2 according to the type of the surface
- $SubCategory(s)$ is a lookup function which returns a value from Table 3.3 according to the type of road above / in close proximity of the pipe
- $Weight(s,i)$ returns the fraction of the intersecting length of pipe i with surface s relative to the total length of the pipe
- i is the index of a pipe in an HM

The value of Category in Eq. (3.27) was multiplied by factor of 10 to represent a hierarchical structure between categories and sub categories. Should the number of sub-categories considered be higher than 9 (see Table 3.3) then a different constant would have to be selected to achieve the desired effect.

The normalised Priority can be computed using the following equation:

$$NormPriority(i) = \frac{Priority(i) - \min_{k \in 1 \dots N_p} (Priority(k))}{\max_{l \in 1 \dots N_p} (Priority(l)) - \min_{k \in 1 \dots N_p} (Priority(k))} \quad (3.28)$$

where:

- $NormPriority$ is the normalised measure of importance of the surface above a pipe
- i, k and l are indices of a pipe in an HM

Table 3.2 Available types of surfaces, their reclassification and category

Description	Reclassified	Category
Building	Building	0
Glasshouse	Building	0
Building; Rail	Building	0
General Feature; General Surface	Land	1
General Surface	Land	1
Landform	Land	1
Natural Environment	Land	1
Unclassified	Land	1
Landform; Rail	Rail	4
Natural Environment; Rail	Rail	4
General Feature; Road Or Track	Land-Road	2
General Surface; Road Or Track	Land-Road	2
Landform; Path	Land-Road	2
Landform; Road Or Track	Land-Road	2
Natural Environment; Road Or Track	Land-Road	2
General Surface; Inland Water	Water	0
Inland Water; Natural Environment	Water	0
Rail	Rail	4
Rail; Road Or Track	Rail	4
Path	Path	2
Road Or Track	Road	3
Roadside	Roadside	3
Path; Structure	Path	2
Road Or Track; Structure	Structure	0
Structure	Structure	0
Inland Water; Structure	Structure	0
Inland Water	Water	0

Table 3.3 Types of roads and their sub-category

Description	Sub-Category
Motorway	9
A Road	8
B Road	7
Minor Road	6
Local Street	5
Pedestrianised Street	4
Private Road - Publicly Accessible	3
Private Road - Restricted Access	2
Alley	1

An example output from the TPD model is shown in Figure 3.20. The “Third Party Damage” (displayed using a red-blue colour gradient) was calculated using Eq. (3.26)

by assuming $\lambda = 0.5$. The flow in the pipes at 8:00AM is displayed using different line thickness.

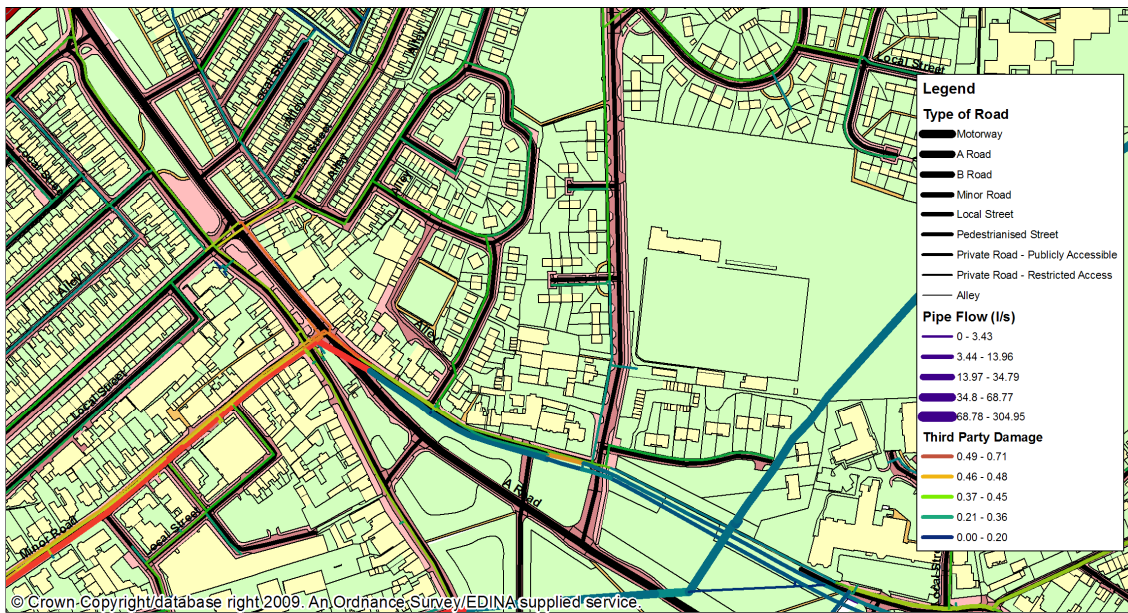


Figure 3.20 An example output from the third party damage model

The values of the Categories and Sub-categories used above were assumed to be linear although it might be necessary to further adjust these values as well as the coefficient λ depending on the preferences of a DM. The current setting of the values might pose a potential threat in situations where long pipes cross railways since, the intersection length with the railway is relatively small (however, so is the likelihood that the pipe burst would occur in the proximity of the rails) and thus the final priority of such pipe might be relatively small.

3.5 Abnormal Event Prioritisation

In the case of large WDS several pipe bursts or other types of failures can occur more or less simultaneously in different DMAs in a similar risk horizon (e.g., during 24 hours). Extreme weather conditions, such as extended periods of frost, are also likely to lead to an increased occurrence of bursts and consequently alarms (i.e., detected anomalies) across the whole WDS. When alarms from multiple DMAs are generated in a similar risk horizon, WDS operators frequently have to prioritise their actions, based on limited information (e.g., affected DMA, magnitude of abnormal flow, etc.) and their experience, since resources to deal with contingency situations are typically limited.

The decision about which alarms should be dealt with first has to be reached promptly to avoid unnecessary customer impact. As discussed by Laffey *et al.* (1987) humans making decisions in Real-Time (R-T) tend to overlook relevant information and respond inconsistently or too slowly if the rate of information flow is too great (e.g., an increased number of alarms received in a control room).

Unlike in other fields, such as the power and chemical industries (Foong *et al.* 2009), operational prioritisation of failures in WDS is not well established. Current research has been mostly concerned with strategic applications such as prioritisation of existing infrastructure for renewal (Giustolisi and Berardi 2009) using evolutionary optimisation methods. The majority of the existing methods of failure detection and prioritisation in process control are based on rule-based Expert Systems (ES) (Foong *et al.* 2009) or model based techniques (Isermann 2005). Fuzzy logic (Zadeh 1975) has also been frequently used in conjunction with the rule-based system to encompass uncertainty by operating with linguistic terms rather than crisp values. The severity of an abnormal event in process control is typically derived from the state of a number of sensors related to a particular process. A rule-based system can contain rules in the following form:

```
IF Temperature > 50°C AND Pressure > 300 kPa THEN  
priority = 10
```

```
IF Temperature > 50°C AND Pressure < 300 kPa THEN  
priority = 5
```

On the other hand a fuzzy rule-based system would capture the critical thresholds using linguistic variables to incorporate the vagueness of the definition of a particular alarm state. An example of a fuzzy-rule is shown below:

```
IF Temperature IS "High" AND Pressure IS "High" THEN  
priority = "Very High"
```

```
IF Temperature IS "High" AND Pressure IS "Normal" THEN  
priority = "Medium"
```

The rule-based prioritisation shown above utilises the observed symptoms caused by a failure, rather than the outcomes of diagnostics of the observed anomaly, to perform the prioritisation. Even model based methods, which typically generate residuals, i.e. differences between observations and model outputs, operate in a similar fashion. The suitability of application of such techniques to prioritise flow alarms (i.e., detected abnormal flows) in a WDS is questionable as will be illustrated later on case studies in section 5.5.

A methodology for an initial automated screening of alarms to help control room personnel better prioritise their actions when investigating several alarms occurring in the same time horizon in different DMAs was developed. The conceptual foundations of this work were laid in section 3.2. Alarms can be presented to operators ranked in the order of their significance, which was determined from the outcomes of a near R-T risk analysis (described in sections 3.3 and 3.4). Alarms representing the highest overall risk to a water utility and customers can then be dealt with first.

3.5.1 Alarm Ranking

The aim of the alarm prioritisation methodology is to determine mutual significance of multiple alarms (i.e., to rank them) rather than to attempt to classify them into predefined categories (e.g., high risk, medium risk, low risk, etc.) The methodology comprises the following steps:

1. **Burst Detection** - Detection of a burst (e.g., using an ANN-FIS), which does not form part of this thesis.
2. **Diagnostics & Risk Assessment** - Identification of potential incidents of an anomaly and estimation of their likelihood of occurrence as well as their impact.
3. **Pipe Burst Risk Aggregation** - Calculation of risk of failure of individual potential incidents.
4. **Overall Risk Aggregation** - Calculation of an overall risk represented by all potential incidents.
5. **Anomaly Ordering** - Sorting of abnormal events according to the level of their overall aggregated risk.

The individual steps defined above are described in detail in the following sub-sections.

3.5.2 Diagnostics and Risk Assessment

In this work it is assumed that an automated pipe burst detection system (Mounce *et al.* 2010) or similar is already in place, providing the following information: (1) date and time of burst occurrence, (2) ID of the affected DMA, and (3) estimated burst flow. It is further assumed here that the detected anomaly (i.e., an alarm) is a result of a single pipe burst only within the reported DMA. This fact does not restrict the potential of the methodology to handle different types of failures (e.g., pump/valve failures) or alternatively handling of multiple failures within a DMA.

Under the above assumptions a one-level fault tree diagnostics, mentioned previously in Figure 3.3, for every active alarm can be performed as shown in Figure 3.21 in a simplified form.

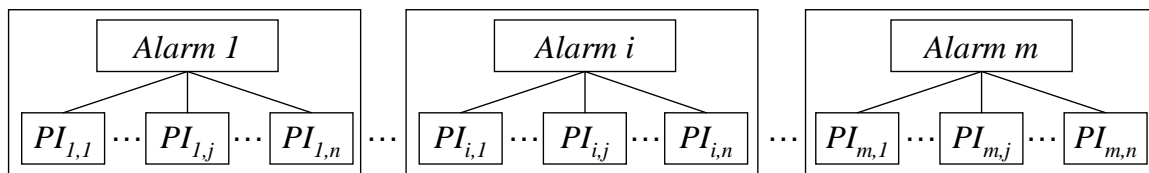


Figure 3.21 A hierarchical representation of alarms and potential incidents

Typically, the set of potential incidents determined for every active alarm as shown in Figure 3.21 contains all pipe segments within the investigated DMA. For the purpose of prioritisation of alarms working with the complete set might not be necessary and only a representative number of pipe segments could be included. This was not investigated as part of this research and the risk of all potential incidents was used here.

Once the set of potential incidents is determined a full risk assessment of all its elements can be carried out. This involves evaluation of the *Likelihood* of occurrence of a burst on every pipe segment (see section 3.3) and estimation of its aggregated *Impact* (see section 3.4) over a given risk horizon.

3.5.3 Pipe Burst Risk Aggregation

For the purpose of decision-making it is important that the risk metric is preserved in a non-aggregated form and as such also presented to a DM. However, as the first step in ranking of multiple alarms, the risk of individual potential incidents was aggregated.

The most commonly applied risk aggregation operation is to represent risk as a product of likelihood and impact (i.e., $R = L \times I$). Such a formulation could well suit problems where the likelihood component of risk reflects the traditional frequentists' probability. However, the likelihood used in this context is a normalised measure indicating, which potential incidents are more likely than others to be the cause of the observed anomaly (i.e., the likelihood normalisation is carried out per alarm) and, therefore, a simple multiplication could completely eradicate potential incidents with very low likelihood and high impact, which might still be interesting for a DM as highly unlikely but disastrous events. To overcome the above issue it is suggested to use the concept of *reference point* (see Figure 3.22) used, e.g., by Zeleny (1973) to represent a risk of a potential incident. The aggregated risk can then be expressed as a distance metric defined as follows:

$$R_{i,j} = \left[\sum_{k \in \{L,I\}} w_k^h (P_k^* - PI_{i,j,k})^h \right]^{1/h} \quad (3.29)$$

where: $R_{i,j}$ is the aggregated risk of a potential incident j being the cause of an alarm i (note: the lower the value of this metric the higher the risk of a particular pipe burst), k is the index corresponding to the likelihood or impact, w_k is a weighting factor reflecting the DM's preference between likelihood and impact subject to $w_L + w_I = 1$, P_k^* is a coordinate of the *reference point* (see Figure 3.22) corresponding to the maximum likelihood (per alarm) or maximum impact (amongst all alarms), $PI_{i,j,k}$ is the coordinate representing the likelihood or impact component of risk of potential incident j , and h is the distance metric exponent, which typically takes value $h = 2$ to represent Euclidean distance.

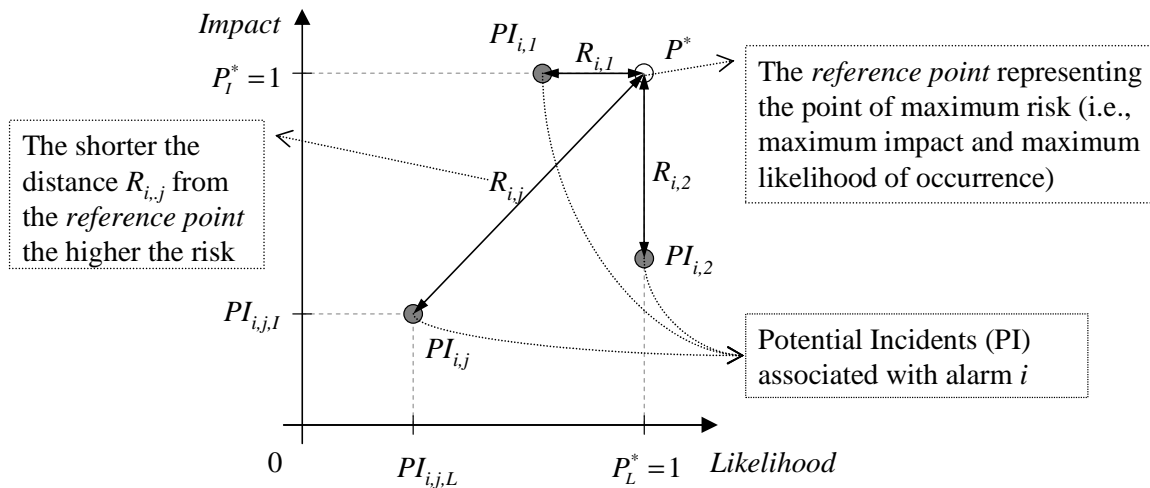


Figure 3.22 Distance metric used to represent aggregated risk of a pipe burst

The *reference point* (see the point P^* in Figure 3.22) does not have to exist in the set of considered potential incidents, as in the case depicted in Figure 3.22, and is typically a fictitious point. In a situation when the potential incident with the highest impact amongst all considered alarms should also be the most likely burst candidate (as part of the alarm it belongs to), it would become the *reference point* and its value of $R_{i,j}$ would be zero.

It is important to note that the normalisation of the likelihood of a burst occurrence is carried out on all potential pipe bursts associated with a single alarm whereas the impact is normalised on all potential incidents of all considered alarms. Only such an approach enables the comparison of the overall risk of alarms.

3.5.4 Overall Risk Aggregation

To represent the overall risk of alarm i the individual risks of all its potential incidents $R_{i,j}$ need to be aggregated. There are three main types of aggregation operators: intersection operators, union operators and averaging operators (Makropoulos and Butler 2006). In this work the Ordered Weighted Averaging (OWA) proposed by Yager (1988) was used. OWA is a flexible aggregation operator, which encompasses operators from minimum to maximum including various averaging operators such as the arithmetic mean. Another interesting property of the OWA is that during the process of generation of the weights applied in the aggregation, it is possible to incorporate the DM's attitude towards risk (e.g., neutral, optimistic, pessimistic, etc.) based on his/her degree of risk aversion (Makropoulos and Butler 2006).

The application of OWA to calculate the overall risk R_i of an alarm is carried out as follows. First a vector v_i , comprising risks $R_{i,j}$ of all potential pipe bursts j associated with alarm i is formed and its elements are sorted in an ascending order of their $R_{i,j}$ values, such as $v_i[x] \leq v_i[y]$ where $x < y$. The overall measure of risk R_i is then obtained by multiplying vector v_i with the transposed vector of weights W of the same dimension using following equation:

$$R_i = \sum_{l=1}^n v_i[l] \cdot W[l], \text{ such that } W = [w_1, \dots, w_l, \dots, w_n], w_l \in \langle 0, 1 \rangle \text{ and } \sum_{l=1}^n w_l = 1 \quad (3.30)$$

As in the case of any aggregation, some information loss inevitably occurs. To maximise the degree of information used from the non-aggregated risk vector v_i a set of maximum entropy (Shannon 1948) weights owa_i is generated given DM's attitude towards risk α according to O'Hagan (1988). Calculation of the maximum entropy weights requires solving the following constrained non-linear problem (O'Hagan 1988):

$$\begin{aligned} & \text{Maximise } \sum_{i=1}^n w_i \ln w_i \\ & \text{subject to } \alpha = \frac{1}{n-1} \sum_{i=1}^n (n-i)w_i, \\ & \sum_{i=1}^n w_i = 1, w_i \in [0, 1], i = (1, \dots, n) \end{aligned} \quad (3.31)$$

Makropoulos (2003) solved the optimisation problem defined in Eq. (3.31) using Sequential Quadratic Programming implemented in Matlab. However, Fullér and Majlender (2001) proposed an analytic solution to the problem defined as follows:

- 1) If $n=2$, then $w_1=\alpha$, $w_2=1 - \alpha$
- 2) If $\alpha = 0$ or $\alpha = 1$, then the associated weighting vectors are uniquely defined as $w = [0, 0, \dots, 1]$ and $w = [1, 0, \dots, 0]$, respectively, with value of dispersion equal to zero.
- 3) If $n \geq 3$ and $0 < \alpha < 1$, then

$$w_j = \sqrt[n]{w_1^{n-j} w_n^{j-1}} \quad (3.32)$$

$$w_n = \frac{((n-1)\alpha - n)w_1 + 1}{(n-1)\alpha + 1 - nw_1} \quad (3.33)$$

$$w_1[(n-1)\alpha + 1 - nw_1]^n = ((n-1)\alpha)^{n-1} [((n-1)\alpha - n)w_1 + 1] \quad (3.34)$$

The maximum entropy weights were calculated here using the analytic solution of Fullér and Majlender (2001). The implicit Eq. (3.34) was solved iteratively using arbitrary precision numbers.

The parameter α defines the level of optimism or pessimism of a DM. The effect of parameter α on the number of elements effectively considered during the aggregation is shown in Figure 3.23. It can be observed that with an increasing level of pessimism only a small number of potential incidents with the highest risk of failure contribute towards the overall aggregated risk representing an alarm. A purely pessimistic attitude ($\alpha = 1$) would mean that the overall risk of an alarm would be represented by only one potential pipe burst with the highest risk (i.e., the maximum operator). On the other hand purely optimistic attitude ($\alpha = 0$) would select the least risky pipe burst as the representative of an alarm (i.e., the minimum operator). A neutral attitude where ($\alpha = 1/n$), where n is the number of potential incidents associated with an alarm would perform aggregation using the arithmetic mean.

In the case of an optimistic attitude towards risk, which does not seem to be appropriate in this decision-making context, the X-axis in Figure 3.23 would be reversed and the less risky pipe bursts would contribute most.

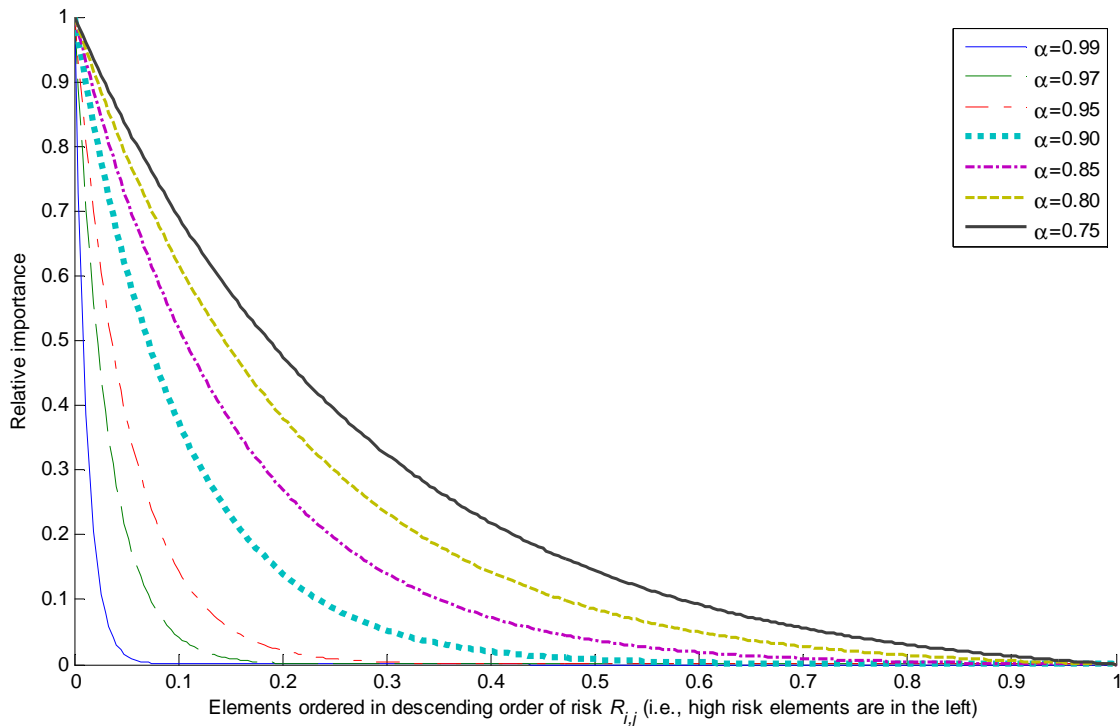


Figure 3.23 The effect of DM's attitude towards risk α on maximum entropy OWA weights

3.5.5 Anomaly Ordering

The above approach, used to calculate the overall measure of risk R_i , is repeated for every active alarm (i.e., an alarm that has not yet been completely resolved). The lower the value of R_i the higher the overall risk associated with a particular alarm. The ranking of an alarm should also reflect the state in which an alarm is. Clearly a confirmed alarm has a higher priority than an unconfirmed one, which, on the other hand, is more important than an alarm that is believed to be a false alarm. This work considers the following alarm states: *active*, *investigated*, *modified*, *real* and *false* that were derived based on an input from a water utility and academic partners in the NEPTUNE project (Savić *et al.* 2008). Figure 3.24 shows the states of an alarm as well as possible transitions between them. The alarm states presented here are not a direct contribution of the author unlike the rest of the methodology presented herein.

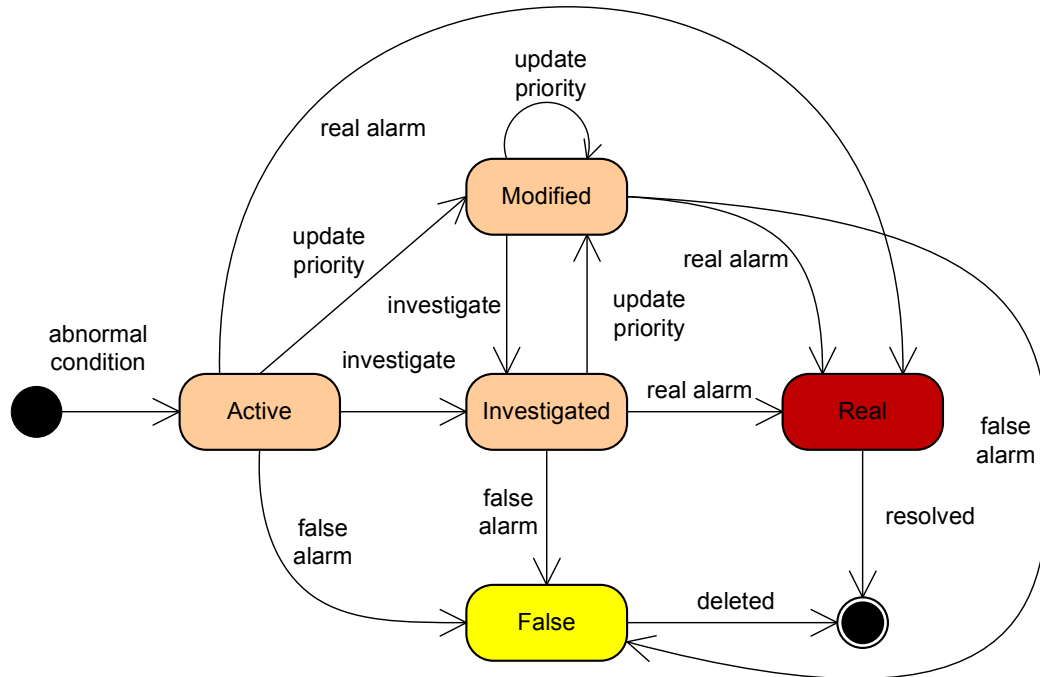


Figure 3.24 An alarm state diagram

An *active* alarm represents a fresh alarm that has just been detected and presented to an operator. The alarm can remain in this state until it is either marked as *false* in which case it was not genuine or as *real* in which case it was a real event. If new evidence becomes available, which affects the priority of an alarm (e.g., a customer call moves the most likely location of the burst to a high impact part of a DMA), while the alarm is in the alarm list, the state of an alarm changes to *modified* to raise the attention of an operator. Alternatively, an alarm can change its state to *investigated* (i.e., from the *active* and *modified* states), which indicates that it is being handled and further explored by an operator (e.g., using an interactive alarm diagnostics user interface discussed in Chapter 4). The *false* and *real* states are only set once the true nature of an alarm is determined (e.g., by a field technician). The alarm remains in the *real* or *false* states until it is manually deleted by an operator as resolved or specific period of time elapses (e.g., 1 week).

To incorporate the alarm state in the ranking, the available states were reclassified into 3 classes, *unconfirmed* (i.e., active, investigated, modified), *confirmed real* and *confirmed false*. It was desirable that a confirmed real alarm always had a higher priority than an unconfirmed one, which in turn had a higher priority than a confirmed false alarm. This

was achieved by assigning a Base_Priority level to every alarm according to the following rules:

```
IF State(i) IN (active, investigated, modified) THEN
    Base_Priority = 1000
ELSE
    IF State(i) IN (real) THEN
        Base_priority = 2000
    ELSE
        Base_priority = 0
```

The final sorting criterion, which encompasses the overall risk of an alarm as well as its state, can then be defined as follows:

$$\text{Sort_Priority}(i) = \text{Base_Priority}(i) + 10 \times \text{Rank}(i) \quad (3.35)$$

where: i is the index of an alarm, Base_Priority is a function defined using the above rules and Rank is a function, which returns the order of an alarm in an alarm list sorted in descending order of R_i so that the alarms with high risk (i.e., low values of R_i) obtain high ranks.

The Base_Priority levels of 1,000, 2,000 and 0 for the unconfirmed, confirmed real and confirmed false alarms, respectively were derived from the assumption that at no point in time there will be more than 100 alarms in each of the categories. The Base_Priorities could be increased (e.g., by multiplying them by 10) should the values above be too restrictive.

The alarms can then be presented to a WDS operator in the form of an alarm list that is sorted in descending order of Sort_Priority (see Eq. (3.35)) of the considered alarms. This ensures that the most severe alarms appear on the top of the list and receive more attention from the control room operators. The Rank of an alarm was multiplied by the factor of 10 since it was believed that higher values will generally receive more attention from the operators. This subjective assumption, however, has no scientific grounds.

3.6 Summary

This chapter presented a methodology for a near R-T risk-based diagnostics of flow anomalies in a WDS. Its key constituents, namely the Likelihood model, Impact model and Alarm prioritisation model, were discussed.

After the introduction in section 3.1, the conceptual foundations of risk-based decision-making in diagnostics of pipe bursts in a WDS were laid in section 3.2. It was suggested that burst investigation within a DMA should be driven by risk maps presenting risk of a failure (i.e., its likely location and impact) in a non-aggregated form. The likelihood component of risk plays a dominant role when dispatching field technicians to investigate potential pipe bursts. On the other hand, the impact can be also considered as a secondary criterion by an operator when a burst in a particular part of a DMA has significant consequences.

Section 3.3 presented a methodology, based on evidential reasoning, to estimate the likely location of a burst pipe within an affected DMA. The outputs of several models (i.e., a PBPM, an HM and a CCM) were combined in order to increase the confidence in the likely location of a burst pipe. A novel calibration procedure, based on multi-objective optimisation was developed, to determine the necessary parameters of the D-S model.

In section 3.4 the development of an impact model based on a pressure driven hydraulic solver and a GIS was described. A number of KPIs were developed to assess the performance of a WDS under failure conditions. MAVT, a technique from the field of MCDA, was used to obtain an aggregated impact of a failure based on a number of criteria and preferences of a DM.

A method for prioritisation of alarms (i.e., detected abnormal events) was proposed in section 3.5. Its application enables the mutual significance of anomalies in situations when multiple failures are detected in a similar time horizon (e.g., 24 hours) in different parts of a WDS to be determined. Aggregated risk was expressed using the concept of a reference point and the DM's preferences between the likelihood and impact components of risk. The OWA operator was applied to calculate an overall aggregated risk of an alarm, which together with the state of an alarm reflected its significance. Based on the outcomes of the alarm prioritisation, WDS operators can pay more attention to the most severe incidents first.

CHAPTER 4 DSS IMPLEMENTATION

4.1 Introduction

This chapter aims to put the methodologies proposed in Chapter 3 into a broader context of a near Real-Time (R-T) DSS for the operation of WDS under abnormal conditions. More specifically the overall architecture of this DSS will be described and details of the implementation of the main DSS modules, arising from the work presented in this thesis, will be discussed. Additional components of the DSS, such as an intervention management module (Vamvakeridou-Lyroudia *et al.* 2009) or an interactive User Interface (UI) described in Morley *et al.* (2009), which were not directly implemented by the author, will not be described here.

First an overview of the whole architecture of the DSS is provided followed by a discussion on the design of a Database (DB), which forms the core of the entire DSS. Then the functionality of background modules, which implement the risk-based diagnostics methodology proposed in Chapter 3, is described. Distributed computing, one of possible solutions to achieve a near R-T performance required in WDS operation and failure management, will be discussed in section 4.4.3.1. The process of R-T visualisation of GIS data as implemented by the author in one of the UIs of the DSS will be briefly mentioned here as well.

4.2 Architecture Overview

As discussed by Morley *et al.* (2009) the DSS was designed in a modular fashion to maximise its extensibility in the future. Figure 4.1 provides a high level overview of a possible architecture of a near R-T DSS for operation of WDS under abnormal conditions. Off-line modules utilised by the DSS for one-off data import or model calibration are not included in the figure. A loose form of coupling between individual modules (i.e., mostly via a DB) was chosen to facilitate their integration within the DSS. All inter-process communication is achieved indirectly by polling information stored in a DB or alternatively through Hypertext Transfer Protocol (HTTP) requests (e.g., the interaction between the “System Overview” and the “Alarm Diagnostics” UI modules of the DSS front-end).

The entire DSS can be divided into several main blocks: (1) Back-end, (2) Front-end and (3) External modules as highlighted in Figure 4.1 using different colours. The focus of this work is on the back-end part, which contains an implementation of the methodologies presented in this thesis.

To maximise the ease of integration of various DSS modules, Microsoft .NET was chosen as the main implementation platform. The majority of the source code was written in the C# programming language. The web-based application providing the “System Overview” was implemented in Personal Home Page (PHP), a server-side scripting language, and JavaScript.

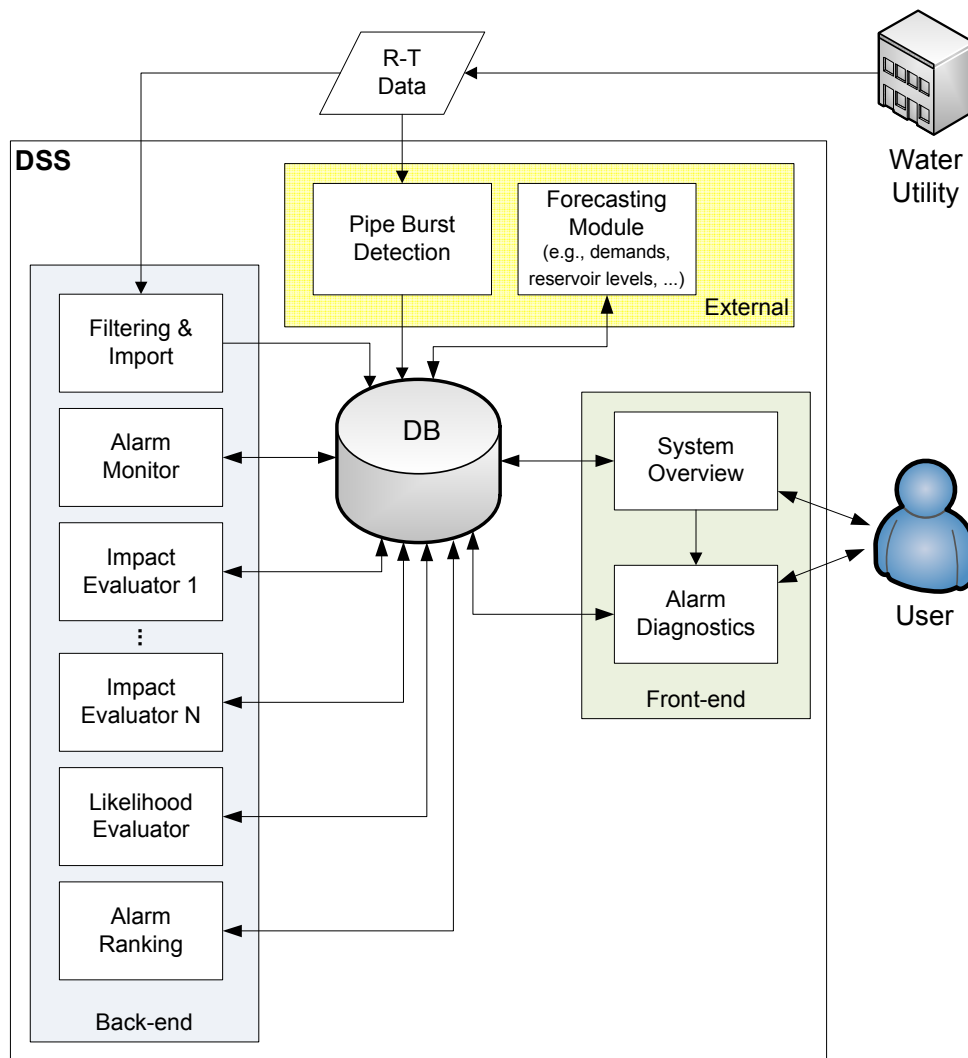


Figure 4.1 A simplified overview of DSS architecture

4.3 Database Management System

A Database Management System (DBMS) was employed by the DSS to provide concurrent access to data utilised by a number of processes that form the DSS as shown in Figure 4.1. Most of the DBMS nowadays are Relational Database Management Systems (RDBMS), which are built upon strong theoretical foundations of relations laid by Edgar F. Codd (1970). Despite the popularity of the object oriented programming paradigm, which was applied in the DSS implementation, purely Object Oriented Database Management Systems (OODBMS) have not become widely used and are typically only deployed in specialised applications. The primary reason for this was the lack of theoretical foundations underlying the OODBMS. The Object-Relational Database Management Systems (ORDBMS) attempt to fill-in the divide between purely RDBMS and OODBMS, exploiting the advantages of both approaches.

ORDBMS were built upon the strong theoretical foundations of RDBMS, however, they offer a number of appealing object oriented features including user defined types, methods and inheritance that can be found in OODBMS. One of the main advantages of an ORDBMS is that it can store complex user defined types, such as geometries containing spatial information associated with a particular record. This allows the storage of GIS data in a relational DB and spatial queries to be performed on the data in an efficient manner thanks to special index structures.

The PostgreSQL (Worsley and Drake 2002) ORDBMS, together with its spatial extension PostGIS (Refractions Research 2009) was chosen as a DBMS platform in this work. This combination allows easy storage and retrieval of relational as well as spatial data. A simplified structure of the DB used by the DSS is shown in Figure 4.2. Only the main tables, out of 54 tables used by the DSS are shown in the figure. The colour coding indicates which datasets were directly provided by a water utility and which were generated or derived during the development of the DSS. The border of the tables in Figure 4.2 identifies whether a particular table contained spatial information or not.

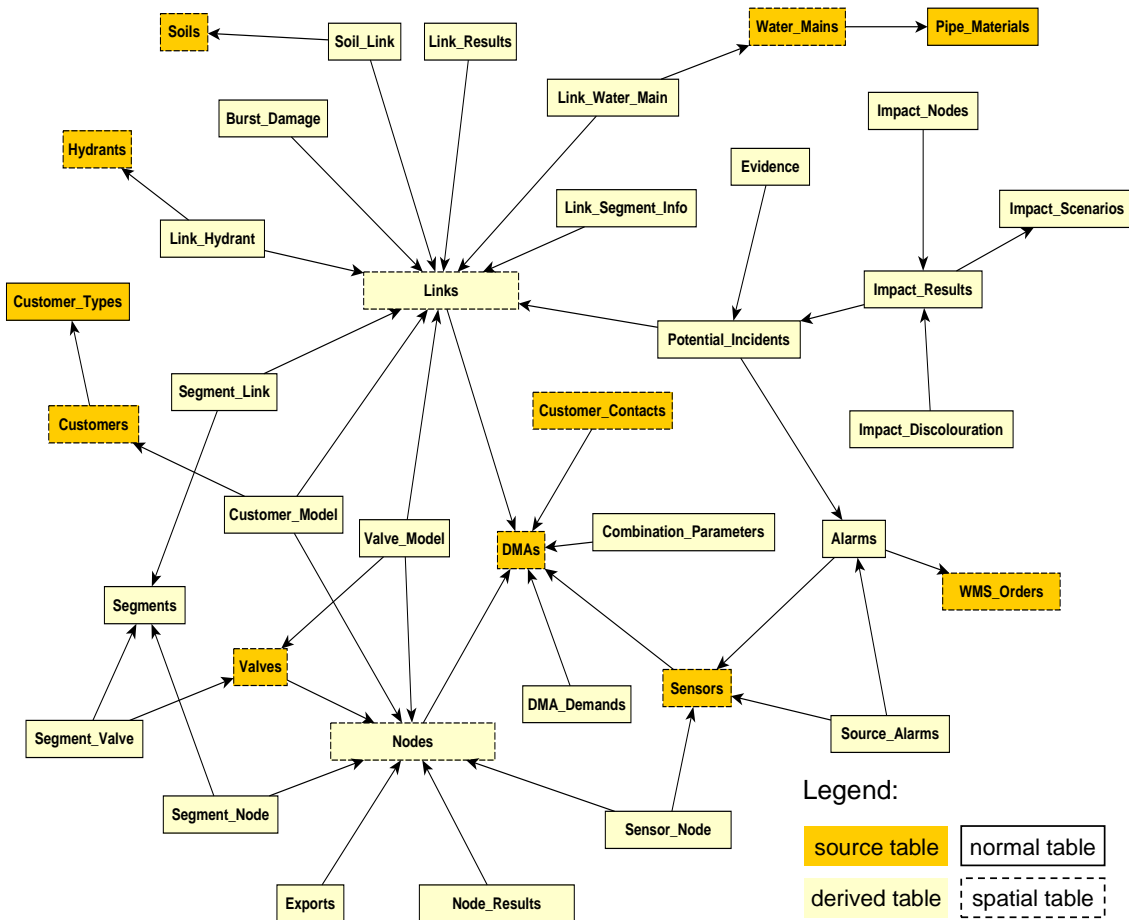


Figure 4.2 An entity-relationship diagram capturing the main tables used by the DSS

The key tables in Figure 4.2 are the “Links” and “Nodes” tables that were imported from an HM of the WDS. A number of associations were then constructed, typically using spatial analysis, representing the mutual relationship between the HM and additional data sources (e.g., Customers, DMAs, Valves, etc.). The second main group of tables (e.g., Source_Alarms, Alarms, Evidence, Potential_Incidents, Impact_Results, etc.) is responsible for the management of alarms and storage of the results of the risk analysis described in Chapter 3.

To maximise the portability of the whole DSS and avoid reliance on a particular type of DBMS used (e.g., PostgreSQL), the Open Database Connectivity (ODBC) standard was employed. ODBC provides a standardised Application Programming Interface (API) to communicate with a DBMS. Every module, which is part of the DSS, uses ODBC to access the PostgreSQL DBMS.

4.4 The Back-End

The back-end part of the DSS comprises a number of non-interactive background processes that are primarily responsible for:

- Import of near R-T data received from a water utility into a DB and its filtering
- Monitoring of newly received alarms (**Alarm Monitor**)
- Distributed evaluation of the impact of a failure (**Impact Evaluator**)
- Evaluation of the likelihood of pipe failure within a DMA (**Likelihood Evaluator**)
- Prioritisation of alarms (**Alarm Ranking**)

The data import and filtering modules are responsible for processing and importing near R-T pressure and flow data (received every 30 minutes), Customer Contact (CC) data and information from a Work Management Systems (WMSY) (received twice per day). The data is transferred from a water utility using the File Transfer Protocol (FTP).

The remaining four back-end processes form the core of the implementation of the risk-based anomaly diagnostics methodology presented in Chapter 3. Figure 4.3 shows an activity diagram in Unified Modelling Language (UML) capturing the interaction of those processes.

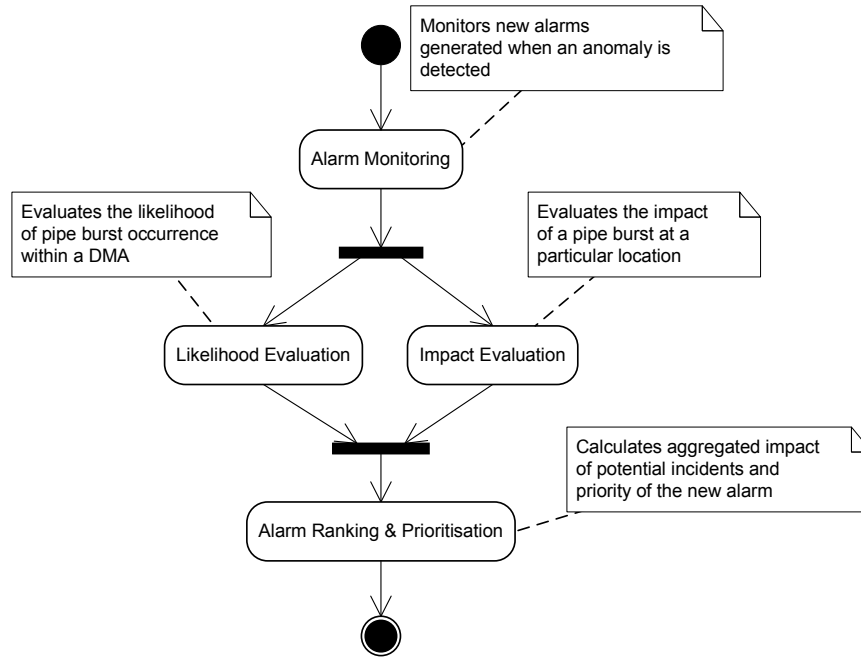


Figure 4.3 The interaction of processes involved in anomaly diagnostics

At first the presence of new alarms generated by the external pipe burst detection module (see section 4.6) is periodically checked by the *Alarm Monitor*, which is described in more detail in section 4.4.1. Once a new alarm is identified, the risk assessment can commence. This is achieved by concurrently evaluating the *Likelihood* and *Impact* of all potential incidents (i.e., possible causes of an alarm). Finally, after the risk assessment is completed, the aggregated impact of possible causes can be computed and all active alarms can be *Ranked and Prioritised* to determine the significance of the most recent event relative to the other active alarms.

4.4.1 Alarm Monitor

An activity diagram, which is similar to a flow diagram, of the Alarm Monitor is shown in Figure 4.4. The process periodically checks the contents of the “source alarm” table in the DB (see DB schema in Figure 4.2) and in case a new (fresh) alarm is discovered, it performs necessary initialisation steps before the risk assessment can be started. The initialisation stage involves generating a set of potential incidents associated with an alarm. This set by default comprises all pipe segments within a DMA from where the alarm originated. The current implementation of the module is only limited to diagnostics of pipe bursts. As previously discussed, extension to include other types of failures is possible. Furthermore, a new HM (i.e., an EPANET input file) of the whole

system (i.e., not necessarily only the investigated DMA) is generated for every alarm, as part of the initialisation stage. The new custom HM contains forecasted boundary conditions and is used in the next Impact Evaluation phase. Should R-T information about active devices (such as valves, pumps, etc.) be available at the time that the custom model is created, it could also be incorporated to provide a more realistic picture of the WDS.

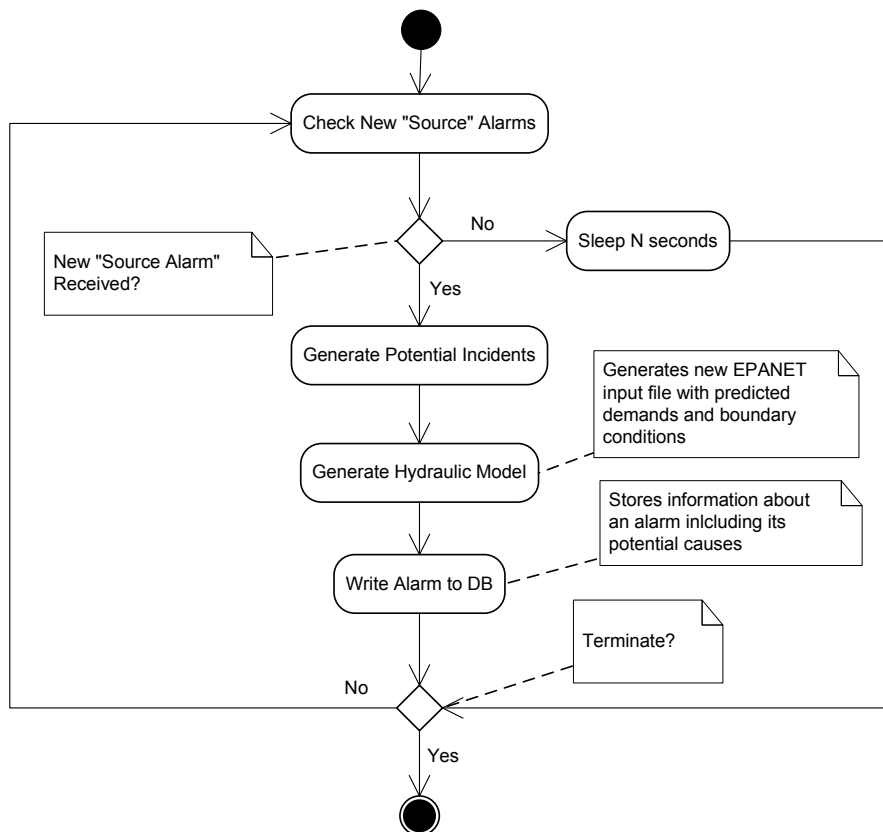


Figure 4.4 An activity diagram describing the Alarm Monitor module

Setting the boundary conditions in the new model involves the calculation of pattern multipliers for all demand nodes and reservoirs at every time step over the next 24 hours (i.e., the default risk horizon). Pre-computed forecasts (i.e., using the external forecasting module shown in Figure 4.1) of relevant variables, i.e., DMA inflows and outflows, exports from the WDS and reservoir levels, are retrieved from a DB. Ideally, the forecasted boundary conditions should be updated every time new measurements are obtained from the field. This would allow a re-evaluation of the impacts of potential incidents using real observations. In the current implementation forecasting is carried out only once in 24 hours. The forecasted boundary conditions are imposed in the new

custom model either directly in case of reservoir levels or exports by modifying their diurnal patterns, or indirectly in case of DMA demands. It is assumed that the increase or decrease of water consumption by all consumers within a DMA is proportional to their average water consumption. On this assumption the average base demands of individual demand nodes at every time step are scaled (up or down) to match the forecasted consumption of the whole DMA at given time.

When a prediction of DMA inflow or outflow is not available (e.g., long term sensor failure preventing the prediction of future demands) the average nodal demands of this particular DMA, stored in the default EPANET input file, are used instead. Should cascading DMAs be present in the system (i.e., a DMA supplies another DMA downstream) and forecasts were not available for any of the downstream DMAs, then average demands are used in all upstream DMAs as well to avoid any flow balance problems.

For the sake of simplicity, pressure measurements from the field were not considered as additional boundary conditions when redistributing nodal demands since this would require the adoption of a more sophisticated state estimation technique (e.g., Machell *et al.* 2009; Preis *et al.* 2009).

Once the new HM is generated, a new alarm record, including a set of potential incidents associated with this alarm, are then stored in a DB. The presence of the new alarm consequently triggers the risk assessment carried out separately by the Likelihood and Impact Evaluators described below.

4.4.2 Likelihood Evaluator

Figure 4.5 shows an activity diagram of the Likelihood evaluator, which is a process responsible for determining the likelihood of occurrence of every potential incident within a DMA where an alarm was generated. The likelihood evaluator periodically checks for new alarms, whose likely cause needs to be identified. Once a new alarm is recognised, the individual models (i.e., a PBPM, a CCM and an HM) are initialised and a set of all potential incidents associated with an alarm (i.e., those previously generated by the Alarm Monitor) are loaded.

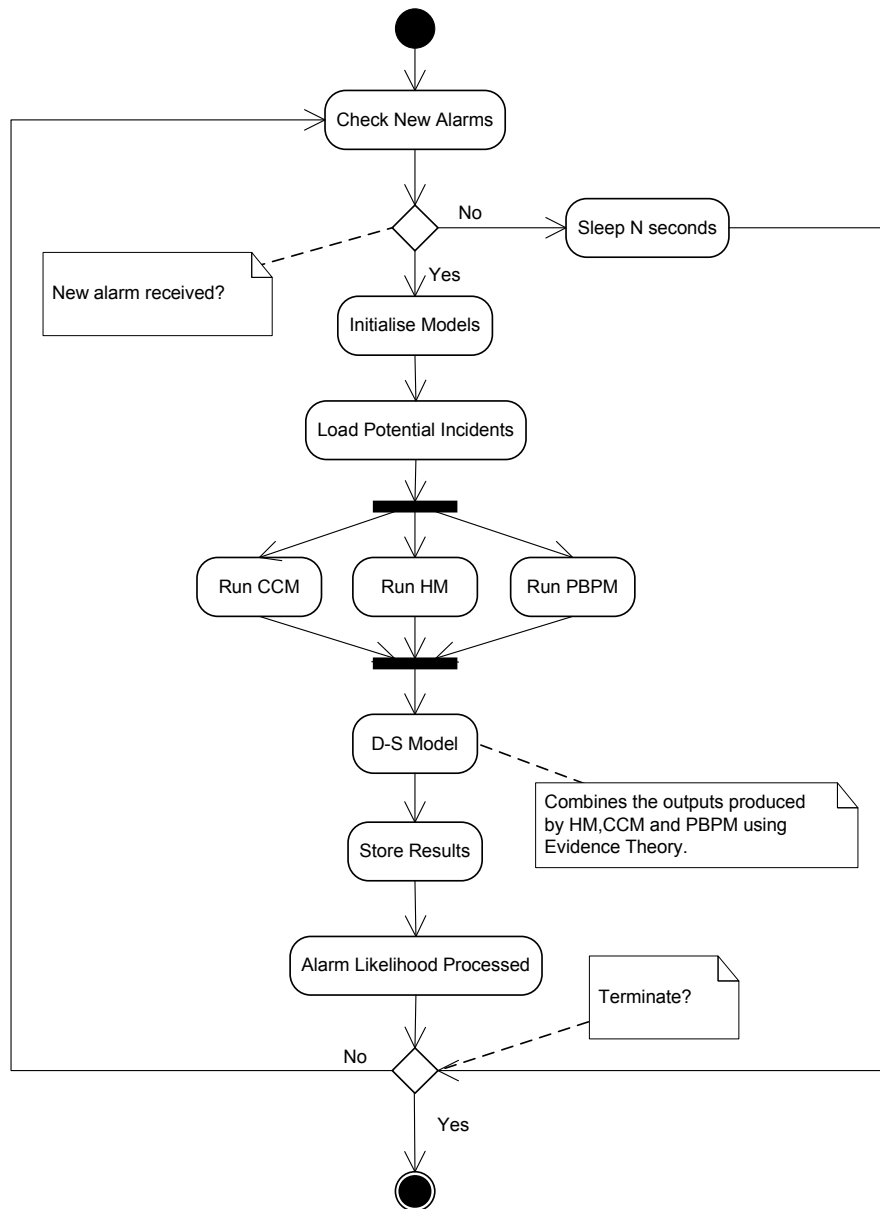


Figure 4.5 An activity diagram describing the Likelihood Evaluator module

The model initialisation stage involves the retrieval of CCs from the affected DMA that were recorded 24 hours before the detection of the burst and during the same day. For the PBPM pipe properties (e.g., age, material, diameter, etc.), the characteristics of the surrounding soil, type of the land above the pipe, average weather conditions and historical burst rates are loaded from a DB. The initialisation of the HM requires the loading of an EPANET model of a given DMA (i.e., not a model of the whole WDS as in the case of the Impact Evaluator) and the retrieval of pressure and flow measurements associated with the DMA (e.g., inflows, outflows and pressures) at the time of the burst detection. The DMA EPANET model is then dynamically adjusted, as described in

section 3.3.2.3, to impose inlet pressure boundary conditions and establish flow balance between the model and flow measurements from the field.

Three different models that are capable of providing evidence about the likely / unlikely location of the burst within a DMA are then executed. Each of the available models (e.g., CCM can be excluded in situations when no CCs were recorded) provides a value of criterion measurement for every potential incident. The model outputs then undergo the information fusion process in the D-S Model as described in section 3.3. Once the information fusion is completed, the combined likelihood (i.e., *BetP*) as well as the underlying evidence provided by the individual models are stored into a DB for future visualisation using the interactive Alarm Diagnostics UI, which is part of the DSS front-end (see Figure 4.1).

4.4.3 Impact Evaluator

A high level activity diagram of the Impact Evaluator is shown in Figure 4.6. The figure describes a distributed implementation of the Impact Evaluator, which can be run on a number of computers simultaneously. Similarly to the Likelihood Evaluator described above, the process also monitors the alarms table for newly generated alarms. If a new alarm, which requires impact assessment, is recognised, the process attempts to load an EPANET model of the whole WDS, which was generated by the Alarm Monitor (described in section 4.4.1) and includes forecasted boundary conditions for this new alarm. Should the custom model be not available for some reason (e.g., the Alarm Monitor process failed to generate an input file) the impact assessment reverts to use the base model of the WDS, with average demands only.

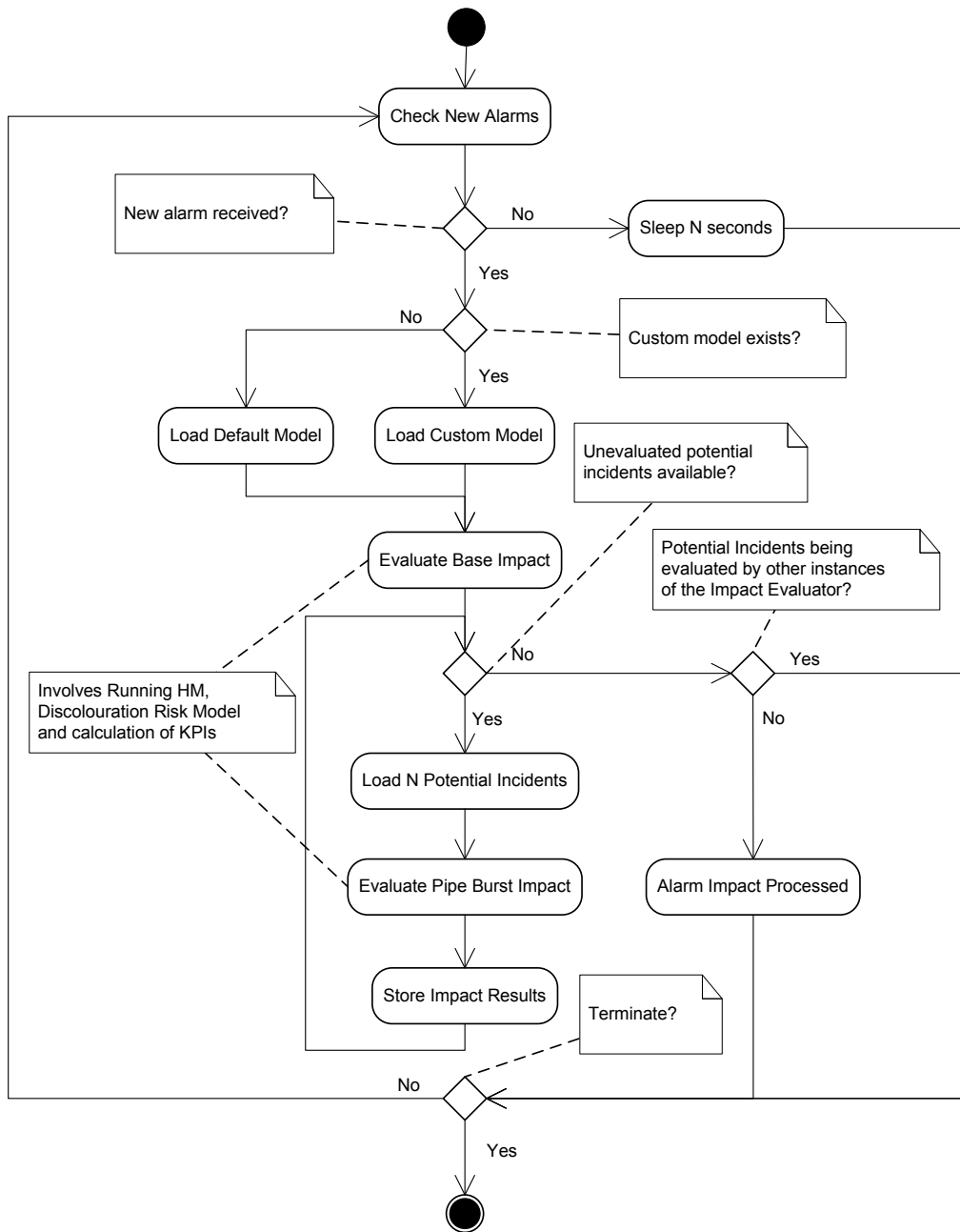


Figure 4.6 An activity diagram describing the Impact Evaluator module

Once the HM is loaded and initialised, first a base line scenario, representing the state of the WDS under normal conditions, is evaluated. The baseline scenario serves to determine normal flows and pressures in the WDS, which are used to calculate the discolouration potential of every pipe in the system under such conditions. Consequently, the Impact Evaluator starts retrieving batches of potential incidents (the number of potential incidents retrieved at a time needs to be selected according to the number of instances of the Impact Evaluator). Only those potential incidents whose

impacts have not yet been evaluated (e.g., by another instance of the Impact Evaluator) are loaded at this stage. For every potential incident, its impact on the whole WDS is evaluated by running an HM, discolouration risk model and calculating KPIs proposed in section 3.4.4. The results are then stored into a DB and the potential incidents are marked as evaluated. In case there are no unevaluated potential incidents available in the DB and no other instances of the impact evaluator are processing potential incidents associated with an alarm, the alarm can be flagged as processed and its impact evaluation is completed. This final step is required only in the distributed version of the Impact Evaluator and assures that an alarm is flagged as processed only after all other instances of the Impact Evaluator (e.g., running on different computers) finished its processing.

Ideally, the pressure driven hydraulic solver should be able to reach a solution for every configuration of a WDS. The gradient algorithm proposed by Todini and Pilati (1988) might be unable to converge under certain circumstances (e.g., when pipe resistances are too high or velocities in the system are too low). If the pressure driven hydraulic solver used (i.e., Morley and Tricarico 2008) fails to converge when simulating a pipe burst, an exception is generated. The potential incident whose impact evaluation failed is then flagged in the DB so that its impact can be excluded from further risk analysis.

4.4.3.1 Distributed Computing

The primary focus of the methodology presented in this thesis is to support near R-T decision-making. Evaluating the impact of all potential failures within a DMA at system level (rather than DMA level only) requires hundreds of runs of a hydraulic solver on a large network, typically containing thousands of nodes and pipes. Therefore, it is computationally demanding as those runs cannot be performed off-line (i.e., pre-computed). This is a consequence of the need to consider the current state of the system based on information from: (i) pressure and flow monitoring devices, (ii) magnitude of abnormal burst flow and also (iii) predictions of demands and reservoir levels. Even with the high-performance personal computers available nowadays impact evaluation of a single failure can take up to several seconds, which makes its application in the near R-T domain difficult. To increase the speed of impact evaluation, a database-centric distributed architecture was implemented (see Figure 4.7).

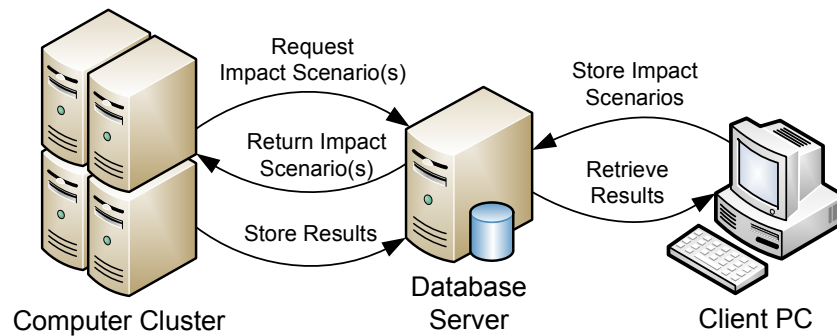


Figure 4.7 A database-centric architecture for distributed impact evaluation

The proposed distributed computing architecture builds upon strong transaction processing capabilities of modern RDBMS. A RDBMS serves as a mediator between a client application and a computer cluster comprising several nodes. The distributed impact evaluation is carried out in following steps: (1) the client application inserts a set of impact scenarios into the DB; (2) each of the processes running on the computing nodes in the cluster periodically attempts to retrieve new scenario(s) from the DB; (3) if a new failure scenario(s) is/are retrieved from the DB, their impact is evaluated; (4) the results are stored back into the DB; and (5) the client application retrieves the results of evaluated impact scenarios.

4.4.3.2 Performance Evaluation

The architecture presented above has proved to be suitable for the given application since the time required to retrieve failure scenario(s) and to store the results into a DB was negligible compared to the time needed to evaluate the impact of one potential incident. Implementation of this distributed application was conceptually simple and the solution should be well scalable.

Evaluation of the performance gains using distributed computing was carried out on a 4 node computing cluster. All the machines in the cluster had identical hardware configuration and were connected using 1Gb/s Ethernet network (to minimise communication latency). The hardware configuration of the nodes was as follows: Intel Core 2 Quad Central Processing Unit (CPU) Q8300 @ 2.5GHz and 4GB of RAM. Different versions of the operating system were installed on each of the computing nodes, which had only a minimum impact on the difference in overall performance of the individual nodes. One of the computing nodes in the cluster acted as a DB server

and its load was always balanced in such a way that the DBMS had sufficient resources available to handle client requests.

The scalability of the current implementation of the distributed impact evaluation is shown in Figure 4.8.

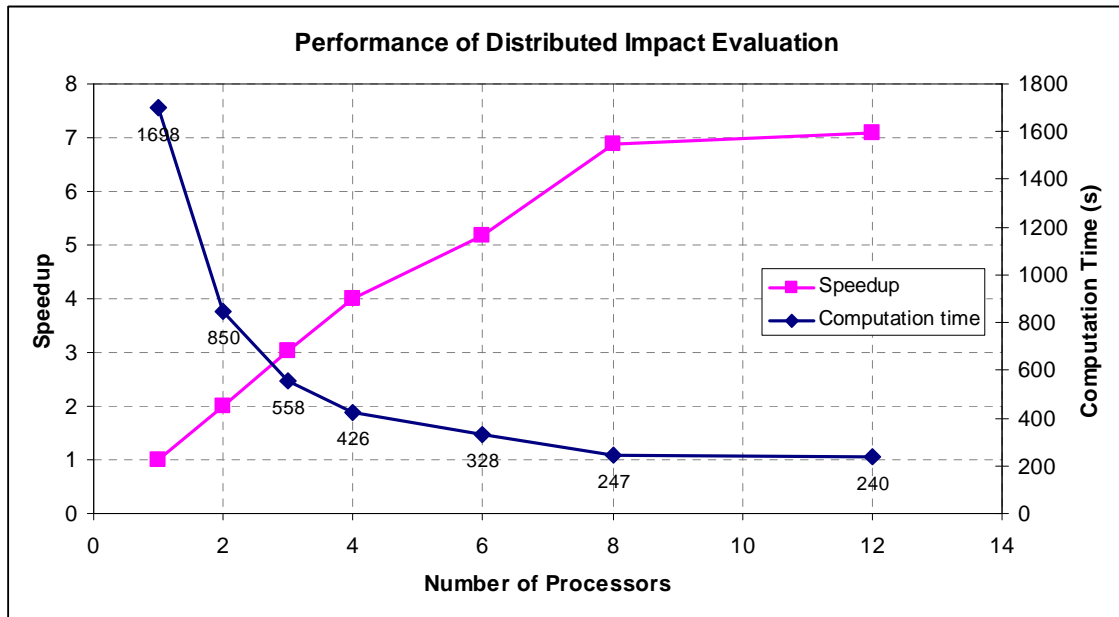


Figure 4.8 Speedup achieved using distributed computing

The figure shows the approximate total time in seconds required to perform a complete impact evaluation of 469 pipe bursts in an urban DMA as well as the speedup achieved (i.e., a ratio of time required by a sequential algorithm and the distributed one) as defined in Eq. (4.1).

$$S_p = \frac{T_1}{T_p} \quad (4.1)$$

where: p is the number of processors, T_1 is the execution time of the sequential algorithm and T_p is the execution time of the parallel algorithm with p processors

The impact assessment was carried out using a pressure driven HM that comprised over 9,000 pipes and 8,700 nodes (i.e., impact of the burst in a DMA was evaluated at system level). The loading of the processes on the nodes was done in such way that the number of processes per node was minimised. Moreover, it was attempted to avoid running any processes on the node with the DB server where possible. The polling frequency (i.e.,

how often the client nodes access the DBMS) as well as the number of impact scenarios retrieved at a time (i.e., one at a time in the current setup) can influence the total duration of the impact evaluation. The influence of these parameters was not studied in detail. It is believed that it is marginal and can be easily tailored to best suit a given distributed environment (i.e., a computing cluster).

As can be seen from Figure 4.8, the solution scaled up almost linearly up to 4 processors (i.e., 1 instance of Impact Evaluator running on all 4 computing nodes). When multiple instances of the impact evaluator were created on a single node the performance has dropped significantly. This can be observed in scenarios with 6 (i.e., 2 processes on each of the 3 nodes used), 8 (i.e., 2 processes on all 4 computing nodes) and 12 (i.e., 4 processes on each of the 3 nodes used).

Figure 4.9 shows the difference in speedup when multiple instances were launched on a single multi-core computer and when the instances were distributed across a number of physical machines. This figure suggests that the scalability issue in current implementation is not caused by communication overheads when impact scenarios are retrieved from and stored into the DB (see the almost linear speedup curve of the configuration with N nodes).

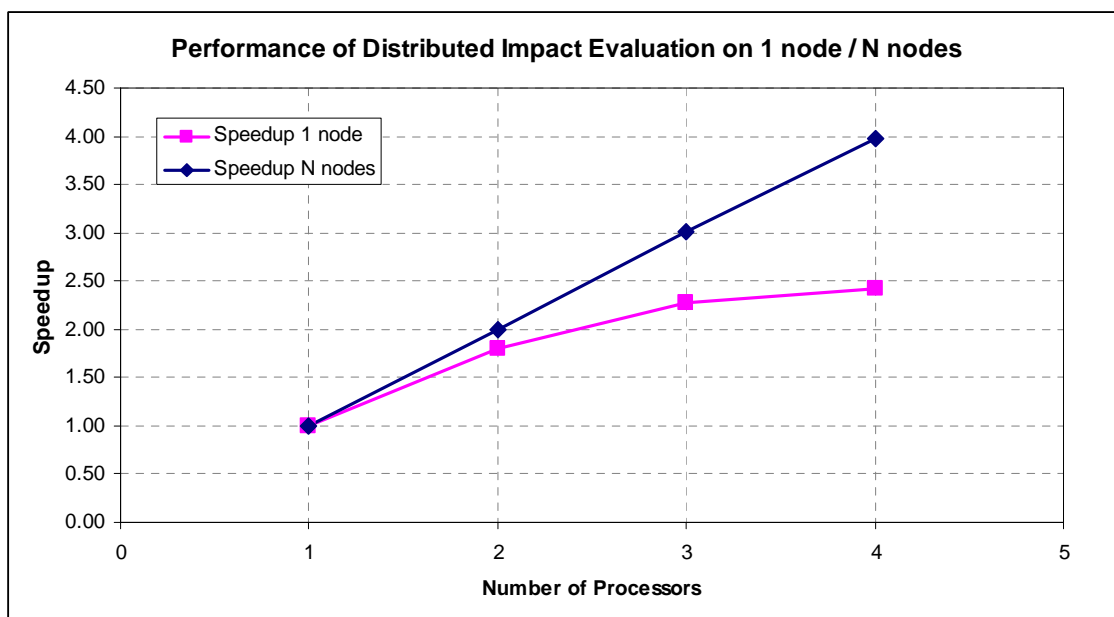


Figure 4.9 Speedup achieved using distributed computing on 1 node vs. N nodes

Profiling of the source code revealed that the slowdown apparent when multiple processes (i.e., instances of the Impact Evaluator) were run on a single computer was most likely caused by an inefficient memory management of the Impact Evaluator. This could be either due to improper use of data structures offered by the Microsoft .NET Framework or possibly by the garbage collection mechanism (i.e., an automatic freeing of unused memory). Table 4.1 shows the time in milliseconds required to perform selected actions as shown in Figure 4.6 to evaluate impact of a single potential incident. The timings of the part of the code responsible for accessing the DB are highlighted in green and it can be observed from the table that the DB access did not vary significantly amongst the different scenarios. On the other hand, the time required to complete memory and CPU intensive operations (i.e., the HM Run, KPI Evaluation and Results Generation), which comprise the Evaluate Pipe Burst Impact block, as shown in Figure 4.6, deteriorated significantly.

Table 4.1 Results of profiling of the distributed Impact Evaluator

Scenario	Load Potential Incident	Evaluate Pipe Burst Impact			Store Results
		HM Run	KPI Evaluation	Results Generation	
Single process	5.3 ms	1742.8 ms	116.3 ms	297.7 ms	8.4 ms
2 Processes 2 machines	4.4 ms	1757.6 ms	116.3 ms	297.3 ms	7.1 ms
2 Processes 1 machine	5.2 ms	2088.6 ms	126.8 ms	361.2 ms	7.7 ms
4 Processes 1 machine	5.1 ms	3467.4 ms	196.1 ms	589.2 ms	7.9 ms

The slowdown when multi-core computers are used can be seen as an obstacle in large scale deployment of the application given the wide availability of multi-core CPUs nowadays. Nevertheless, the distributed impact evaluation as proposed in this work is generally a well scalable problem. The sequential part of the algorithm, which includes mostly loading of required data and initialisation of the HM takes approx. 10s (i.e., 0.5% of the overall sequential runtime on 469 potential incidents) on the hardware described above.

4.4.4 Alarm Ranking

Figure 4.10 depicts an activity diagram of the Alarm Ranking process. This process concludes the risk-based methodology by performing impact aggregation and alarm prioritisation. Similarly to the Likelihood and Impact Evaluators, the process also monitors the alarms table in the DB. Once an alarm that underwent the complete risk

analysis (i.e., the likelihood and impact of all its potential incidents were evaluated) is found, then the ranking process is initiated. At first, all active alarms that need to be re-prioritised are loaded. Next, the process retrieves all potential incidents, including their non-aggregated impact metrics at a given risk horizon (i.e., 24 hours), associated with those alarms. The aggregation of impacts of potential incidents can only take place once the KPIs off all considered potential incidents are known since the normalisation of impact KPIs (described in section 3.4) takes place across all active alarms. Once the aggregated impacts of all potential incidents are re-computed, the alarm ranking methodology (see section 3.5) can be applied.

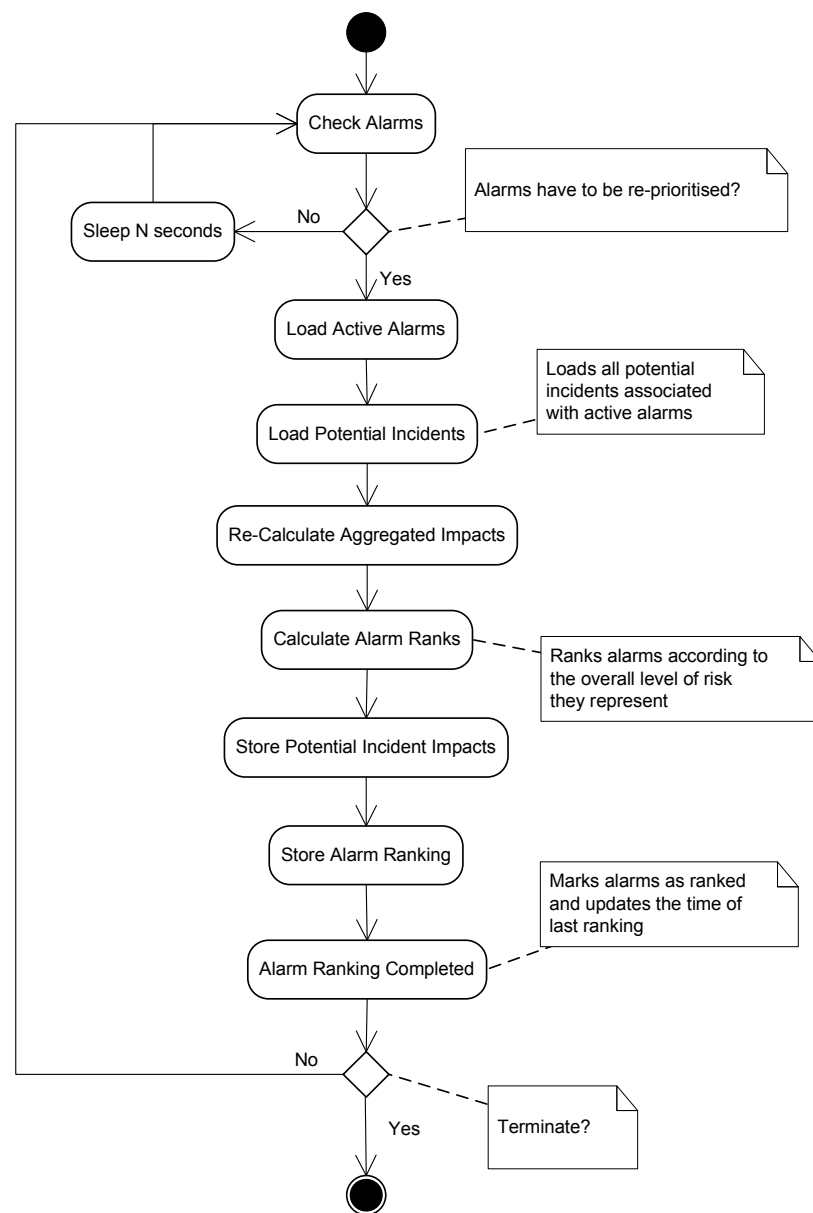


Figure 4.10 An activity diagram describing the Alarm Ranking module

A caching mechanism was implemented to improve the efficiency of calculating the maximum entropy weights. The weights for a particular value of parameters α and n are stored in a DB and can be efficiently retrieved when needed. When a desirable value of parameter α is determined by the DM, the cache could be seeded with all weights for common values of n (i.e., the number of potential incidents within a DMA) and given a level of attitude towards risk α . The structure of the tables used to store the weights is shown in Figure 4.11.

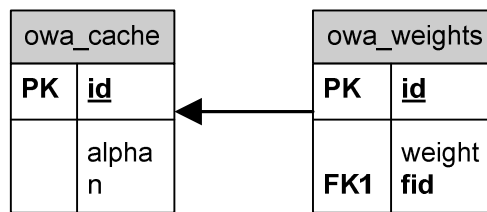


Figure 4.11 Table structure of the cache used to store maximum entropy weights

Once the alarm ranking is completed, results, including the newly computed aggregated impacts and alarm priorities, are stored into the DB. The alarm can then be flagged as ranked and only at this point it is presented to an operator through the “System Overview” UI, described further in section 4.5.1.

4.5 The Front-End

The processes that form part of the front-end (see Figure 4.1) are responsible for presenting the outcomes of the risk-analysis as well as additional relevant information to the end user (i.e., a control room operator) of the DSS. At any time, an overview of the near R-T state of the entire WDS is available to the operator through a prioritised list of all alarms (i.e., detected anomalies) as well as through using a GIS interface. This is achieved by a multi-user web-based application, which is introduced in the following section. Detailed results of the risk analysis are then made available to the end user through the “Alarm Diagnostics” UI, which has not been developed as part of this thesis and will not be described here.

4.5.1 System Overview User Interface

This section discusses the development of a web-based application that provides the DSS user with a near R-T overview of alarms in a WDS through a GIS and an alarm list. The GIS visualisation comprises several layers overlaid on top of a background

map as illustrated in Figure 4.12. The GIS layers contain information about sensors that were in an alarm state (note the red dots in Figure 4.12) over a specified period of time (e.g., 7 days), DMA boundaries, topology of the WDS, etc.

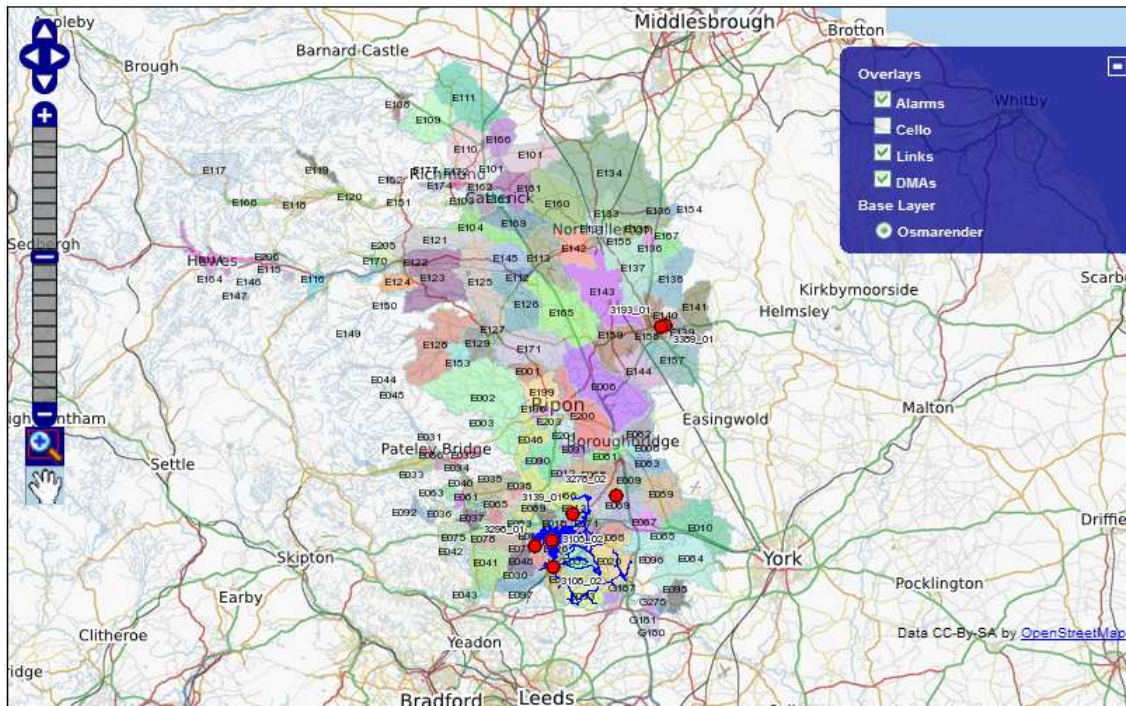


Figure 4.12 A screen capture of GIS layers projected on top of a background map

A number of approaches to visualise data stored in a spatial DB (e.g., sensors in an alarm state) can be adopted. Figure 4.13 shows a possible setup used to serve GIS layers to end users using a MapServer (Kropla 2005). MapServer provides a number of interfaces to access spatial data (e.g., stored in a PostgreSQL DB with PostGIS spatial extensions). The most commonly used protocols to access GIS data nowadays are the Web Map Service (WMS) and Web Features Service (WFS) standards developed by the Open Geospatial Consortium (OGC). The WMS and WFS standards are supported by all major GIS software packages, including ArcGIS.

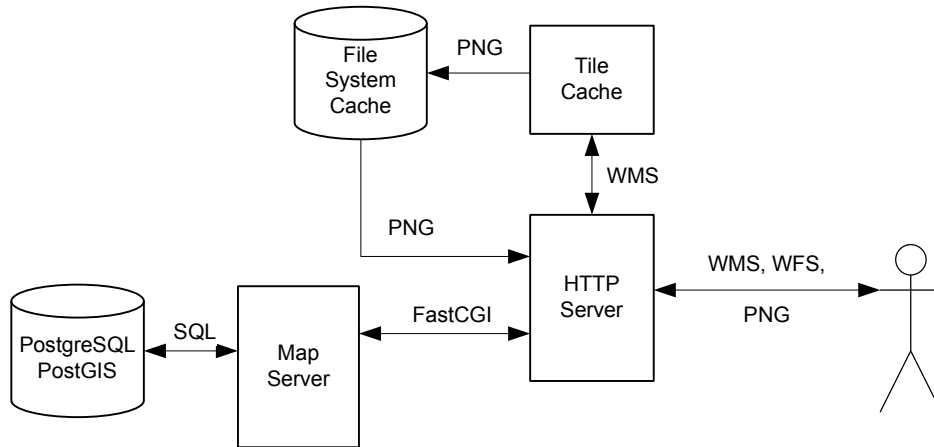


Figure 4.13 Online generation of GIS layers from a spatial DB

MapServer can be accessed by end users (or other processes such as a Tile cache) as a web application hosted on a HTTP server (e.g., Apache HTTP server). Users are thus allowed to retrieve layers using HTTP requests in a number of formats. GIS layers rendered in raster format can be retrieved using the WMS protocol or alternatively vector data can be requested using the WFS protocol. In case of WMS, the most commonly used format to render GIS data is the Portable Network Graphics (PNG) format thanks to its suitable compression.

To request a GIS layer, a MapServer needs to perform a spatial query on a DB, then retrieve and process the results. Such an approach might represent a potential performance bottle neck when the number of requests is too high. It is frequently the case that web-based GIS visualisation frameworks (e.g., OpenLayers) split an image into a number of smaller tiles to allow smooth panning and navigation over a GIS map. Since information in some of the layers presented to the user does not change frequently (e.g., DMA boundaries) it is possible to store such layers in the form of cached tiles (i.e., images of fixed size, typically 256x256 pixels containing the graphical representation of a particular area at given zoom level). The tiles that are rendered off-line can then be efficiently served to the end user without requiring any additional resources of the DBMS as well as the MapServer. The Tile cache can be periodically refreshed when needed (e.g., during night hours) to reflect long term changes in the underlying data.

4.5.1.1 Alarm List

Information about sensors in an alarm state is also available through an alarm list (see Figure 4.14), which lets the user perform further actions. The alarm list contains information such as (1) the time when an alarm was received; (2) Alarm ID (in the “Investigate” column) in case further investigation is possible; (3) Alarm state; (4) Alarm priority; (5) ID of a sensor, which triggered the alarm; (6) ID of an affected DMA; (7) estimated burst flow; (8) Control button; and (9) additional information about the alarm.

Operators can start the investigation of an alarm, which allows the exploration of detailed results of risk-based diagnostics of possible causes of an alarm, using the interactive Alarm Diagnostics UI. The interaction between the web application and the Alarm Diagnostics UI is achieved by sending an HTTP request. The HTTP request acts as a message and carries information about an alarm to be investigated. This allows asynchronous communication between the two main front-end applications.

The alarm list also allows users to invoke a trend display to visualise data associated with a particular sensor in an interactive way. The trend display contains 2 panes, where the bottom pane provides an overview of the trend over the past 2 weeks and the main top pane provides the trend of a dynamically selected period of time using the bottom pane.

Time	Investigate	State	Priority	Sensor	DMA	Burst Flow	Update	Notice
16. 03. 2010 04:15	3234	Active <input type="button" value="v"/>	Processing (0.0%)	3105_02	E021	2.7 l/s	<input type="button" value="Update"/>	FULL DATA FOR TRAINING
14. 03. 2010 22:17	-	Active <input type="button" value="v"/>	-	3278_02	E070	1.0 l/s	<input type="button" value="Update"/>	FULL DATA FOR TRAINING
13. 03. 2010 22:15	3232	Active <input type="button" value="v"/>	Processing (0.0%)	3108_02	E054	0.7 l/s	<input type="button" value="Update"/>	FULL DATA FOR TRAINING
13. 03. 2010 17:18	-	Active <input type="button" value="v"/>	-	3389_01	E140	-	<input type="button" value="Update"/>	FULL DATA FOR TRAINING
13. 03. 2010 16:19	-	Queued	?	3581_01	?	-		FULL DATA FOR TRAINING
13. 03. 2010 16:16	-	Active <input type="button" value="v"/>	-	3193_01	E159	-	<input type="button" value="Update"/>	FULL DATA FOR TRAINING

Figure 4.14 An example of an alarm list

When the nature of an alarm is verified (e.g., by a field technician dispatched to the field) it is also possible to change the state of an alarm (e.g., to Real or False) and thus affect its overall priority. Should the automatic prioritisation performed by the DSS

(using methodology described in chapter 3.5) provide priorities that are not in agreement with the judgement of the operators, these can be manually overridden. In the current implementation the manually overridden priority has only a temporary effect and is reset when alarm re-prioritisation takes place with the arrival of a new alarm.

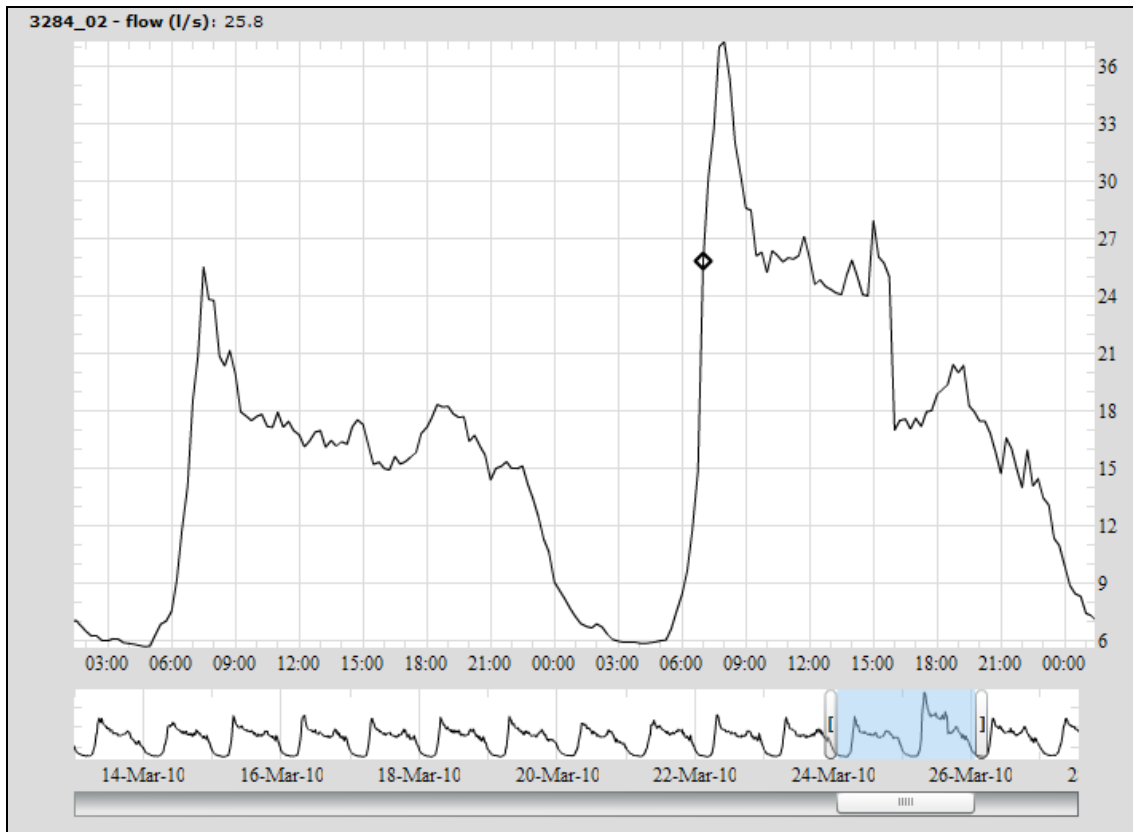


Figure 4.15 An interactive trend display

The alarm list could be easily extended to capture the exact cause of real alarms by associating them with main pipe repairs from a WMSY. Such feedback could then be used by the DSS to re-calibrate the D-S model used by the Likelihood Evaluator. The functionality to carry out the automatic re-calibration was not implemented since it represents a number of challenges and is suggested as part of future research in section 6.3.1.

4.6 External Modules

The DSS utilises two external modules responsible for near R-T detection of pipe bursts and forecasting of trend data. These modules were provided by academic partners as part of the NEPTUNE project (Savić *et al.* 2008).

The *Pipe Burst Detection Module* was developed by the University of Sheffield (Mounce *et al.* 2010). An ANN was trained on continually updated historic data to predict future flow profiles. The flow data measured every 15 minutes and provided by a water company once per hour is then compared with the predicted flows over a given time window using a Fuzzy Inference System (FIS). An alarm to notify control room personnel is generated and stored in a DB in case a significant discrepancy between observed and predicted data is discovered.

A *Forecasting Module*, to predict future water DMA demands, export flows and reservoir levels was developed by De-Montfort University. The module was part of an optimal pump scheduling software package FINESSE (Rance *et al.* 2001). The prediction is done in three stages: (1) screening, (2) smoothing and (3) forecasting. At first outliers in the data set are removed. Fast Fourier transform is then applied to reveal trends in the historical data. Finally, the Triple Exponential Smoothing is used to extrapolate the smoothed trend into the future.

4.7 Summary

This chapter provided details about the possible implementation of the risk-based decision support methodology for near R-T WDS operation under abnormal conditions presented in Chapter 3. The focus of the description was on the implementation of processes responsible for the background risk-analysis that were designed and implemented by the author.

A loosely coupled design of the risk-analysis and alarm prioritisation modules was used here to facilitate their integration. The methodology presented in Chapter 3 was broken down to 4 main modules, namely the Alarm Monitor, Likelihood Evaluator, Impact Evaluator and the Alarm Ranking and Prioritisation module. The functionality as well as implementation details of each of the aforementioned modules were discussed.

It was demonstrated that distributed computing can be exploited to speed up risk assessment of potential incidents. Given the reliance of impact evaluation on the use of an HM and the requirement to run an EPS, any overhead of inter-process communication is negligible compared to the computational time required to evaluate a single impact scenario. A database-centric distributed architecture was designed and

implemented. The theoretical scalability of such a solution should be very good (i.e., almost linear), however, the current implementation suffered serious slow down on multi-core CPUs.

The use of ORDBMS with spatial extensions has proved as beneficial since it significantly facilitated operating with GIS data. Thanks to the adopted approach, GIS data was effortlessly made available and visualised in a number of formats including WMS, WFS and PNG, using a MapServer. A web-based application, utilising the WMS technology, providing an overview of the near R-T state of a WDS (i.e., alarms) was implemented. To ensure scalability of the visualisation solution, its performance can be further improved by caching the static contents in the form of graphic tiles.

CHAPTER 5 CASE STUDIES

5.1 Introduction

This chapter illustrates the application of the models and methodologies presented in Chapter 3 on a number of real life and semi-real case studies. The software implementation of the back-end modules described in Chapter 4 was used to perform the testing. The availability of required data in sufficient quality and quantity was in some cases limited, which prevented the entire risk-based pipe burst diagnostics methodology being demonstrated on data collected from a real WDS.

This chapter is organised as follows. First, the use of a Hydraulic Model (HM) as a Real-Time (R-T) source of evidence suggesting the likely location of a burst pipe is demonstrated on real life Engineered Events (EE) in section 5.2. Second, the potential of applying information fusion, using the Dempster-Shafer (D-S) model presented in section 3.3, to locate a burst pipe is shown in section 5.3 on a number of historical pipe bursts with synthetic noisy pressure and flow measurements. Section 5.4 provides details of the calibration of the impact model introduced in Chapter 3.4. Results of an online questionnaire survey were analysed to derive a number of weighting factors reflecting the preferences of a water company. Finally, the automated prioritisation of alarms (i.e., detected abnormal events) is described in section 5.5 on a number of real life alarms detected over a period of two years.

The case studies presented in this thesis are based on data from a real life WDS located in the Harrogate and Dales area in North Yorkshire, UK as shown in Figure 5.1. The WDS in question supplied water to almost 25,000 properties with an average daily water consumption of 37 MI/d (in March 2010).

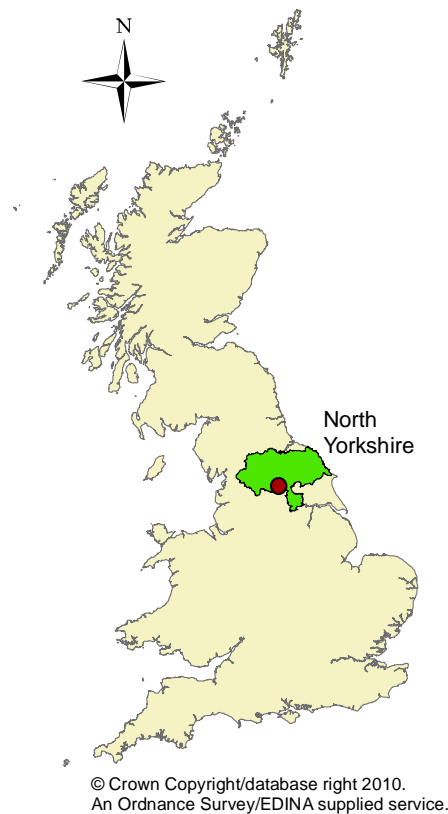


Figure 5.1 Location of the case study area in the UK

5.2 Hydraulic Model Evidence

The aim of this case study is to demonstrate the possibility of using calibrated HMs together with near R-T pressure and flow measurements to estimate the location of a burst pipe within a DMA. HMs were previously used in the attempts to locate leakage / bursts in a WDS and a number of methods similar to the one used here were proposed in the literature. Their validation using real field data was lacking and, therefore, the potential of the HM is demonstrated here. Hydrant openings were used in the past (e.g., Mounce *et al.* 2003) to simulate effects of pipe bursts. Similarly, in this case study data collected during a set of EEs, when fire hydrants were flushed at different locations within a DMA to simulate bursts, was used.

In EEs the application of the whole information fusion methodology as described in section 3.3 does not make sense since the location of the hydrant opening has, unlike a real burst, no correlation with the results provided by a Pipe Burst Prediction Model (PBPM). The abnormal flows introduced during EEs are within safe thresholds so that customers are not affected by low pressures. An EE will, therefore, not be reported by

customers since it is supervised by a field technician and, therefore, the use of a Customer Contacts Model (CCM) cannot yield any benefit. Therefore, the Likelihood Evaluator process, whose implementation was described in section 4.4.2 was modified, to exclude the information fusion portion and to output only the criterion measurements (i.e., the Sum of Squared Errors (SSE)) produced by an HM in this case.

First, results from two sets of EEs carried out in a relatively simple, tree-like DMA (see Figure 5.2) in a predominantly rural area will be presented here followed by an application of the HM in a more complex DMA (see Figure 5.7) with only a small number of pressure sensors. The first set of EEs in a simple DMA (section 5.2.1) was based on large burst flow simulations (i.e., approx. 36% of an average peak DMA inflow or 63% of an average inflow in April 2010) whereas the second set of EEs (section 5.2.2) was based on medium burst flows (i.e., approx. 10% of an average peak DMA inflow or 18% of an average inflow in April 2010). Section 5.2.3 presents the results achieved on medium burst flow simulations (i.e., approx. 6% of an average peak DMA inflow or 10% of an average inflow in April 2010) conducted in a highly looped urban DMA.

5.2.1 Large Burst Flow Simulations (EE1)

Figure 5.2 shows the layout of a predominantly dendritic DMA comprising 390 demand nodes and 373 pipes where the first set of large and medium burst flow simulations were conducted. The total mains length was 17.8 km. The DMA had 1 inlet, shown as a reservoir in Figure 5.2, and 2 metered exports to other DMAs in the northern part of the DMA at the location of sensors 3276 and 3277. The DMA supplied water to 897 domestic and 28 commercial properties (annual water consumption greater than 400 m³). There were no tanks, pumps or PRVs installed in this DMA. The real location of the hydrant opening is denoted using an **X** symbol and a number corresponding to a particular event. The large burst flow simulations took place on 7 August 2008.

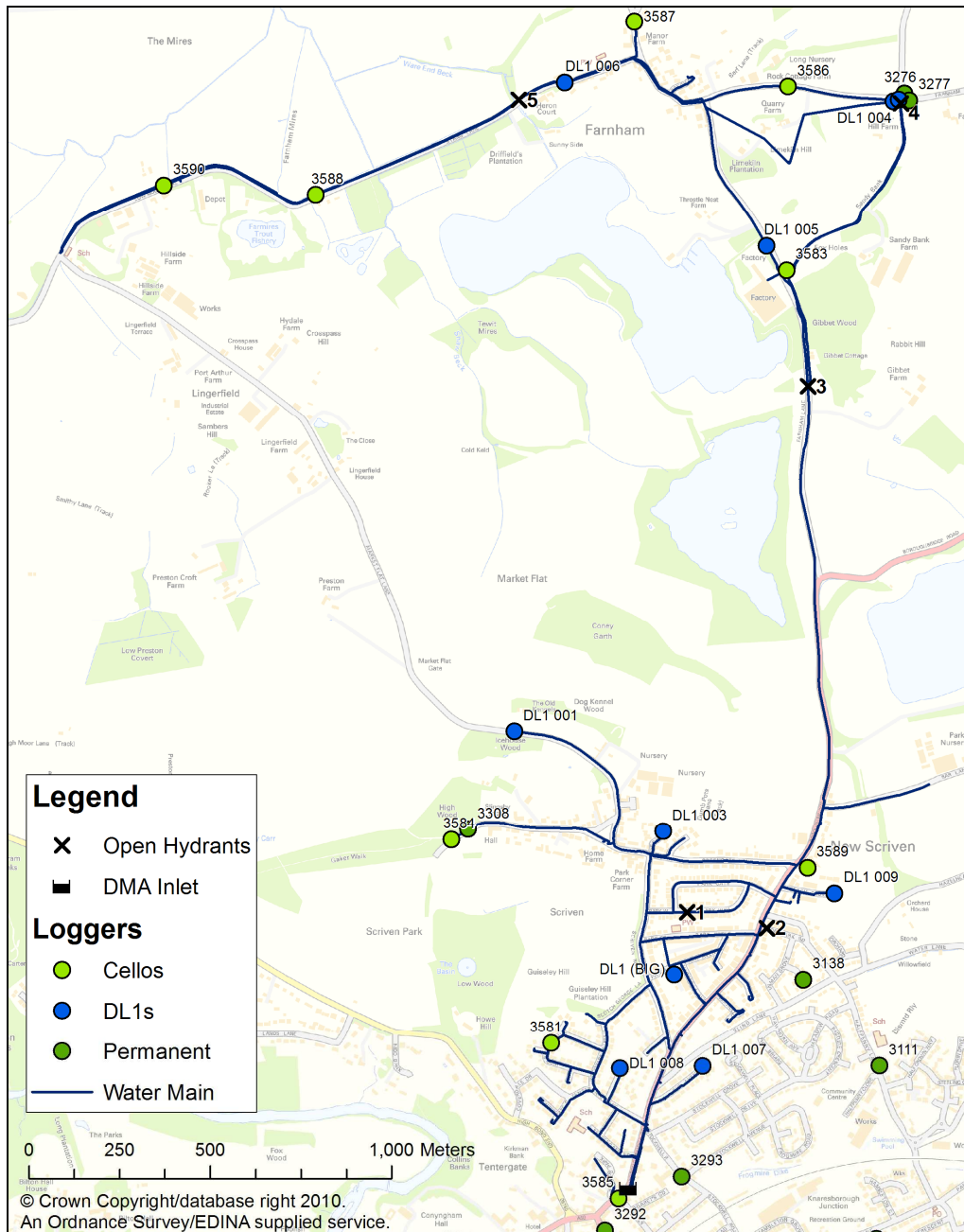


Figure 5.2 An overview of the case study area for EE1 and EE2

Under normal conditions, there are only 4 loggers installed in the DMA (denoted as “Permanent” in Figure 5.2). One logger is at the inlet of the DMA (pressure + flow), two loggers are at the exports to other DMAs (pressure + flow) and the fourth logger (pressure only) is located at the highest elevation point of the DMA (i.e., the highest DMA elevation DG2 point). Before the EEs were conducted, 19 additional loggers were installed in the DMA at locations shown in Figure 5.2, to achieve an even coverage of the whole DMA (without taking optimal sampling design into consideration). There

were two types of loggers deployed in the field, 9 normal Cello loggers (Technology 2010), and 10 high speed (i.e., 100Hz) loggers (Race Technology 2010) denoted as DL1 in Figure 5.2 that were equipped with pressure transducers supplied by SensorsOne Ltd (2010). The accuracy of the Cello loggers, the DL1 loggers and the Permanent loggers was ± 0.5 m (i.e., $\pm 0.5\%$ on 100 m range), ± 0.64 m (i.e., $\pm 0.25\%$ on 255 m range) and ± 1 m (i.e., $\pm 1\%$ on 100 m range) of head, respectively.

Due to equipment failures only 9 out of the 10 high speed loggers were operational. The existing (i.e., “Permanent”) Cello logger 3308 at DG2 (i.e., high elevation) point was malfunctioning during the EEs and was not used either. Further analysis of the data recorded by the loggers revealed unexpected readings from loggers 3583 and 3587, which lead to their exclusion from the analysis. As can be seen from Figure 5.3 the data from sensors 3583 and 3587 seemed to be delayed in comparison with the data from other sensors (e.g., 3588, 3590 and 3589). The portion of the trend highlighted in green indicates the return of the majority of the loggers to normal (i.e., a hydrant was shut off) whereas the parts of the trend highlighted in yellow show when the excluded sensors 3583 and 3587 returned to normal.

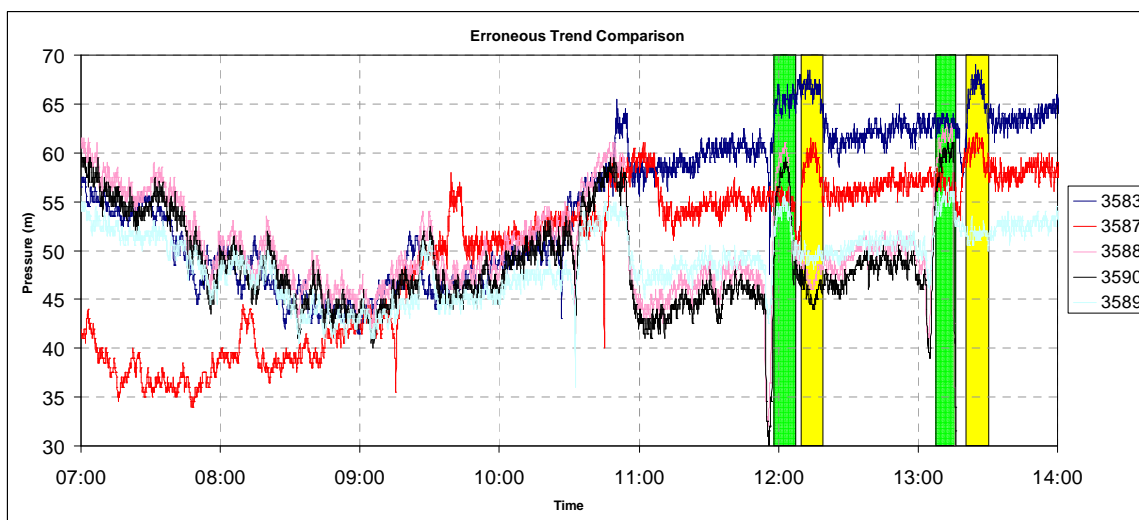


Figure 5.3 Erroneous data from sensors 3583 and 3587

One of the Cello loggers (i.e., 3585) was used to measure pressure at the inlet to establish boundary conditions of the DMA. In total, data from 15 newly installed loggers and two existing loggers at DMA exports was used in the analysis.

The quality of the HM, which was not recalibrated prior to the EEs, was tested on field data recorded under normal conditions (i.e., before the EEs were conducted). The Table 5.1 shows differences of pressures obtained by running the HM with updated boundary conditions (i.e., DMA inflows, outflows and inlet pressure) and field observations. The rows highlighted in red correspond to the two loggers (i.e., 3583 and 3587) excluded from the analysis.

Table 5.1 Difference between pressure measurements and the HM in m of head

Node Id	Cello	Pressure Difference (m)					AVG	Offset
		06/08 18:00	07/08 00:00	07/08 07:00	07/08 08:00			
5JYT466T2U	3581	-1.89	-2.05	-2.12	-2.33	-2.1	2.1	
5LLWL6C8E7	3583	2.6	-0.15	-0.74	4.99	1.7		
5JA10688K4	3584	-3.93	-4.5	-4.39	-4.23	-4.3	4.3	
5LMBK6DIBA	3586	-1.88	-3.42	-2.9	-0.79	-2.2	2.2	
5KJNJ6DYU8	3587	8.15	6.67	-3.52	7.36	4.7		
5IBN06CRID	3588	1.79	0.17	0.68	3.1	1.4	-1.4	
5LRX2681QL	3589	2.12	1.62	1.75	2.13	1.9	-1.9	
5H9CQ6CTQY	3590	0.8	-0.85	-0.17	1.77	0.4	-0.4	
5JPYD690DW	DL1 001	4.96	4.55	4.45	4.35	4.6	-4.6	
5MDFP6DERE	DL1 002	1.37	0.03	0.4	2.28	1.0	-1	
5KRGF68AIV	DL1 003	-0.51	-0.71	-0.32	-0.27	-0.5	0.5	
5MEMV6DF8F	DL1 004	2.92	1.59	2.21	4.1	2.7	-2.7	
5LH486CE8V	DL1 005	4.19	2.57	2.99	5.1	3.7	-3.7	
5L1XM66MJ2	DL1 007	5.99	6.7	6.09	4.41	5.8	-5.8	
5KG7R66M2K	DL1 008	-1.17	-0.71	-1.14	-1.35	-1.1	1.1	
5LYDR67UPL	DL1 009	5.86	5.49	5.43	5.73	5.6	-5.6	
5KU4F67AHI	DL1 BIG	-10.85	-11.98	-11.83	-10.35	-11.3	11.3	
5MFXU6DGYF	3276	2.55	2.12	2.07	5.9	3.2	-3.2	
5MHXC6DF7U	3277	1.55	1.12	1.08	4.9	2.2	-2.2	

The table further shows that some of the loggers exhibited a systematic discrepancy that could be either caused by incorrect calibration of the HM (e.g., node elevation error), calibration of the pressure transducers or noise. Rather than recalibrating the HM of the studied DMA to match the observed pressures, which would be the most appropriate approach, it was assumed that the pressure measurements were not entirely correct and were either increased or decreased by applying a constant offset to match the HM results (under normal operating conditions) as closely as possible. The actual value of the applied adjustment is reported in the “Offset” column in Table 5.1. It was calculated as an average discrepancy between model results and field measurements computed over 4 randomly chosen time steps.

5.2.1.1 Data Pre-Processing

It was discovered that the data collected during the EEs was in different time zones. Typically, all measurements are recorded in Greenwich Mean Time (GMT), however, the newly deployed loggers, due to incorrect setting, recorded time in British Summer Time (BST), which is equal to GMT+1. Given the fact that the EEs took place in the summer, failure to synchronise the time zones would yield erroneous results. The common time base used needs to consider the local time of a particular country to reflect the current water consumption trends and, therefore, the time base of all measurements was converted to BST to correspond with the HM.

The transient DL1 loggers recorded pressures at 100 Hz frequency, whereas the Cello loggers recorded data every 5 seconds. So a high sampling rate is unrealistic for long term deployment of battery-only powered sensors since it would lead to fast battery depletion. Moreover, given the 15 minute time steps of the HM, all pressure data had to be down sampled to 15 minute time step using a moving average to reduce the effect of noise (the averaging window was 2 minutes). Pressure at the N^{th} minute was calculated by averaging pressure readings in the $(N-1)^{\text{th}}$ and the N^{th} minute. Detailed analysis of the influence of the size of the averaging window used was not carried out. The average difference of pressures aggregated over a 1-minute time window was approx. 0.52%, which seemed insignificant compared to the drops in pressure observed during the EEs.

5.2.1.2 Event Detection

As stated in section 3.3.2.3 the HM requires the detection time of a burst as well as the estimated magnitude of burst flow as inputs. These input parameters are normally provided by an automated pipe burst detection system (Mounce *et al.* 2010). In case of EE1 and EE2 the aforementioned system could not readily detect consecutive hydrant openings carried out within one day. The burst detection times were determined in this particular case manually by visual inspection of pressure data from a selected pressure sensor, whose trend during two consecutive days is shown in Figure 5.4. The hydrant openings correspond to pressure drops lasting approximately 1 hour and could be easily recognised in the trends.

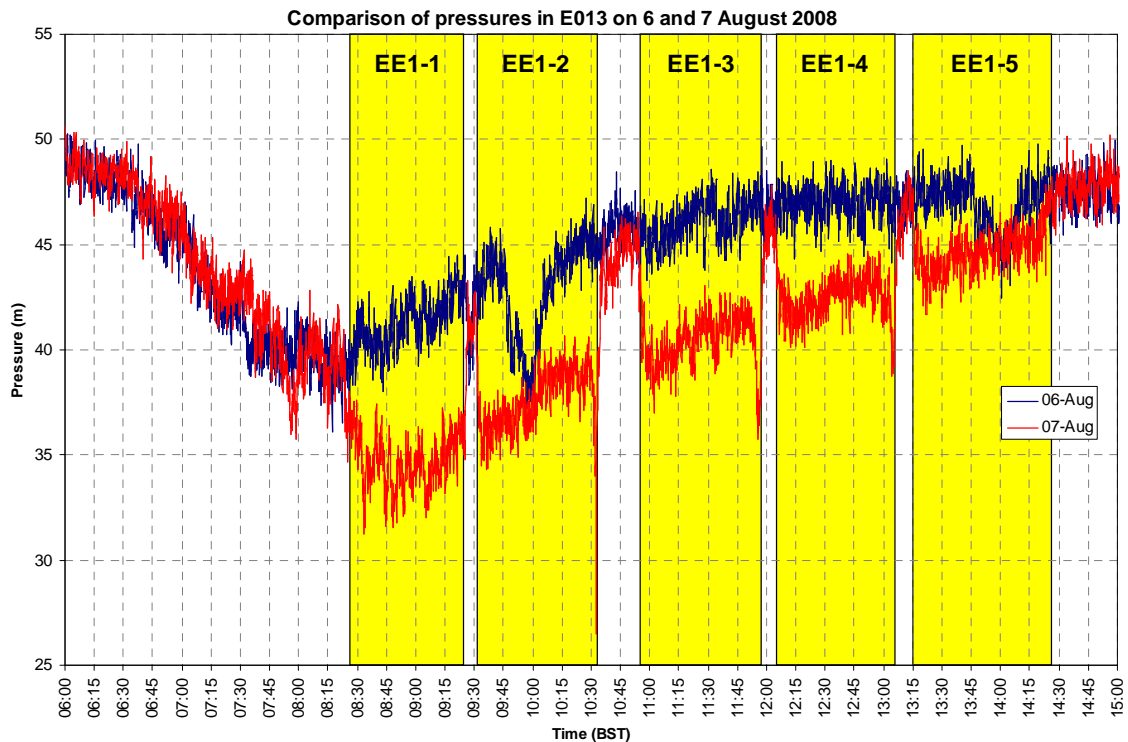


Figure 5.4 Pressure data of a selected logger for event detection on 6 and 7 August 2008

The manually detected and actual hydrant opening times are shown in Table 5.2. The table suggests that the manually detected hydrant openings closely corresponded to the actual times when the hydrants were opened.

Table 5.2 Detected and actual hydrant opening times of EE1

EE1	Hydrant Opening Times (BST)					
	Manually Detected			Actual		
1	08:24	–	09:26	08:25	–	09:29
2	09:31	–	10:34	09:33	–	10:37
3	10:56	–	11:58	10:56	–	11:58
4	12:07	–	13:08	12:06	–	13:09
5	13:15	–	14:24	13:17	–	14:20

5.2.1.3 Abnormal Flow Estimation

Under normal conditions an automated pipe burst detection system (Mounce and Boxall 2010) is able to provide a good estimate of the abnormal flow. As discussed in the previous section, the system was not used during these EEs and it was therefore necessary to estimate the burst flow manually. To estimate the flow from the open

hydrants during the first set of EEs the difference between an average demand over the past 3 days (i.e., from 4 to 6 August) and the actual demand on 7 August was taken. The estimated abnormal flow was required as one of the inputs to the HM.

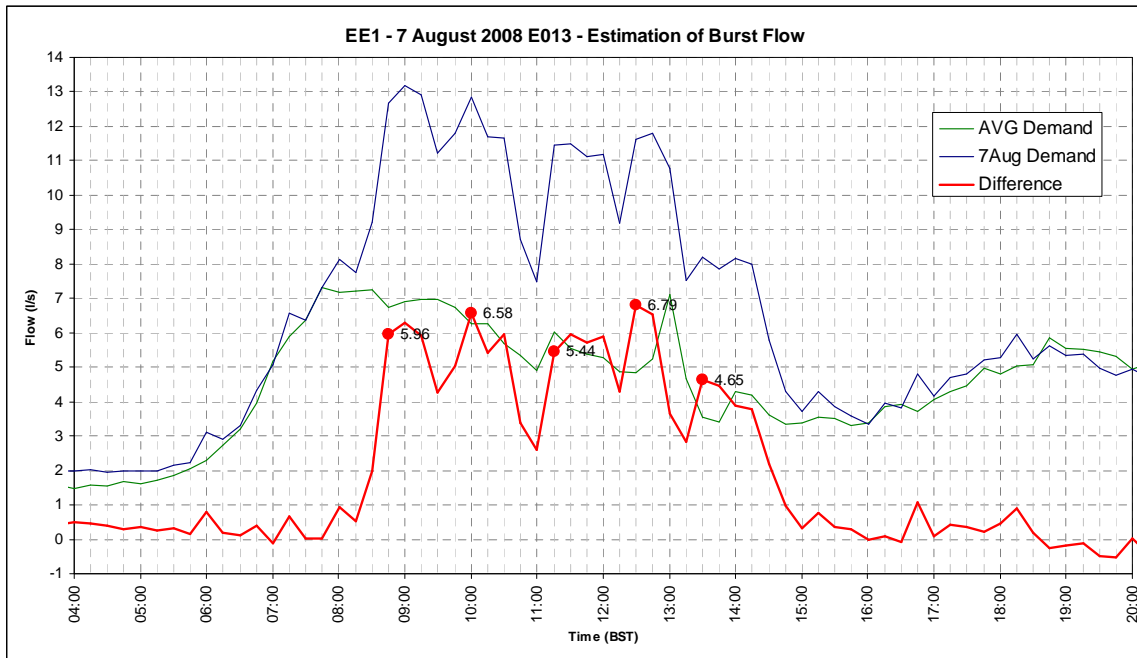


Figure 5.5 Comparison of flow data on 7 August 2008 with an average demand

Table 5.3 provides a summary of abnormal flows estimated by comparing flow patterns under normal and abnormal conditions in the network using Figure 5.5. The column “Difference” corresponds to the estimated flow rate used by the HM whereas the “Real Flow” column contains observed flow measurements, disclosed after the analysis. The flow rate from the hydrant was measured using a hydrant pipe flow meter which, although digital, is prone to error. The five manually detected events (i.e., the assumed burst detection times) are highlighted in yellow in Table 5.3.

Table 5.3 Summary of times and abnormal flows used by the HM

Date	AVG Outflow (l/s)	AVG Inflow (l/s)	AVG Demand (l/s)	7 Aug Demand (l/s)	Difference (l/s)	Real Flow (l/s)
07/08/2008 08:00	9.75	16.93	7.18	8.13	0.94	
07/08/2008 08:15	10.03	17.25	7.22	7.74	0.52	
07/08/2008 08:30	9.95	17.19	7.24	9.23	1.99	
07/08/2008 08:45	10.03	16.76	6.73	12.69	5.96	6.6
07/08/2008 09:00	9.90	16.80	6.90	13.20	6.30	
07/08/2008 09:15	9.49	16.46	6.97	12.91	5.93	
07/08/2008 09:30	8.80	15.77	6.97	11.22	4.25	
07/08/2008 09:45	8.82	15.57	6.75	11.80	5.05	
07/08/2008 10:00	10.16	16.42	6.26	12.84	6.58	6.2
07/08/2008 10:15	8.93	15.19	6.26	11.69	5.43	
07/08/2008 10:30	8.00	13.69	5.68	11.65	5.97	
07/08/2008 10:45	7.44	12.78	5.34	8.72	3.38	
07/08/2008 11:00	7.30	12.21	4.90	7.49	2.58	
07/08/2008 11:15	6.37	12.41	6.03	11.47	5.44	7.3
07/08/2008 11:30	6.15	11.68	5.53	11.51	5.97	
07/08/2008 11:45	5.96	11.35	5.40	11.12	5.72	
07/08/2008 12:00	5.70	10.96	5.27	11.17	5.90	
07/08/2008 12:15	5.77	10.64	4.87	9.17	4.30	
07/08/2008 12:30	5.44	10.27	4.83	11.62	6.79*	7.3
07/08/2008 12:45	4.18	9.44	5.26	11.79	6.52	
07/08/2008 13:00	4.89	12.00	7.11	10.78	3.66	
07/08/2008 13:15	6.19	10.87	4.68	7.52	2.84	
07/08/2008 13:30	6.00	9.54	3.54	8.19	4.65	7.5
07/08/2008 13:45	5.98	9.38	3.40	7.87	4.47	
07/08/2008 14:00	5.85	10.14	4.28	8.18	3.89	

*) The estimated hydrant flow of 6.79 l/s at 12:30 seemed too high (without knowing the real flow) and the HM identified the same burst location as was the case at 11:15. Therefore, the burst flow was reduced by 1 l/s to 5.79 l/s. This globally reduced the SSE, which suggested it was likely that the initial burst flow had not been estimated correctly. After the locations of hydrant openings, their times and the measured hydrant outflows were revealed, it was found out that the actual hydrant outflow was higher than the estimated one. This might indicate an incorrect calibration of the hydraulic model. The actual measurement (i.e., Real Flow) recorded using a digital hydrant pipe flow meter could also be subject to errors.

5.2.1.4 Results and Discussion

The results obtained for locating the open hydrant are summarised in Table 5.4, which reports a topological distance of the pipe identified by the HM as a burst location from

the actual hydrant opening. The topological distance was measured here as the shortest path between two points in the network by tracing the network connectivity schematics. The column “All loggers” corresponds to a scenario when all (15+2) loggers were used to determine the location using an HM. In the “Cello only” scenario only (6+2) Cello loggers were used. The “DL1” scenario considered only 9 DL1 loggers and Cello loggers at exports. In the “Selection” scenario measurements from only 2 additional loggers (i.e., 3590 and 3584) were used.

Table 5.4 HM hydrant opening results for EE1

EE1	Time	Distance from an open hydrant (m)			
		All loggers	Cello only	DL1 only	Selection
1	08:45	346	346	346	346
2	10:00	42	42	85	85
3	11:15	157	157	45	157
4	12:30	194	194	194	194
5	13:30	603	603	1,140	1,210

Table 5.4 shows that the increased number of pressure sensors used in a relatively simple DMA did not necessarily yield an extra benefit in identifying the location of the open hydrant more accurately. In the majority of cases very similar results could be obtained just by using 2 additional loggers deployed at suitable locations sensitive to changes in pressure. Where only a small number sensors were used (e.g., the “Selection” scenario) a higher number of pipes received very similar value of criterion measurement and the method would be more prone to measurement errors.

Detailed results of the analysis are shown in Appendix C.1 in the form of GIS maps, showing the spatial distribution of SSE for each of the “All loggers” scenario considered in Table 5.4. From the figures presented in Appendix C.1, it can be observed that the HM in the majority of cases (i.e., except EE1-5) managed to identify a burst hotspot (i.e., a group of pipes having a similar SSE value). EE1-5 was conducted at 13:30 (see Figure C.5) and it can be observed that the HM did not manage to identify a burst hotspot in the proximity of the open hydrant. This can also be seen in Table 5.4, where the distance from the open hydrant was significantly higher (i.e., 603 m) than other EEs. The most likely explanation for this failure could be the poor calibration of the HM, which was over predicting head losses in pipes in the top part of the DMA.

5.2.1.5 Summary

The above case study was carried out as a blind test and the actual locations of the hydrant openings as well as the opening times and flush flow rates were unknown to the author before submitting the results. From the results presented in Table 5.4 and Appendix C it can be concluded that the adopted method has the potential to provide an estimated location of a large pipe burst within a relatively simple DMA where a reasonably calibrated HM exists and a sufficient number of suitably located pressure monitoring points are available. The combined model calibration and burst location as suggested by Wu *et al.* (2010) as well as the use of multiple measurements taken at different times (ideally during minimum night flow hours) is likely to lead to further improved results. However, if multiple measurements or night flow values had been used, it would have caused a delay to the investigation. Therefore, these were not considered in this work, which required near R-T burst location.

5.2.2 Medium Burst Flow Simulations (EE2)

Similarly to the first set of EEs presented in section 5.2.1, another hydrant flushing exercise took place in the same DMA on 8 August 2008. This time the flow rates were significantly reduced. The same set of sensors as described above (see Figure 5.2) was used. The pressure data was pre-processed in the same way as in the case of EE1 (e.g., time shift, moving average applied, etc.). The pressure measurements from the field were corrected in the same way as in EE1 by applying constant offsets as shown in Table 5.1.

On 8 August 2008 the flow data of the exports (i.e., loggers 3276 and 3277) was corrupted (see Figure 5.6). In order to utilise the dataset it was necessary to synthetically generate the outflows. Average values over the period from 4 - 7 August 2008 (Monday to Friday) were used to fill-in the missing data. This might have affected the results to some extent.

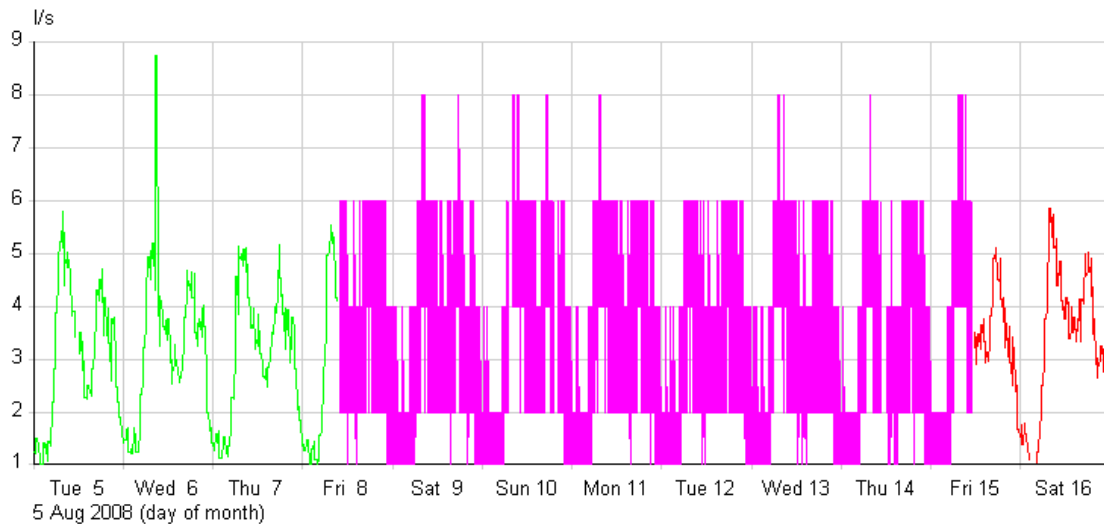


Figure 5.6 Corrupt flow data of logger 3276

5.2.2.1 Event Detection & Abnormal Flow Estimation

Detecting the time of the hydrant opening and estimating the flow would be difficult in this case since the magnitude of abnormal flow was much lower than in case of the large burst flow simulations. Such situations would certainly benefit from a more advanced automated approach (Mounce *et al.* 2010). Unlike in the previous case, here the known hydrant opening times and measured flush flow rates were used. The actual considered input parameters can be found in Table 5.5. The assumed conditions might represent a significant challenge for an online pipe burst detection system and could be seen as ideal, however, they were partially compensated by the unknown outflows from the DMA exports.

Table 5.5 Time schedule and hydrant flow rate of EE2

EE2	Time	Abnormal flow
5	09:00	2 l/s
4	11:00	2 l/s
1	12:30	2 l/s
2	14:30	2 l/s

The ID of an EE corresponds to the location of hydrant opening as shown in Figure 5.2. In case of EE2, only four hydrant openings were carried out and their order was different to that in EE1.

5.2.2.2 Results & Discussion

Similarly to the previous set of EEs (i.e., EE1) a different number of pressure sensors were used in the attempt to determine the location of an open hydrant. The distances of the most likely burst location from the actual hydrant opening are presented in Table 5.6.

Table 5.6 HM hydrant opening results for EE2

EE2	Time	Distance from an open hydrant (m)			
		All loggers	Cello only	DL1 only	Selection
5	09:00	340	1,940	340	1,090
4	11:00	25	25	25	25
1	12:30	324	395	324	376
2	14:30	270	270	270	270

Table 5.6 shows that the performance of the HM in this DMA was similarly to EE1 still acceptable even when a smaller number of sensors were used. Detailed results of the analysis of EE2 are presented in Appendix C.2 in the form of GIS maps, showing the spatial distribution of SSE for each of the “All loggers” scenarios considered in Table 5.6. The most likely hydrant opening locations identified by the HM were slightly different in case of EE2 compared to EE1. Whereas the differences in the values of SSE between differently colour coded classes in the figures presented in Appendix C.1 (i.e., EE1) were significant, the lower hydrant flush rates generated smaller drops in pressure and the values of SSE in case of EE2 (see Appendix C.2) were much more similar across a number of pipes. Similarly to the scenario EE1-5 discussed above, even the scenario EE2-5 (i.e., the same location of an open hydrant) generated much higher values of SSE. This further supports the hypothesis of inadequate calibration of the HM (i.e., at least in the top part of the DMA).

5.2.2.3 Summary

This set of EEs was not a blind test and the locations of open hydrants as well the opening times and flows used during the flushing were known *a priori*. Even the significantly lower abnormal flows (i.e., 2 l/s) generated in the DMA sufficient head losses, which were picked up by the sensors. Therefore, the methodology performed similarly to the large burst flow simulations presented in section 5.2.1. In this case the estimated abnormal flow was considered as known, which represented an ideal case. On

the other hand, the measured outflows from the DMA were only approximated based on average values, which to some extent compensated the advantage of the known abnormal flows. Similarly to EE1 even in this case (i.e., a simple DMA) an increased number of pressure monitoring points did not yield substantial benefit that would justify the additional investment.

5.2.3 Engineered Events in a Typical DMA (EE3)

This section provides details of the performance of the HM in the attempt to locate an open hydrant in a highly looped urban DMA (see Figure 5.7). The studied DMA contained 698 demand nodes and 738 pipes. The total mains length was 19.2 km. The DMA had 1 inlet shown as a reservoir in Figure 5.7 and 1 metered export to other DMA in the eastern part of the network at the location of sensor 3122. The DMA supplied water to 2,640 domestic and 122 commercial properties (annual water consumption greater than 400 m³). There was one major metered consumer (i.e., monitored by a dedicated logger) in the DMA, having demand greater than 10,000 m³/year or 5% of the total DMA inflow. No tanks, pumps or PRVs were installed in this DMA.

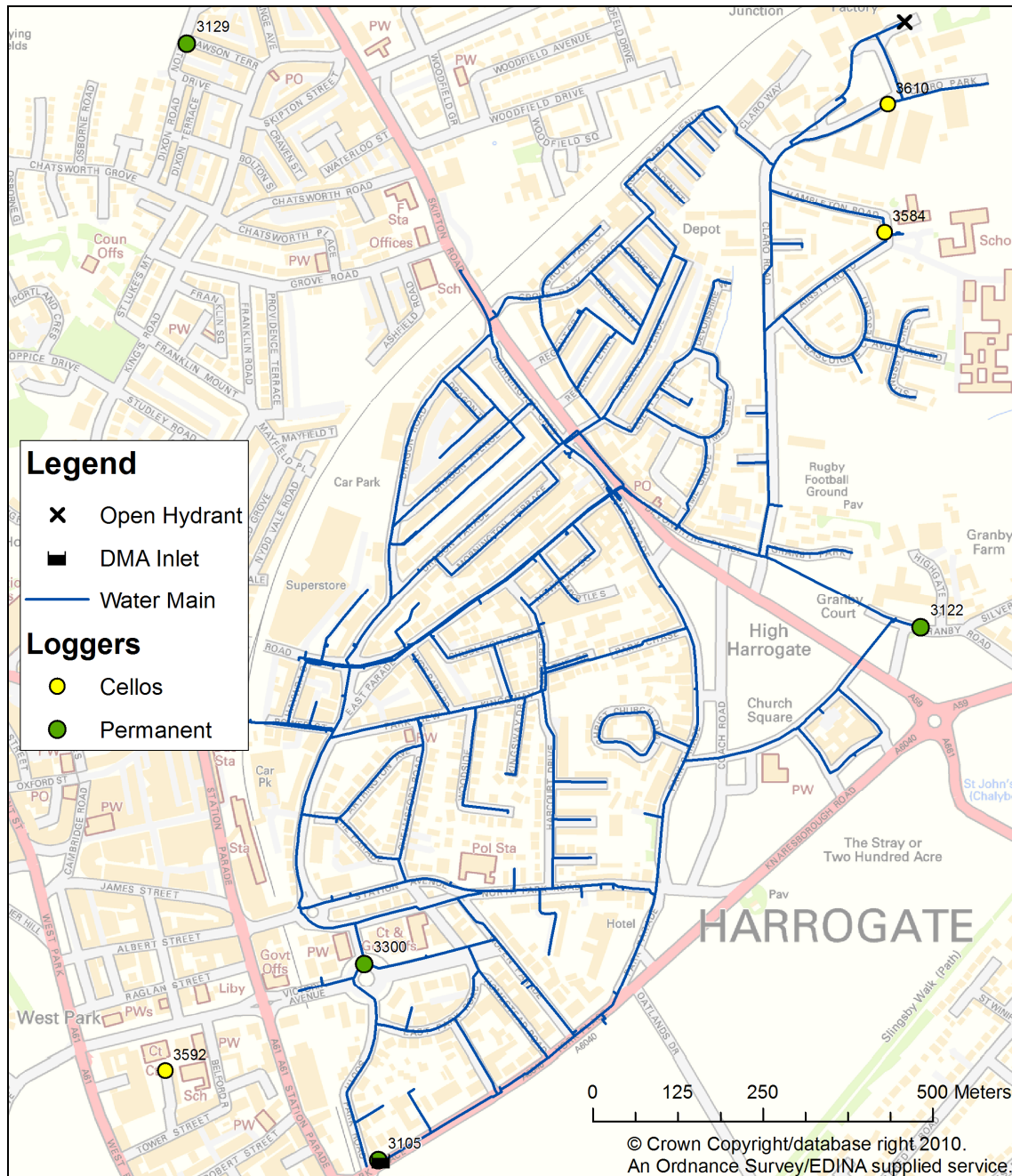


Figure 5.7 An overview of the case study area for EE3

The number of pressure sensors deployed in the DMA was relatively small (i.e., only 2 additional loggers) compared to the previous EEs. However, the additional sensors (see the yellow dots in Figure 5.7) were deployed at strategic locations as identified by Farley *et al.* (2008). The EE was a part of validation tests of the whole DSS described in Chapter 4. Unlike in the case of EE1 and EE2, this time the hydrant opening was automatically detected by the ANN-FIS (Mounce *et al.* 2010), denoted as an external Pipe Burst Detection module in Figure 4.1. All required inputs, such as the affected

DMA, detection time and the estimated burst flow, were stored in the DB (see Table 5.7) and marked as a fresh alarm. After being first processed by the Alarm Monitor (see section 4.4.1), the alarm was passed to the Likelihood Evaluator (described in section 4.4.2), where the evidence of the HM was computed. The time considered for burst location is highlighted in yellow in Table 5.7 and corresponds to the end of the time window used by the ANN-FIS for burst detection. Ideally, a much narrower time window should be used for burst detection as well as estimation of the abnormal flow. This should be possible as Romano *et al.* (2009) reported successful burst detections with only a 30 minute time window.

Table 5.7 Alarm information provided by a pipe burst detection module

EE3	Alarm Received	ANN-FIS Window Start	ANN-FIS Window End	Burst flow	DMA
1	02/03/2010 15:15	01/03/2010 17:30	02/03/2010 05:30	1.7 l/s	E021

The estimated burst flow of the EE3 was 1.7 l/s (see Table 5.7) and corresponded to approx. 15% of DMA inflow at 7AM (i.e., peak demand). The automatically estimated flow was close to the actual flow used during the hydrant flushing (i.e., 2 l/s). As in the previous EEs, offsets to pressure measurements (calculated under normal operating conditions) had to be applied to achieve a closer match between the HM and field observations. Table 5.8 provides details of the actual values of constant pressure offsets used.

Table 5.8 Pressure measurement corrections for EE3

Logger	Pressure measurement corrections (m) on 01/03/2010							AVG Offset (m)
	00:00	04:00	05:00	05:15	05:30	05:45	06:00	
3610	0.55	-0.31	0.16	-0.43	0.5	-0.08	0.69	0.06
3584	1.14	0.79	0.75	1.16	1.09	0.51	1.28	0.91
3300	0.9	1.25	1.23	2.18	2.14	1.09	1.97	1.47
3122	1.65	1.39	2.28	2.21	2.11	2.04	2.74	1.95

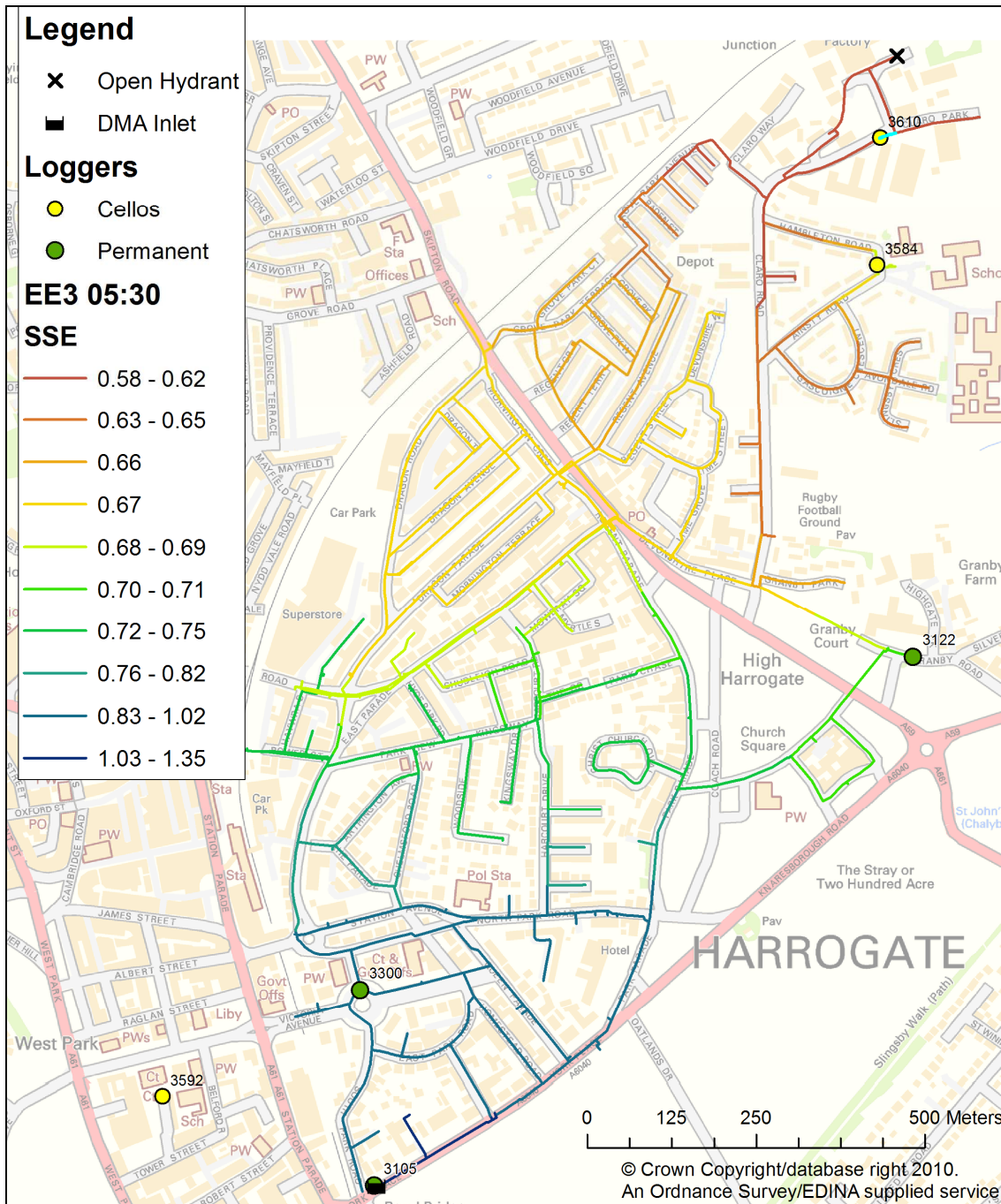


Figure 5.8 A map showing the most likely location of hydrant opening of EE3

Figure 5.8 shows the performance of the HM after applying pressure offsets presented in Table 5.8. The distance from the location with lowest SSE (i.e., the most likely location of the open hydrant), identified by the HM, to the actual location of the open hydrant was 165 m. However, the hydrant flushing caused pressure drops across the DMA in the range from 0 - 0.55 m. The abnormal flow of 1.7 l/s did not generate pressure drops above 0.5 m at the location of the newly deployed sensors (i.e., 3610,

3584) and nor at the location of the permanent sensors (3300, 3122) with a 1 m accuracy. The HM in this case, therefore, could not provide a sensible answer. The promising result shown in Figure 5.7 was, therefore, obtained only by chance. If the HM had been run at a different time (i.e., other than 5:30AM) during the EE an entirely different location could be identified.

5.2.3.1 Summary

EE3 shows that the use of HM as a source of evidence suggesting the likely location of a burst pipe might be problematic in situations when the abnormal flow escaping from the system does not generate sufficient pressure drops at the locations of pressure sensors. Moreover, the accuracy of the pressure sensors can play an important role, particularly in highly looped urban DMAs where the effects of a burst will be mitigated since the additional flow can reach the burst through a number of alternative paths.

The number of accurate pressure sensors (i.e., having accuracy of 0.1 m) that would have to be deployed in an urban DMA in order to be able to locate a burst pipe might be uneconomical, at least at current price levels. The accuracy necessary to locate such bursts might furthermore impose significant challenges on the quality of calibration of the HM.

5.3 Dempster-Shafer Model: Semi-Real Case Study

This section provides the results of an application of the D-S model presented in section 3.3 of this thesis on a number of semi-real case studies in a large urban DMA in the Harrogate & Dales area in North Yorkshire, UK (see Figure 5.1). The aim of the case study is to show that combining realistic evidence, which can be obtained from a number of models in an effort to locate a burst pipe within a DMA, yields additional benefits.

The layout of the highly looped urban DMA, which was subject of this study, is shown in Figure 5.9. The DMA had two inlets and no exports. A total of 10 pressure sensors were used in this case study. The DG2 pressure sensor, which was located at the critical point of the DMA (i.e., location with the highest elevation), and 9 additional sensors were placed according to an optimal sampling methodology developed by Farley *et al.* (2008).

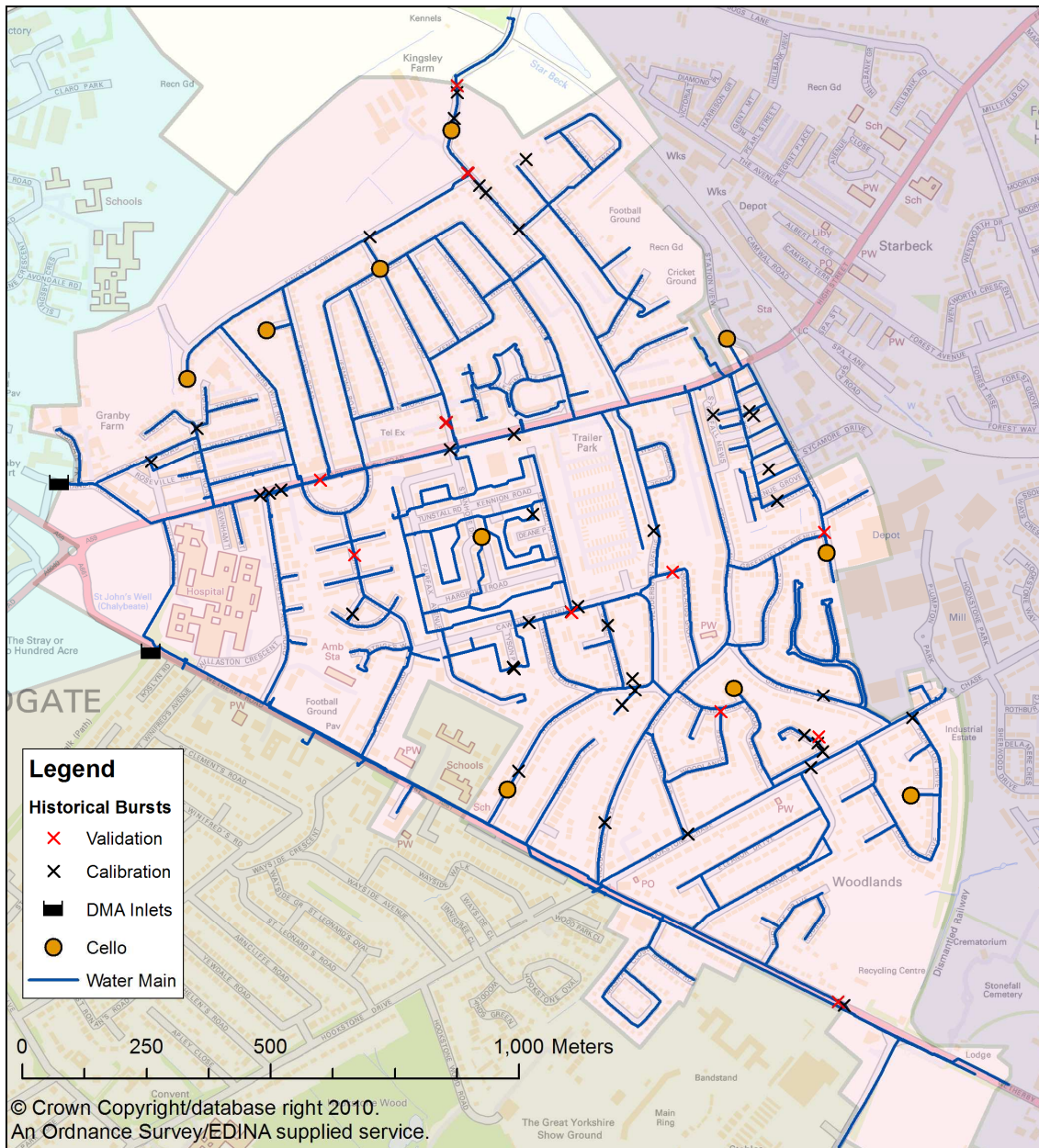


Figure 5.9 An overview of DMA E022

The selected case study area was one of the largest DMAs in the Harrogate and Dales area, supplying water to over 4,500 properties (almost 69% unmetered). The DMA comprised 998 demand nodes and 1,052 pipes (i.e., potential burst locations). The total length of water mains in this DMA was 33.5 km. There were only 6 commercial properties with an annual water consumption greater than 400 m³ and 1 major consumer (i.e., demand > 10,000 m³/year or 5% of the total DMA inflow), which was monitored by a standalone logger.

5.3.1 Individual Model Screening

Before attempting to apply the information fusion methodology, the performance of individual models was evaluated first. The findings obtained during the application of the individual models (i.e., the HM, CCM and PBPM) on a selection of calibration cases in the DMA E022 are summarised in the following sub-sections.

5.3.1.1 Hydraulic Model

By modelling artificial bursts in the DMA it was observed that the HM was generally not very sensitive to noise added to nodal demands because these were substantially lower than the outflows from the simulated pipe bursts. Variation of nodal demands of 20% (i.e., +/- 10% uniformly distributed) did not cause any major errors in determining the location of a burst pipe, since there were only very few major customers in the DMA.

On the other hand, it was observed that the pressure measurements were very sensitive to the added noise. In the DMA, pressures generally ranged from 40 m up to 90 m due to the differences in elevation. A 2% error (i.e., +/- 1% uniformly distributed) added to pressure measurements for a 5 l/s burst (i.e., 12.5% of average peak demand or 20% of average DMA inflow) was still found acceptable. The HM performed reasonably well in most tested scenarios. The accuracy of the HM required by this method might be very difficult to achieve in real life conditions since it is close to the threshold of acceptable level of calibration (for this type of modelling), as discussed by Walski *et al.* (2003). Also the accuracy of commonly available pressure transducers is approx. +/- 0.5% of their full range, which might be insufficient under some conditions.

5.3.1.2 Customer Contacts Model

Two main data sources, provided by a water utility, were used during the development of the CCM. The first dataset contained classified CCs received by phone, containing the date and time of the complaint, its nature and geographic coordinates associated with the contact (i.e., either the coordinates of the property or geo-referenced location of a burst provided by a customer). The second dataset contained information from a Work Management System (WMSY), which contained a date when a mains repair was carried out as well as coordinates where it took place.

It was assumed here that a burst was repaired during the same day it was detected. Under such an assumption, the time window over which CCs were considered to be related to a particular burst event was established by performing spatial analysis of CCs and WMSY data of 15 DMAs collected over the period of 6 years (2002 - 2007). The size of the window was chosen according to Table 5.9 as the best trade-off maximising the number of CCs associated with pipe bursts (i.e., the “Bursts with CC” row) and minimising the distance of those contacts from the location of a burst pipe (i.e., the “AVG Dist” row).

Table 5.9 An average distance of CCs from a burst pipe

Criterion	Same Day	Same Day & 12h Before	Same Day & 24h Before	Same Day & 36h Before	36h Before +12h After	24h Before +12h After	12h Before +12h After	24h Before +24h After
Bursts with CC	143	171	183	192	199	190	178	193
AVG CC Count / Burst	1.0	1.1	1.2	1.3	1.4	1.3	1.2	1.4
AVG Dist (m)	233.9	240.2	239.3	277.8	307.6	272.0	275.2	284.5

The “AVG CC Count / Burst” row provides information about the average number of CCs per burst given a particular size of time window and is correlated to the “Bursts with CC” row. The typical number of CCs per burst for a particular time window is then shown in detail in Table 5.10. It can be observed that for the chosen time window of 24 hours before the repair and during the same day the repair took place, the majority of the bursts were not reported by any customer and if a burst was reported it was mainly by 1 or 2 customers.

Table 5.10 A histogram showing frequency of CCs per pipe burst

Customer Contacts	Same Day	Same Day & 12h Before	Same Day & 24h Before	Same Day & 36h Before	36h Before +12h After	24h Before +12h After	12h Before +12h After	24h Before +24h After
0	214	186	174	165	159	167	179	164
1	60	75	80	81	84	83	78	80
2	39	44	49	47	48	51	45	53
3	20	24	24	32	31	23	23	25
4	10	11	10	12	11	9	11	9
More	14	17	20	20	24	24	21	26

Figure 5.10 shows that most of the CCs (i.e., 70.6%) were typically within 200 m from the True Burst Location (TBL) for the time window of 24 hours before the WMSY

order creation date and the same day. Moreover, almost 40% of the CCs lay within 50 m from the TBL. However, almost 13% of the contacts lay further than 500 m from the TBL, which might indicate either incorrect association with a WMSY record or an error in WMSY or CC data (e.g., a misleading report).

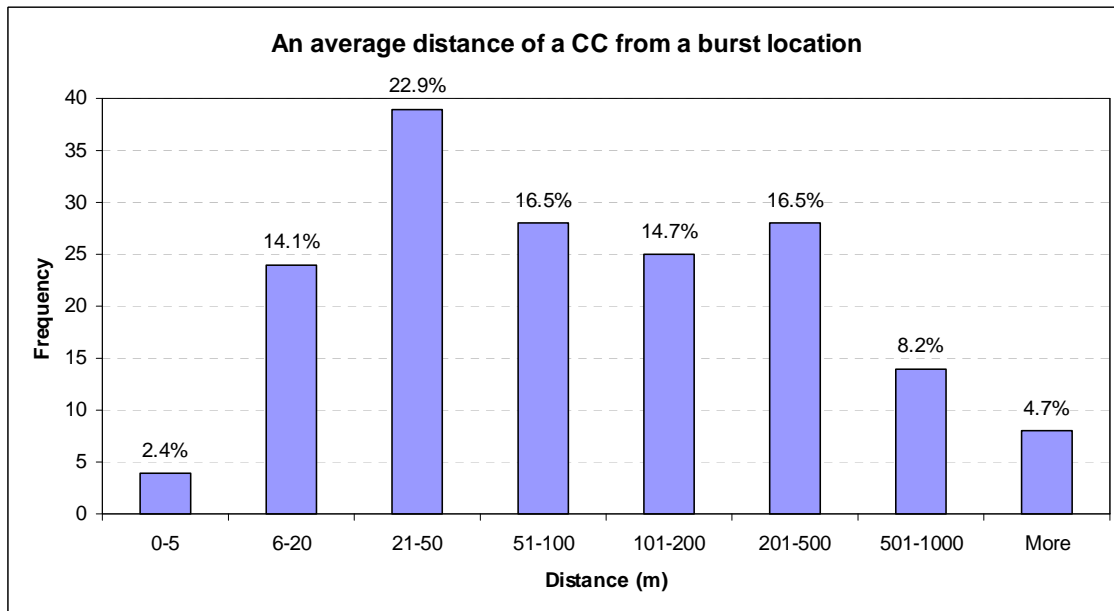


Figure 5.10 A histogram of an average distance of customer contact from a burst location

The CCM seemed to perform relatively well in the DMA. Typically the CCs associated with a burst event originated almost exactly from the area where a burst occurred or were misleading (i.e., came from a different part of the DMA). The time window (i.e., the CCs reporting Burst / Leak during the 24 hours before and during the same day when a WMSY entry was created were considered as related to a burst) identified in Table 5.9 seemed to be appropriate for this case study because only less than 30% of CCs were more than 200 m from the TBL.

An attempt was made to combine multiple CCs hierarchically (see Appendix A.1 for additional details). This, however, brought certain difficulties related to an increased influence of the combined result, compared to other information sources (i.e., HM and PBPM). Also some performance issues related to the combination of many information sources (in some cases) were encountered, which could be overcome using a more efficient implementation of the D-S model.

5.3.1.3 Pipe Burst Prediction Model

PBPMs are typically used for strategic planning to identify the most suitable assets for rehabilitation or replacement. Their predictions are generally not of a very high quality for operational use. The PBPM used in this work, which was built by a consultancy company, was treated as a black box and was not validated prior to use. As shown later, even such a model can bring certain benefits, despite its different primary use.

5.3.2 Dempster-Shafer Model Calibration

To calibrate the D-S model a number of historical cases are required so that its various parameters (e.g., the type of the normalisation functions, shape of the mapping functions, etc.) can be set to achieve the best gains from the information fusion. Since it was not possible to use real life examples due to missing or insufficient data, a number of semi-real case studies were created. In order to make these as realistic as possible, historical pipe burst events were first obtained from a WMSY. Where applicable, the CC DB was queried to retrieve CCs reporting burst pipe or a leak.

Poor calibration of the available HM of the study area as well as missing historical pressure and flow records prevented the use of real data from pressure and flow sensors deployed in the field. Synthetic pressure measurements were generated by simulating a medium sized burst (i.e., 5 l/s = 12.5% of peak DMA inflow or 20% of average DMA inflow) as a fixed (i.e., pressure insensitive) demand added to the centre of the burst pipe at the location and date obtained from a WMSY. Pressures in the studied DMA were generally high due to significant differences in elevation and ranged from 40 m to 90 m of head during minimum night flow hours (i.e., 4:00 AM). The chosen value of burst flow of 5 l/s, which seemed to generate sufficient pressure drops in the DMA, could be seen as representative for medium to large bursts. The time of burst detection / occurrence was randomly chosen between 0 and 24 hours. Pressures in the network obtained at demand nodes closest to the real locations of sensors in the WDS were recorded and used as reference pressures representing a pipe burst. White noise was added to the reference pressure values (i.e., $\pm 1\%$ uniformly distributed) as well as nodal demands (i.e., $\pm 7.5\%$ uniformly distributed). The base values were either increased or decreased by a given percentage, to more closely reflect the reality. Without adding the noise the HM would always find the right location of the burst and would significantly outperform the remaining information sources. In fact, there would

be no need to use information fusion to include information from additional data sources. The chosen values of added noise were selected according to observations during preliminary screening of the HM to allow the model to provide imperfect but still acceptable results.

5.3.2.1 Calibration and Validation Data Sets

A dataset comprising 54 historical pipe bursts in the DMA (see Figure 5.9) was formed and split into a calibration set comprising 41 cases and a validation set comprising 13 cases (approx. ratio 75% calibration / 25% validation). The split between calibration and validation data was done in such a way that both datasets had similar properties (e.g., in terms of number of CCs received and the performance of individual models). Both calibration and validation sets contained similar numbers of CCs, i.e., 27 (66%) and 8 (62%), respectively. The performance of the models was measured using the average likelihood attributed to the 10 nearest pipes in the proximity of the TBL (see section 3.3.5). The pipes included in the “10 nearest” category are represented by the “Inner” region shown in Figure 5.11

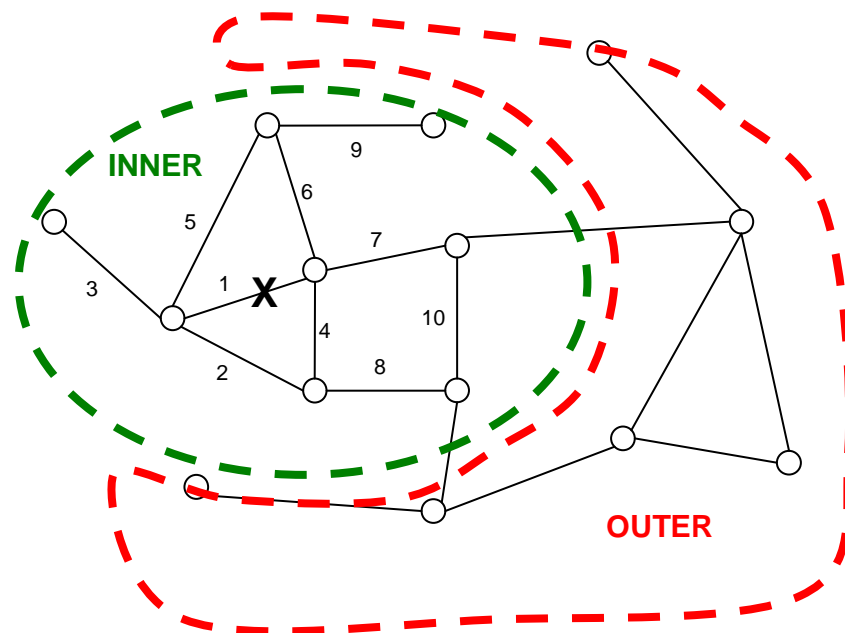


Figure 5.11 Illustration of the Proximity function

The split of data into calibration and validation sets was performed using GANetXL (Bicik *et al.* 2008), an optimization add-in for Microsoft Excel[®], by applying a single objective GA (Goldberg 1989) where the objective was to minimize the difference in

performance of individual models (i.e., the PBPM, the HM and the CCM) between the calibration and validation sets while maintaining the chosen size of the calibration and validation sets (i.e., 41/13) and ensuring that the cases where CCs were present were proportionally split between the two sets. Decision variables in this case formed a vector of binary numbers, where the value of 0 indicated that a particular case should be included in the calibration dataset, whereas the value of 1 suggested including a case into the validation dataset. The objective function was defined by following equations:

$$f = |Performance(calibration\ set) - Performance(validation\ set)| \quad (5.1)$$

$$Performance(X) = \frac{1}{|X|} \sum_{\forall cases \in X} (Perf(PBPM) + Perf(HM)) + \frac{1}{|Z|} \sum_{\forall cases \in Z} (Perf(CCM)) \quad (5.2)$$

where:

- f is the objective function,
- $Performance$ is the function representing the overall performance of a given set X ,
- X represents the chosen set, i.e., calibration set or validation set,
- $Perf$ is a function returning the average likelihood of the 10 nearest pipes from the True Burst Location (TBL), which represents the performance of a particular individual model on a given case, and
- Z is a subset of X ($Z \subseteq X$) representing only those cases where CCs were available.

Even though some of the calibration and validation cases were located close to each other in Figure 5.9, the bursts were simulated during different times of day and different sources of evidence, such as CCs, were available. Each of the models, therefore, performed differently, despite their geographical closeness. The above procedure was applied prior to any attempts to calibrate the D-S model, purely to determine representative calibration and validation data sets. The calibration of the D-S model presented in the following section was carried out only on the calibration dataset.

5.3.2.2 Multi-Objective Optimisation of the D-S Model

The calibration of the D-S model defined in section 3.3.5 was solved using a multi-objective GA (Goldberg 1989). GAs are population-based heuristic search algorithms, particularly suitable to solve complex non-linear problems, which was the case in this work. The particular type of multi-objective GA used here was the Non-dominated Sorting Genetic Algorithm (NSGA-II) proposed by Deb *et al.* (2002). The optimisation problem comprised 24 real decision variables, 4 integer variables and 3 objectives. The population size was set at between 100-240 solutions, crossover type: Simulated Binary Crossover (SBX) (Deb and Agrawal 1995), real crossover rate: 0.95, $\eta_c = 1-3$, real mutation type: polynomial mutation, mutation rate: $1/24$ and $\eta_m = 1-3$, binary crossover rate: 0.9 and binary mutation rate: 0.1-0.25. The suitable ranges of parameters of the GA shown above were determined manually by trial and error. A number of runs were conducted prior to the main optimisation to establish an understanding of the influence of the parameters on the convergence and diversity of solutions produced by the GA.

Given the stochastic nature of GAs it is not guaranteed that they converge to a global optimum (i.e., a Pareto front in the case of a multi-objective problem). Their strength lies in their ability to produce a good approximation of the Pareto front. The convergence can be influenced by the randomly generated initial population and, therefore, multiple runs were conducted. Figure 5.12 shows the final Pareto Front produced by combining the frontiers obtained from 4 independent optimisation runs with different initial populations (i.e., random seeds) and parameters of the GA.

5.3.2.3 Calibration Results

The algorithm produced an approximation of a Pareto-front of non-dominated solutions from which a single set of parameters was selected based on subjective criteria outlined in section 3.3.5. The selected solution (see the black circle in Figure 5.12) contained sigmoid normalisation function for the PBPM and logit normalisation function for the HM and the CCM. The preferred combination rule was the original Dempster's combination rule in this instance.

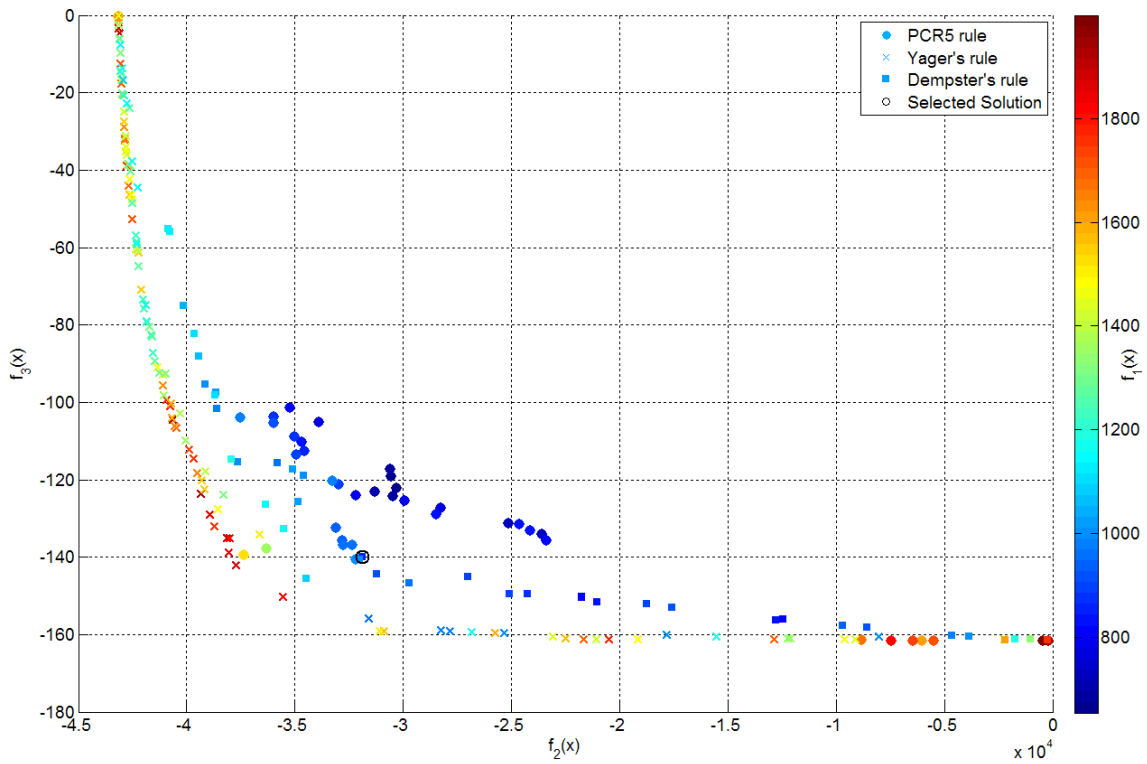


Figure 5.12 A 2D View of the 3D Pareto front showing the chosen solution

The shapes of the mapping functions as shown in Figure 5.13, Figure 5.14 and Figure 5.15 were suggested for the PBPM, the HM and the CCM, respectively.

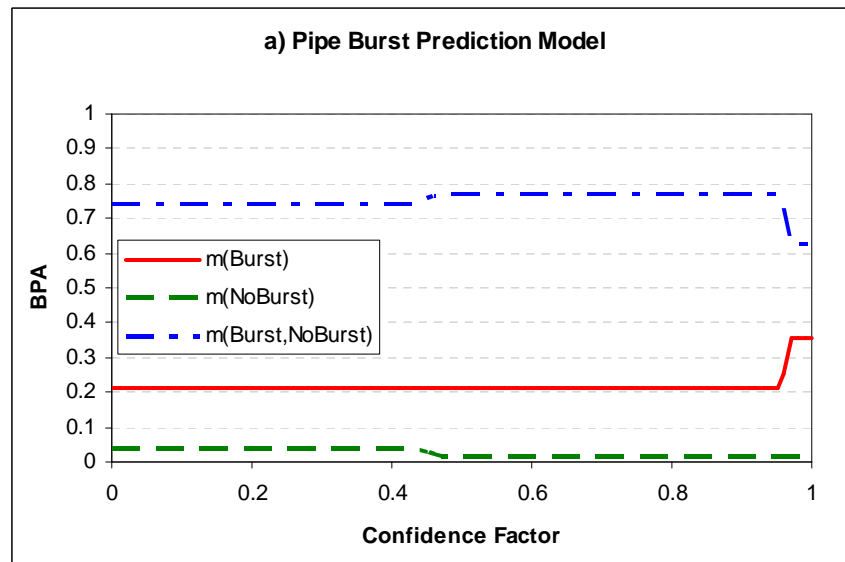


Figure 5.13 Mapping functions of the PBPM

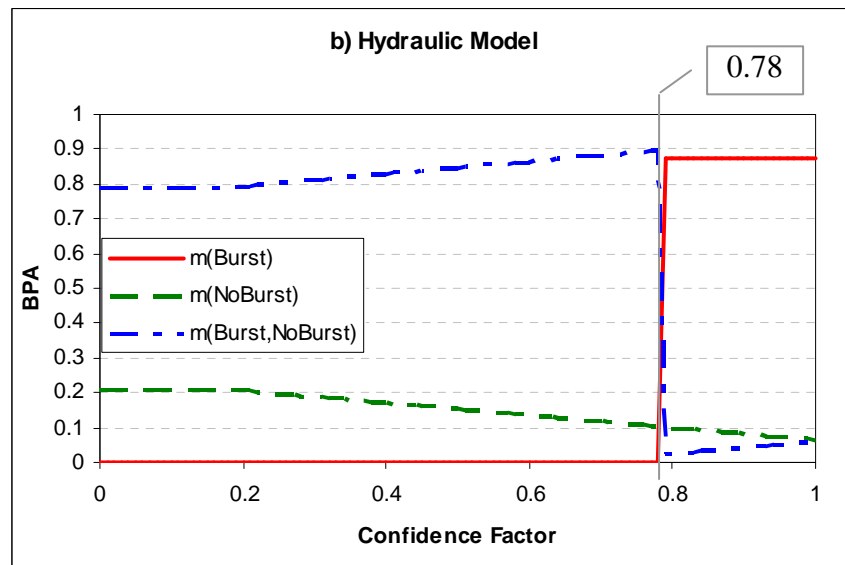


Figure 5.14 Mapping functions of the HM

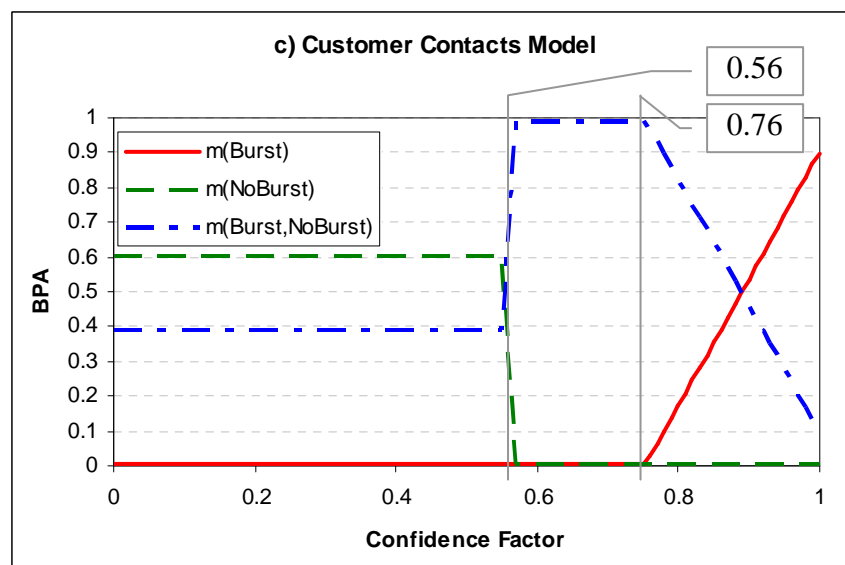


Figure 5.15 Mapping functions of the CCM

The above curves capture information about the overall performance of the individual models on calibration cases. The fact that the mapping curves are available and can be analysed by a DM can be seen as a benefit of the methodology over, e.g., ANNs (Haykin 1999), which behave as a “black box” and their internal structure remains hidden.

From the mapping curves presented in Figure 5.13, Figure 5.14 and Figure 5.15, it can be concluded that the PBPM (see Figure 5.13) played a less significant role in terms of

contributing to the fact that a particular element was the TBL (because of its lower credibility). It also did not provide much “negative” evidence suggesting that a particular pipe was not the TBL, which suggests that the PBPM would normally generate a high number of false positive locations.

Both the CCM and the HM were capable of narrowing down the search area where the TBL might be. Interestingly, in the case of the studied DMA the HM (see Figure 5.14) attributed equal level of belief (i.e., $m(\{Burst\})$) to a number of potential incidents whose value of the normalised confidence factor was greater than 0.78. This might suggest that the model was typically unable to distinguish the TBL within those potential incidents (e.g., because of the noise added to pressure measurements and nodal demands) and only perceived potential incidents with a high value of confidence factor as more plausible.

On the other hand, the CCM (see Figure 5.15) clearly showed that belief attributed to a potential incident was decreasing with an increase in distance of a pipe from CCs. The mapping curves of the CCM reflect the fact that it can be in some cases significantly wrong, which can be explained by the generally large level of epistemic uncertainty in the range of a confidence factor from 0.56 to 0.76. All potential incidents within this range are still entirely plausible burst locations. Only potential incidents whose value of confidence factor was below 0.56 were deemed as significantly less plausible burst locations.

The mapping curves presented above are likely to be valid for a single DMA only and a different set of curves needs to be obtained for other DMAs depending on the performance of the three individual models in those DMAs. The calibration of the curves for other DMAs might be difficult when only a short burst record history is available. The D-S model could be recalibrated as new historical cases become available. Such a process was not fully automated as part of this work since no rules were created to select a solution from the Pareto front produced during the calibration. For future calibration / re-calibration of the D-S model it is, therefore, vital to capture as much information about every burst pipe as possible (i.e., at least the exact date and time of burst detection and the location of the burst).

The mapping curves also justify the adoption of D-S theory, compared to a traditional Bayesian approach. As discussed in section 3.3.1 and in more detail in Appendix A, one of the distinguishing features of D-S theory is its ability to assign probability mass to subsets of the frame of discernment Θ . The mapping functions in Figure 5.13, Figure 5.14 and Figure 5.15 show that in all cases a significant amount of probability mass was attributed to the whole frame of discernment Θ representing complete lack of knowledge. The adopted calibration approach could, however, converge to a solution, where no or very little probability mass was assigned to Θ . This was not the case, which leads to the conclusion that the D-S theory was in this context a better mathematical framework than the traditional Bayesian approach.

5.3.3 Results and Discussion

The main aim of information fusion applied in the context of pipe burst diagnostics is to identify hotspots, comprising a small number of pipes, where the burst is most likely to be located. Table 5.11 gives detailed results about the performance of the individual models as well as the D-S model on all of the 54 calibration and validation cases considered in this case study. Besides providing information about a particular historical burst, such as its WMSY ID, date when it was repaired, ID of a burst pipe (i.e., the TBL) it also reports Belief (Bel), Plausibility (Pl) and pignistic probability (BetP) attributed to the TBL by the D-S model. Most importantly the last four columns (i.e., the D-S M, PBPM, HM and CCM) show the rank of the TBL provided by each of the individual models as well as the D-S model. The lower the value of the rank, the better is the performance of a particular model. It is, therefore, possible to assess the scale of improvement (or deterioration of performance) in identifying the TBL for every case in Table 5.11.

Table 5.11 Detailed results of the performance of the D-S model

	Burst ID	Order Date	Link Id	Bel	Pl	BetP	D-S M	PBPM	HM	CCM
calibration cases no CC	6038359	13/04/2004 12:00	0004G302	0.90	0.93	0.91	85	1049	47	-
	6588773	16/12/2004 05:00	0004G39H	0.92	0.94	0.93	22	149	77	-
	7701432	24/04/2006 07:00	0004G30E	0.92	0.94	0.93	23	104	50	-
	7719426	02/05/2006 08:00	0004G30A	0.92	0.95	0.93	6	104	13	-
	4998859	10/01/2003 07:00	0EJ9KB3F	0.92	0.94	0.93	27	287	62	-
	5600831	30/09/2003 03:00	0004G37I	0.92	0.93	0.92	3	167	50	-
	5710918	18/11/2003 05:00	0004E11L	0.90	0.92	0.91	74	1049	63	-
	9540594	28/04/2008 17:00	0EJ9KAGM	0.90	0.94	0.92	15	305	11	-

	Burst ID	Order Date	Link Id	Bel	PI	BetP	D-S M	PBPM	HM	CCM	
CC	8640654	23/05/2007 12:00	0004E11G	0.90	0.94	0.92	4	588	5	-	
	8681541	05/06/2007 02:00	0EJ9KB36	0.92	0.93	0.92	1	24	37	-	
	5468788	04/08/2003 01:00	0EJ9KB36	0.90	0.94	0.92	80	287	70	-	
	4398117	23/04/2002 03:00	0EIJ3F3	0.92	0.93	0.92	21	244	163	-	
	4533556	19/06/2002 11:00	0004G39H	0.92	0.94	0.93	10	149	94	-	
	5571373	17/09/2003 06:00	0004G2F0	0.90	0.94	0.92	74	406	6	-	
	4651377	06/08/2002 07:00	0EJ9KDNN	0.81	0.84	0.83	10	167	81	1036	
	8230257	11/12/2006 10:00	0004E119	0.78	0.80	0.79	105	655	126	562	
	5523071	27/08/2003 12:00	0004G3AI	0.90	0.92	0.91	63	975	57	410	
	8343335	31/01/2007 01:00	0004G28G	0.92	0.93	0.92	11	26	197	346	
	8120373	22/10/2006 17:00	0004E9G5	0.90	0.94	0.92	3	765	7	304	
	8375245	13/02/2007 05:00	0EIII5H	0.90	0.94	0.92	8	764	4	284	
	5003372	13/01/2003 15:00	0004E1G2	0.90	0.94	0.92	58	616	18	224	
	8044356	17/09/2006 17:00	0004G393	0.90	0.93	0.92	39	631	48	153	
	9085548	08/11/2007 01:00	0004E1M5	0.20	0.89	0.55	106	605	181	93	
	7575245	02/03/2006 14:00	0004G36G	0.93	0.95	0.94	7	232	81	7	
	5773552	17/12/2003 03:00	0EJ9KC14	0.91	0.95	0.93	4	512	1	4	
	6004593	29/03/2004 09:00	0004E1EK	0.99	0.99	0.99	0	144	10	0	
	6565521	04/12/2004 01:00	0004G28G	0.99	0.99	0.99	0	672	7	0	
	7435423	03/01/2006 08:00	0004E1II	0.99	0.99	0.99	0	21	0	0	
	9298957	30/01/2008 21:00	0004G2MM	0.99	0.99	0.99	0	16	2	0	
	8914690	03/09/2007 07:00	0004G370	0.99	0.99	0.99	0	490	119	0	
	4953310	18/12/2002 01:00	0EJ9LH1N	0.99	0.99	0.99	0	616	115	0	
	5000220	11/01/2003 11:00	0004G283	0.99	0.99	0.99	0	565	19	0	
	5871806	01/02/2004 08:00	0004G38H	0.99	0.99	0.99	0	406	46	0	
	7879730	09/07/2006 21:00	0004G38I	0.99	0.99	0.99	0	406	15	0	
	8284538	07/01/2007 15:00	0004G2N6	0.99	0.99	0.99	0	948	26	0	
	8732007	24/06/2007 02:00	0004G38E	0.91	0.98	0.95	0	451	121	0	
	5251001	01/05/2003 05:00	0004E1J3	0.99	0.99	0.99	0	636	49	0	
	6911300	11/05/2005 23:00	0004G2DG	0.99	0.99	0.99	0	708	17	0	
	7180113	09/09/2005 22:00	0004G2MM	0.99	0.99	0.99	0	261	0	0	
	7354905	26/11/2005 20:00	0004G37I	0.99	0.99	0.99	0	167	5	0	
	5553615	09/09/2003 22:00	0004E1IL	0.99	0.99	0.99	0	1049	46	0	
	validation cases	no CC	4396152	22/04/2002 17:00	0004G37A	0.90	0.92	0.91	35	548	20
4396389			22/04/2002 08:00	0004G3AB	0.90	0.94	0.92	93	416	108	-
8005667			31/08/2006 04:00	0004G38E	0.19	0.89	0.54	500	406	458	-
8606121			09/05/2007 19:00	0004G2FE	0.90	0.93	0.91	36	179	38	-
4639990			01/08/2002 21:00	0004E1KJ	0.90	0.93	0.91	66	512	87	-
6283602			28/07/2004 09:00	0EJ9LG5E	0.81	0.84	0.83	9	232	6	694
CC		7080348	26/07/2005 06:00	0EJ9L2BD	0.79	0.82	0.80	97	287	25	575
		9315021	05/02/2008 13:00	0EIII5H	0.90	0.94	0.92	7	742	0	10
		8905881	31/08/2007 05:00	0EJ9L2BF	0.93	0.95	0.94	9	291	54	9
		8583704	30/04/2007 10:00	0004G2FE	0.98	0.99	0.98	3	179	9	3
		5957590	09/03/2004 09:00	0EJ9LHHD	0.99	0.99	0.99	1	672	1	2
		6657966	22/01/2005 19:00	0EJ9LHHD	0.99	0.99	0.99	2	672	7	2
		5086020	19/02/2003 22:00	0004G37I	0.99	0.99	0.99	0	167	197	0

If the combined results were compared to the best individual model (i.e., based on the results presented in Table 5.11), it can be seen that the D-S model results were equal or better than the best individual models in 61% and 75% of validation and calibration cases, respectively. It should be noted, however, that such information (i.e., which is the “best” individual model) would not be *a priori* known in real decision-making situations. The D-S model provided better result than any of the individual models in 23% and 34% of validation and calibration cases, respectively.

5.3.3.1 D-S Model Example Application

Figure 5.16 illustrates the performance of the D-S model on a historical pipe burst selected from the calibration dataset. In this case, the burst was reported by two customers and, therefore, all three sources of evidence were available.

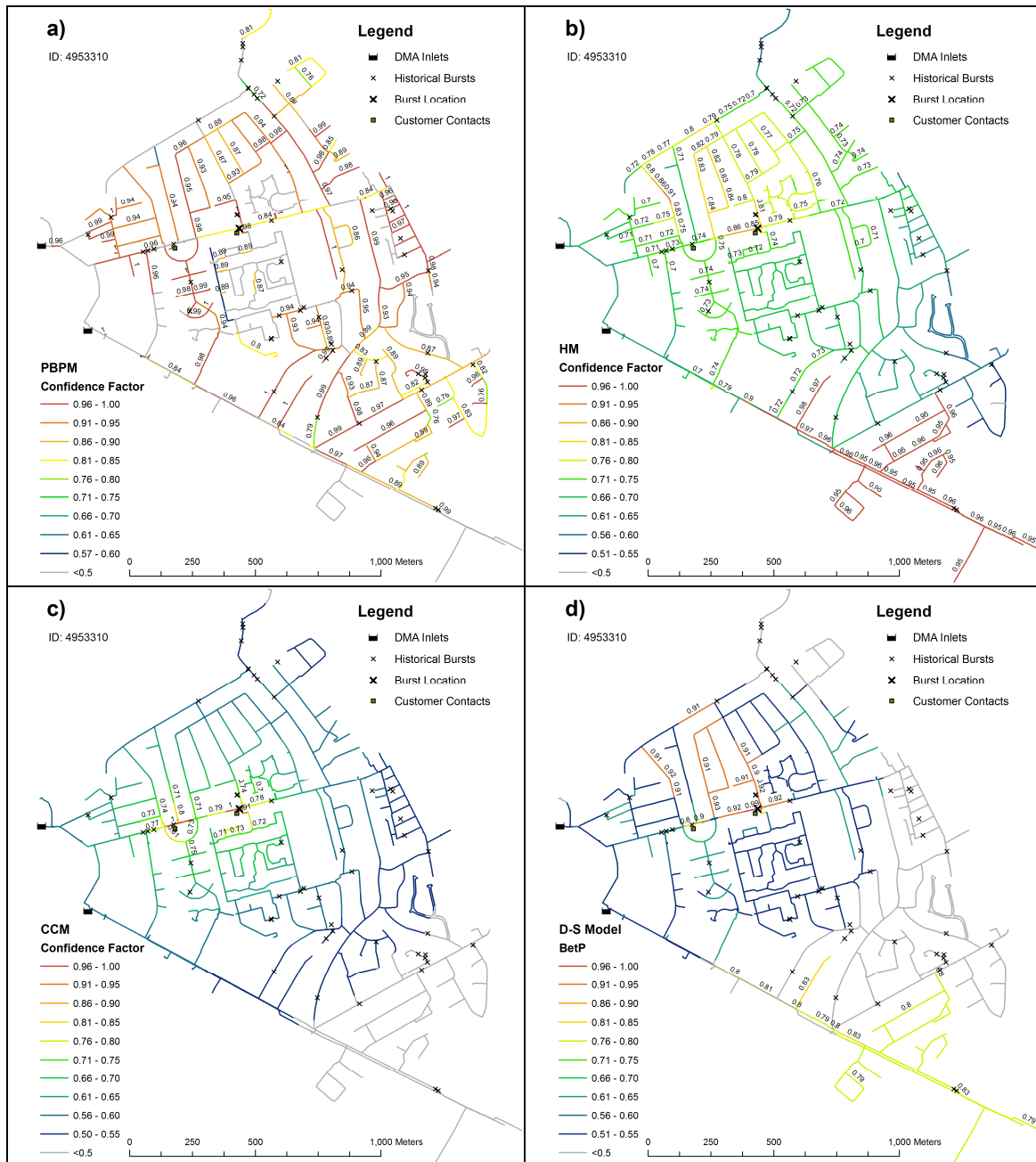


Figure 5.16 An example output from the a) PBPM, b) HM, c) CCM and d) the D-S model: $BetP(\{Burst\})$

The accuracy of the PBPM was limited and a large number of pipes received the same value of confidence factor (see Figure 5.16a). The HM performed poorly in this particular case and identified two possible pipe burst hotspots, with the most likely location being far from the burst pipe (see Figure 5.16b). One of the CCs was received from a location in close proximity to the burst pipe whereas the other one was more than 250 m away from the burst location (see Figure 5.16c). Mostly based on the input of the

CCM, the D-S model attributed higher levels of $BetP(\{Burst\})$ (see Figure 5.16d) to the pipes in the proximity of the second pipe burst hotspot previously identified by the HM, supporting the proposition that this was the TBL (i.e., according to a record in WMSY that a burst was repaired there). The pipes close to the second customer contact, which was further away from the TBL, received a lower level of $BetP(\{Burst\})$. Therefore, a field investigation, based on the results of the D-S model, could focus on the first customer contact and thus reduce the time needed to locate the burst, decrease the amount of water lost from the system and the possible follow-on (socio-economic) impact on customers.

Figure 5.17 shows spatial distribution of *Belief* and *Plausibility*. It can be observed that after the information fusion high levels of belief are typically attributed to only a small number of potential incidents. On the other hand a high number of potential incidents typically receive a high level of plausibility, suggesting that no evidence exists, supporting the fact that those pipes could not be the TBL.

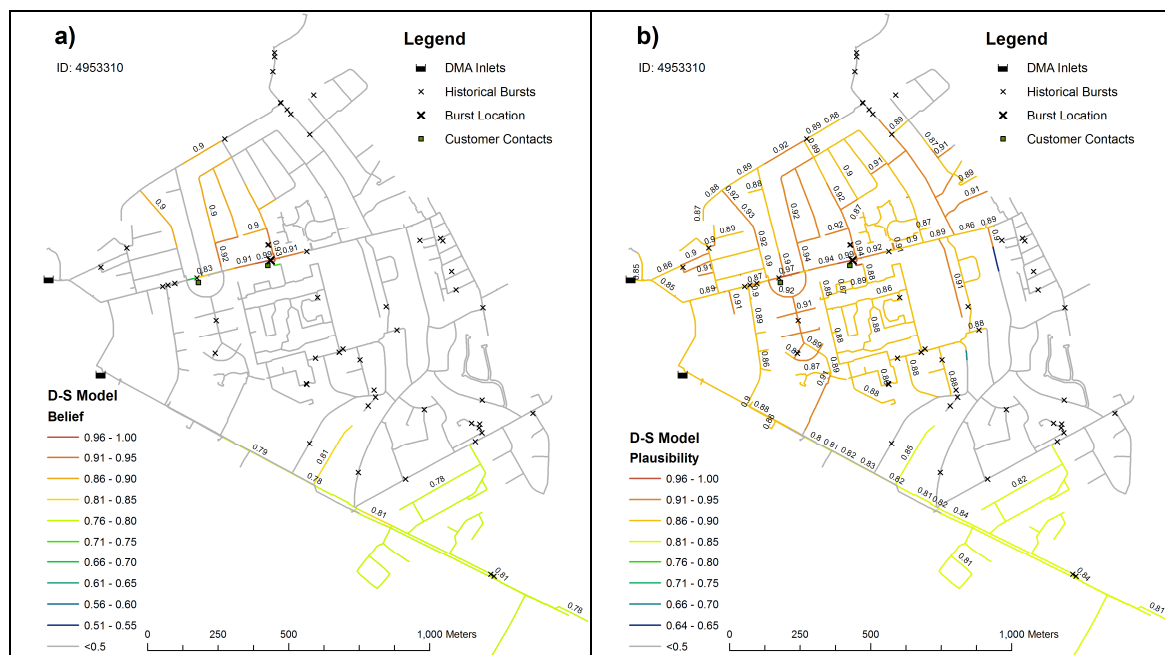


Figure 5.17 Belief and Plausibility maps produced by the D-S model

Additional detailed examples of four cases selected from the validation dataset shown in Table 5.11 are given in Appendix D. The examples provided aim to demonstrate the properties of the D-S model in situations when evidence from some data sources (e.g.,

the CCM) was conflicting or missing entirely. The importance of considering both, Belief and Plausibility by the DM under certain circumstances is also illustrated.

5.3.3.2 Performance Comparison

Table 5.12 shows the performance of the D-S model and the individual models on calibration and validation cases. These were further split depending on the presence of CCs. The comparison was based on the ranking (see section 3.3.5) of the TBL according to the output of the D-S model (i.e., the $BetP(\{Burst\})$) and the ranking assigned by individual models (i.e., based on their criterion measurement). The performance of any model was considered good if the TBL was amongst the top 10 burst candidates identified by the respective model. As can be seen from Table 5.12 none of the individual input models, i.e., the PBPM, HM and CCM, was able to achieve the above goal in all of the situations (i.e., 54 historical pipe bursts) considered in the case study. The degree of success in identifying the location of a burst pipe varied significantly amongst the models. According to this assessment criterion the overall performance of the D-S model was on average in every scenario either equally good or better than the performance of any of the individual models. Similar performance can be observed when the number of potential burst candidates was increased from 10 to 50 (i.e., the area of the burst hotspot was expanded).

Table 5.12 An overview of the performance of the D-S model

Scenario	Rank of TBL < 10				Rank of TBL < 50			
	D-S Model	PBPM	HM	CCM	D-S Model	PBPM	HM	CCM
Calibration (No CC)	28.6%	0.0%	14.3%	0.0%	71.4%	7.1%	42.9%	0.0%
Calibration (CC)	74.1%	0.0%	29.6%	66.7%	85.2%	11.1%	66.7%	66.7%
Validation (No CC)	0.0%	0.0%	0.0%	0.0%	40.0%	0.0%	40.0%	0.0%
Validation (CC)	87.5%	0.0%	62.5%	62.5%	87.5%	0.0%	75.0%	75.0%

The D-S Model, however, as well as the HM and CCM significantly outperform random identification of the TBL, which would yield less than 1% and less than 5% for the “Rank of TBL < 10” and the “Rank of TBL < 50” scenarios, respectively. The performance of the PBPM might in this sense be seen as disappointing. This can be explained by the fact that a relatively high number of potential incidents receive the same value of criterion measurement from the PBPM. The TBL, therefore, does not fall within the top 10 or 50 potential incidents (i.e., due to the way the rank was calculated),

despite having the highest value of criterion measurement (i.e., likelihood of failure occurrence).

Evaluating the benefits of information fusion algorithms is not simple and using only the measure above would not reflect the additional advantages of this approach. A particular model might fail to identify the correct burst location according to the criteria used above but can, on the other hand, still identify a number of locations where the burst pipe is unlikely to be located. To take this fact into the account and to compare the quality of the output of the D-S model and the individual models, the following set of performance indicators was established:

Likelihood concentration. For the method to be useful operationally, it is important that the likelihood of burst occurrence assigned to the pipes near the TBL is significantly higher than the likelihood assigned to pipes further away. This can be expressed using the ratio of the average likelihood of occurrence of the burst assigned to pipes close to the TBL over the average likelihood of burst occurrence assigned to all remaining pipes. The higher this ratio, the better the overall performance of a particular model. The set of pipes in the proximity of the TBL was assumed here as the 10 topologically nearest pipes. Given that the average length of pipes in the case study area was 30 m and that the network was highly looped, such resolution should be considered acceptable.

Certainty. According to Yager (2004), Shannon entropy (Shannon 1948) was used to characterise the certainty of the outputs of the individual models and the D-S model. The entropy of an information source (i.e., output of a particular model) was calculated using Eq. (5.3) and its certainty can be expressed using Eq. (5.4). The higher the certainty of a particular model the better its performance was.

$$H = -\sum_{k=1}^{N_p} p_k(Burst) \ln(p_k(Burst)) \quad (5.3)$$

$$Certainty = 1 - \frac{H}{\ln(N_p)} \quad (5.4)$$

where: H is Shannon entropy, p_k is either the normalised $BetP_k(\{Burst\})$ or the normalised value of confidence factor of a potential incident (pipe) k in the case of the D-S model and the individual models, respectively and N_p is the number of potential incidents (i.e., pipes) in the DMA.

The results of the comparison based on the two additional criteria suggested above are shown in Table 5.13. The table indicates in how many calibration and validation cases the D-S model was better than the individual models (values above 50% indicate that the D-S model on average improved over the prediction of an individual model and 100% means that the D-S model was better in all considered cases than a particular individual model). Again, cases were further split into scenarios where CCs were and were not available.

Table 5.13 Performance of the D-S model compared with PBPM, HM and CCM based on spatial distribution of the likelihood of potential incidents

Scenario	Likelihood concentration			Certainty		
	D-S > PBPM	D-S > HM	D-S > CCM	D-S > PBPM	D-S > HM	D-S > CCM
Calibration (No CC)	100.0%	100.0%	-	85.7%	28.6%	-
Calibration (CC)	96.3%	100.0%	100.0%	96.3%	44.4%	100.0%
Validation (No CC)	80.0%	80.0%	-	80.0%	0.0%	-
Validation (CC)	100.0%	100.0%	100.0%	100.0%	75.0%	100.0%

Table 5.13 shows that the D-S model yields better results (e.g., D-S > PBPM) in terms of the Likelihood concentration in a higher number of cases when compared to the individual models. The D-S model was significantly better than the PBPM and CCM in view of the Certainty criterion, however, in some situations, it performed worse than the HM. This fact is most apparent in scenarios where no CCs were received and only the outputs of the HM and PBPM were combined. In such situations the most likely locations of the burst pipe typically form a number of scattered hotspots rather than a relatively well confined area as shown in Figure 5.16d. Despite this fact the use of the PBPM as an information source still yields certain benefits as demonstrated in Table 5.12.

5.3.4 Sensitivity Analysis

To investigate the sensitivity of individual model outputs as well as the D-S model output to noisy inputs, a global sensitivity analysis using Monte Carlo simulation (1,000 samples) was performed on the example presented in Figure D.5. The selected case represented a suitable scenario from the validation data set since at least two of the individual models (i.e., the HM and the CCM) performed acceptably and, therefore, the effect of the added noise could be observed. Various levels of uniformly distributed

noise as indicated in Table 5.14 were added to the inputs of the individual models, namely the HM (observed pressures, demands and estimated burst flow) and the CCM (Easting and Northing). Adding noise to the PBPM would be problematic (e.g., because it uses a number of non-numerical inputs, such as pipe material, etc.) and given its relatively low credibility it would not make a significant difference in this case. The AVG rank of the PBPM was, therefore, the same for all scenarios and had the value of 742.0 out of 1,052 potential incidents (i.e., poor performance in this case).

Table 5.14 Results of a global sensitivity analysis (case 9315021)

Scenario	Burst Flow	Pressure Noise	Demands Noise	Burst Flow Noise	CC Noise	AVG D-S Rank	AVG HM Rank	AVG CCM Rank
A	5	1.0%	5.0%	0.5%	0.01%	6.4	4.8	10.2
B	5	2.0%	10.0%	1.0%	0.01%	7.2	5.4	10.2
C	3	2.0%	7.5%	1.0%	0.01%	62.6	84.0	10.2
D	5	3.0%	10.0%	2.0%	0.02%	24.8	16.5	14.4
E	5	4.0%	10.0%	2.0%	0.02%	42.9	52.5	14.4
F	7	3.0%	10.0%	5.0%	0.03%	8.1	5.2	20.1
G	5	2.0%	7.5%	2.0%	0.03%	8.4	5.5	20.1
H	5	2.0%	7.5%	4.0%	0.03%	9.9	5.6	20.1
I	5	3.0%	7.5%	1.0%	0.03%	26.4	16.3	20.1
J	3	2.0%	7.5%	1.0%	0.03%	66.9	84.0	20.1
K	5	1.0%	7.5%	0.5%	0.05%	8.1	4.8	37.5
L	5	2.0%	10.0%	1.0%	0.05%	8.9	5.4	37.5
M	3	2.0%	10.0%	1.0%	0.05%	78.0	84.0	37.5
N	7	2.0%	10.0%	2.0%	0.08%	8.2	4.9	70.1
O	7	5.0%	10.0%	2.0%	0.08%	26.5	9.8	70.1

The “AVG Rank” shown in Table 5.14 is the rank as described in section 3.3.5, averaged over 1,000 samples. The lower the value of the “AVG Rank” the better the performance of a particular model was. Table 5.14 suggests that the combined results were in all scenarios (for this particular case) slightly worse than those of the best model (such information is, however, unknown until the burst is located by a field technician). On the other hand, the D-S model outputs were to some extent less sensitive to the noise added to the inputs of individual models. If the performance of only one of the models degraded significantly, the two remaining models (the CCM or HM in particular) would still influence the combined results so that they did not degrade as fast as the worst model. However, in cases where the quality of evidence of the most influential input models (i.e., the HM and the CCM) deteriorated at the same time (e.g., because of the

amount of noise present in the data or due to low burst flow; illustrated in scenarios D and I in Table 5.14), then the combined results were worse than those of any of the two key input models.

5.3.5 Comparison with Other Methods

The performance of the newly proposed D-S model was compared with other simple information fusion methods, such as Mean, Weighted Average (WA), Product and Generalised Mean (GM) (Polikar 2006). The comparison of the performance was again based on the rank of the TBL when all potential incidents were sorted in a descending order according to their likelihood of occurrence (i.e., $BetP(\{Burst\})$ in case of the D-S model or criterion measurement in case of the individual models). In the case of the WA and GM methods the values of required parameters were optimised to achieve the best possible results in all 54 cases (i.e., not only on the calibration data set). Table 5.15 shows that the combination of the model outputs using Evidence theory dominates the other methods' outputs in majority of the cases analysed.

Table 5.15 Comparison of the performance of the D-S theory with other combination functions

	Mean	WA	Product	GM
D-S equal or better [%]	94.4	75.9	96.3	83.3
D-S better [%]	87.0	64.8	96.3	55.6

The relatively high number of cases where the D-S model performed equally well with the WA and GM functions can be explained by the fact that in these cases all methods managed to correctly identify the burst pipe and, therefore, there was no potential for further improvement.

5.4 Impact Model

This section describes the calibration of the impact model developed in Chapter 3.4, by conducting a quantitative questionnaire survey. Detailed outputs of the impact model are not presented here due to the amount of data produced by the model and difficult visualisation of its outputs in a non-interactive way. Instead, the aggregated outputs of the impact model are presented as part of section 5.5, which discusses the automated

alarm prioritisation, where the impact model was used to provide one part of the risk metric.

5.4.1 Impact Importance Survey

To determine the preferences of a water utility in terms of importance of different types of impacts a questionnaire survey (see Appendix B) was conducted in two UK water utilities. For confidentiality reasons, the results presented here do not refer to a specific company.

The questionnaire comprised four main sections, excluding an introduction. First, the purpose of the survey was explained to the respondents and guidance on how to answer the questions used in the survey was provided. Contact details of the author were available to allow the respondents to get support in case of any problems. The respondents were asked to answer all 9 questions in the survey from the perspective of an employee of a particular water company rather than its customers. The four main sections of the questionnaire were as follows:

- **Customer Importance** (1 question) – to determine the mutual importance of different customer types
- **Types of Impact** (5 questions) – to determine the mutual importance of different types of impact, their duration and scale
- **Personal Information** (2 questions) – to determine the role of the respondent within a company
- **Other** (1 question) – to allow respondents to provide further comments

Table 5.16 provides a summary of the questions included in the survey for each of the above categories.

Table 5.16 A summary of questions included in the online survey

Group	Id	Question
<i>Customer Importance</i>	1	Please, indicate the mutual importance of the following types of customers according to their vulnerability in case of a failure in a water distribution system (e.g., a pipe burst causing low pressure or supply interruption).
<i>Types of Impact</i>	2	Please, indicate the importance of the following economic impacts, having equal scale (i.e., financial losses), which affect the water utility (company). Bear in mind that the impacts might negatively affect the public image of the company.
	3	Please, indicate the importance of the duration of supply interruption affecting the same number of customers of the same type (e.g., residential).
	4	Please, indicate the importance of the duration of low pressure problems affecting the same number of customers of the same type (e.g., residential).
	5	Please, indicate the importance of the scale of the same impact (e.g., supply interruption) on the customers of the same type (e.g., residential) for the same period of time.
	6	Please, indicate the mutual importance of the following types of impacts affecting the same number of properties for the same period of time (where applicable).
<i>Personal Information</i>	7	Please, select the company / organisation you work for:
	8	Please, select your occupation
<i>Other</i>	9	Please, provide additional comments

The questions were set up in a way that would allow easy extraction of the preferences in form of a vector of weights using the AHP developed by Saaty (1980). AHP is a well established method for solving complex decision-making problems using a number of pairwise comparisons between a set of criteria. One of the advantages of AHP is also its capability to determine consistency of the responses.

The respondents were asked to indicate the mutual importance of two criteria (e.g., Supply Interruption and Discolouration) according to their preferences. A 9-point linguistic scale adapted from Saaty (1980) shown in Table 5.17 was used.

Table 5.17 Arithmetic scale used in AHP (adapted from (Saaty (1980))

Linguistic Preference	Importance (arithmetic scale)
Unquestionably more important	9
Much more important	7
More important	5
Rather more important	3
Equally important	1
Rather less important	1/3
Less important	1/5
Much less important	1/7
Unquestionably less important	1/9

Apart from the arithmetic scale, other scales such as the exponential and fuzzy scale exist (Vamvakeridou-Lyroudia *et al.* 2006) but these were not applied in this work. One of the disadvantages of applying AHP is that the number of criteria to be compared needs to be small (e.g., less than 5) otherwise the number of pairwise comparisons required from a respondent would be too high. To determine preference weights of N criteria $\frac{N(N-1)}{2}$ pairwise comparisons are required. Therefore, the number of criteria used in this survey was a maximum of four, requiring at most six pairwise comparisons to be entered by a respondent.

An online form of delivery of the questionnaire was chosen to facilitate its creation and analysis of the results. The questionnaire was created and deployed using the LimeSurvey (2010) software package. A printed copy of the questionnaire is included in Appendix B.

To ensure that the questionnaire was designed well to provide answers to the unknown impact preferences of water companies, a small scale pilot study was first carried out within the Centre for Water Systems at the University of Exeter. The very specific target group for the pilot was particularly chosen to resemble the highly skilled and experienced employees of a water company. The pilot study revealed a small number of issues in the questionnaire that were corrected to improve the clarity of the questions before the survey was conducted at selected water utilities, which were participating in the aforementioned NEPTUNE project (Savić *et al.* 2008).

In total 26 responses were received from Company 1 and only 6 responses from Company 2. Out of the 26 responses (approx. 25% return rate) of Company 1, two were incomplete and an additional five questionnaires had to be discarded due to highly inconsistent answers or misunderstanding of the linguistic scale used. For the analysis considered here, 19 questionnaires from Company 1 and all 6 responses from Company 2 were used. Figure 5.18 shows the distribution of the respondents depending on their role in the company. Due to the small sample of respondents in this survey, a comparison of responses from people of different positions in the companies could not be carried out.

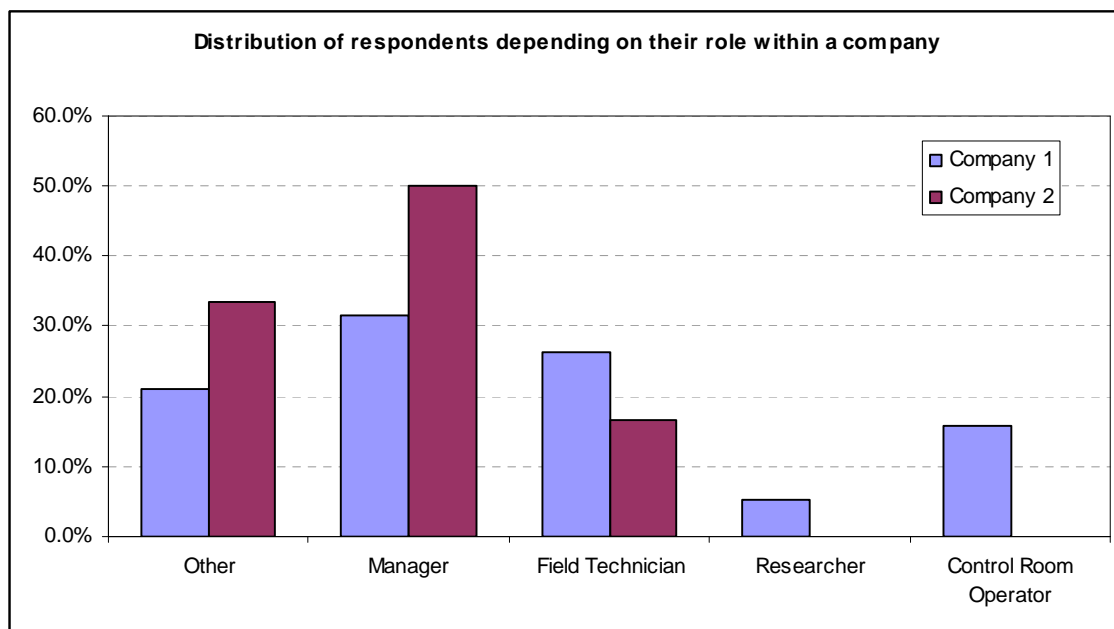


Figure 5.18 Distribution of respondents depending on their role within a company

5.4.2 Questionnaire Survey Analysis Methodology

The responses collected were analysed separately for each of the two companies to allow a comparison of the preferences. The aim of the survey was to derive preferences of the company as a whole (i.e., a group decision-making context) rather than of the individual participants of the survey. Given the chosen mode of delivery of the survey (i.e., an online questionnaire), consensus voting, which requires direct involvement of the DMs to reach agreement for each pairwise comparison, could not be used. As discussed by Mikhailov (2004) a number of group decision-making methods exist to aggregate the opinions of a group. The aggregation can take place at two different levels

(Forman and Peniwati 1998) depending on how the group wants to act, i.e., as a unit or as individuals. In the first case, referred to as Aggregation of Individual Judgements (AIJ), the individual pairwise comparisons are first aggregated before the AHP is applied. The second method, sometimes also called the Aggregation of Individual Priorities (AIP), applies AHP separately to the pairwise comparisons of every group member and then aggregates the weights derived using AHP. The arithmetic mean and the geometric mean are commonly applied to aggregate group preferences for both aggregation levels (i.e., AIJ and AIP) (Mikhailov 2004). As suggested by Forman and Peniwati (1998) the geometric mean is more suitable for the AIJ aggregation, whereas both the arithmetic mean and the geometric mean could be used in case of the AIP aggregation. Forman and Peniwati (1998) further suggested that in situations when the importance of the DMs is not equal then weighted alternatives of the means could be used.

It was decided here to follow the AIJ approach and first aggregate the pairwise comparisons of individuals within a group before applying AHP only once. The chosen approach not only emphasises that the group (i.e., a water company) acts as a unit but also overcomes problems of slightly inconsistent responses of some individuals, which were softened during the aggregation of judgements. Moreover, by aggregating the individual judgements first, AHP only has to be applied once, which could save computational time if it was necessary to derive the priorities in R-T. However, this was not needed in the work presented here since the impact preferences were derived only once. The influence of individuals within the group was considered equal, whereas in reality it is likely that the managers would have a higher decision-making power compared to other employees of a water utility. The geometric mean (Eq. (5.5)) was used to aggregate the individual judgements.

$$a_{i,j} = \left(\prod_{k=1}^{N_R} a_{i,j,k} \right)^{1/N_R} \quad (5.5)$$

where: $a_{i,j}$ is the preference of a group with respect to pairwise comparison of criteria i and j , $a_{i,j,k}$ is the numerical representation (see Table 5.17) of pairwise comparison of criteria i and j of respondent k and N_R is the number of respondents considered in the survey.

Table 5.18 shows an example of a pairwise comparison matrix \mathbf{A} built based on aggregated responses $a_{i,j}$ (i.e., Eq. (5.5)) of survey participants.

Table 5.18 A pairwise comparison matrix \mathbf{A} for Customer importance (Company 1)

	Critical	Residential	Commercial	Industrial
Critical	1.00	6.81	7.28	5.48
Residential	0.15	1.00	1.57	0.95
Commercial	0.14	0.64	1.00	0.41
Industrial	0.18	1.05	2.45	1.00

Every element in the pairwise comparison matrix suggests the mutual importance of criteria in a row of the element compared to the criteria in the column of the element. E.g., the value of 7.28 in the second row and the fourth column of Table 5.18 (i.e., the first row and the third column of matrix \mathbf{A}) suggests that the impact on Critical customers is perceived by a company as “much more important” (i.e., according to the linguistic scale in Table 5.17) than the impact on Commercial customers.

The values of elements of the lower triangular of the pairwise comparison matrix \mathbf{A} , generated from the questions included in the survey, correspond to the inverse values of the elements in the upper triangular of the matrix \mathbf{A} (i.e., $a_{i,j} = 1 / a_{j,i}$). This is the result of the formulation of the pairwise comparisons in the questionnaire survey and the above relationship does not have to hold every time. Situations when $a_{i,j} \neq 1 / a_{j,i}$ typically indicate inconsistency in the pairwise comparisons.

Once the opinion of a group of DMs regarding all pairwise comparisons was expressed using the pairwise comparison matrix above, the AHP was applied. A number of prioritisation methods can be used within AHP (e.g., Eigenvalue Method, Logarithmic Least Squares Method, Least Squares Method, etc.) (Saaty and Vargas 1984; Srdjevic 2005). Here the Eigenvalue Method (EM) method as originally proposed by Saaty (1980) was used to derive a vector of preference weights w from the pairwise comparison matrix \mathbf{A} . The preference (priority) weights can be expressed using the EM method as follows:

$$\sum_{j=1}^n a_{ij} w_j = \lambda_{max} w_i, \quad i = 1, 2, \dots, n \quad (5.6)$$

where: λ_{max} is the principal eigenvector and n is the number of criteria in the pairwise comparison matrix \mathbf{A} , $a_{i,j}$ is an element of matrix \mathbf{A} .

As noted by Srdjevic (2005) the EM gives a reasonably good approximation of the preference weights when inconsistency is small. The consistency of the preferences of the pairwise comparisons provided by a DM can be quantified using the Consistency Index (CI) (Saaty 1980). If the EM method was used to derive weights from the pairwise comparison matrix, the CI is defined using the following equation:

$$CI = \frac{\lambda_{max} - n}{n - 1} \quad (5.7)$$

Consistency can be also expressed using the Consistency Ratio (CR), which is shown in Eq. (5.8) as a fraction of CI and the Random Index (RI). RI is the average CI of randomly generated pairwise comparisons. Values of RI for a particular number of criteria are given in Table 5.19. (Saaty 1980)

$$CR = \frac{CI}{RI_n} \quad (5.8)$$

Table 5.19 Values of Random Index for a given number of criteria

n	1	2	3	4	5	6	7	8	9	10
RI_n	0	0	0.58	0.9	1.12	1.24	1.32	1.41	1.45	1.49

Generally, values of $CR < 0.1$ are considered as consistent. Higher values indicate inconsistencies in the pairwise comparison matrix and might require the collection of new data or additional corrections of the pairwise comparison matrix.

5.4.3 Questionnaire Survey Results

The analysis of the data collected revealed that the consistency of answers to all three questions 3, 4 and 5 that tried to determine importance of different duration or scale of supply interruption or low pressure impact, was very low. Given the poor results obtained from questions 3, 4 and 5, question 5 (i.e., the duration and scale of impact) was excluded from the questionnaire given to Company 2, since the questionnaires were not distributed at the same time. As can be seen from Table 5.20, the CR index for questions 3, 4 and 5 exceeded the 0.1 threshold in most cases, which is an indication of

poor consistency. The aim of those questions was to find out whether the effect of duration or scale of the impact had a linear relationship or could be described by some other mathematical function. It seems that those questions were either misunderstood by the survey participants or the chosen type of question (i.e., the 9-point preference scale) was not suitable to determine such information. Those questions were discarded and not considered further in this work. Equal importance between the duration and scale of an impact was assumed. Similarly, no preference between the scale of an impact and its magnitude in the case of discolouration impact was presumed. The assumption of equal importance between the above criteria was chosen because of its simplicity and because it could be adjusted if more data was available.

The responses to the remaining questions were more consistent (see Table 5.20) and almost all of them had $CR < 0.1$. Responses from Company 1 to question no. 6 were slightly less consistent (i.e., having $CR = 0.101$), which was still considered acceptable.

Table 5.20 An overview of consistency of the responses

Id	Question	CR	
		Company 1	Company 2
1	Customer Importance	0.016	0.022
2	Economic Impact Type	0.000	0.065
3	Duration of Supply Interruption	0.321	0.174
4	Duration of Low Pressure Impact	0.285	0.049
5	Scale of Impact	0.326	N/A
6	Impact Type	0.101	0.041

The outcomes of the questionnaire analysis are shown in Figure 5.19, Figure 5.20 and Figure 5.21. The importance of different customer types from the point of view of a water utility is shown in Figure 5.19. Critical customers (e.g., hospitals, schools, etc.) ranked highest, whereas commercial customers obtained the lowest priority. Both companies in this case seemed to have very similar preferences.

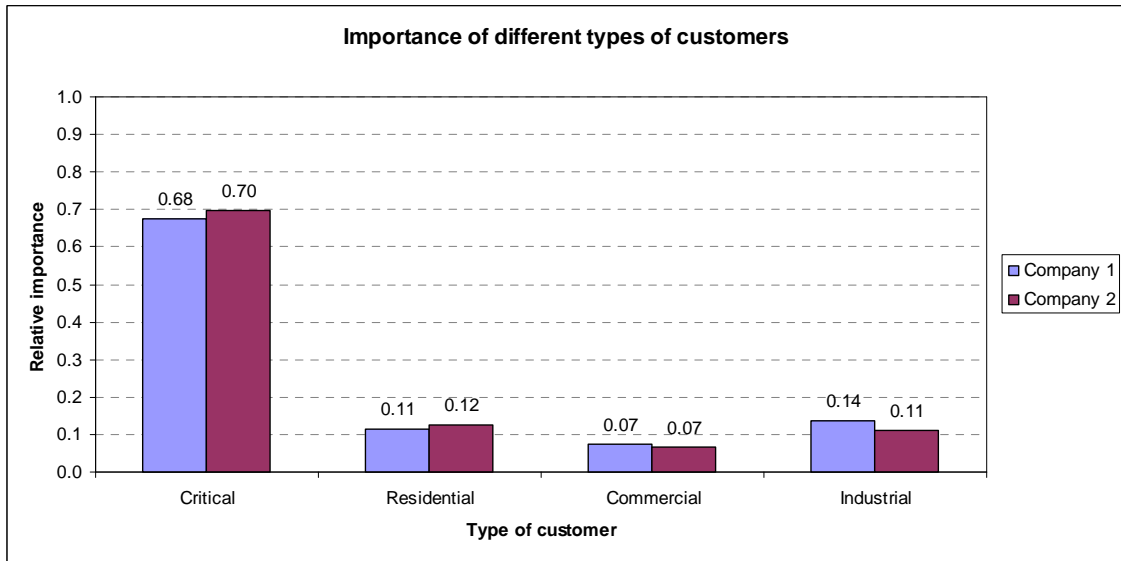


Figure 5.19 The relative importance of various types of customers

Figure 5.20 displays the importance of different impact categories (i.e., objectives) from a hierarchy shown in Figure 3.17. Both companies ranked the impact categories in the same order of significance, however, attributed different levels of priority particularly to Supply Interruption and Discolouration. The similar value of weighting factor attributed to Supply Interruption and Discolouration by Company 2 (i.e., in contrast to Company 1) could be explained by the fact that, in neither of the cases the consumers can use water (i.e., people would not drink discoloured water).

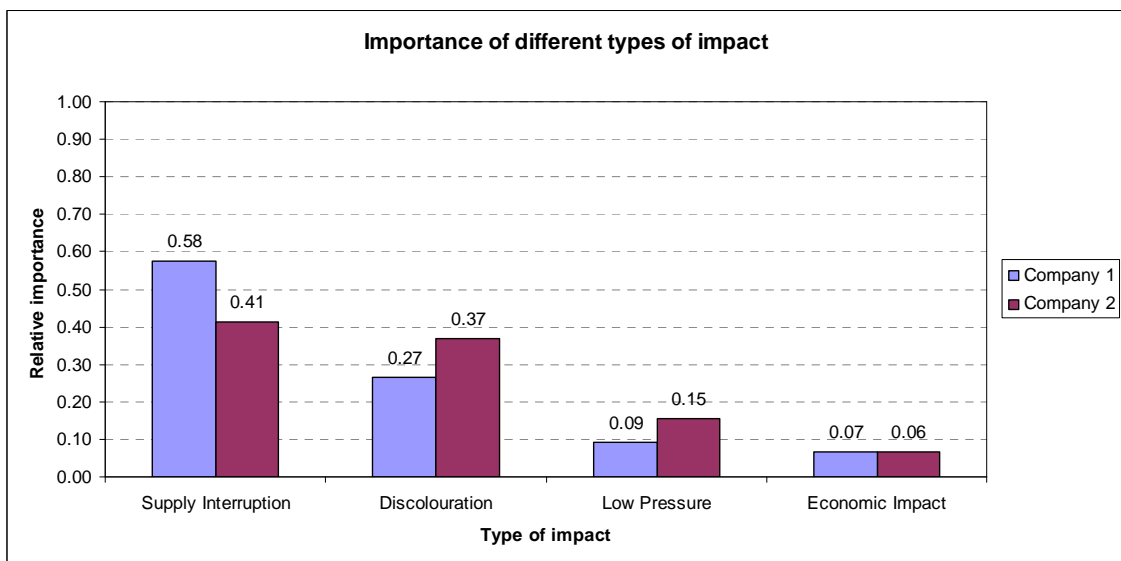


Figure 5.20 The relative importance of different types of impact

The preferences related to different types of economic impact are shown in Figure 5.21. The weights obtained do not differ too significantly between the two companies. Company 2 put much more emphasis on Third Party Damage impact, perhaps since it can be associated with negative public image.

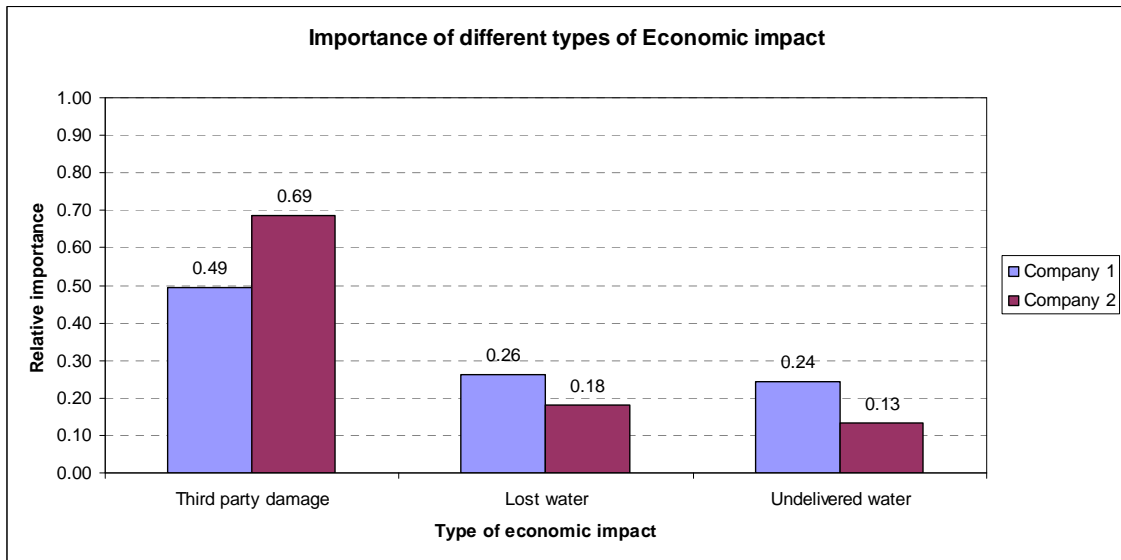


Figure 5.21 The relative importance of different types of Economic impact

Based on the above results, the preferences obtained can be put into the objective tree from Figure 3.17. An updated objective tree with specific values for water Company 1 is illustrated in Figure 5.22.

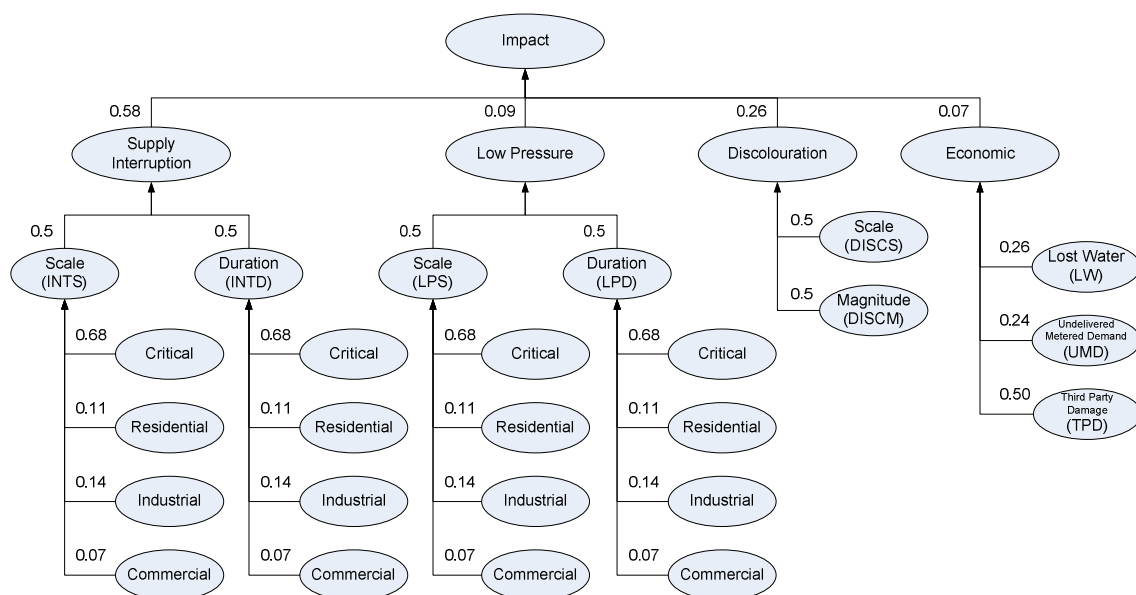


Figure 5.22 An objective tree used in impact aggregation with determined weights

To calculate the overall impact of a failure, the values of KPIs proposed in section 3.4.3 are substituted in the leaves in Figure 5.22 and propagated through a hierarchy of weights as suggested in Eq. (3.17).

5.5 Alarm Prioritisation Case Study

The alarm ranking methodology proposed in section 3.5 was tested on a number of real-world alarms detected by an automated pipe burst detection system (Mounce *et al.* 2010) applied to the Harrogate & Dales case study area. Only 11 out of all 15 DMAs were considered here (e.g., because of missing / malfunctioning sensors). Every DMA had its inflow monitored in the period from November 2008 to January 2010. Figure 5.23 shows the layout of the WDS, including the DMA boundaries and location of the flow meters as well as the number of alarms per sensor.

The primary purpose of the alarm prioritisation methodology is to rank alarms occurring more or less simultaneously in a similar time horizon. The number of simultaneous alarms generated in the small number of DMAs was not significant. To demonstrate the full potential of the methodology, all 50 alarms detected throughout the above study period were prioritised regardless of their date/time of occurrence. Nevertheless, the exact date and time of burst detection affected the likelihood of potential incidents occurring as well as their impact. The state of the considered alarms (e.g., real or false) as well as their true nature (i.e., location of the burst pipe in case of a real alarm) remained unknown. It was assumed that all alarms were in an *active* state and, therefore, their priority was purely determined by the outcomes of the risk-based ranking (i.e., the rules presented in section 3.5.5 played no effect).

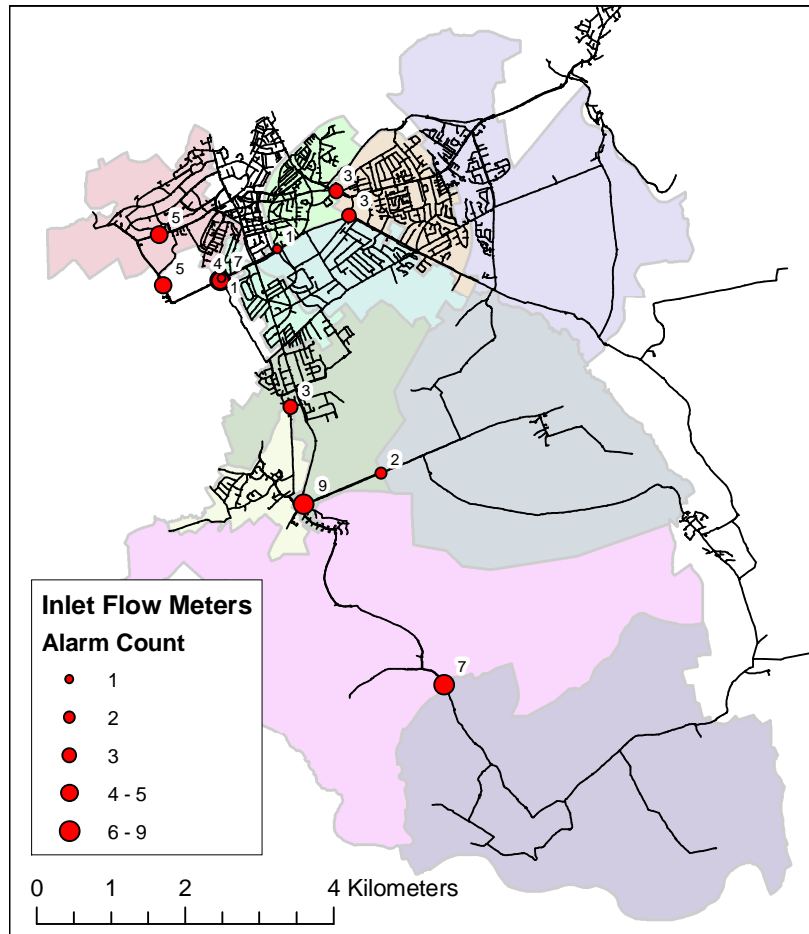


Figure 5.23 Case study area overview with locations of inlet flow meters and alarms

The risk $R_{i,j}$ of failure of every pipe segment within a DMA associated with an alarm was first evaluated using a number of back-end processes described in Chapter 4 of this thesis. A ‘neutral’ preference between likelihood and impact components of risk was chosen (i.e., $w_L = w_I = 0.5$). For the purpose of ranking, a DM’s pessimistic attitude towards risk (i.e., $\alpha = 0.8$) was selected here so that the riskiest potential pipe bursts contribute most to the overall risk of an alarm.


5.5.1 Main Results

Table 5.21 provides an overview of the ranking of all 50 alarms. Four different rankings are presented in the table, where the first one (Ranking $\alpha = 0.8$) corresponds to the parameter set as described above. The highlighted lines in the table correspond to alarms that are discussed in more detail below.

The “Ranking Histogram” and “AVG ranking” were based on the outcomes of sensitivity analysis described below in section 5.5.3. The ranking based on a histogram

chose the most frequent rank of an alarm evaluated across a range of parameter values, whereas the average ranking was obtained by averaging all possible ranking outcomes produced during the sensitivity analysis as illustrated in Figure 5.24 on an example.

	α	w_L	w_I	8603	8644	8933	
Scenario 1	0.72	0.5	0.5	3	2	4	
Scenario 2	0.72	0.48	0.52	3	2	4	
Scenario 3	0.72	0.46	0.54	4	2	3	



Alarm ID	Ranking Hist.	Ranking AVG
8603	3	3.33
8644	2	2.00
8933	4	3.67

Figure 5.24 An example of ranking based on histogram and an average

The last column of Table 5.21 (i.e., “Pairwise comparison”) was obtained by performing $N \times (N - 1)$ pairwise rankings of all 50 alarms and counting for every alarm the number of times it ranked higher than the other alarms (when compared mutually). The purpose of this ranking technique was to observe the effect of global (i.e., across all alarms) and local (i.e., pairwise) impact normalisation on the alarm ranking.

Table 5.21 A list of 50 alarms considered in this case study

Alarm ID	Created Data	DMA	Flow	Ranking $\alpha=0.8$	Ranking Histogram	Ranking AVG	Pairwise comparison
8581	14/12/2008 12:10	E057	20.2	50	50	43.98	50
9036	06/06/2009 18:10	E011	10.3	49	49	47.25	49
8836	04/01/2010 12:42	E011	6.6	48	48	47.72	48
8802	19/11/2009 12:59	E011	5.4	47	47	45.19	46
8660	14/12/2008 07:12	E026	14.4	46	46	43.63	47
8738	18/12/2008 10:12	E024	7.2	45	45	43.28	45
8815	10/09/2009 13:05	E024	9.4	44	44	42.43	44
9032	02/07/2009 21:15	E024	7.8	43	43	41.34	43
9009	11/01/2010 08:41	E055	2.1	42	31	35.54	42
8695	26/09/2009 21:05	E024	6	41	42	39.64	41
8591	20/04/2009 00:10	E011	3.1	40	40	37.43	40
8777	01/06/2009 07:10	E023	1.4	39	39	38.34	33
9038	09/06/2009 08:13	E024	4.4	38	38	35.82	39
8997	23/04/2009 01:12	E026	4.1	37	35	32.61	38
9031	12/02/2009 17:13	E026	5.2	36	34	32.91	36
8702	15/11/2008 22:13	E026	5	35	33	30.82	35
8565	11/01/2010 01:40	E023	1.7	34	50	36.06	32
8653	24/12/2009 19:40	E023	1.1	33	47	35.09	30
8700	16/09/2009 09:04	E026	4.1	32	31	27.52	28
8756	12/12/2008 19:10	E011	1.7	31	32	29.67	25
8783	24/07/2009 04:10	E023	0.9	30	30	30.77	23
8966	15/08/2009 02:04	E093	0.6	29	27	26.68	37
8931	27/08/2009 09:57	E021	2.4	28	29	24.49	18
9030	07/11/2008 04:16	E093	0.4	27	26	21.21	24

Alarm ID	Created Data	DMA	Flow	Ranking $\alpha=0.8$	Ranking Histogram	Ranking AVG	Pairwise comparison
8563	11/01/2010 00:41	E026	4.9	26	28	23.49	17
8996	22/04/2009 12:12	E055	3.9	25	25	28.52	29
8888	04/10/2009 18:05	E022	5.4	24	29	32.15	34
8771	19/03/2009 18:14	E093	0.4	23	16	22.41	26
8610	18/04/2009 08:13	E093	0.5	22	14	19.36	20
8819	16/09/2009 06:59	E204	5.8	21	17	19.81	15
8638	05/01/2010 12:41	E022	2.3	20	19	20.71	22
8936	04/09/2009 18:06	E022	5.1	19	28	29.35	31
8906	05/01/2010 13:40	E022	1.2	18	11	13.90	13
8772	30/05/2009 22:13	E093	0.8	17	12	22.55	27
8611	19/04/2009 23:10	E057	1.1	16	20	15.30	11
8609	07/01/2009 15:10	E054	1.2	15	11	12.74	16
8781	14/06/2009 03:15	E093	0.7	14	10	15.87	19
8778	01/06/2009 13:10	E057	1.4	13	13	19.39	10
8854	23/12/2009 13:41	E026	5.6	12	24	21.21	21
8869	07/01/2009 08:11	E022	0.5	11	11	19.33	14
8701	16/09/2009 23:59	E022	1.2	10	12	16.29	9
8841	20/12/2009 10:41	E093	0.4	9	1	13.04	12
8965	14/08/2009 04:31	E054	0.7	8	9	8.40	5
8588	08/01/2010 18:45	E054	1	7	8	7.78	8
8840	20/12/2009 11:40	E054	0.7	6	7	7.13	6
8780	13/06/2009 22:10	E054	1	5	5	5.40	7
8933	29/08/2009 21:57	E054	0.7	4	4	2.96	1
8644	23/05/2009 07:10	E054	0.5	3	3	2.88	3
8603	07/11/2008 09:16	E054	0.5	2	4	3.64	4
8555	11/12/2008 14:10	E054	0.4	1	1	1.99	2

Detailed results of the initial risk analyses are presented in form of risk maps (see e.g., Figure 5.25). The thickness of the pipes reflects how likely it is that a burst has occurred in that part of the network, based on the output of the D-S model, and the colour (i.e., red = high impact and blue = low impact) corresponds to the aggregated impact that a burst of a given magnitude would cause at that location over a 24h risk horizon. The identification of impact and likelihood classes (i.e., breaks) used in the risk maps was done using the Natural Breaks algorithm (Jenks 1967), which tries to group similar values in the attempt to maximise the differences between the classes.

AlarmId: 8777, DMA: E023, Burst flow: 1.4, Date: 01/06/2009 07:10:13, Rank: 390



Figure 5.25 A risk map of alarm 8777

Certain pipes were excluded from the impact aggregation (and thus also from the alarm ranking). Pipes excluded from the ranking are shown using a light grey dashed line on the risk maps. There were several reasons why a pipe was excluded from the ranking process. Sometimes, it was not possible to evaluate the impact of a burst on that pipe (e.g., the system was hydraulically unbalanced and it was not possible to find a solution to the governing mass and energy conservation equations). Also, on several occasions the evaluation of likelihood of failure of that pipe did not succeed for some reason (e.g., no evidence was available).

5.5.2 Detailed Alarm Prioritisation Results

As discussed in section 3.5 the impact of a pipe burst has to be compared across all potential incidents of all active alarms to establish a common scale. This fact was reflected in Table 5.21, however, the detailed risk maps presented below were re-normalised in pairs (i.e., only the two alarms were considered as active) to emphasise

the differences only between the impacts of potential incidents associated with the two alarms. The alarm ranking examples described below were included to demonstrate following:

- *Alarms 8966 & 9030* – to show that the methodology produces an expected ranking in case of similar alarms that differ predominantly in the magnitude of abnormal flow.
- *Alarms 8802 & 8660* – to illustrate the advantages of the alarm ranking methodology to take into account the usually complex development of the impact of potential incidents associated with an alarm.
- *Alarms 8854 & 8563* – to highlight a limitation of the methodology when dealing with outliers caused by potential incidents with very high values of impact or likelihood of occurrence.

5.5.2.1 Alarms 8966 & 9030

As discussed in section 3.5.2, the alarm ranking methodology assumes only one failure at a time from the same DMA. The majority of the alarms presented in Table 5.21 originating from the same DMA at a similar time of day, show a strong positive correlation between their ranking and the magnitude of abnormal flow. Such behaviour is typically caused by the impact component of risk of potential incidents associated with an alarm and does not have to hold every time (i.e., because of the likelihood of occurrence of potential incidents). Figure 5.26 and Figure 5.27 show risk maps of two alarms 8966 and 9030 respectively that originated from the same DMA at approximately the same time, but at different dates. The likelihood component of potential incidents associated with each of the alarms is very similar. This fact can be explained by an incorrect calibration of the HM used, which affected both alarms in a similar way. In terms of impact, it can be observed from the risk maps and a scatter plot in Figure 5.28 that the higher burst flow increased the impact level of alarm 8966. This alarm consequently received a higher ranking and was perceived as more important.

AlarmId: 8966, DMA: E093, Burst flow: 0.6, Date: 15/08/2009 02:04:06, Rank: 280

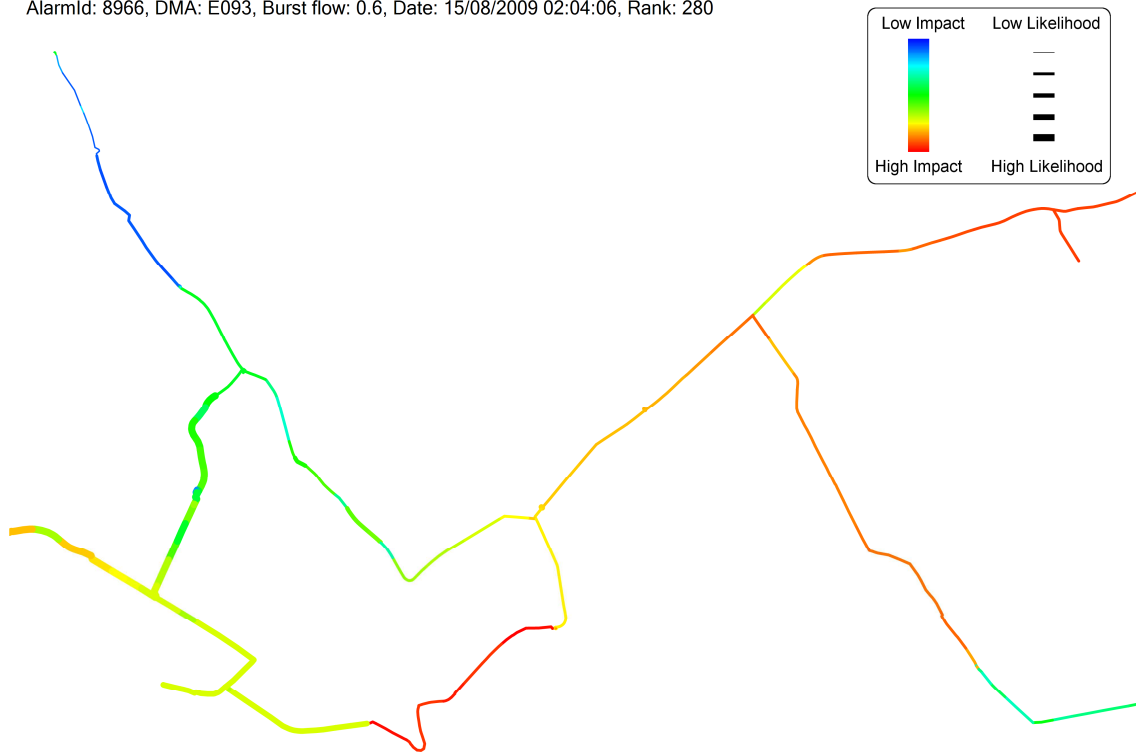


Figure 5.26 A risk map of alarm 8966

AlarmId: 9030, DMA: E093, Burst flow: 0.4, Date: 07/11/2008 04:16:00, Rank: 260

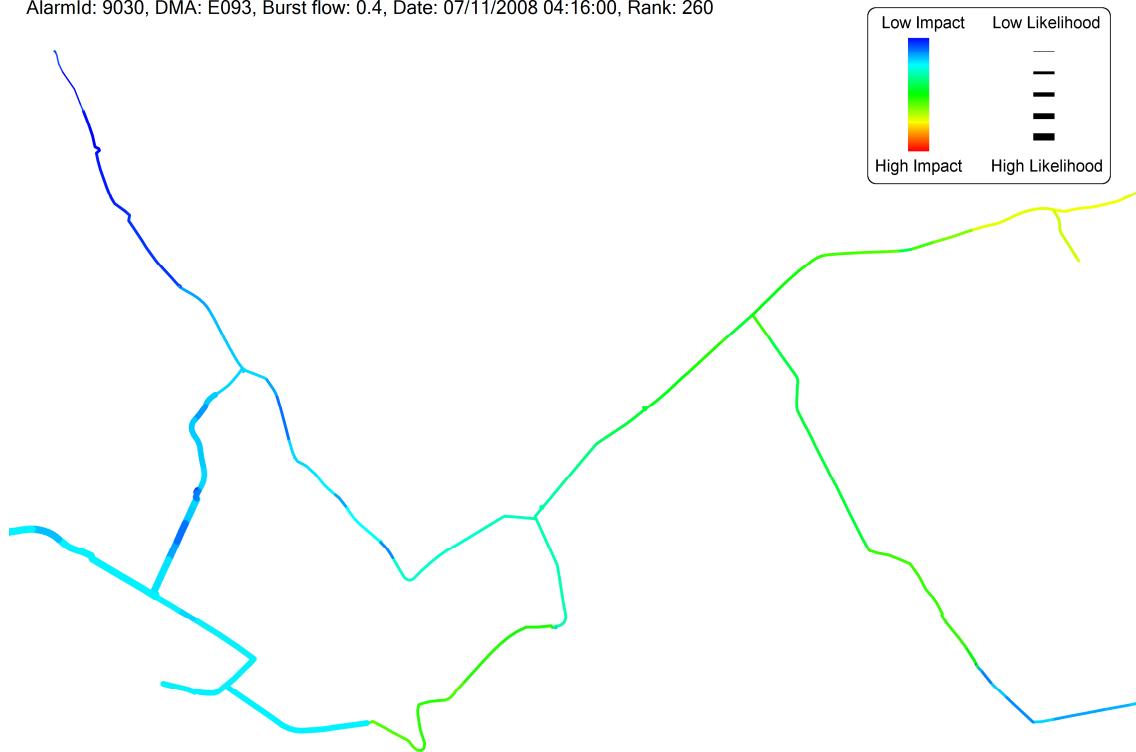


Figure 5.27 A risk map of alarm 9030

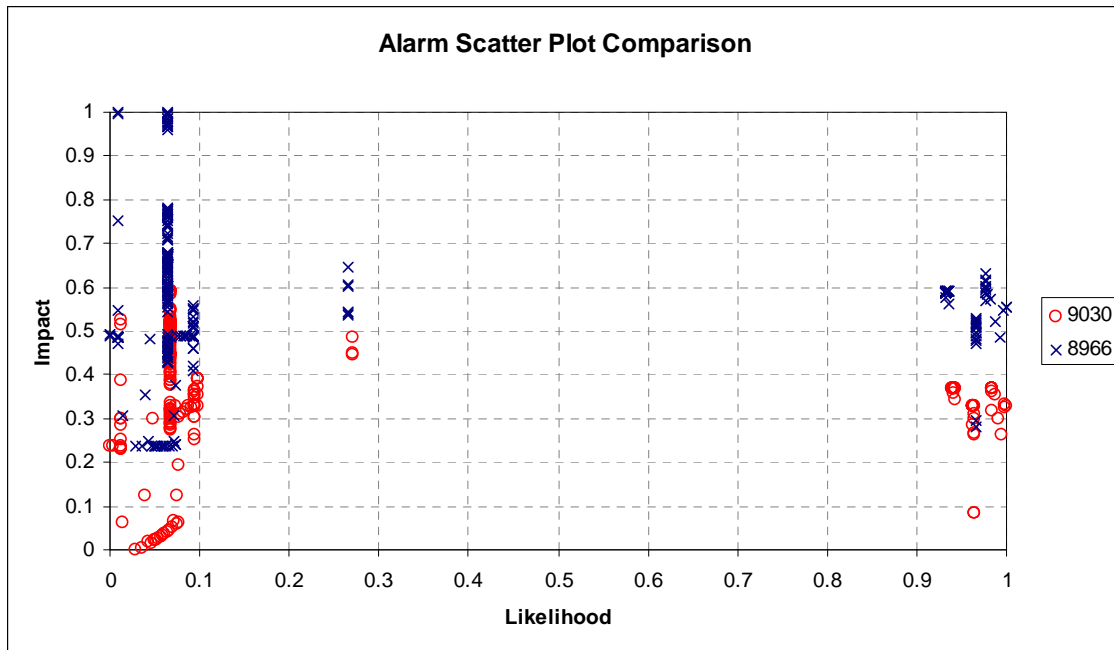


Figure 5.28 A scatter plot of alarms 8966 and 9030

5.5.2.2 Alarms 8802 & 8660

The following example demonstrates the advantage of the risk-based approach to alarm prioritisation, in comparison to simply relying on the abnormal flow of an event, which could serve as a good indicator of alarm severity in a number of situations. In this case, the alarms 8802 (see Figure 5.29) and 8660 (see Figure 5.30) originated from different DMAs. As can be seen in Figure 5.29 and Figure 5.30, in both cases the most likely location of the burst coincided with the part of the DMA where the burst would have the highest impact.

Despite the fact that the burst flow of the alarm 8802 ($5.4 \text{ l/s} = 25\%$ of max. DMA inflow) was lower than in the case of alarm 8660 ($14.4 \text{ l/s} = 30\%$ of max. DMA inflow), it obtained higher priority than the alarm 8660 due to a higher impact on customers in the north-west part of the DMA. If, however, at the time of the risk analysis there had been evidence available suggesting that the alarm 8802 was most likely to have been caused by a burst pipe in the southern part of the DMA, then ranking results would have been the opposite, since that burst would have caused much lower impact there (e.g., due to different topography and elevation).

AlarmId: 8802, DMA: E011, Burst flow: 5.4, Date: 19/11/2009 12:59:13, Rank: 470



Figure 5.29 A risk map of alarm 8802

AlarmId: 8660, DMA: E026, Burst flow: 14.4, Date: 14/12/2008 07:12:14, Rank: 460

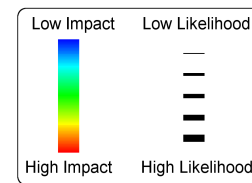


Figure 5.30 A risk map of alarm 8660

5.5.2.3 Alarms 8854 & 8563

This example shows one of the weaknesses of the alarm ranking methodology in situations when outliers are present in the set of potential incidents associated with an alarm. Outliers typically manifest themselves as potential incidents with very high values of likelihood, impact or both. A group of outliers with high values of likelihood (compared to the rest of potential incidents) is highlighted in Figure 5.31. Those four outliers, associated with alarm 8854 affected the likelihood scale of that alarm and caused it to be ranked lower (i.e., less risky) than the alarm 8563. The presence of the outliers can be explained by an incorrectly calibrated HM, whose evidence was dominant in this case.

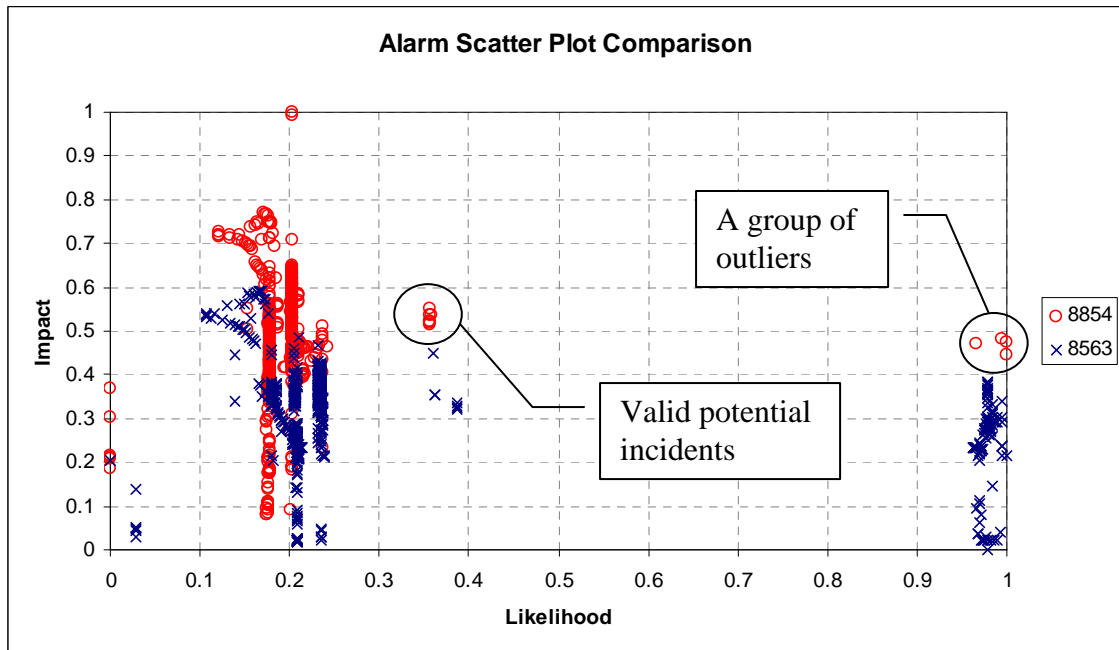


Figure 5.31 An original (un-filtered) scatter plot of alarms 8854 and 8563

After the outliers were excluded from the alarm ranking, the alarms were then ranked in a different order to the one shown in Table 5.21 (i.e., alarm 8854 ranked higher than alarm 8563). This fact can be seen from an updated scatter plot in Figure 5.32 where the potential incidents represented by red circles (i.e., alarm 8854) dominate the blue crosses representing potential incidents associated with alarm 8563.

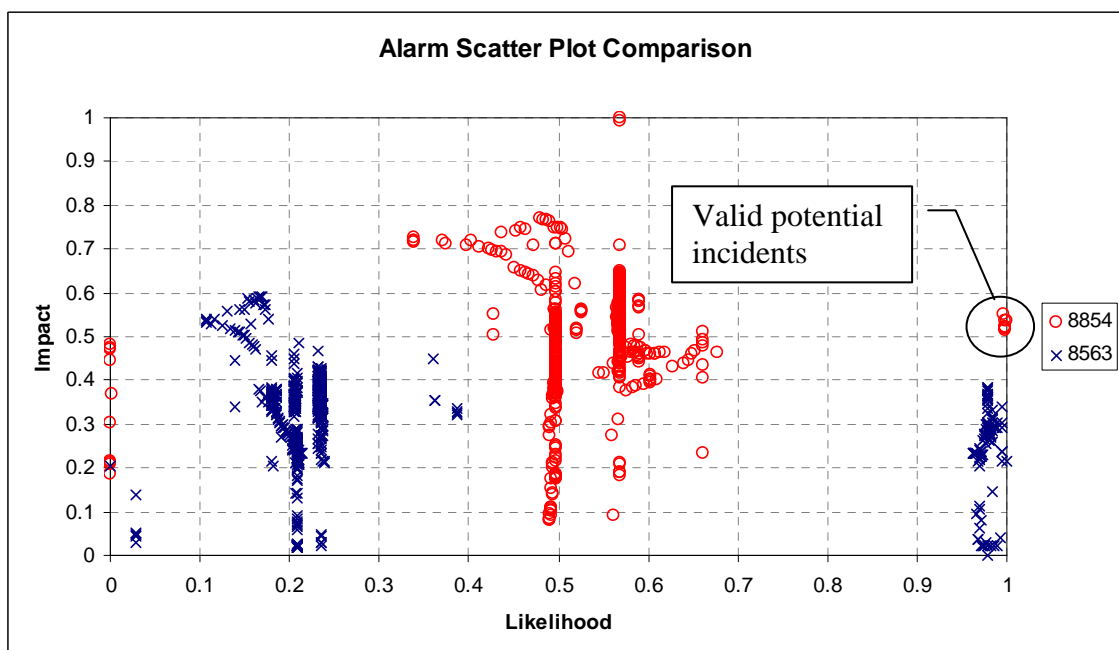


Figure 5.32 A filtered scatter plot of alarms 8854 and 8563

The presence of outliers can affect the entire scale of impacts and likelihoods of the alarms being considered and could cause a rank reversal – a situation when a less significant alarm is treated as a more important one. Currently, the impact and likelihood components are normalised using Eq. (5.9)

$$Norm(x) = \frac{x - \min(x)}{\max(x) - \min(x)} \quad (5.9)$$

where: $Norm(x)$ is normalised value of attribute x , $\min(x)$ is the minimum value of attribute x and $\max(x)$ is the maximum value of attribute x .

The influence of outliers could be reduced by adopting a different normalisation procedure. Mavrotas and Trifillis (2006) suggested using the fifth and ninety-fifth percentile in the normalisation procedure as shown in Eq. (5.10) instead of the minimum and maximum to alleviate this problem.

$$NormP(x) = \frac{\max(\min(x, p_{0.95}(x)), p_{0.05}(x)) - p_{0.05}(x)}{p_{0.95}(x) - p_{0.05}(x)} \quad (5.10)$$

where: $p_{0.05}$ is the fifth percentile of attribute A and $p_{0.95}$ is the ninety-fifth percentile of attribute x

The use of percentiles was not applied in this work, although it might potentially reduce the risk of an incorrect prioritisation of alarms.

5.5.3 Sensitivity Analysis

A sensitivity analysis was carried out to investigate the influence of parameters used by the alarm ranking methodology (i.e., the operators' attitude towards risk α and likelihood and impact preference weights w_L and w_I , respectively). Ranking of all 50 alarms presented in this case study was done with parameter values varied across their entire feasible range. The results of sensitivity analysis are plotted in the form of a contour map (see Figure 5.33), where every point on the map represents a particular ranking obtained using a corresponding value of parameter α and likelihood weight w_L (note that the weight w_I is given by $w_I + w_L = 1$). The colour of every point corresponds to the distance of the rankings of alarms from a reference solution ($\alpha = 0.8$ and $w_L = 0.5$) presented in Table 5.21.

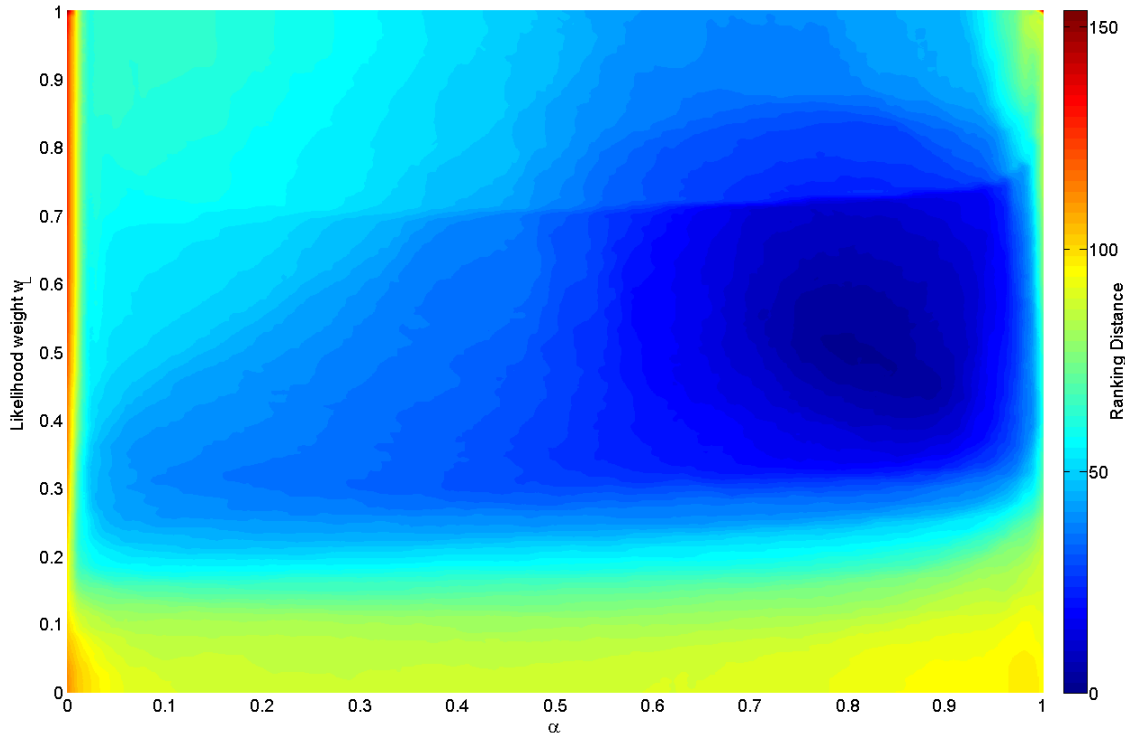


Figure 5.33 Influence of parameter values on distance from a reference solution

The distance between the reference solution and ranking obtained using different values of parameters α and w_L was expressed using the following equation:

$$RankingDistance(i) = \sqrt{\sum_{i=1}^{N_A} (Rank_{ref}(i) - Rank(i))^2} \quad (5.11)$$

where: N_A is the number of alarms considered (in this case 50), $Rank_{ref}(i)$ is the ranking of the i -th alarm of the reference solution and $Rank(i)$ is the ranking of the i -th alarm obtained using different parameter values α and w_L .

The reference solution itself at coordinates $\alpha = 0.8$ and $w_L = 0.5$ clearly has a ranking distance equal to 0. As can be further seen from Figure 5.33, the ranking methodology provides very similar rankings for a wide range of values of input parameters α and w_L . A significantly different ranking of alarms would be obtained for values of α close to its limits (i.e., 0 and 1). Similar phenomenon could be observed in cases when the value of the likelihood weight w_L drops below 0.3 or exceeds the value of 0.7. It can, therefore, be concluded that the method is likely to produce an expected alarm ranking across a wide range of parameter inputs, which can be seen as a positive feature since high sensitivity could make the calibration difficult.

5.5.4 Discussion

Prioritisation of alarms is a complex process, which needs to consider multiple criteria. An expert's judgement based only on limited information such as the time of detection of an alarm, DMA characteristics and estimated magnitude of the burst flow might be insufficient to assess thoroughly the severity of an alarm. Alarm priority depends on the state of a WDS as a whole and might vary significantly depending on water consumption and pressures in the system.

Manual ranking of alarms by visual comparison of risk maps has proved to be subjective and also difficult since both the likelihood and impact components of risk have to be considered simultaneously. An attempt was made to rank alarms manually by a visual comparison of their risk maps. This manual ranking seemed to lack consistency and put more emphasis on the impact component of risk, which might be also caused by the way the risk maps were visualised (i.e., visually the line colour seems to dominate its thickness).

In situations where the likely location of the burst is confined to a small area, the overall risk of such an alarm is reduced since a higher number of less likely burst locations play a more important role during the aggregation. This might produce counterintuitive ranking in some cases when a high impact, well located burst would have lower rank than an average impact burst, whose location within a DMA is unknown (i.e., a large number of pipes have a high likelihood of bursting). Such behaviour could be reduced to a certain extent by increasing the level of pessimism of the DM (i.e., increasing the value of α or reducing the likelihood weighting factor w_L).

5.6 Summary

This chapter has demonstrated the application of the individual constituents of the risk-based pipe burst diagnostics methodology proposed in Chapter 3 on a number of real life and semi-real case studies. The results presented in this chapter were obtained using the background processes (i.e., the Alarm Monitor, Likelihood Evaluator, Impact Evaluator and the Ranking module) described in section 4.4.

Section 5.1 provided a brief introduction to the case studies presented here and explained the obstacles, which prevented the application of some of the methodologies, namely the D-S model on real life data.

The possibility of using an HM and near R-T pressure and flow measurements from the field to locate a burst within a DMA was demonstrated in section 5.2. It was concluded that the magnitude of burst flow, calibration of the HM as well as the number of measurement points and their location (i.e., sensitivity to changes in pressure in a DMA) play an important role in the successful location of a burst. Small pipe bursts do not generate sufficient pressure drops and, therefore, cannot be located using measurements of current commonly used pressure transducers that have typical accuracy of +/- 0.5 m of head. On the other hand, such bursts are unlikely to significantly impact customers and do not require an immediate attention.

Section 5.3 presented results of an application of the D-S model (see section 3.3) on a number of historical pipe bursts. It was shown that the long term credibility of individual information sources (i.e., the PBPM, CCM and HM) can be captured in the form of mapping curves during a multi-objective calibration procedure. Validation of the D-S model showed better performance than any of the individual models achieved on a high number of unseen validation cases (i.e., in terms of certainty in identifying the correct burst location and likelihood concentration).

A possible way to determine weights used by the impact model was presented in section 5.4. To gather data required to calibrate the impact model, an online questionnaire survey was conducted in two water utilities. First, a group decision-making approach was used to aggregate outcomes of the questionnaire survey within a company. The aggregated results were then analysed using the AHP, which was applied to derive preference weights from comparison matrices formed after the aggregation of individual judgements. Consequently, these weights were put into an objective tree, which reflected an overall aggregated impact of a failure on a water utility.

The alarm ranking methodology, which combines the likelihood and impact components of the risk of potential incidents associated with an alarm to determine its severity, was demonstrated in section 5.5. The methodology produced intuitive ranking of real life alarms with only a small number of disputable cases (e.g., caused by the

presence of outliers). Based on the results achieved, it can be concluded that the measure of risk used in this work provides a suitable indicator for systematic alarm prioritisation. The newly proposed alarm prioritisation methodology enables control room personnel to identify and then pay more attention to the most severe failures first, leading to an improved response time and better quality of service.

CHAPTER 6 CONCLUSIONS

6.1 Summary

The concept of risk has been widely applied across the water industry, however, primarily from a strategic perspective. The main objective of this thesis was to introduce risk-based decision-making into the near Real-Time (R-T) operational management of WDS under failure conditions. In particular the aim was to support the process of diagnostics and prioritisation of abnormal flow conditions typically caused by burst pipes.

A novel methodology for diagnostics of WDS failures (i.e., pipe bursts) based on the measure of risk associated with a failure was developed. The methodology allows better informed decisions to be made about where to dispatch field crews to investigate possible problems, not only based on information about the likelihood of a suspected failure occurring, but also according to the estimated impact such failure would have on the water utility and its customers.

Suitable models to quantify the fundamental components of the risk metric, i.e., the likelihood of adverse effects occurring and their impact on the stakeholders concerned were first developed and implemented. The likely location of the burst pipe was estimated using a novel Dempster-Shafer (D-S) model by combining evidence from multiple information sources (i.e., a Pipe Burst Prediction Model (PBPM), a Customer Contact Model (CCM) and a Hydraulic Model (HM)) to increase confidence in the results. An impact model based on the Multi-Attribute Value Theory (MAVT), capable of incorporating Decision-Makers' (DM) preferences, was created to capture operational aspects of a failure in a WDS during a risk horizon.

The full potential of the risk-based approach towards failure diagnostics was exploited in a novel alarm ranking methodology. The proposed method is able to suggest mutual significance of multiple alarms (i.e., detected abnormal events), occurring more or less simultaneously during similar time horizon, based on the DM's attitude towards risk and the level of aggregated risk they represent. Alarms are presented to a human DM in order of their importance and therefore the most severe failures can be dealt with first. In severe weather conditions, such as extended periods of frost, when multiple pipe

bursts are most likely to occur more or less simultaneously, the cognitive load of the operators can be effectively reduced using this approach.

A possible implementation of individual constituents of the risk-based pipe burst diagnostics methodology was suggested in Chapter 4. The methodology presented in this thesis was then also put into a broader context of a Decision Support System (DSS) for near R-T WDS operation under abnormal conditions. A simplified design of a relational Database (DB) (with spatial extension), which formed the core of the proposed DSS, was presented. The possibility of using distributed computing in order to increase the computational efficiency of the impact evaluation, to gain the requested near R-T performance, was demonstrated. A scalable solution for the visualisation of GIS data, representing the current state of a WDS, directly from a spatial DB was also suggested.

The risk-based decision support methodology was applied to a number of real life as well as semi-real case studies, which show its potential to improve the current practices of failure management in WDS, when pipe bursts occur. The control room operators can make better informed decisions, which are likely to ensure an improved level of service of delivery of potable water.

6.1.1 Summary of the Contributions

The main contributions of the work presented in this thesis are:

- A novel D-S model, inspired by ensemble classifiers, to provide an estimate of the likelihood of burst occurrence at a particular location within a DMA by combining outputs from multiple information sources (i.e., a PBPM, a CCM and an HM).
- A novel multi-objective calibration methodology to determine input parameters used by the D-S model, including a suitable combination rule, in order to learn the credibility of the individual information sources and achieve maximum benefits from the information fusion process.
- A novel tree-like impact model based on the MAVT theory, which aggregates a number of KPIs computed using a pressure driven hydraulic solver coupled with

a GIS in order to estimate the relative importance of failure impact in accordance with preferences of a water utility represented by a group of DMs.

- A novel risk-based pipe burst investigation method, to drive the burst diagnostics not only by the likelihood of burst location but also the impact of a burst in different parts of a DMA to enhance the decision-making of control room operators.
- A novel alarm prioritisation methodology, which uses an overall aggregated risk of all potential incidents (i.e., causes) of an alarm (i.e., a detected anomaly), capable of determining mutual significance of a number of simultaneously occurring alarms according to the DM's attitude towards risk.

6.2 Main Conclusions

The main conclusions are given here with respect to the individual constituents of the overall risk-based pipe burst diagnostics methodology presented in this thesis.

6.2.1 Risk-Based Pipe Burst Diagnostics

From the risk-based pipe burst diagnostics presented in Chapter 3.2, the following conclusions can be drawn:

- Presenting risk in an aggregated form (e.g., by multiplying likelihood and impact) is a misapprehension frequently held by practitioners. It is important that the risk metric is presented in a non-aggregated form (i.e., the likelihood and the impact measures are treated separately where possible). This was achieved here using risk maps, which use varying line thickness and colour to separately present both components of risk.
- Investigation of burst pipes is most likely to be driven primarily by the likelihood component of risk, whereas the impact only serves as a secondary indicator. On the other hand, impact plays a dominant role in alarm prioritisation, where it represents the primary feature that enables DMs to determine the mutual significance of several alarms.

6.2.2 Dempster-Shafer Model

The Dempster-Shafer model presented in Chapter 3.3, which provides an estimated likelihood of burst occurrence at a particular location within a DMA, shows:

- Locating a pipe burst within a DMA using data driven or conventional model-based methods is a challenging problem. The main constraint of such methods is typically the lack of data or insufficient calibration of the models used. Under such conditions of uncertainty, when no single model is able to provide a satisfactory answer, it is beneficial to combine the outputs from several models, in order to improve confidence in the overall result. This thesis presented a methodology based on the D-S Theory which combines evidence from several independent sources/models (i.e., a PBPM, an HM and a CCM) to locate a pipe burst within a DMA. It is argued that this methodology is able to fully exploit all the information sources available in a WDS control room, reduce the information load faced by a human operator and facilitate targeted field investigations.
- A limiting factor to a wider application of HMs in near R-T burst diagnostics is the unavailability of pressure and flow data in sufficient quantity and quality. In certain WDS deployment of a sufficient number of sensors might be uneconomical since the potential benefits from timely burst identification would not justify the cost of the sensors and their maintenance. However, stringent requirements on delivered levels of service and customer satisfaction might support more investment into monitoring technology in the not-too-distant future, which, coupled with the availability of cheaper sensors, due to technological advances, may tip the balance of the cost benefit analysis in favour of more sensors.
- The performance of the information sources used in this work varies significantly, which makes information fusion difficult. Such phenomena can be observed for example in the case of the CCM which tends to be either completely correct or completely wrong. Ideally, all the information sources should perform similarly. Furthermore, the PBPM, which has significantly lower

credibility than the other remaining information sources, does not contribute much when the HM and CCM are in conflict.

- A major strength of the proposed methodology is its potential to learn from the performance of the individual models during the calibration stage and successfully apply this knowledge to unseen cases. As information about new pipe bursts becomes progressively available, the D-S model can be recalibrated in order to better reflect the evolving performance of the input models. Moreover, additional models suggesting the location of a burst pipe (e.g., based on the information of third parties working in the system, weather information, etc.) can be readily incorporated acting as additional information sources, to further improve the performance and benefits of information fusion.
- The novel multiple-objective calibration procedure developed, allows the D-S model to learn the credibility of the underlying information sources based on a set of historical events. However, criteria for selecting the most suitable non-dominated solution from the Pareto front need to be established to allow for automation of the learning process.
- Importantly, the calibration procedure selects the most suitable combination rule since, as stated by many, the choice of a particular rule for information fusion is problem specific and no single combination rule can yield optimal results in all decision-making contexts.
- The results of calibration of the D-S model suggest that the D-S theory of Evidence is a suitable mathematical framework for information fusion applied in the context discussed in this work. In contrast to the traditional Bayesian theory, the ability of the D-S theory to handle epistemic uncertainty seems to yield certain advantages.
- The initial calibration and maintenance of the mapping curves, which reflect the credibility of the input models, is not straightforward and represents a challenge that needs to be addressed.

- The results obtained by running the D-S model on a number of semi-real historical cases suggest that the methodology is capable of:
 - Identifying parts of the network where the problem is least likely to be located rather than providing an increased resolution of burst location. This could possibly help exclude areas where the burst may not have occurred from expensive field investigations.
 - Suggesting that conflicts exist between individual information sources, which might influence the decision-making processes. This would, however, require the “likelihood” to be presented using *Belief* and *Plausibility* instead of the pignistic probability (*BetP*), which might be impractical for WDS operators.
 - Providing an insight into the performance of individual models using the “mapping curves”, which reflect their credibility and specificity, presents an advantage over “black box” models such as ANNs.
- No conclusions can be drawn about the performance and suitability of different combination rules since the solutions in the non-dominated set obtained during the calibration procedure contained all the three combination rules considered (i.e., Dempster’s rule, Yager’s rule and PCR5 rule). However, Yager’s rule seemed to generate results impractical for decision-making due to large differences between Belief and Plausibility, which was not observed in the case of the other two combination rules.

6.2.3 Impact Model

An impact model was developed (see Chapter 3.4) and implemented, based on an HM (i.e., a pressure driven modification of EPANET2) coupled with a GIS, in order to assess the impact of failures (i.e., pipe bursts) from an operational, rather than strategic perspective.

- A set of KPIs capturing the impact of a pipe burst on a water utility, as well as its customers, was developed. The proposed KPIs are able to model the

following impact categories: supply interruption, low pressure, discolouration, and economic impacts.

- The KPIs reflecting impact on customers explicitly differentiate the following types of customers: residential, industrial, commercial, and critical. This is not the case of the KPIs used by OFWAT to monitor long term performance of water utilities.
- It is suggested that the impact of pipe bursts needs to be evaluated on a system level, rather than within a single DMA since phenomena such as discolouration can affect much larger parts of the network (i.e., outside of the boundaries of an affected DMA) depending on the network topology.
- A questionnaire survey was conducted in two UK water utilities in order to determine their perception of the impact of various failures in a WDS. The results identified very similar preferences in the two participating water utilities in terms of significance of different aspects of considered impacts.
 - Regarding the significance of different impacts of a pipe burst, full supply interruption was perceived as the most severe impact, followed by discolouration, low pressure and economic impacts.
 - Impact on critical customers (e.g., hospitals, schools, etc.) was perceived as being significantly more serious in comparison to the other customer categories (i.e., residential, commercial and industrial users) considered in this thesis.
 - In terms of economic impact, damage to third parties (e.g., damage to a road caused by a burst) was identified as the most severe economic impact, followed by undelivered demand and lost water.
- Distributed computing was successfully applied in order to increase the performance of the impact evaluation of potential incidents, associated with an alarm in a particular DMA in order to reach a near R-T character of the methodology.

6.2.4 Alarm Prioritisation & Ranking

Prioritisation of abnormal flow events (i.e., alarms) has received only a little attention by the water sector. The following conclusions can be drawn regarding the alarm prioritisation methodology proposed in Chapter 3.5.

- A novel methodology for automatic prioritisation of flow alarms (i.e., detected flow anomalies) was developed. The methodology provides a DM with the means to determine mutual significance of multiple alarms occurring simultaneously in different parts of a WDS (e.g., during periods of abnormal frost). The risk of individual possible causes of an alarm was used here to calculate an overall aggregated risk associated with that alarm, depending on the DM's preferences and attitude towards risk (e.g., pessimistic / optimistic).
- Prioritisation of flow alarms in a WDS was found to be a complex and a highly subjective task. The information currently available to the control room operators might not be sufficient to assess the priority of an alarm. Estimating the alarm priority based on the magnitude of abnormal flow (or its fraction compared to the total DMA inflow only) might lead to incorrect conclusions. The risk-based alarm ranking methodology offers a systematic approach to alarm prioritisation.
- The performance of the method can be negatively affected by the presence of outliers (i.e., potential incidents associated with an alarm that have unrealistically high impact or likelihood of occurrence compared to neighbouring pipes in the same DMA). Possible ways of overcoming this problem were suggested in section 6.3.3. Counterintuitive ranking might be also produced in situations when the likely location of the burst is confined to a small area since the aggregated risk of such an alarm might be lower than when the location of the burst is completely unknown.
- The alarm ranking methodology on its own is a computationally efficient algorithm, where the calculation of the maximum entropy weights takes most of the time. These were stored in a cache for a given value of parameter α to improve the performance. The major computational burden lies in the pipe burst

risk analysis (primarily in the impact evaluation), which typically involves running hundreds of extended period simulations of an HM.

6.3 Future Research

This section suggests possible directions of further research to extend and improve the methodologies presented in this thesis. Generally, with the exception of the D-S model, uncertainty was not thoroughly considered in this work. The majority of the models developed here were deterministic (e.g., the impact model). Incorporating methods of uncertainty handling into near R-T environment represents an intriguing challenge that certainly deserves more attention in the future.

Specific recommendations for further research are given separately for each key constituent of the risk-based pipe burst diagnostics methodology.

6.3.1 Dempster-Shafer Model

It is recommended that future research into the D-S Model (see chapter 3.3), utilised to estimate the likelihood of burst occurrence at a given pipe within a DMA, might include the following:

- A method for automatic selection of the most suitable solution from the Pareto front produced during the calibration stage should be developed. This would facilitate automated re-training of the D-S model when new feedback about historical pipe bursts becomes available.
- The mapping curves generated for each source of evidence should be parameterised to account for specific factors (e.g., magnitude of abnormal flow in case of the HM) temporarily affecting the performance of a particular information source (i.e., an input model).
- To better utilise the uncertain output of the D-S model at credal level (i.e., Beliefs and Plausibilities) in the decision-making process. Methods for intuitive visualisation of such information to a DM in conjunction with risk-maps should be researched.

- Additional information sources or new models capable of suggesting the likely location of a burst pipe within a WDS could be utilised to strengthen the synergetic effect of information fusion. These might be based on information from a WMSY containing details about third party works, models using transient analysis or turbidity measurements. Alternatively, subjective human judgement could be also incorporated, together with new combination rules that take the inter-dependencies of such type of evidence into account.
- The CCM could be further extended to take into account different types of CCs (e.g., low pressure problems, discolouration reports, etc.). In the case of such reports, the relationship between distance from the location of the caller and the actual location of the burst pipe is likely to be highly non-linear and the use of an HM would be required to incorporate this kind of evidence.
- A number of enhancements could be implemented in the HM. First, flow measurements within a DMA as well as flow imbalance of multi-inlet DMAs should be incorporated in the error function (see Eq. (3.10)). Multiple field measurements taken at different time steps, after the burst detection, should be utilised. Pressure measurements recorded during minimum night flow hours could be particularly suitable when variation caused by regular water consumption during day time is significant. A combination of burst location together with automatic re-calibration of an HM as suggested by Wu *et al.* (2010) should be taken into account and further explored together with the use of emitters to model the pressure sensitive outflow from a burst.

6.3.2 Impact Model

The functionality of the Impact model proposed in chapter 3.4 could be enhanced as follows:

- The set of KPIs proposed in section 3.4.3 could be further extended to better account for social aspects of the impact caused by failures. Moreover, better ways of quantification of water quality problems should be explored. In the case of discolouration risk state of the art models, based on shear stress (Boxall and Saul 2005), should be applied.

- A more detailed quantitative as well as qualitative survey on a wider sample including both key stakeholders (i.e., the water utility and its customers) should be conducted to gain better understanding of their preferences regarding various aspects of failure impact.
- Possible ways to speed-up the impact evaluation, which was identified as the main bottleneck affecting the application of the risk-based burst diagnostics in near R-T, should be explored. Such techniques might include the use of ANNs to capture the knowledge of an HM (Salomons *et al.* 2007), dynamic skeletonisation (Shamir and Salomons 2008) or regression-based methods (Burrows *et al.* 2000), that would have to be extended to account for possible topological changes in the network.
- Explore the use of fuzzy logic to quantify the impact in linguistic terms, rather than using crisp values, which give a DM a false impression of certainty and confidence in the accuracy of the results.

6.3.3 Alarm Prioritisation & Ranking

The alarm ranking methodology presented in chapter 3.5 could be further extended and improved in the following directions:

- Better handling of possible outliers in the set of potential incidents, which could negatively affect the scale of impact and likelihood and, therefore, the priority of alarms. This could be achieved by introducing different normalisation schemes or intelligent filtering of potential incidents.
- Currently, the alarm ranking methodology produces a relative rather than an absolute priority. By providing reference examples of alarm severity, alarms could then be classified to fall into several priority categories (e.g., high, medium and low risk), which would immediately tell an operator that urgent action (i.e., intervention) is required.
- The feedback from an operator (e.g., manual overriding of alarm priority) currently only has a temporary effect and is not preserved when alarms are re-prioritised (e.g., when a new alarm arrives). An operator's feedback could be

better incorporated into the alarm ranking methodology. Various parameters (e.g., attitude towards risk, impact and likelihood preferences, etc.) could be recalibrated in order to find a ranking that best mimicked the one of a human expert.

- Suitable methodology should be developed to determine an optimal sample of potential incidents that could reliably reflect the overall aggregated risk of an alarm. This could reduce the number of potential incidents that need to undergo the complete risk analysis and improve the performance dramatically, allowing a truly near R-T application even without the use of distributed computing.

APPENDIX A EVIDENCE THEORY

Most decisions in real life have to be made without complete knowledge of the given problem. To reduce the uncertainty and thus make a better decision a Decision Maker (DM) typically tries to find various information sources that would either increase or decrease confidence in a particular hypothesis. Tackling the uncertainty and the combination of evidence coming from several sources are key features of the Theory of Evidence which forms the mathematical foundation used in this work. This appendix provides a more detailed overview of the theory to allow the reader to better understand the information fusion methodology presented in section 3.3.

The mathematical Evidence Theory also known as Dempster-Shafer theory was founded in the late 70's by Dempster (1967) and later extended by Shafer (1976). The Evidence Theory stemmed from Bayesian probability theory (Bayes 1763) by extending it to take into account epistemic uncertainty. The Bayesian probability theory can be thus considered as a special case of the Evidence Theory.

The Evidence Theory operates on the “*frame of discernment*” Θ which is a finite set of mutually exclusive and exhaustive hypotheses. Whereas in classic probability theory where probability p is assigned to an event and $(1-p)$ is automatically assigned to its negation, in the Evidence Theory, the remaining probability can be “unassigned” reflecting the lack of knowledge about a given phenomenon (i.e., ignorance).

The number of all subsets in a frame Θ (i.e., the number of elements in its power set) is $2^{|\Theta|}$ since each element is either included in the subset or it is not.

In Evidence Theory the evidence is distributed amongst sets of hypotheses (propositions) by attributing probability mass to these subsets of the frame of discernment Θ using the Basic Probability Assignment (BPA). The BPA is a function $m: 2^{\Theta} \rightarrow [0,1]$ complying with following conditions:

$$\begin{aligned}
 m(\emptyset) &= 0 \\
 m(A) &\geq 0 \text{ for every } A \subseteq \Theta \\
 \sum_{A \in 2^{\Theta}} m(A) &= 1
 \end{aligned}
 \tag{A.1}$$

where:

- A is a non-empty subset of Θ

It is important to note that **no** probability mass can be assigned to the empty set (i.e., $m(\emptyset) = 0$).

“ $m(A)$ measures the total portion of belief that is confined to A yet none of which is confined to any proper subset of A .” (Shafer 1976) According to Klir (1994) the quantity $m(A)$ “represents the degree of evidential support that a specific element of Θ belongs to the set A **but not to any** particular subset of A ”. A BPA m is said to be vacuous if $m(\Theta)=1$ and $m(A)=0$ for all $A \neq \Theta$.

We call all subsets $A \subseteq \Theta$, for which $m(A) > 0$, “focal sets” or “focal elements”.

Belief and *Plausibility* are functions associated with the BPA.

$$Bel : 2^\Theta \rightarrow [0,1] \quad \text{and} \quad Bel(A) = \sum_{B \subseteq A} m(B) \tag{A.2}$$

where:

- B is a non-empty subset of Θ

Belief corresponds to the total probability mass which supports A and all of its subsets.

$$Pl : 2^\Theta \rightarrow [0,1] \quad \text{and} \quad Pl(A) = \sum_{B \cap A \neq \emptyset} m(B) \tag{A.3}$$

Plausibility corresponds to the total mass of evidence which is not in contradiction with hypothesis A . From the definitions above it is apparent that the relationship between *Bel* and *Pl* is as follows:

$$Pl(A) = 1 - Bel(\bar{A}) \tag{A.4}$$

Our belief in A can be considered to be somewhere between $[Bel(A), Pl(A)]$ where the *Bel* function is the lower bound whereas *Pl* represents the upper bound. The difference between the *Bel* and *Pl* functions is depicted in Figure A.1.

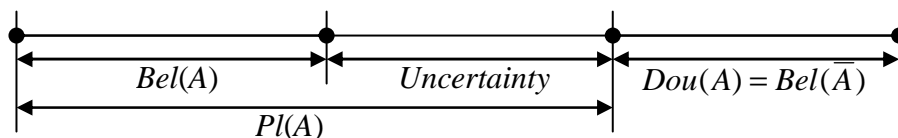


Figure A.1 A relationship between *Bel* and *Pl* functions (Agarwal *et al.* 2004)

A belief function on 2^Θ is said to be a Bayesian belief function if:

$Pl(A) = Bel(A)$ for all $A \subset \Theta$

This implies that m takes non-zero values only for singletons (Yager 1983).

Other functions also used in Evidence Theory are *Doubt* and *Commonality*. These are defined as:

$$\text{Doubt: } Dou(A) = 1 - Pl(A) = Bel(\bar{A}) \quad (\text{A.5})$$

Doubt represents the probability mass in contradiction with hypothesis A .

$$\text{Commonality: } Q(A) = \sum_{B \supseteq A} m(B) \quad (\text{A.6})$$

The commonality function represents the mass of evidence equally in support of all the elements of A , i.e., the evidence focused on supersets of A . The use of the commonality function will be demonstrated later in relation to the computation of Dempster's combination rule. The relationship between Bel and Q functions is described in Eq. (A.7) and Eq. (A.8).

$$Bel(A) = \sum_{B \subset A} (-1)^{|B|} Q(B) \quad \text{for all } A \subset \Theta \quad (\text{A.7})$$

$$Q(A) = \sum_{B \subset A} (-1)^{|B|} Bel(\bar{B}) \quad \text{for all } A \subset \Theta \quad (\text{A.8})$$

An inverse relationship exists between BPAs and the functions presented in this section (i.e., Bel , Pl , and Q). So, the BPA can be calculated from, e.g., a belief function in the following way:

$$m(A) = \sum_{B \subset A} (-1)^{|A-B|} Bel(B) \quad \text{for all } A \subset \Theta \quad (\text{A.9})$$

A.1 Combining the Evidence

Making judgements about a particular hypothesis is usually not easy given the rather scarce and scattered information available. The various pieces of evidence can thus be combined to facilitate the decision-making. The requirement of the bodies of evidence to be independent has to be stressed, since in reality it is very difficult to achieve as noted by Dempster (1967). The term “body of evidence” and “source of evidence” will be used interchangeably in this work. The problem of dependencies between bodies of evidence has been thoroughly studied by Ferson *et al.* (2004). Marashi *et al.* (2008) stated that “The assumption of independence and randomness may well suit the problem

domains like pattern recognition and sensors information fusion, but it seems to be less realistic in the case of human subjective judgements.” Given the similarities of this work and sensors information fusion, all the bodies of evidence used in this work were considered as probabilistically independent.

The combination of evidence coming from N independent bodies of evidence is depicted in Figure A.2 . The combined evidence forms a new BPA which can again be combined with other evidence and thus form a hierarchical structure as shown in Figure A.3.

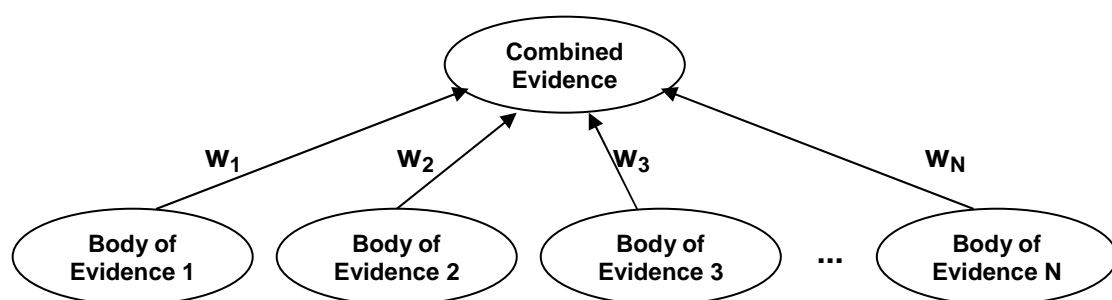


Figure A.2 Combination of N independent bodies of evidence

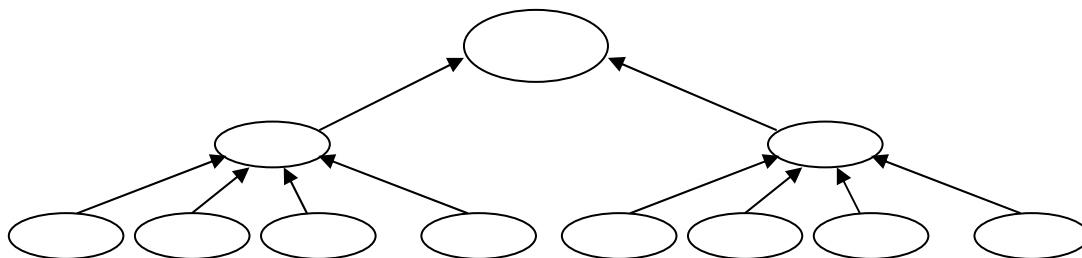


Figure A.3 A hierarchical structure of evidence

There are several combination rules, each having different properties, which can be used in the Evidence Theory. The original rule was introduced by Dempster (1967) and formed a fundamental part of the Evidence Theory.

A.1.1 Dempster’s Rule of Combination

This combination rule can be seen as an orthogonal sum followed by a normalisation process, which has to be performed in case the evidence provided contains some level of conflict.

$$m_{1,2}(A) = \frac{\sum_{B \cap C = A} m_1(B)m_2(C)}{1 - K} \text{ when } A \neq \emptyset \quad (\text{A.10})$$

$$K = \sum_{B \cap C = \emptyset} m_1(B)m_2(C) \quad (\text{A.11})$$

$$m_{1,2}(\emptyset) = 0 \quad (\text{A.12})$$

where:

- $m_{1,2}$ is the combined BPA
- m_1, m_2 are BPAs
- A, B and C are non-empty subsets of Θ

In the case of conflicting evidence when $K \neq 0$, without normalising the combined BPA $m_{1,2}(A)$ by the factor $1 / (1 - K)$, some probability mass would be assigned to the empty set, which violates the condition in Eq. (A.1): $m(\emptyset) = 0$. Dempster (1967) avoided this by scaling the combined BPA and distributing the conflicting mass amongst the focal sets of Θ .

Definition:

Let us denote \otimes a binary operation on a set S . We say that the operation \otimes is associative if: $(a \otimes b) \otimes c = a \otimes (b \otimes c)$ for all $a, b, c \in S$

In particular associativity in terms of the Evidence Theory is defined as: Let \otimes be a combination rule (e.g., Dempster's rule, etc.) on a frame of discernment Θ . We say that the operation \otimes is associative if: $(A \otimes B) \otimes C = A \otimes (B \otimes C)$ for all $A, B, C \in \Theta$

The distinguishing feature of Dempster's rule is that it is associative and thus allows evidence to be updated. Its major drawback, however, is that it can produce unexpected results under certain circumstances of conflicting evidence as pointed out by Zadeh (1984).

The following example demonstrates this counterintuitive behaviour. Let us assume following situation of two engineers providing evidence about a particular failure. The frame of discernment $\Theta = \{\text{pipe burst}, \text{valve blockage}, \text{pump failure}\}$

Engineer 1:

$$\begin{aligned} m_1(\{\text{pipe burst}\}) &= 0.90 \\ m_1(\{\text{valve blockage}\}) &= 0.1 \end{aligned}$$

Engineer 2:

$$m_2(\{pump\ failure\}) = 0.90$$

$$m_2(\{valve\ blockage\}) = 0.10$$

$$K = m_{1,2}(\emptyset) = m_1(\{pipe\ burst\}) \cdot m_2(\{pump\ failure\}) +$$

$$m_1(\{valve\ blockage\}) \cdot m_2(\{pump\ failure\}) +$$

$$m_1(\{pipe\ burst\}) \cdot m_2(\{valve\ blockage\}) = 0.9 \times 0.9 + 0.1 \times 0.9 + 0.9 \times 0.1 = 0.99$$

Combining the available evidence using Dempster's rule gives a single result:

$$m_{1,2}(\{valve\ blockage\}) = 0.1 \times 0.1 / (1 - 0.99) = 1$$

Dempster's rule is also unsuitable to combine completely conflicting evidence because in those situations the denominator of Equation (3.3) would be equal to zero. To prevent situations like this and to yield more intuitive results the conflicting evidence can be either discounted as described later in section A.3 to reduce the level of conflict, completely discarded by not considering it in the aggregation, or some other combination rules can be applied which handle the conflict in a different way. A review of additional combination rules can be found in Sentz and Ferson (2002).

A.2 Combining Conflicting Evidence

Aggregation of conflicting evidence has been studied by several researchers, for example, (Murphy 2000; Lefevre *et al.* 2002). Murphy (2000) pointed out the problems related to Dempster's combination rule when conflicting evidence is aggregated and suggested the use of averaging, which avoids most of the problems related to conflicting evidence. Amongst the main advantages of averaging are identification of possible combination problems, preservation of ignorance (unassigned belief) and distribution of belief. Murphy (2000) also noted that the probability mass assigned to the empty set can be used as a warning indicator, however, setting the threshold level determining when the conflict is high enough to warn a DM, was difficult. In situations where the level of conflict is greater than 90% it can be considered as a good indicator of some problems.

The Evidence Theory is based on the "close-world" assumption which requires that exactly one of the hypotheses in the frame of discernment is true. This assumption can be questionable when the evidence is contradicting and a significant amount of the probability mass is assigned to the empty set. This indicates a high level of conflict, which might stem from the fact that it is likely that the truth lies outside of the frame of

discernment in a hypothesis which had not been initially considered. Smets (1990) in his Transferable Belief Model (TBM) introduced the idea of the “open-world” assumption, allowing the probability mass to be assigned to the empty set and eliminating the need to normalise belief functions (unlike in the case of Dempster’s combination rule).

A.2.1 Yager’s Combination Rule

Yager’s rule of combination stems from the original work of Dempster, however, conceptualises the conflicting mass as part of the uncertainty pertaining to the problem and assigns it to the whole frame of discernment Θ . In Yager’s approach the combined basic probability assignment can be computed as:

$$m_Y(A) = q(A) \tag{A.13}$$

$$m_Y(\Theta) = q(\Theta) + q(\emptyset) \tag{A.14}$$

$$q(A) = \sum_{B \cap C = A} m_1(B)m_2(C) \tag{A.15}$$

$$q(\emptyset) = K = \sum_{B \cap C = \emptyset} m_1(B)m_2(C) \tag{A.16}$$

where:

- m_Y is the combined BPA
- m_1, m_2 are BPAs
- q is a ground probability assignment which is different from the BPA obtained by Dempster’s combination rule in a way that that it allows $q(\emptyset) \geq 0$. It is consequently transformed to BPA by attributing all $q(\emptyset)$ to the frame of discernment.

Applying Yager’s combination rule on the example of two engineers yields the following results:

$$m_Y(\{\text{valve blockage}\}) = m_1(\{\text{valve blockage}\}) \times m_2(\{\text{valve blockage}\}) = 0.01$$

$$m_Y(\Theta) = m_Y(\{\text{pipe burst, pump failure, valve blockage}\}) = 0.99$$

The result obtained using Yager’s combination rule is more intuitive since conflict reinforces uncertainty rather than one of the alternatives. Unfortunately, Yager’s rule is not associative and thus cannot be applied for updating of evidence. However, as its quasi-associative form exists, the evidence can be re-combined to overcome this issue.

A.2.2 PCR5 Combination Rule

A detailed description of the PCR5 combination rule is beyond the scope of this thesis and readers are referred to Smarandache and Dezert (2006) for exhaustive information. Only a version of the PCR5 combination rule that supports two information sources will be discussed here. According to Smarandache and Dezert (2006) the simplified version of the PCR5 rule can be defined as follows:

$$m_{PCR5}(A) = q(A) + \sum_{\substack{B \in 2^\Theta \setminus \{A\} \\ A \cap B = \emptyset}} \left[\frac{m_1(A)^2 m_2(B)}{m_1(A) + m_2(B)} + \frac{m_2(A)^2 m_1(B)}{m_2(A) + m_1(B)} \right] \quad (\text{A.17})$$

where:

- m_{PCR5} is the combined BPA
- m_1, m_2 are BPAs of the individual information sources
- q is a ground probability assignment defined in Eq. (A.15)

If the denominators in Eq. (A.17) are zero, that fraction is discarded.

The application of the PCR5 combination rule on the example of two Engineers illustrated above yields following results:

$$\begin{aligned} m_{PCR5}(\{valve\ blockage\}) &= 0.01 + 0.009 + 0.009 = 0.028 \\ m_{PCR5}(\{pump\ failure\}) &= m_{PCR5}(\{pipe\ burst\}) = 0 + 0.405 + 0.081 = 0.486 \\ m_{PCR5}(\{pipe\ burst, pump\ failure, valve\ blockage\}) &= 0 \end{aligned}$$

The result obtained using the PCR5 combination rule is quite different from Yager's and Dempster's combination rules and certainly not counter-intuitive (as in the case of Dempster's rule). Similarly to Yager's combination rule, PCR5 is not associative and thus cannot be directly applied for updating the evidence. However, its quasi-associative form also exists.

A.3 Discounting of Evidence

As confidence in the reliability of a certain information source can vary, it is also possible to take this into account and apply a “discounting” operation to reduce the credibility of a particular source of evidence. In situations where there is a significant conflict in evidence, discounting reduces the level of conflict. The application of discounting to tackle conflicting evidence is also suggested in Lefevre *et al.* (2002), who further noted that the conflict amongst sources generally increases with their number. Discounting by a coefficient $(1 - \alpha)$ was defined by Shafer (1976) as follows:

$$m(A) = \alpha m(A) \text{ for all } \alpha \in [0, 1] \quad (\text{A.18})$$

$$m(\Theta) = \alpha m(\Theta) + (1 - \alpha) \quad (\text{A.19})$$

For:

- $\alpha = 0$ discounting renders the source as completely unreliable and effectively discards all the evidence by assigning all the probability mass to the frame of discernment Θ ,
- $\alpha = 1$ represents a full confidence in the source and has no effect on the BPAs

A.4 Computational Complexity of Dempster's Combination Rule

Let us begin with two fundamental definitions which are essential in order to assess the complexity of an algorithm. Complexity of an algorithm is typically measured in terms of computational time and memory used. If not explicitly stated otherwise, by complexity we mean the time complexity equivalent to the number of basic computational steps.

Definition:

Let us say that a function $f(n)$ is $O(g(n))$ whenever there exist constants c and n_0 such that $|f(n)| \leq c \cdot |g(n)|$ for all $n \geq n_0$ (Knuth 1976)

where:

- n is the length of the input (size of the problem)

The function $O(g(n))$ thus represents an asymptotic upper bound of function $f(n)$.

Definition:

A *polynomial time algorithm* is defined as one whose time complexity function is $O(p(n))$ for some polynomial function p (e.g., n^b where $b > 1$)

The computational complexity of Dempster's combination rule belongs to the class of #P-Complete problems as proven by Orponen (1990) (equivalent to NP-Complete for decision problems). The class of NP-Complete¹ (Garey and Johnson 1979) is characterised by the fact that no polynomial-time algorithm is known to exist to solve

¹ NP stands for Non-deterministic Polynomial time

any of the problems belonging to this class. The complexity of the combination rule can be considered as one of the major barriers preventing wide spread application of the Evidence Theory.

Haenni and Lehmann (2003) showed that for small problems, an efficient implementation of Dempster's combination rule makes the computation time acceptable. In situations where an exact solution cannot be obtained in a reasonable time, approximate methods have to be applied. A review and comparison of some approximate methods can be found, for example, in Tessem (1993) and Bauer (1996).

Xu and Kennes (1994) proposed three techniques to speedup the computation of Dempster's combination rule. They suggested the use of local computation using Markov chains, implementation of belief functions using bit-arrays (used in this work) and finally using the commonality functions and Möbius transformation (which is in fact generalised Fourier transformation used to compute the commonality function $Q(A)$ defined in Eq. (A.8) from $BPA(A)$). The major advantage of the commonality function is shown in Eq. (A.20). The orthogonal sum can be calculated simply by multiplying two commonality functions instead of by computing a sum every time.

$$Q_{m_1 \oplus m_2}(A) = Q_{m_1}(A) \cdot Q_{m_2}(A) \quad (\text{A.20})$$

Similarly, Denoeux and Yaghlane (2002) proposed an approximation algorithm to combine evidence based on fast Möbius transformation which can be computed in $O(n^2 \cdot 2^n)$. They also manipulated the size of the frame of discernment Θ to reduce the computational complexity.

Kreinovich *et al.* (1994) developed an approximation algorithm employing Monte-Carlo simulation in order to avoid the computational complexity of combining evidence. They also pointed out that their approach can be easily parallelised.

APPENDIX B FAILURE IMPACT SURVEY

Dear Participant,

This survey was designed to determine the severity of various types of impacts caused by failures (e.g., pipe bursts) in a water distribution system. You are going to be asked to indicate mutual importance of several criteria *from the perspective of an employee of a water utility (i.e., NOT from the perspective of a customer)*.

The questionnaire is anonymous and the information provided will be confidential and used only for the purposes of this study carried out as part of the [NEPTUNE](#) project. There are **9 questions** in the survey and it should not take more than **10 minutes** to complete. Thank you very much for your time and kind support of this research. In case of any questions please do not hesitate and contact Josef Bicik (E-mail: j.bicik@exeter.ac.uk, phone: 01392 263730).

Below is an answer to an imaginary question indicating that *Quality* is **much more important** than *Price*.

	Unquestionably more important	Much more important	More important	Rather more important	Equally important	Rather less important	Less important	Much less important	Unquestionably less important	
Quality	<input type="radio"/>	<input checked="" type="radio"/>	<input type="radio"/>	<input type="radio"/>	<input type="radio"/>	<input type="radio"/>	<input type="radio"/>	<input type="radio"/>	<input type="radio"/>	Price

To indicate the opposite, i.e., that *Quality* is **much less important** than *Price* select an option on the right-hand side from the **Equally important** answer as shown in the following figure:

	Unquestionably more important	Much more important	More important	Rather more important	Equally important	Rather less important	Less important	Much less important	Unquestionably less important	
Quality	<input type="radio"/>	<input type="radio"/>	<input type="radio"/>	<input type="radio"/>	<input type="radio"/>	<input type="radio"/>	<input type="radio"/>	<input checked="" type="radio"/>	<input type="radio"/>	Price

Please try to answer all questions in the survey and be consistent in your answers as much as possible (i.e., **AVOID** situations where Price>Quality, Quality>Design and Price<Design).

Customers

1. Please, indicate the mutual importance of following types of customers according to their vulnerability in case of a failure in a water distribution system (e.g., a pipe burst causing low pressure or supply interruption).

- critical (e.g., hospitals, schools and other vulnerable customers, etc.),
- residential (e.g., flats, houses, etc.),
- commercial (e.g., shops, businesses, etc.),
- industrial (e.g., factories, mills, etc.)

	Unquestionably more important	Much more important	More important	Rather more important	Equally important	Rather less important	Less important	Much less important	Unquestionably less important	No answer
Critical	<input type="checkbox"/>	<input type="checkbox"/>	<input type="checkbox"/>	<input type="checkbox"/>	<input type="checkbox"/>	<input type="checkbox"/>	<input type="checkbox"/>	<input type="checkbox"/>	<input type="checkbox"/>	Residential <input type="checkbox"/>
Critical	<input type="checkbox"/>	<input type="checkbox"/>	<input type="checkbox"/>	<input type="checkbox"/>	<input type="checkbox"/>	<input type="checkbox"/>	<input type="checkbox"/>	<input type="checkbox"/>	<input type="checkbox"/>	Commercial <input type="checkbox"/>
Critical	<input type="checkbox"/>	<input type="checkbox"/>	<input type="checkbox"/>	<input type="checkbox"/>	<input type="checkbox"/>	<input type="checkbox"/>	<input type="checkbox"/>	<input type="checkbox"/>	<input type="checkbox"/>	Industrial <input type="checkbox"/>

Residential	<input type="checkbox"/>	<input type="checkbox"/>	<input type="checkbox"/>	<input type="checkbox"/>	<input type="checkbox"/>	<input type="checkbox"/>	<input type="checkbox"/>	<input type="checkbox"/>	<input type="checkbox"/>	Commercial	<input type="checkbox"/>
Residential	<input type="checkbox"/>	<input type="checkbox"/>	<input type="checkbox"/>	<input type="checkbox"/>	<input type="checkbox"/>	<input type="checkbox"/>	<input type="checkbox"/>	<input type="checkbox"/>	<input type="checkbox"/>	Industrial	<input type="checkbox"/>
Commercial	<input type="checkbox"/>	<input type="checkbox"/>	<input type="checkbox"/>	<input type="checkbox"/>	<input type="checkbox"/>	<input type="checkbox"/>	<input type="checkbox"/>	<input type="checkbox"/>	<input type="checkbox"/>	Industrial	<input type="checkbox"/>

Types of Impact

2. Please, indicate the importance of following economic impacts, having equal scale (i.e., financial losses), which affect the water utility (company). Bear in mind that the impacts might negatively affect the public image of the company.

	Unquestionably more important	Much more important	More important	Rather more important	Equally important	Rather less important	Less important	Much less important	Unquestionably less important	No answer
Third party damage	<input type="checkbox"/>	<input type="checkbox"/>	<input type="checkbox"/>	<input type="checkbox"/>	<input type="checkbox"/>	<input type="checkbox"/>	<input type="checkbox"/>	<input type="checkbox"/>	<input type="checkbox"/>	Lost water
Third party damage	<input type="checkbox"/>	<input type="checkbox"/>	<input type="checkbox"/>	<input type="checkbox"/>	<input type="checkbox"/>	<input type="checkbox"/>	<input type="checkbox"/>	<input type="checkbox"/>	<input type="checkbox"/>	Undelivered water
Lost water	<input type="checkbox"/>	<input type="checkbox"/>	<input type="checkbox"/>	<input type="checkbox"/>	<input type="checkbox"/>	<input type="checkbox"/>	<input type="checkbox"/>	<input type="checkbox"/>	<input type="checkbox"/>	Undelivered water

Third party damage represents the estimated damage to third parties (e.g., damage to the road, flooding of basements, etc.).

Lost water represents the amount of water escaped from the system due to a leak or pipe burst.

Undelivered water represents loss of revenue of the water company due to pressure sensitive demand that was not delivered because of low pressure at consumers' taps (e.g., a garden hose).

3. Please, indicate the importance of the **duration** of supply interruption affecting the same number of customers of the same type (e.g., residential):

	Unquestionably more important	Much more important	More important	Rather more important	Equally important	Rather less important	Less important	Much less important	Unquestionably less important	No answer
>24h	<input type="checkbox"/>	<input type="checkbox"/>	<input type="checkbox"/>	<input type="checkbox"/>	<input type="checkbox"/>	<input type="checkbox"/>	<input type="checkbox"/>	<input type="checkbox"/>	<input type="checkbox"/>	13-24h
>24h	<input type="checkbox"/>	<input type="checkbox"/>	<input type="checkbox"/>	<input type="checkbox"/>	<input type="checkbox"/>	<input type="checkbox"/>	<input type="checkbox"/>	<input type="checkbox"/>	<input type="checkbox"/>	7-12h
>24h	<input type="checkbox"/>	<input type="checkbox"/>	<input type="checkbox"/>	<input type="checkbox"/>	<input type="checkbox"/>	<input type="checkbox"/>	<input type="checkbox"/>	<input type="checkbox"/>	<input type="checkbox"/>	3-6h
13-24h	<input type="checkbox"/>	<input type="checkbox"/>	<input type="checkbox"/>	<input type="checkbox"/>	<input type="checkbox"/>	<input type="checkbox"/>	<input type="checkbox"/>	<input type="checkbox"/>	<input type="checkbox"/>	7-12h
13-24h	<input type="checkbox"/>	<input type="checkbox"/>	<input type="checkbox"/>	<input type="checkbox"/>	<input type="checkbox"/>	<input type="checkbox"/>	<input type="checkbox"/>	<input type="checkbox"/>	<input type="checkbox"/>	3-6h
7-12h	<input type="checkbox"/>	<input type="checkbox"/>	<input type="checkbox"/>	<input type="checkbox"/>	<input type="checkbox"/>	<input type="checkbox"/>	<input type="checkbox"/>	<input type="checkbox"/>	<input type="checkbox"/>	3-6h

>24h represents interruption of water supply of the same number of customers lasting more than 24 hours.

4. Please, indicate the importance of the **duration** of low pressure problems affecting the same number of customers of the same type (e.g., residential):

	Unquestionably more important	Much more important	More important	Rather more important	Equally important	Rather less important	Less important	Much less important	Unquestionably less important	No answer
>24h	<input type="checkbox"/>	<input type="checkbox"/>	<input type="checkbox"/>	<input type="checkbox"/>	<input type="checkbox"/>	<input type="checkbox"/>	<input type="checkbox"/>	<input type="checkbox"/>	<input type="checkbox"/>	13-24

>24 h	<input type="checkbox"/>	<input type="checkbox"/>	<input type="checkbox"/>	<input type="checkbox"/>	<input type="checkbox"/>	<input type="checkbox"/>	<input type="checkbox"/>	<input type="checkbox"/>	<input type="checkbox"/>	7-12 h	<input type="checkbox"/>
>24 h	<input type="checkbox"/>	<input type="checkbox"/>	<input type="checkbox"/>	<input type="checkbox"/>	<input type="checkbox"/>	<input type="checkbox"/>	<input type="checkbox"/>	<input type="checkbox"/>	<input type="checkbox"/>	3-6h	<input type="checkbox"/>
13-24h	<input type="checkbox"/>	<input type="checkbox"/>	<input type="checkbox"/>	<input type="checkbox"/>	<input type="checkbox"/>	<input type="checkbox"/>	<input type="checkbox"/>	<input type="checkbox"/>	<input type="checkbox"/>	7-12 h	<input type="checkbox"/>
13-24h	<input type="checkbox"/>	<input type="checkbox"/>	<input type="checkbox"/>	<input type="checkbox"/>	<input type="checkbox"/>	<input type="checkbox"/>	<input type="checkbox"/>	<input type="checkbox"/>	<input type="checkbox"/>	3-6h	<input type="checkbox"/>
7-12h	<input type="checkbox"/>	<input type="checkbox"/>	<input type="checkbox"/>	<input type="checkbox"/>	<input type="checkbox"/>	<input type="checkbox"/>	<input type="checkbox"/>	<input type="checkbox"/>	<input type="checkbox"/>	3-6h	<input type="checkbox"/>

>24h represents low pressure problems affecting the same number of customers for more than 24 hours.

5. Please, indicate the importance of the **scale** of the same impact (e.g., supply interruption) on the customers of the same type (e.g., residential) for the same period of time:

	Unquestionably more important	Much more important	More important	Rather more important	Equally important	Rather less important	Less important	Much less important	Unquestionably less important	No answer	
>1000	<input type="checkbox"/>	<input type="checkbox"/>	<input type="checkbox"/>	<input type="checkbox"/>	<input type="checkbox"/>	<input type="checkbox"/>	<input type="checkbox"/>	<input type="checkbox"/>	<input type="checkbox"/>	201-1000	<input type="checkbox"/>
>1000	<input type="checkbox"/>	<input type="checkbox"/>	<input type="checkbox"/>	<input type="checkbox"/>	<input type="checkbox"/>	<input type="checkbox"/>	<input type="checkbox"/>	<input type="checkbox"/>	<input type="checkbox"/>	51-200	<input type="checkbox"/>
>1000	<input type="checkbox"/>	<input type="checkbox"/>	<input type="checkbox"/>	<input type="checkbox"/>	<input type="checkbox"/>	<input type="checkbox"/>	<input type="checkbox"/>	<input type="checkbox"/>	<input type="checkbox"/>	<50	<input type="checkbox"/>
201-1000	<input type="checkbox"/>	<input type="checkbox"/>	<input type="checkbox"/>	<input type="checkbox"/>	<input type="checkbox"/>	<input type="checkbox"/>	<input type="checkbox"/>	<input type="checkbox"/>	<input type="checkbox"/>	51-200	<input type="checkbox"/>
201-1000	<input type="checkbox"/>	<input type="checkbox"/>	<input type="checkbox"/>	<input type="checkbox"/>	<input type="checkbox"/>	<input type="checkbox"/>	<input type="checkbox"/>	<input type="checkbox"/>	<input type="checkbox"/>	<50	<input type="checkbox"/>
51-200	<input type="checkbox"/>	<input type="checkbox"/>	<input type="checkbox"/>	<input type="checkbox"/>	<input type="checkbox"/>	<input type="checkbox"/>	<input type="checkbox"/>	<input type="checkbox"/>	<input type="checkbox"/>	<50	<input type="checkbox"/>

<50 represents less than 50 customers of the same type affected for the same period of time.
 >1000 represents more than 1000 customers of the same type affected for the same period of time.

6. Please, indicate the mutual importance of following types of impacts affecting the same number of properties for the same period of time (where applicable):

	Unquestionably more important	Much more important	More important	Rather more important	Equally important	Rather less important	Less important	Much less important	Unquestionably less important	No answer	
Supply interruption	<input type="checkbox"/>	<input type="checkbox"/>	<input type="checkbox"/>	<input type="checkbox"/>	<input type="checkbox"/>	<input type="checkbox"/>	<input type="checkbox"/>	<input type="checkbox"/>	<input type="checkbox"/>	Discolouration	<input type="checkbox"/>
Supply interruption	<input type="checkbox"/>	<input type="checkbox"/>	<input type="checkbox"/>	<input type="checkbox"/>	<input type="checkbox"/>	<input type="checkbox"/>	<input type="checkbox"/>	<input type="checkbox"/>	<input type="checkbox"/>	Low pressure	<input type="checkbox"/>
Supply interruption	<input type="checkbox"/>	<input type="checkbox"/>	<input type="checkbox"/>	<input type="checkbox"/>	<input type="checkbox"/>	<input type="checkbox"/>	<input type="checkbox"/>	<input type="checkbox"/>	<input type="checkbox"/>	Economic (company) losses	<input type="checkbox"/>
Discolouration	<input type="checkbox"/>	<input type="checkbox"/>	<input type="checkbox"/>	<input type="checkbox"/>	<input type="checkbox"/>	<input type="checkbox"/>	<input type="checkbox"/>	<input type="checkbox"/>	<input type="checkbox"/>	Low pressure	<input type="checkbox"/>
Discolouration	<input type="checkbox"/>	<input type="checkbox"/>	<input type="checkbox"/>	<input type="checkbox"/>	<input type="checkbox"/>	<input type="checkbox"/>	<input type="checkbox"/>	<input type="checkbox"/>	<input type="checkbox"/>	Economic (company) losses	<input type="checkbox"/>
Low pressure	<input type="checkbox"/>	<input type="checkbox"/>	<input type="checkbox"/>	<input type="checkbox"/>	<input type="checkbox"/>	<input type="checkbox"/>	<input type="checkbox"/>	<input type="checkbox"/>	<input type="checkbox"/>	Economic (company)	<input type="checkbox"/>

losses

Supply interruption represents a situation when pressure in the water distribution system drops below 7 m of head.

Low pressure is defined as situation when pressure in the water distribution system drops below 15 m of head (but is still above 7 m).

Discolouration is characteristic by increased turbidity of water due to high levels of suspended particles.

Economic losses represent direct or indirect financial losses sustained by the water company (e.g., lost water, third party damage, etc.)

Personal Information

7. *Please, select the company / organisation you work for:
Choose one of the following answers



8. Please, select your occupation:
Choose one of the following answers



Other

9. Please provide additional comments:

APPENDIX C HYDRAULIC MODEL RESULTS

This Appendix contains detailed results of locations of open hydrants identified by the Hydraulic Model. The pipe with the lowest value of SSE (i.e., the most likely location of the hydrant opening was highlighted in cyan). The actual location of the open hydrant is denoted using symbol **X**. Remaining pipes are colour coded using a red – blue gradient in an ascending order of their Sum of Squared Errors (SSE) (i.e., red refers to the likely hydrant opening locations with low SSE).

C.1 Large Burst Flow Simulations EE1 (All Sensors)

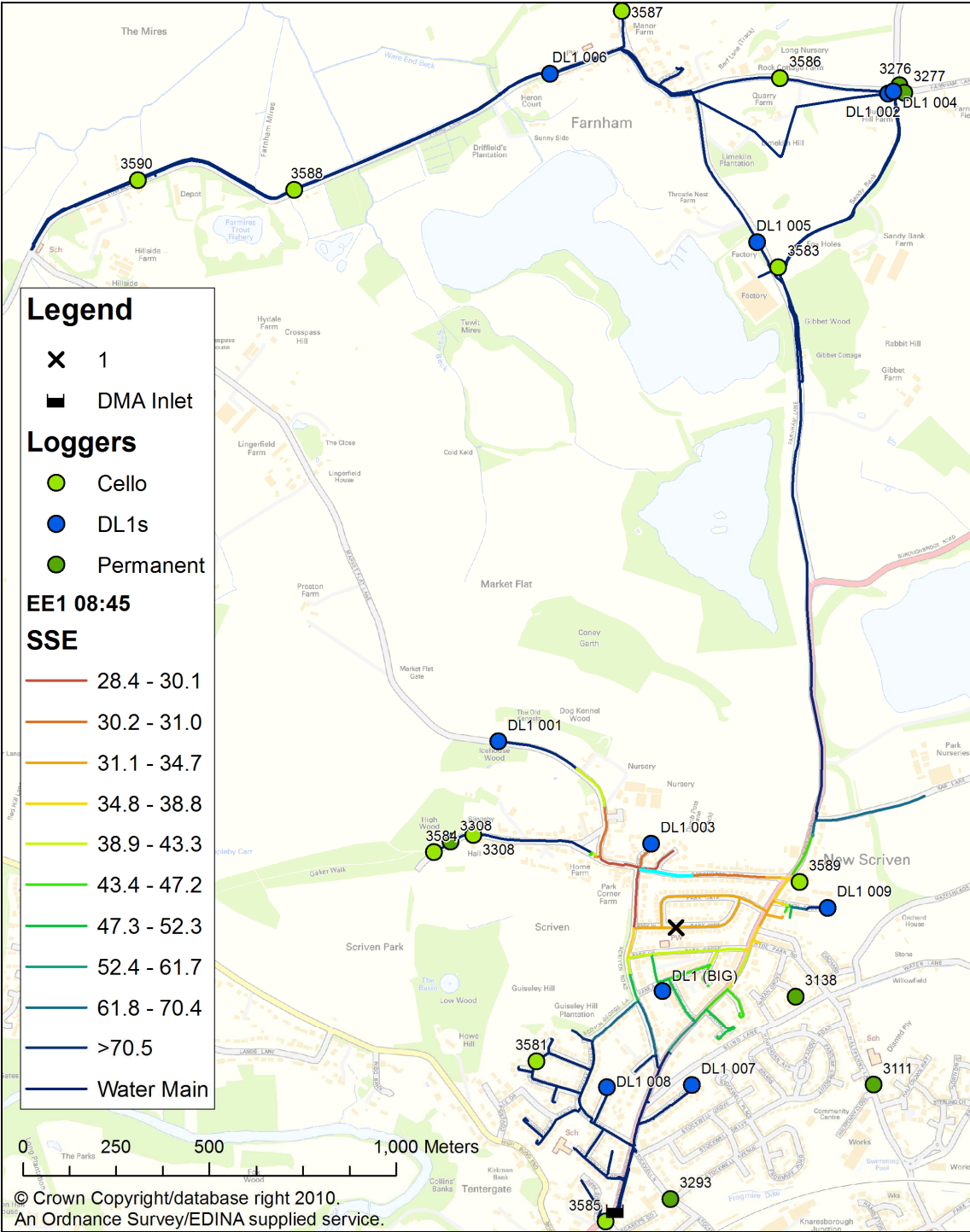


Figure C.1 The most likely location of hydrant opening for EE1-1

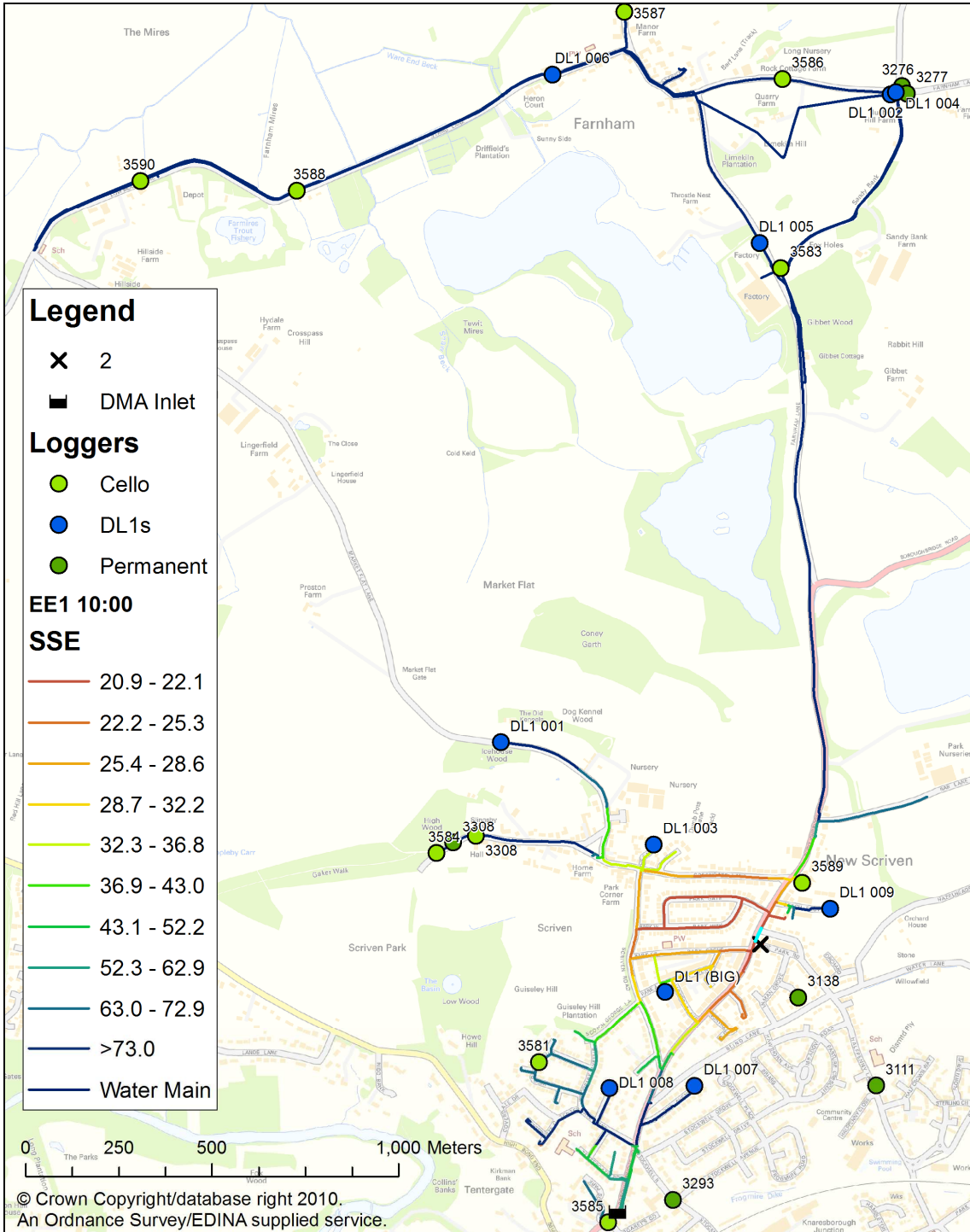


Figure C.2 The most likely location of hydrant opening for EE1-2

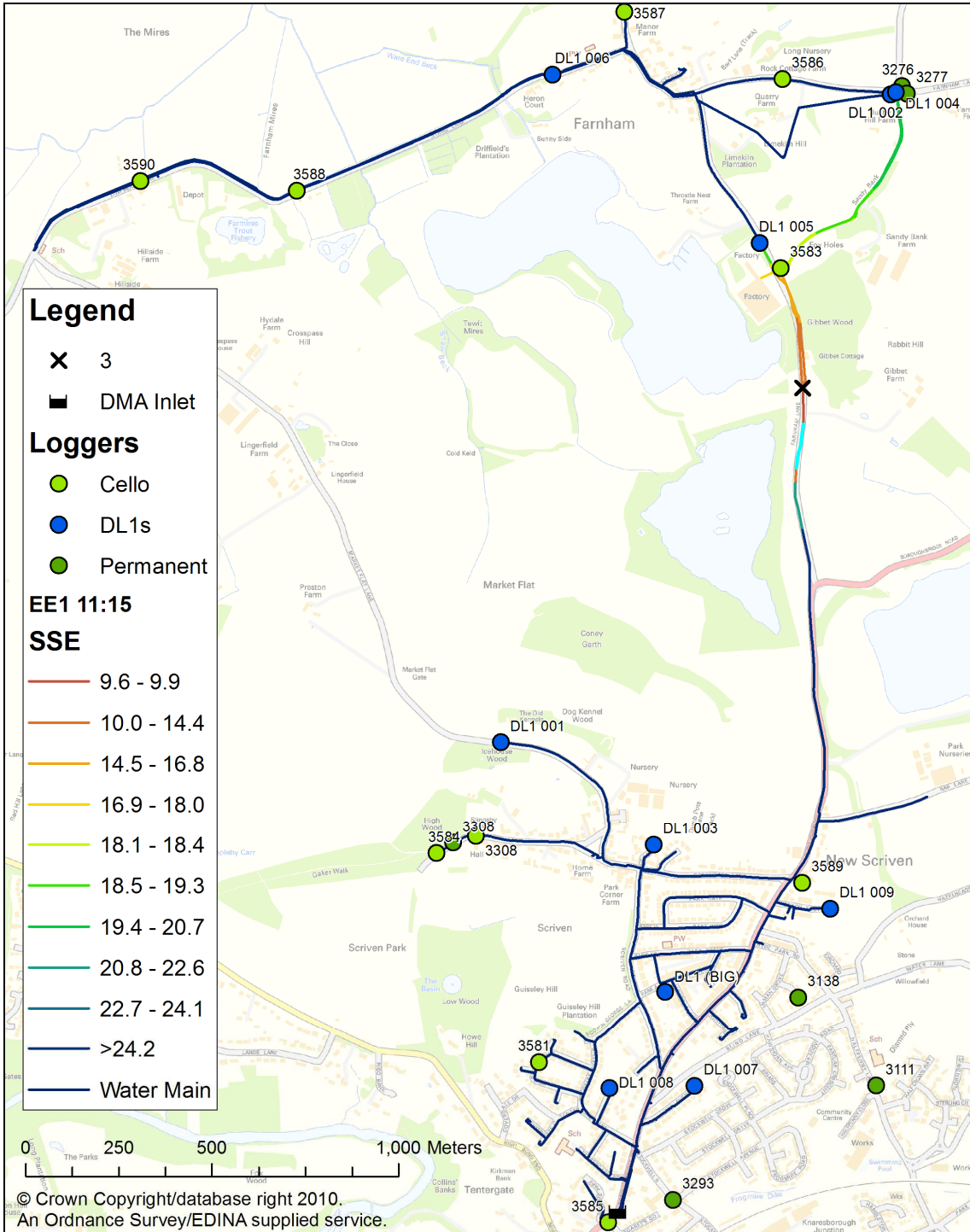


Figure C.3 The most likely location of hydrant opening for EE1-3

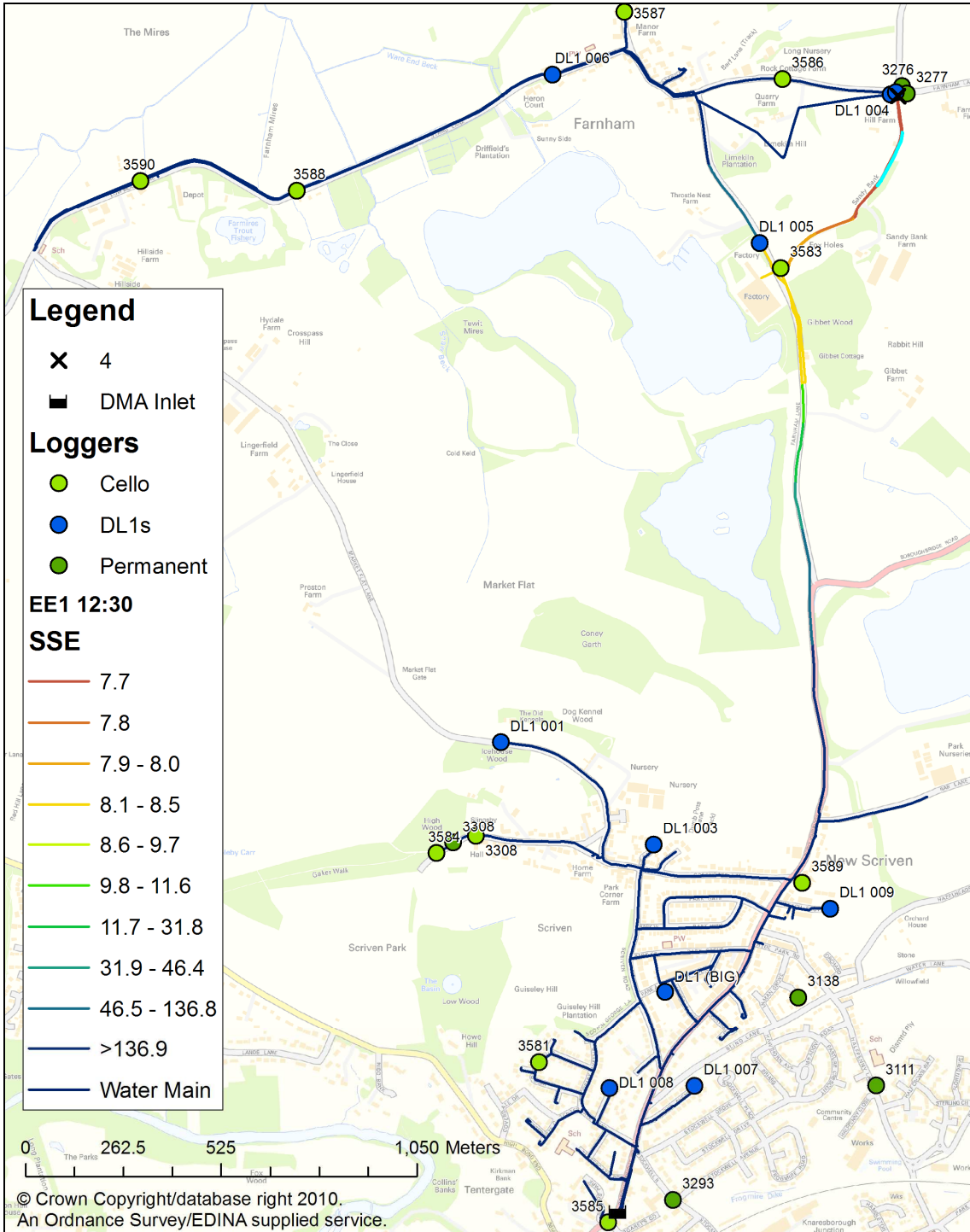


Figure C.4 The most likely location of hydrant opening for EE1-4

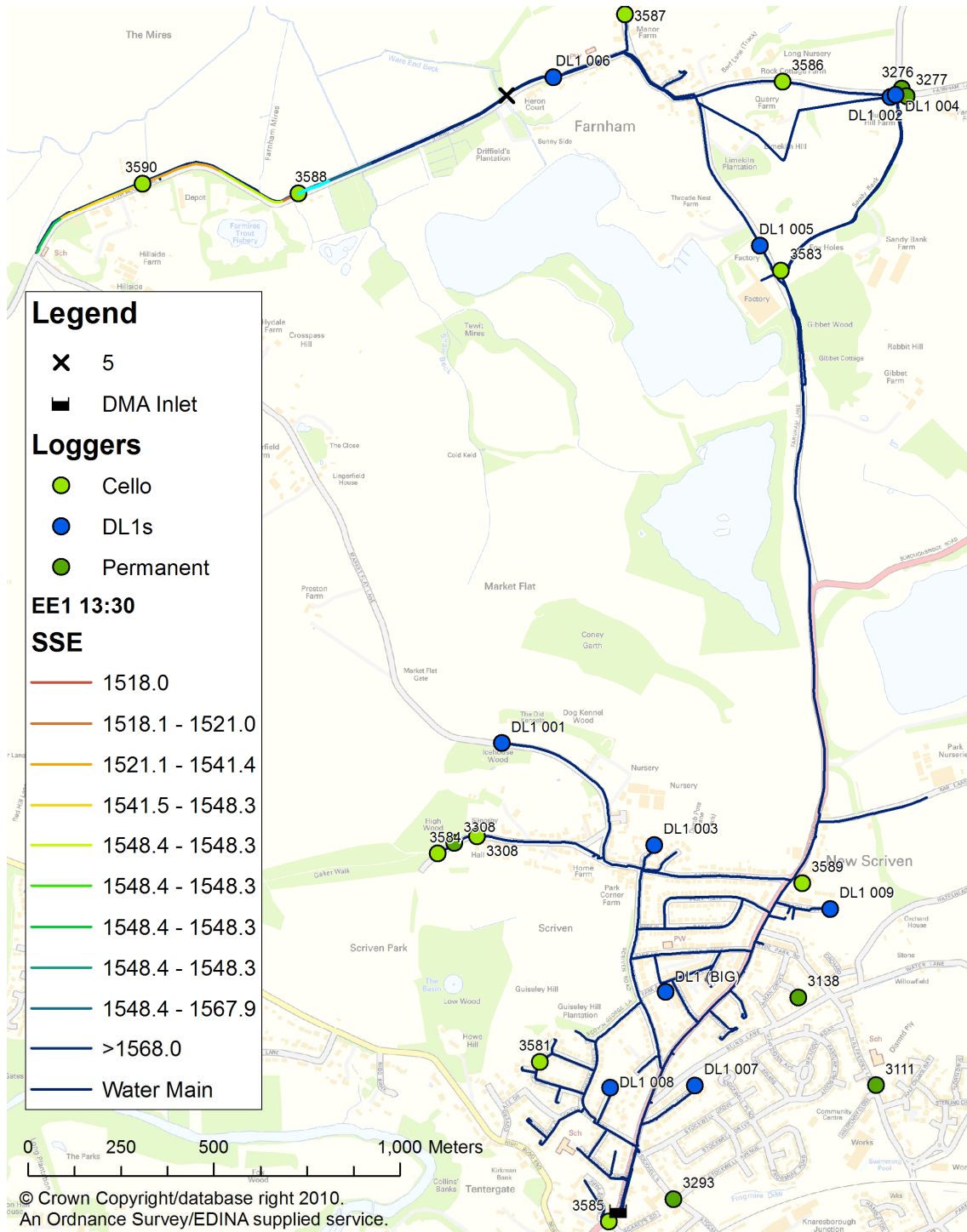


Figure C.5 The most likely location of hydrant opening for EE1-5

C.2 Medium Burst Flow Simulations EE2 (All Sensors)

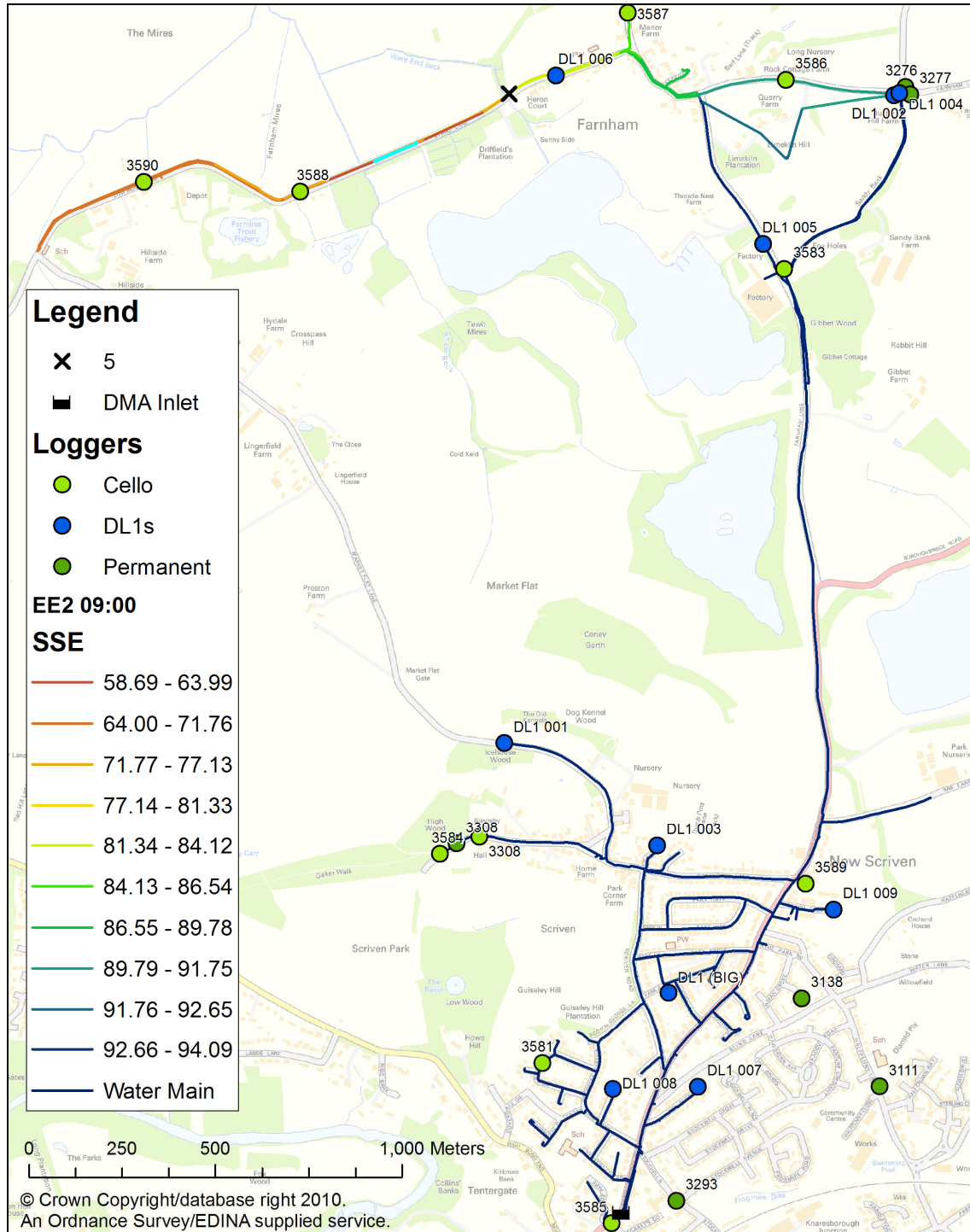


Figure C.6 The most likely location of hydrant opening for EE2-5

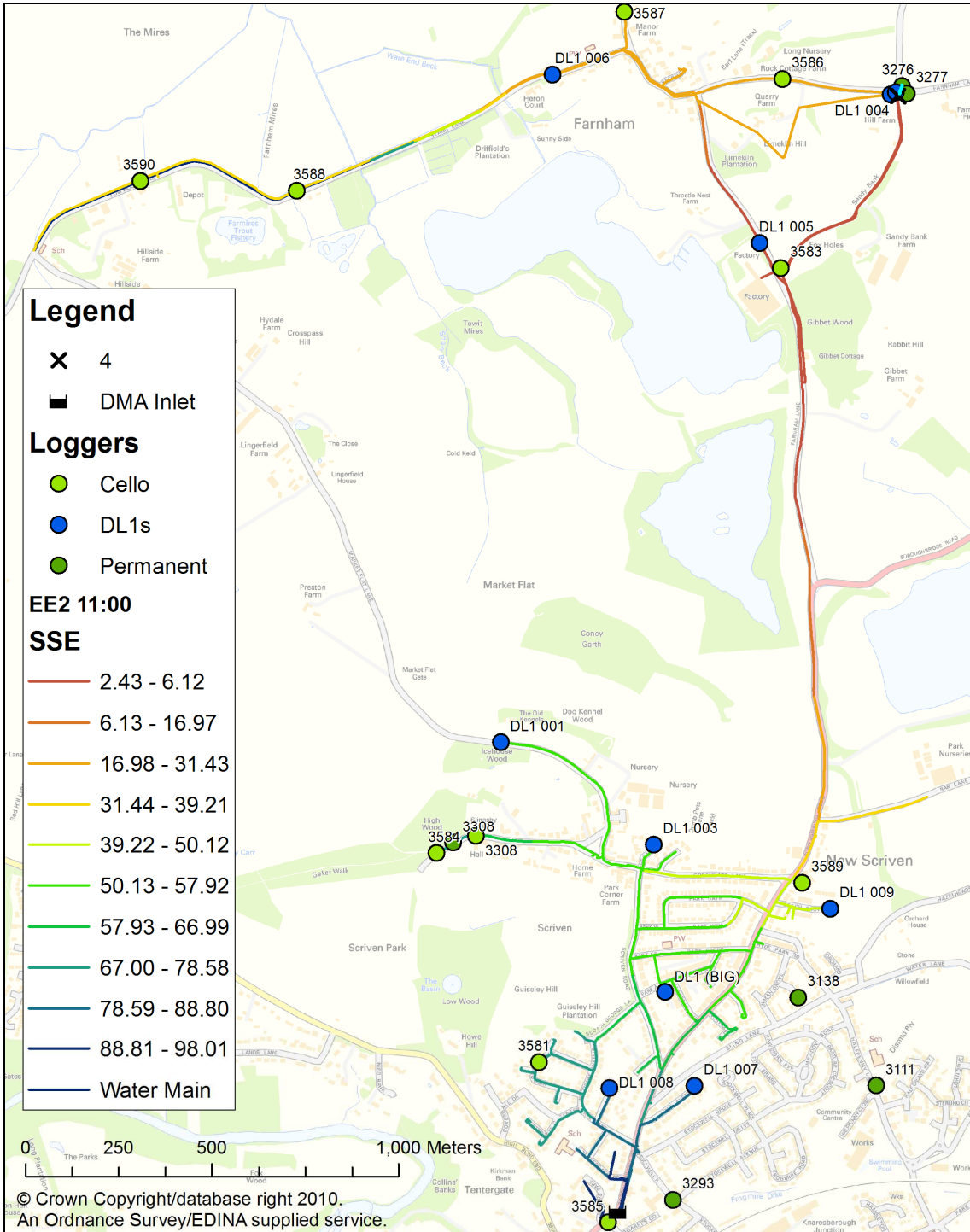


Figure C.7 The most likely location of hydrant opening for EE2-4

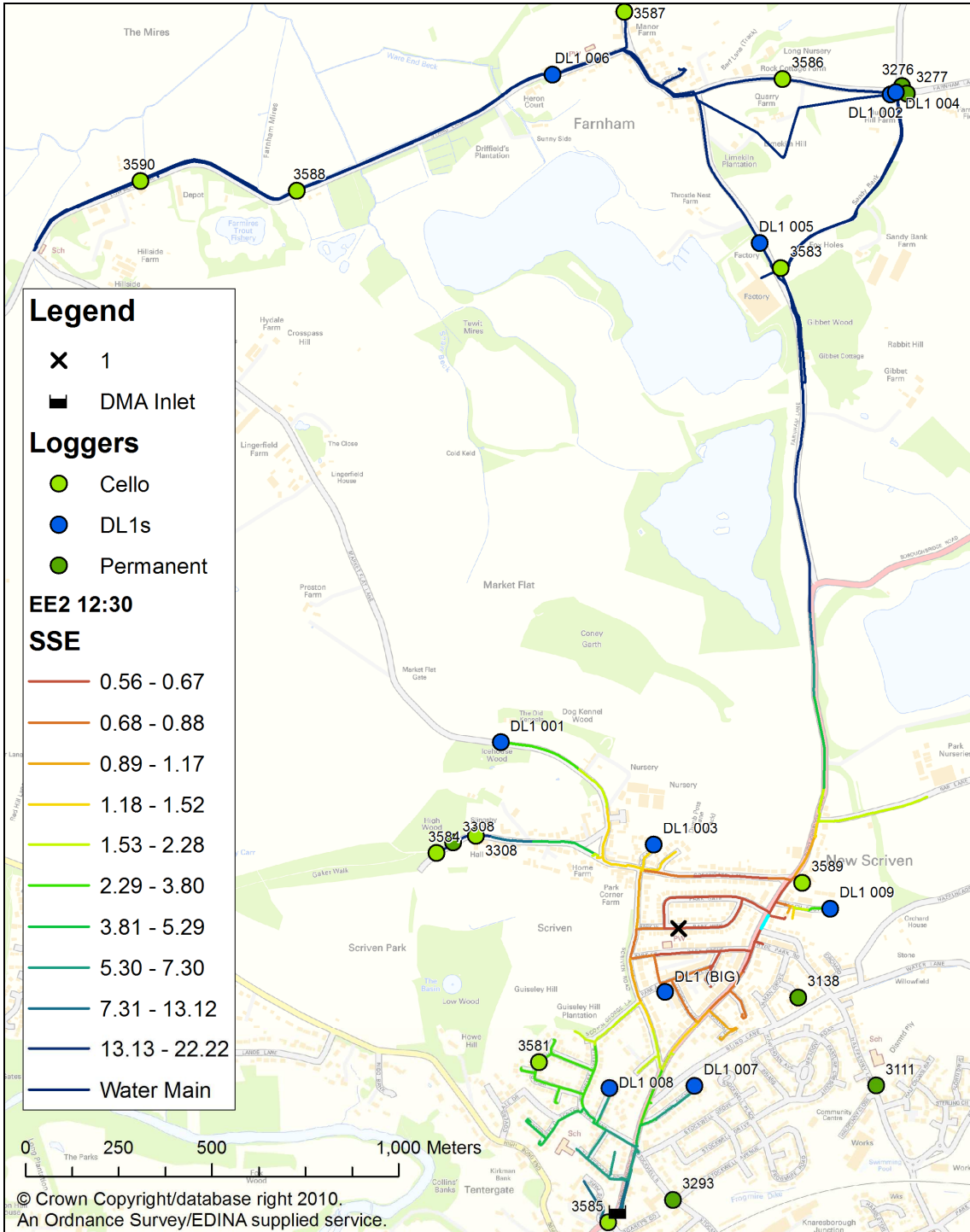


Figure C.8 The most likely location of hydrant opening for EE2-1

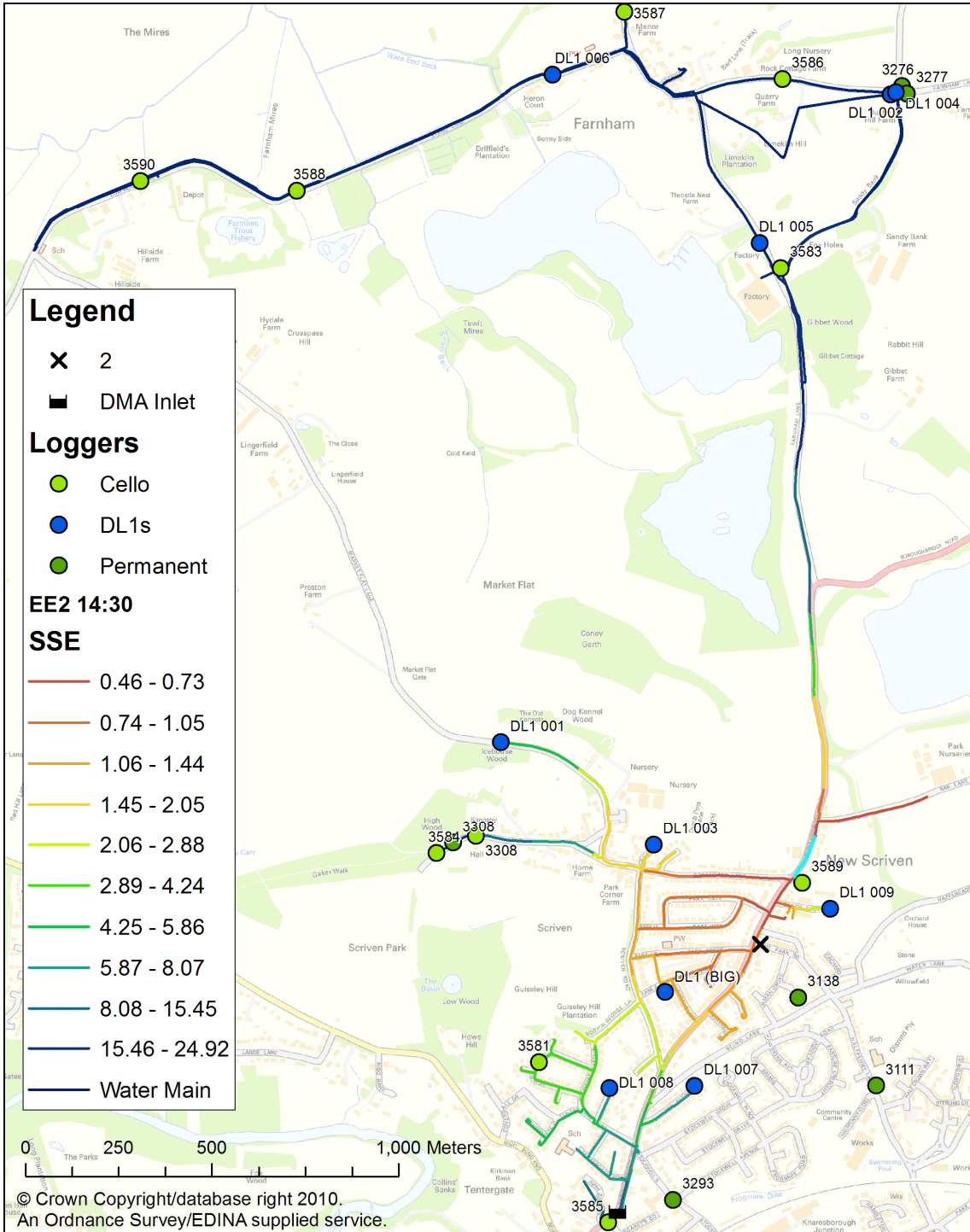


Figure C.9 The most likely location of hydrant opening for EE2-2

APPENDIX D D-S MODEL PERFORMANCE

This appendix contains detailed results and discussion of the application of the Dempster-Shafer (D-S) model on several cases selected from Table 5.11. The colour coding used in the figures (i.e., “likelihood“ maps) presented here was chosen so that the pipes in red are the most likely potential incidents whereas those in dark blue are less likely to be the True Burst Location (TBL). Pipes whose level of likelihood was below 0.5 were shown in light gray to suggest that these were unlikely to be the TBL. Labels were added only to those pipes whose likelihood was greater than 0.7 in order to preserve the clarity of the figures. All the distances reported in the appendix were estimated by tracing the pipe network rather than by calculating the Euclidean distance.

D.1 Detailed results for case #7080348

This example was taken from the validation data set presented in Table 5.11. The historical burst occurred on 26 July 2005. One customer contact was received in the time window being considered (i.e., 24 hours before the burst repair took place or during the same day). The burst report in this case might have been incorrectly associated with this burst event since it was located far from the location where the burst was later found and repaired.

The Pipe Burst Prediction Model (PBPM) (see Figure D.1a) failed to provide a good indication of the most likely location of the TBL. On the other hand the Hydraulic Model (HM) (see Figure D.1b) in this particular case, given the added levels of noise to pressure measurements and magnitude of abnormal flow, managed to locate the likely burst location accurately (i.e., the TBL was approx. 250 m from the pipe identified as the most likely burst location by the HM). Apart from identifying a relatively well confined pipe burst hotspot in the proximity of the TBL, the HM also identified a number of pipes in the south east part of the DMA as likely burst candidates (note the pipes with Confidence factor around 0.71 in Figure D.1b). The Customer Contacts Model (CCM) shown in Figure D.1c identified the most likely burst location, which was more than 1,250 m from the TBL.

The combined results from the D-S Model presented in Figure D.1d were worse than those provided by the HM. Such information would, however, be unknown in a real

decision-making situation until the TBL was found. The most likely pipe burst location would be where the Customer Contact (CC) originated. The second most likely pipe burst area would be 350 m from the TBL. One of the advantages of the combined result could be seen in the fact that the secondary burst hotspot in the south east part of the DMA identified originally by the HM, received significantly lower level of likelihood from the D-S Model and could be excluded from field investigations.

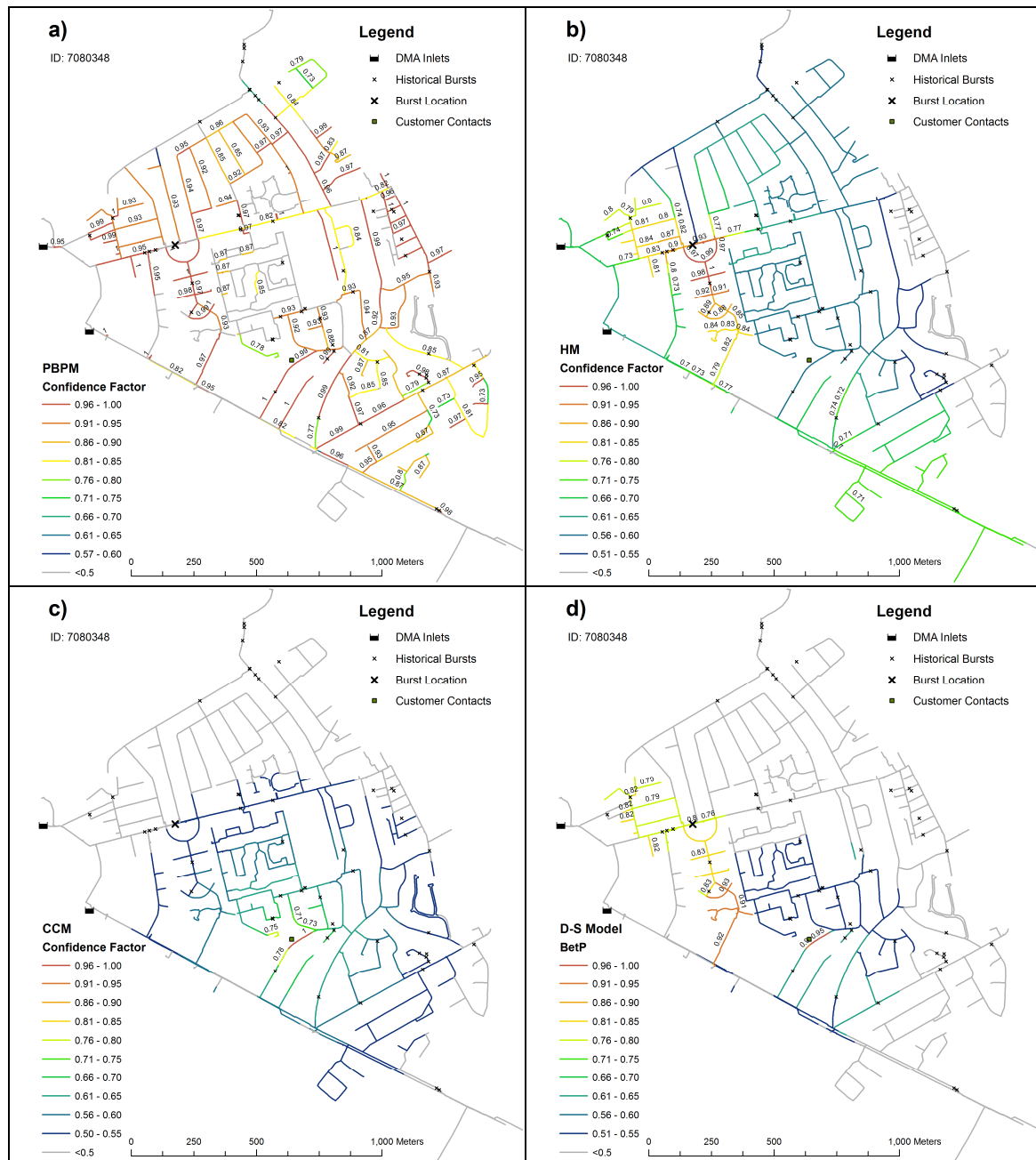


Figure D.1 a) PBPM, b) HM, c) CCM and d) D-S Model results for case #7080348

Figure D.2 provides an overview of the spatial distribution of Belief and Plausibility returned by the D-S model. Figure D.2b suggests that potential incidents in a large portion of the DMA are not very plausible burst candidates and, therefore, the investigation could be better focused, starting with pipes with the highest levels of Belief.

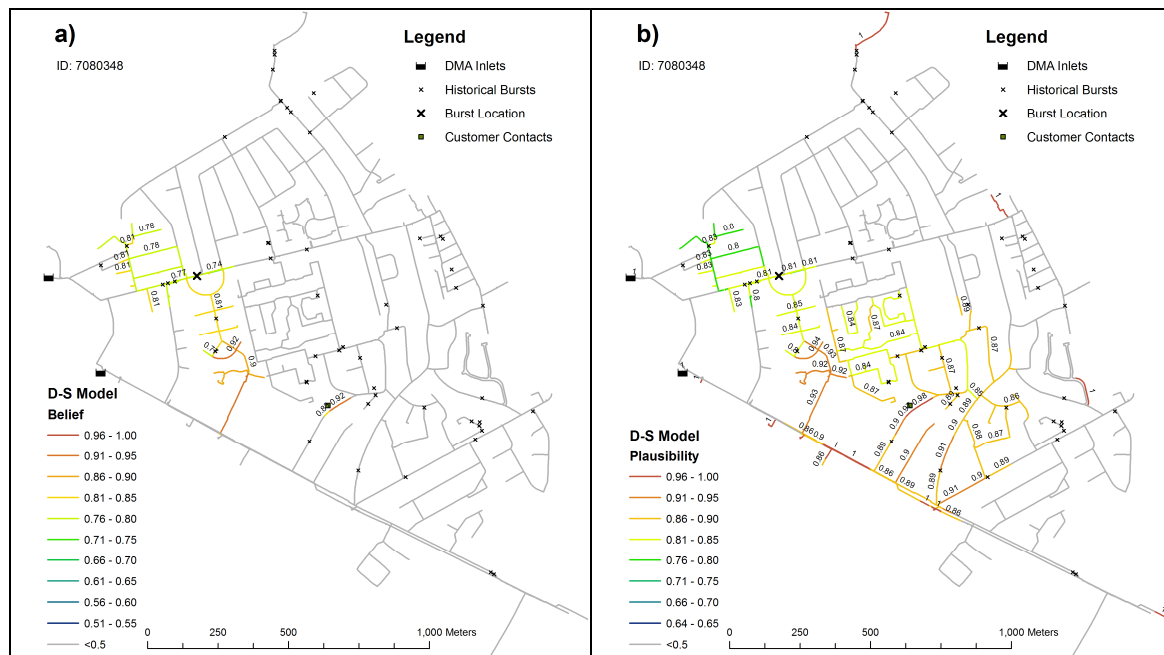


Figure D.2 a) Belief and b) Plausibility of the D-S Model for case #7080348

No evidence was available in this case for a small number of potential incidents. Such potential incidents are, therefore, entirely plausible pipe burst candidates for the D-S model. As can be seen in Figure D.2b a pipe in the north part of the DMA has maximum plausibility (i.e., $Pl_{pipe}(\{Burst\}) = 1$) and minimum belief (i.e., $Bel_{pipe}(\{Burst\}) = 0$) implying that the D-S model was unable to make any judgement about such pipe. It is left up to a human Decision Maker (DM) to handle such potential incidents.

D.2 Detailed results for case #8905881

Figure D.3 presents results of the individual models as well as the D-S model on a historical pipe burst taken from the validation set in Table 5.11. The burst occurred on 31 August 2007 and was reported by one customer. As can be seen from Figure D.3a the PBPM performed very strangely in this case and highlighted only very few pipes as potential burst candidates. Both, the HM (see Figure D.3b) and the CCM (see Figure D.3c) identified locations in very close proximity of the TBL. The HM again

highlighted the south west part of the DMA as a likely location of the burst, which could be due to limited pressure sensor coverage of that area (see Figure 5.9). The combined results of the D-S model in Figure D.3d are less specific than those of the CCM, however, better than the results provided by the HM.

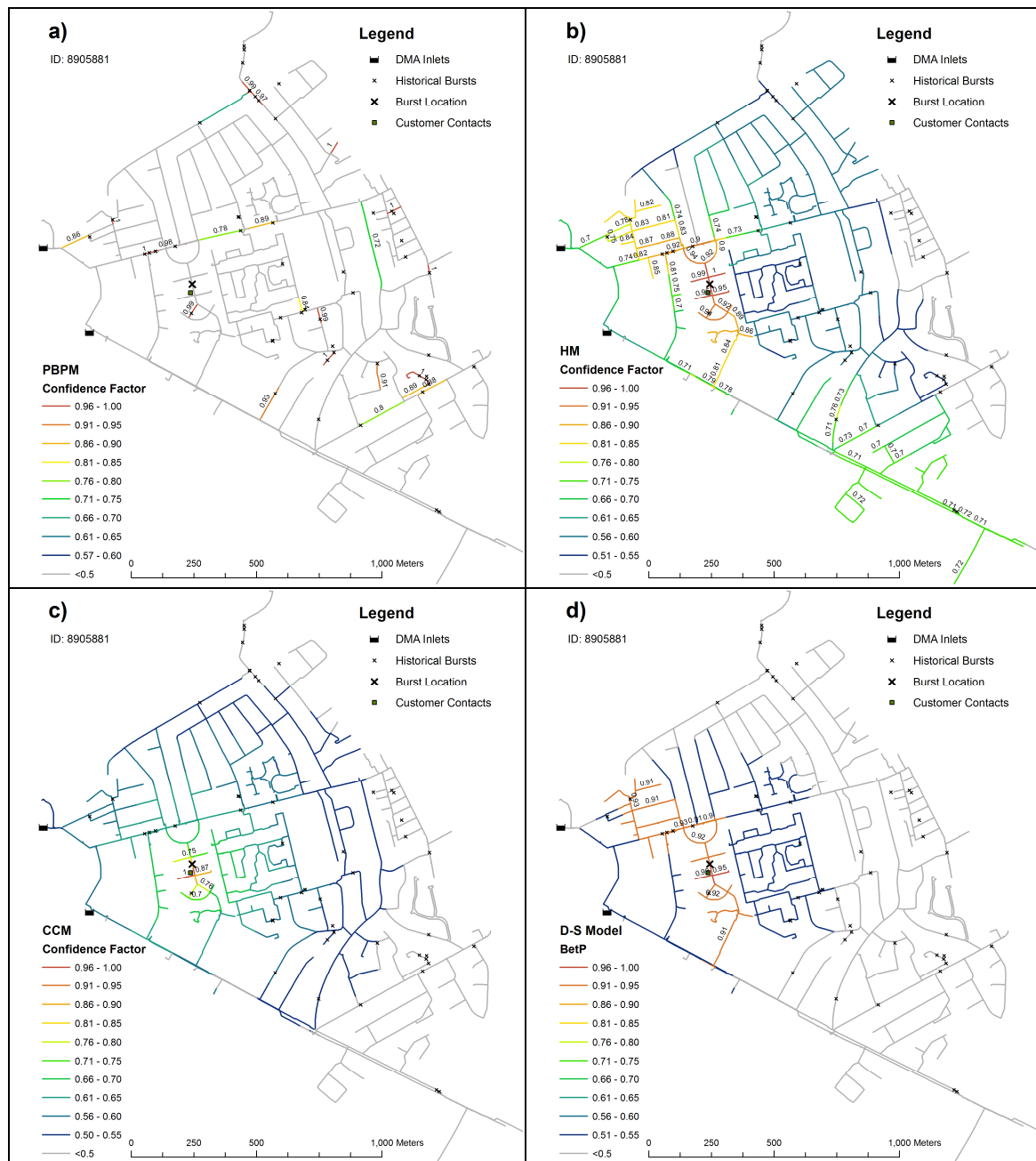


Figure D.3 a) PBPM, b) HM, c) CCM and d) D-S Model results for case #8905881

The Belief and Plausibility maps shown in Figure D.4a and Figure D.4b, respectively, are similar to the previous case, which can be explained by the closeness of the TBL in both cases and, therefore, a similar performance of the HM (despite the different time of

day, pressure measurements and demands). Unlike in the previous case, the levels of Belief and Plausibility of potential incidents in the proximity of the TBL are very similar, which suggests that the individual models were in an agreement.

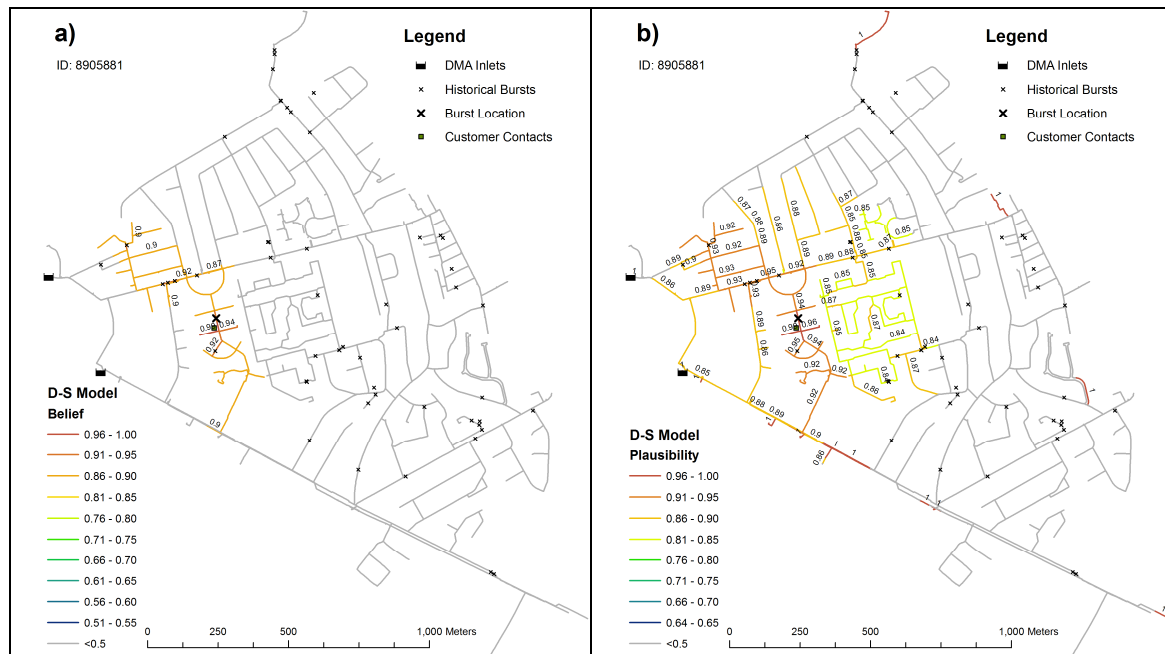


Figure D.4 a) Belief and b) Plausibility of the D-S Model for case #8905881

D.3 Detailed results for case #9315021

Figure D.5 shows the results of another validation example from Table 5.11. The historical burst occurred on 5 February 2008 and was reported by three customers. The origin of the CCs (see, e.g., Figure D.5c) did not favour the fact that when a customer reports a burst, the actual coordinates of a geocoded location provided by the customer were stored in the CC database. In this case it seemed that the location of the caller was recorded rather than the location of the burst, which would explain why the CCs formed a triangle surrounding the TBL (which was not a common situation in the CC dataset). The HM (see Figure D.5b) managed to identify the location of the burst pipe precisely, since it was in close proximity of a pressure sensor. The PBPM (see Figure D.5a) did not perform very well in this case. The combined result shown in Figure D.5d was negatively affected by the CCM, which overweighed the HM and the most likely burst location was 650 m from the TBL. To facilitate the decision-making process (i.e., to avoid the need to use both Belief and Plausibility maps) only the pignistic probability $BetP$ generated by the D-S model was primarily presented to a DM. The inevitable

information loss caused by the aggregation of Belief and Plausibility brings some disadvantages and represents a trade-off between quality and quantity of information.

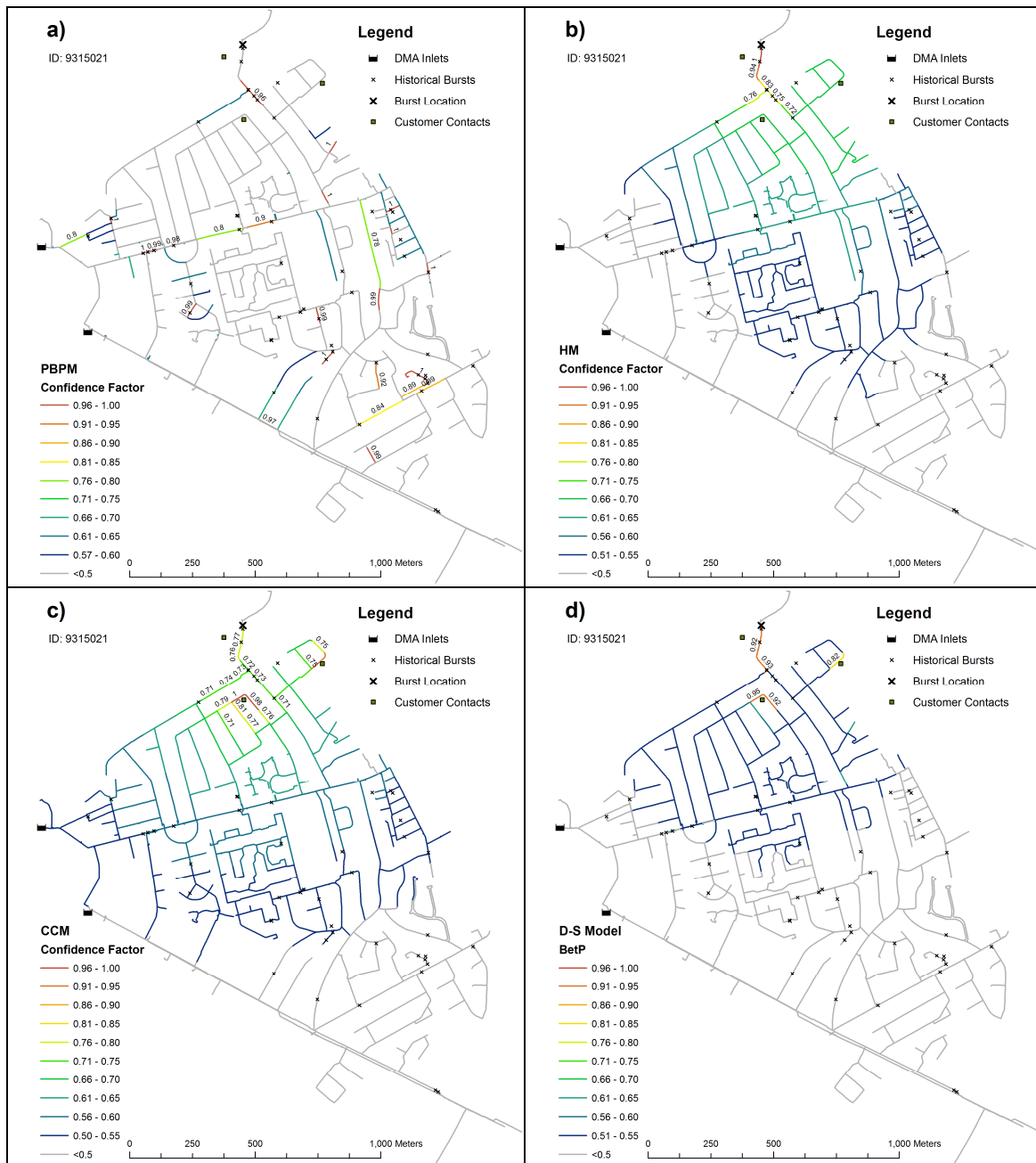


Figure D.5 a) PBPM, b) HM, c) CCM and d) D-S Model results for case #9315021

Although the most likely location identified by the D-S model had the highest *BetP* (see Figure D.5d), it did not have the highest level of Belief as shown in Figure D.6a. The pignistic probability *BetP* provides a quick overview of the likely location of the burst and can be sufficient to make an informed decision in most cases. However, some

situations (e.g., as shown in Figure D.6) warranted more detailed inspection using the Belief and Plausibility maps.

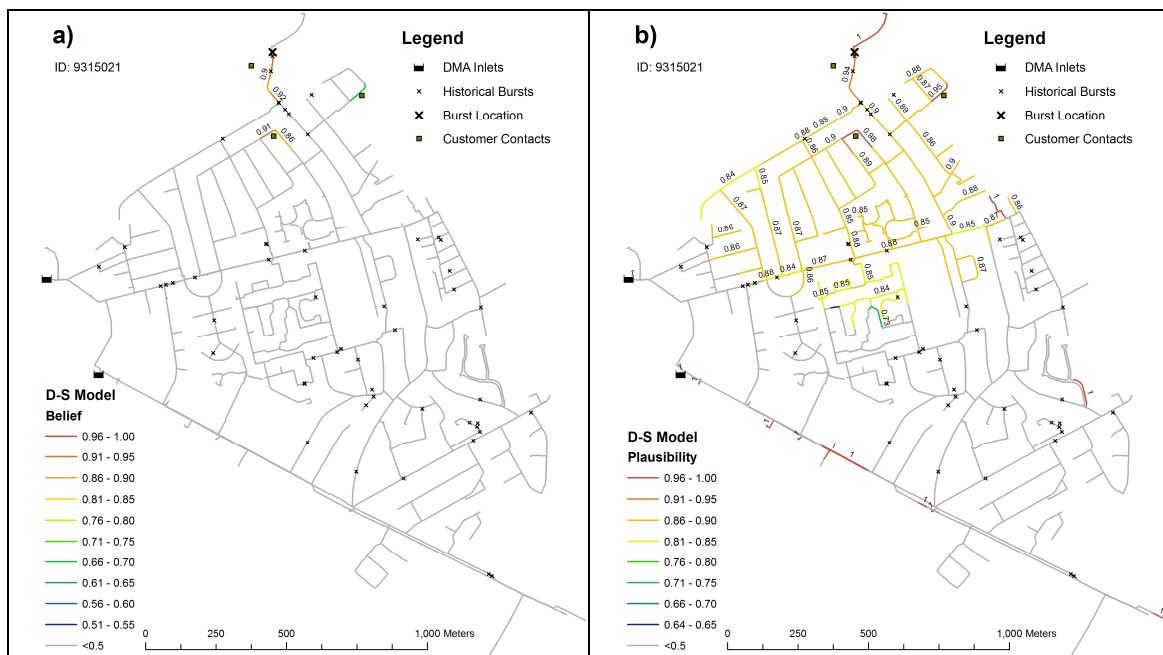


Figure D.6 a) Belief and b) Plausibility of the D-S Model for case #9315021

The advantage of the results provided by the D-S model could be also seen in the fact that one of the CCs (i.e., the one located in the north east part of the DMA) received a significantly lower level of *BetP* as well as Belief and would be probably investigated as the last one after the other two pipe burst hotspots identified by the D-S model.

D.4 Detailed results for case #4639990

This example shows a historical pipe burst repaired on 1 August 2002, which was taken from the validation dataset. The burst was not reported by any customers and, therefore, only evidence from the PBPM and the HM was available. Figure D.7 provides the outputs of the PBPM (see Figure D.7a), the HM (see Figure D.7b) and the D-S model (see Figure D.7c). As can be seen from the figures, the PBPM highlighted a number of likely locations, however, also identified possible pipes, which were unlikely to burst. The HM identified two large pipe burst hotspots. The combined results in this particular case (see Figure D.7c) significantly reduced the area of the two hotspots and as can be seen from Table 5.11 even managed to improve the ranking of the TBL compared to the rankings of the other two models. The pipe burst hotspot in the south east part of the

DMA received only a slightly higher level of BetP compared to the other hotspot located in the south central part of the DMA.

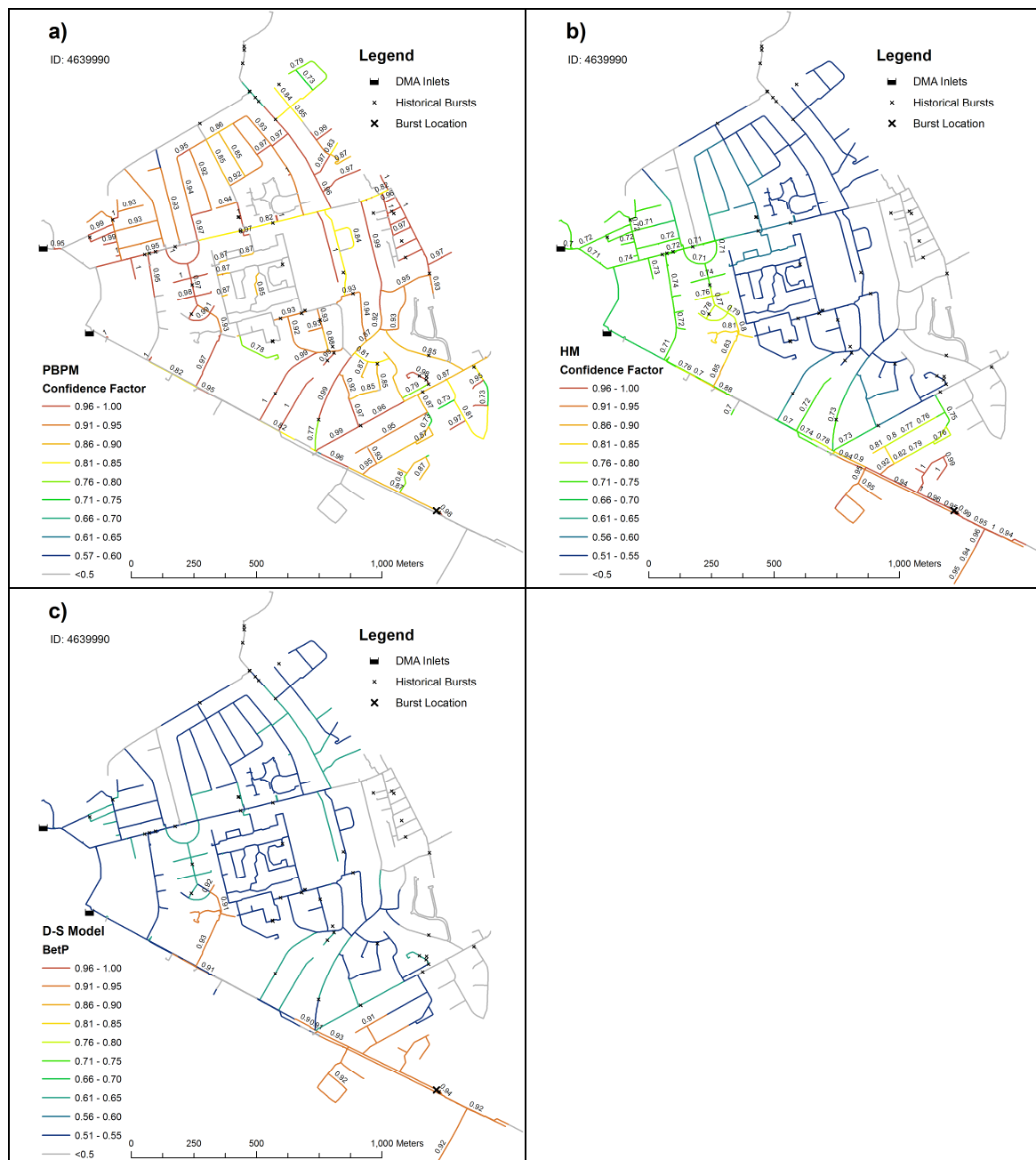


Figure D.7 a) PBPM, b) HM and c) D-S Model results for case #4639990

The spatial distribution of Belief (see Figure D.8a) provided by the D-S Model was well confined, which was not the case of Plausibility as shown in Figure D.8b. The plausibility map depicted below represents a typical situation, when the HM is combined only with the PBPM. This usually results in little “negative” evidence supporting the hypothesis that certain potential incidents were unlikely the TBL.



Figure D.8 a) Belief and b) Plausibility of the D-S Model for case #4639990

GLOSSARY

Background leakage is typically caused by a number of small leaks that are very difficult to detect. (van Zyl and Clayton 2007)

Belief corresponds to the total probability mass which supports a proposition and all of its subsets. (Shafer 1976) It can be seen as a lower probability bound.

Burst is a large individual leak that emerges on to the surface or is found through active leakage initiatives. (van Zyl and Clayton 2007)

Decision Support System is an interactive computer-based system, which helps decision makers utilise data and models to solve unstructured problems. (Gorry and Scott-Morton 1971)

Expert System is a decision-making and/or problem solving package of computer hardware and software that can reach a level of performance comparable to - or even exceeding that of - a human expert in some specialised and usually narrow problem area. (Turban 1995)

Failure can be defined as the inability to achieve a defined level of performance. (Sayers *et al.* 2003)

Hazard is defined as a situation with the potential to result in harm, however, it does not necessarily lead to harm. (Sayers *et al.* 2003).

Intervention is a planned activity designed to achieve an improvement in an existing system. (Sayers *et al.* 2003)

Likelihood is a general concept relating to the chance of an event occurring. (Sayers *et al.* 2003).

Plausibility corresponds to the total probability mass which is not in contradiction with a proposition. (Shafer 1976) It can be seen as an upper probability bound.

Potential Incident refers to a suspected failure, which has not been confirmed.

Risk is a measure of the probability and severity of adverse effects. (Lowrance 1976)

Risk analysis is part of the risk assessment procedure and comprises the identification of hazards and estimation of the risks.

Risk assessment is defined as a process of identifying hazards and consequences, estimating the magnitude and probability of consequences and assessing the significance of the risk(s). (Kaplan and Garrick 1981)

Risk management is following the IEC60300-3-9 standard defined as “a systematic application of management policies, procedures and practices to the tasks of analysing, evaluating and controlling risk.” (Tuhovcak *et al.* 2006)

Uncertainty refers to randomness, which cannot be explained (Knight 1921). It can be broadly classified into **aleatory uncertainty**, which refers to natural variability, or stochastic uncertainty, and **epistemic uncertainty**, representing knowledge uncertainty or incompleteness.

BIBLIOGRAPHY

Papers Presented by the Candidate

- Bicik, J., Kapelan, Z., Makropoulos, C., and Savić, D. A. (Accepted). "Pipe Burst Diagnostics Using Evidence Theory." *Journal of Hydroinformatics*.
- Bicik, J., Kapelan, Z., and Savić, D. A. (Accepted). "Risk-Based Prioritisation of Alarms in Water Distribution System Operations." *Proceedings of the 9th International Conference on Hydroinformatics 2010*, Tianjin, China.
- Bicik, J., Savić, D. A., and Kapelan, Z. (2009). "Operation of WDS using risk-based decision making." *Proceedings of the Computing and Control in the Water Industry 2009 (CCWI 2009)*, University of Sheffield, UK, 143-149.
- Bicik, J., Kapelan, Z., and Savić, D. A. (2009). "Operational Perspective of the Impact of Failures in Water Distribution Systems." *Proceedings of the World Environmental & Water Resources Congress 2009 (WDSA 2009)*, Kansas City, Missouri, 305-314.
- Bicik, J., Makropoulos, C., Kapelan, Z., and Savić, D. A. (2009). "The Application of Evidence Theory in Decision Support for Water Distribution System Operations." *Proceedings of the 8th International Conference on Hydroinformatics*, Concepcion, Chile.
- Bicik, J., Morley, M. S., and Savić, D. A. (2008). "A Rapid Optimization Prototyping Tool for Spreadsheet-Based Models." *Proceedings of the 10th Annual Water Distribution Systems Analysis Conference (WDSA 2008)*, Kruger National Park, South Africa, 472-482.
- Bicik, J., Makropoulos, C., Joksimović, D., Kapelan, Z., Morley, M. S., and Savić, D. A. (2008). "Conceptual Risk-Based Decision Support Methodology for Improved Near R-T Response to WDS Failures." *Proceedings of the 10th Annual Water Distribution Systems Analysis Conference (WDSA 2008)*, Kruger National Park, South Africa, 510-519.
- Morley, M. S., Bicik, J., Vamvakeridou-Lyroudia, L. S., Kapelan, Z., and Savić, D. A. (2009). "Neptune DSS: A Decision Support System for Near-Real Time Operations Management of Water Distribution Systems." *Proceedings of the Computing and Control in the Water Industry 2009 (CCWI 2009)*, Sheffield, UK, 249-255.
- Vamvakeridou-Lyroudia, L. S., Bicik, J., Awad, H., Savić, D. A., and Kapelan, Z. (2009). "Developing and implementing a R-T intervention management model for WDS." *Proceedings of the Computing and Control in the Water Industry 2009 (CCWI 2009)*, Sheffield, UK, 339-345.
- Vamvakeridou-Lyroudia, L. S., Morley, M. S., Bicik, J., Green, C., Smith, M., and Savić, D. A. (2009). "AquatorGA: Integrated optimisation for reservoir

operation using multiobjective genetic algorithms." *Proceedings of the Computing and Control in the Water Industry 2009 (CCWI 2009)*, Sheffield, UK, 493-500.

List of References

- Adams, R. W. (1961). "Distribution Analysis by Electronic Computer." *Institute of Water Engineers*, 15, 415-428.
- Agarwal, H., Renaud, J. E., Preston, E. L., and Padmanabhan, D. (2004). "Uncertainty quantification using evidence theory in multidisciplinary design optimization." *Reliability Engineering & System Safety*, 85(1), 281-294.
- Almoussawi, R., and Christian, C. (2005). "Fundamentals of quantitative risk analysis." *Journal of Hydroinformatics*, 7(2), 61-77.
- Andersen, J. H., and Powell, R. S. (2000). "Implicit state-estimation technique for water network monitoring." *Urban Water*, 2(2), 123-130.
- Ang, W. K., and Jowitt, P. W. (2006). "Solution for Water Distribution Systems under Pressure-Deficient Conditions." *Journal of Water Resources Planning and Management*, 132(3), 175-182.
- Bai, H., Sadiq, R., Najjaran, H., and Rajani, B. (2008). "Condition Assessment of Buried Pipes Using Hierarchical Evidential Reasoning Model." *Journal of Computing in Civil Engineering*, 22(2), 114-122.
- Basir, O., and Yuan, X. (2007). "Engine fault diagnosis based on multi-sensor information fusion using Dempster-Shafer evidence theory." *Information Fusion*, 8(4), 379-386.
- Bauer, M. (1996). "Approximations for decision making in the Dempster-Shafer theory." *Uncertainty in Artificial Intelligence*, Saarbrücken, 339-344.
- Bayes, T. (1763). "An essay towards solving a problem in the doctrine of chances." *Philosophical Transactions of the Royal Society*, 53, 370-418.
- Beuken, R. H. S., Konings, L. J. M., Poortema, K. H., and Blokker, E. J. M. (2006). "External Effects of Pipe Bursts." *Water Distribution Systems Analysis*, Cincinnati, Ohio.
- Beuken, R. H. S., van den Boomen, M., Blaauwgeers, H. G. P., and van Daal, H. A. (2008). "Feasibility Study on Quantitative Risk Analysis of Drinking Water Networks." *Proceedings of the 10th Annual Water Distribution Systems Analysis Conference (WDSA2008)*, Kruger National Park, South Africa, 665-675.
- Beynon, M. J. (2005). "A novel technique of object ranking and classification under ignorance: An application to the corporate failure risk problem." *European Journal of Operational Research*, 167(2), 493-517.

-
- Bhave, P. R. (1981). "Node Flow Analysis of Water Distribution Systems." *Transportation engineering journal of ASCE*, 107(4), 457-467.
- Bi, Y., Guan, J., and Bell, D. (2008). "The combination of multiple classifiers using an evidential reasoning approach." *Artificial Intelligence*, 172(15), 1731-1751.
- Bicik, J., Morley, M. S., and Savić, D. A. (2008). "A Rapid Optimization Prototyping Tool for Spreadsheet-Based Models." *Proceedings of the 10th Annual Water Distribution Systems Analysis Conference WDSA2008*, Kruger National Park, South Africa, 472-482.
- Borovik, I., Ulanicki, B., and Skworcow, P. (2009). "Bursts Identification in Water Distribution Systems." *World Environmental and Water Resources Congress 2009*, Kansas City, Missouri, USA.
- Boxall, J. B., and Saul, A. J. (2005). "Modeling Discoloration in Potable Water Distribution Systems." *Journal of Environmental Engineering*, 131(5), 716-725.
- Brunone, B. (1999). "Transient test based technique for leak detection in outfall pipes." *Journal of Water Resources Planning and Management*, 125(5), 302-306.
- Buchberger, S. G., and Nadimpalli, G. (2004). "Leak Estimation in Water Distribution Systems by Statistical Analysis of Flow Readings." *Journal of Water Resources Planning and Management*, 130(4), 321-329.
- Burrows, R., Crowder, G. S., and Zhang, J. (2000). "Utilisation of network modelling in the operational management of water distribution systems." *Urban Water*, 2(2), 83-95.
- Cassa, A. M., van Zyl, J. E., and Laubscher, R. F. (2010). "A numerical investigation into the effect of pressure on holes and cracks in water supply pipes." *Urban Water Journal*, 7(2), 109-120.
- Chen, Q., and Aickelin, U. (2006). "Anomaly Detection Using the Dempster-Shafer Method." *International Conference on Data Mining, DMIN 2006*, Las Vegas, Nevada, USA.
- Cheung, P. B., Van Zyl, J. E., and Reis, L. F. R. (2005). "Extension of EPANET for Pressure Driven Demand Modeling in Water Distribution System." *Computers and Control in the Water Industry (CCWI 2005)*, Exeter, UK, 311-316.
- Christodoulou, S., Deligianni, A., Aslani, P., and Agathokleous, A. (2009). "Risk-based asset management of water piping networks using neurofuzzy systems." *Computers, Environment and Urban Systems*, 33(2), 138-149.
- Codd, E. F. (1970). "A relational model of data for large shared data banks." *Communications of the ACM*, 13(6), 377-387.
- Colombo, A. F., Lee, P., and Karney, B. W. (2009). "A selective literature review of transient-based leak detection methods." *Journal of Hydro-environment Research*, 2(4), 212-227.

-
- Cooper, N. R., Blakey, G., Sherwin, C., Ta, T., Whiter, J. T., and Woodward, C. A. (2000). "The use of GIS to develop a probability-based trunk mains burst risk model." *Urban Water*, 2(2), 97-103.
- Cross, H. (1936). "Analysis of Flow in Networks of Conduits or Conductors." *University of Illinois. Engineering Experiment Station. Bulletin no. 286.*
- Deagle, G., Green, A., and Scrivener, J. (2007). "Advanced tools for burst location." *Water Management Challenges in Global Change (CCWI2007)*, De Montfort University, Leicester, UK, 307-312.
- Deb, K., and Agrawal, R. B. (1995). "Simulated Binary Crossover For Continuous Search Space." *Complex Systems*, 9, 115–148.
- Deb, K., Pratap, A., Agarwal, S., and Meyarivan, T. (2002). "A fast and elitist multiobjective genetic algorithm: NSGA-II." *Evolutionary Computation, IEEE Transactions on*, 6(2), 182-197.
- Demotier, S., Denoeux, T., and Schon, W. (2003). "Risk Assessment in Drinking Water Production Using Belief Functions." *Symbolic and Quantitative Approaches to Reasoning with Uncertainty*, T. D. Nielsen and N. L. Zhang, eds., Springer, Heidelberg, 319-331.
- Dempster, A. P. (1967). "Upper and Lower Probabilities Induced by a Multivalued Mapping." *The Annals of Mathematical Statistics*, 38(2), 325-339.
- Denoeux, T., and Yaghlane, A. B. (2002). "Approximating the combination of belief functions using the fast Mobius transform in a coarsened frame." *International Journal of Approximate Reasoning*, 31(1-2), 77-101.
- Department of Defense. (1980). "Procedures for Performing a Failure Mode, Effects and Criticality Analysis." *MIL-STD-1629A*, Washington, DC.
- Dewis, N., and Randall-Smith, M. (2005). "Discolouration Risk Modelling." *Computers and Control in the Water Industry (CCWI 2005)*, Exeter, UK, 223-228.
- Dey, P. K. (2001). "A risk-based model for inspection and maintenance of cross-country petroleum pipeline." *Journal of Quality in Maintenance Engineering*, 7(1), 25-41.
- Dezert, J., Tchamova, A., Smarandache, F., and Konstantinova, P. (2006). "Target Type Tracking with PCR5 and Dempster's rules: A Comparative Analysis." *9th International Conference on Information Fusion*, Florence, 1-8.
- Dillon, R. L., Liebe, R. M., and Bestafka, T. (2009). "Risk-Based Decision Making for Terrorism Applications." *Risk Analysis*, 29(3), 321-335.
- Duan, N., Mays, L. W., and Lansey, K. E. (1990). "Optimal Reliability-Based Design of Pumping and Distribution Systems." *Journal of Hydraulic Engineering*, 116(2), 249-268.

-
- Egerton, A.-J. (1996). "Achieving reliable and cost effective water treatment." *Water Science and Technology*, 33(2), 143-149.
- Egerton, A.-J. (1999). "Risk Assessment Techniques in the Water Industry." *CIWEM National Conference (4 November 1999)*.
- Eom, S. B., Lee, S. M., Kim, E. B., and Somarajan, C. (1998). "A Survey of Decision Support System Applications (1988-1994)." *The Journal of the Operational Research Society*, 49(2), 109-120.
- Farley, B., Boxall, J. B., and Mounce, S. R. (2008). "Optimal Locations of Pressure Meters for Burst Detection." *Proceedings of the 10th Annual Water Distribution Systems Analysis Conference WDSA2008*, Kruger National Park, South Africa, 747-757.
- Farmani, R., Savić, D. A., and Walters, G. A. (2005a). "Fuzzy Rules for Hydraulic Reliability-Based Design and Operation of Water Distribution Systems." *World Water Congress 2005*, Anchorage, Alaska, USA, 21.
- Farmani, R., Walters, G. A., and Savić, D. A. (2005b). "Trade-off between Total Cost and Reliability for Anytown Water Distribution Network." *Journal of Water Resources Planning and Management*, 131(3), 161-171.
- Person, S., Nelsen, R. B., Hajagos, J., Berleant, D. J., Zhang, J., Tucker, T. T., Ginzburg, L. R., and Oberkampf, W. L. (2004). "Dependence in probabilistic modeling, Dempster-Shafer theory, and probability bounds analysis." *SAND2004-3072*, Sandia National Laboratories.
- Filion, Y. R., Adams, B. J., and Karney, B. W. (2007). "Stochastic Design of Water Distribution Systems with Expected Annual Damages." *Journal of Water Resources Planning and Management*, 133(3), 244-252.
- Foong, O. M., Sulaiman, S. B., Rambli, D. R., and Abdullah, N. S. (2009). "ALAP: Alarm Prioritization System for Oil Refinery." *Proceedings of the World Congress on Engineering and Computer Science 2009*, San Francisco, USA, 1012-1017.
- Forman, E., and Peniwati, K. (1998). "Aggregating individual judgments and priorities with the analytic hierarchy process." *European Journal of Operational Research*, 108(1), 165-169.
- Francisque, A., Rodriguez, M. J., Sadiq, R., Miranda, L. F., and Proulx, F. (2009). "Prioritizing monitoring locations in a water distribution network: a fuzzy risk approach." *Journal of Water Supply: Research and Technology-AQUA*, 58(7), 488-509.
- Fujiwara, O., and Li, J. (1998). "Reliability analysis of water distribution systems considering pressure dependency of outflows." *Water Resources Research*, 34(7), 1843-1850.

-
- Fullér, R., and Majlender, P. (2001). "An analytic approach for obtaining maximal entropy OWA operator weights." *Fuzzy Sets and Systems*, 124, 53-57.
- Gabrys, B., and Bargiela, A. (1999). "Neural Networks Based Decision Support in Presence of Uncertainties." *Journal of Water Resources Planning and Management*, 125(5), 272-280.
- Garey, M. R., and Johnson, D. S. (1979). *Computers and intractability : a guide to the theory of NP-completeness*, W. H. Freeman, San Francisco.
- Gass, S. I. (1985). *Decision making, models and algorithms : a first course*, Wiley, New York.
- Germanopoulos, G. (1985). "A technical note on the inclusion of pressure dependent demand and leakage terms in water supply network models." *Civ. Eng. Syst.*, 2(3), 171-179.
- Giustolisi, O., and Doglioni, A. (2005). "Water Distribution System Failure Analysis." *Computers and Control in the Water Industry (CCWI 2005)*, Exeter, UK, 51-56.
- Giustolisi, O., and Doglioni, A. (2007). "A Pressure Driven Approach for Water Distribution System Modelling." *Water Management Challenges in Global Change (CCWI2007)*, De Montfort University, Leicester, UK.
- Giustolisi, O., Kapelan, Z., and Savić, D. A. (2008a). "Extended Period Simulation Analysis Considering Valve Shutdowns." *Journal of Water Resources Planning and Management*, 134(6), 527-537.
- Giustolisi, O., Kapelan, Z., and Savić, D. A. (2008b). "Algorithm for Automatic Detection of Topological Changes in Water Distribution Networks." *Journal of Hydraulic Engineering*, 134(4), 435-446.
- Giustolisi, O., Savić, D. A., and Kapelan, Z. (2008c). "Pressure-Driven Demand and Leakage Simulation for Water Distribution Networks." *Journal of Hydraulic Engineering*, 134(5), 626-635.
- Giustolisi, O., and Berardi, L. (2009). "Prioritizing Pipe Replacement: From Multiobjective Genetic Algorithms to Operational Decision Support." *Journal of Water Resources Planning and Management*, 135(6), 484-492.
- Goldberg, D. E. (1989). *Genetic Algorithms in Search, Optimization, and Machine Learning*, Addison-Wesley, Reading, MA.
- Gorry, G. A., and Scott-Morton, M. S. (1971). "A framework for management information systems." *Sloan Management Review*, 13(1), 55-70.
- Gupta, R., and Bhawe, P. R. (1994). "Reliability Analysis of Water-Distribution Systems." *Journal of Environmental Engineering*, 120(2), 447-461.

-
- Gupta, R., and Bhawe, P. R. (1996). "Comparison of Methods for Predicting Deficient-Network Performance." *Journal of Water Resources Planning and Management*, 122(3), 214-217.
- Haenni, R., and Lehmann, N. (2003). "Implementing belief function computations." *International Journal of Intelligent Systems*, 18(1), 31-49.
- Haimes, Y. Y. (2004). *Risk Modeling, Assessment, and Management*, John Wiley & Sons, Hoboken, New Jersey.
- Hall, D. L., and Garga, K. A. (1999). "Pitfalls in Data Fusion (and How to Avoid Them)." *The 2nd international Conference on Information Fusion*, Sunnyvale, California, USA.
- Haykin, S. S. (1999). *Neural Networks: A Comprehensive Foundation*, Prentice Hall, Upper Saddle River, N.J.
- Hayuti, M. H., and Burrows, R. (2004). "Sequential Solution Seeking DDA based HDA (SSS-DDA/HDA) Approach." *Decision Support in the Water Industry Under Conditions of Uncertainty (ACTUI2004)*, Exeter, UK, 44-49.
- Hayuti, M. H., and Burrows, R. (2005). "Synthesizing real water distribution network performance under pressure deficiency." *Computing and Control for the Water Industry (CCWI 2005)*, Centre for Water Systems, Exeter, UK, 229–234.
- Hayuti, M. H., Naga, D., Zhang, Y., and Burrows, R. (2006). "An evaluation of the robustness of sample U.K. water distribution system configurations to operational stresses." *8th Annual Int. Symp. on Water Distribution Systems Analysis*, Cincinnati, Ohio, USA.
- Hayuti, M. H., Burrows, R., and Naga, D. (2007). "Modelling water distribution systems with deficient pressure." *Proceedings of ICE, Water Management*, 160(WM4), 215–224.
- Holloway, C. A. (1979). *Decision making under uncertainty : models and choices*, Prentice-Hall, Englewood Cliffs, N.J.
- Holnicki-Szulc, J., Kolakowski, P., and Nasher, N. (2005). "Leakage Detection in Water Networks." *Journal of Intelligent Material Systems and Structures*, 16(3), 207-219.
- Isermann, R. (2005). "Model-based fault-detection and diagnosis - status and applications." *Annual Reviews in Control*, 29(1), 71-85.
- Izquierdo, J., Lopez, P. A., Martinez, F. J., and Perez, R. (2007). "Fault detection in water supply systems using hybrid (theory and data-driven) modelling." *Mathematical and Computer Modelling*, 46(3-4), 341-350.
- Jamieson, D. G., Shamir, U., Martinez, F., and Franchini, M. (2007). "Conceptual design of a generic, real-time, near-optimal control system for water-distribution networks." *Journal of Hydroinformatics*, 9(1), 3-14.

- Jenks, G. F. (1967). "The Data Model Concept in Statistical Mapping." *International Yearbook of Cartography*, 7, 186-190.
- Jun, H., and Loganathan, G. V. (2007). "Valve-controlled segments in water distribution systems." *Journal of Water Resources Planning and Management*, 133(2), 145-155.
- Jun, H., Loganathan, G. V., Deb, A. K., Grayman, W., and Snyder, J. (2007). "Valve Distribution and Impact Analysis in Water Distribution Systems." *Journal of Environmental Engineering*, 133(8), 790-799.
- Jun, H., Loganathan, G., Kim, J., and Park, S. (2008). "Identifying Pipes and Valves of High Importance for Efficient Operation and Maintenance of Water Distribution Systems." *Water Resources Management*, 22(6), 719-736.
- Kapelan, Z., Savić, D. A., and Walters, G. A. (2003). "A Hybrid Inverse Transient Model for Leakage Detection and Roughness Calibration in Pipe Networks." *Journal of Hydraulic Research*, 41(5), 481-492.
- Kapelan, Z., Savić, D. A., and Walters, G. A. (2005a). "Decision-support tools for sustainable urban development." *Engineering Sustainability*, 153(3), 135-142.
- Kapelan, Z., Savić, D. A., and Walters, G. A. (2005b). "Multiobjective Design of Water Distribution Systems Under Uncertainty." *Water Resources Research*, 41(11), W11407.
- Kapelan, Z., Savić, D. A., Walters, G. A., and Babayan, A. V. (2006). "Risk- and robustness-based solutions to a multi-objective water distribution system rehabilitation problem under uncertainty." *Water Science & Technology*, 53(1), 61-75.
- Kapelan, Z., Giustolisi, O., and Savić, D. A. (2007). "Risk Assessment of Water Supply Interruptions Due to Mechanical Pipe Failures." *Water Management Challenges in Global Change (CCWI2007)*, De Montfort University, Leicester, UK.
- Kapelan, Z. S., Savić, D. A., and Walters, G. A. (2005c). "Optimal Sampling Design Methodologies for Water Distribution Model Calibration." *Journal of Hydraulic Engineering*, 131(3), 190-200.
- Kaplan, S., and Garrick, B. J. (1981). "On the Quantitative Definition of Risk." *Risk Analysis*, 1(1), 11-27.
- Keeney, R. L., and Raiffa, H. (1976). *Decisions with multiple objectives : preferences and value tradeoffs*, Wiley, London.
- Khan, K., Widdop, P. D., Day, A. J., Wood, A. S., Mounce, S. R., and Machell, J. (2002). "Low-cost failure sensor design and development for water pipeline distribution systems." *Water Science and Technology*, 45(4-5), 207-215.

-
- Klir, G. J. (1994). "Measures of uncertainty in the Dempster-Shafer theory of evidence." *Advances in the Dempster-Shafer theory of evidence*, R. R. Yager, M. Fedrizzi, and J. Kacprzyk, eds., John Wiley & Sons, Inc., New York, 597.
- Knight, F. (1921). *Risk, uncertainty, and profit*, Houghton Mifflin, Boston.
- Knuth, D. E. (1976). "Big Omicron and big Omega and big Theta." *SIGACT News*, 8(2), 18-24.
- Koutsoyiannis, D., Karavokiros, G., Efstratiadis, A., Mamassis, N., Koukouvinos, A., and Christofides, A. (2003). "A decision support system for the management of the water resource system of Athens." *Physics and Chemistry of the Earth, Parts A/B/C*, 28(14-15), 599-609.
- Kreinovich, V. Y., Bernat, A., Borrett, W., Marsical, Y., and Villa, E. (1994). "Monte-Carlo methods make Dempster-Shafer formalism feasible." *Advances in the Dempster-Shafer theory of evidence*, R. R. Yager, M. Fedrizzi, and J. Kacprzyk, eds., John Wiley & Sons, Inc., New York, 597.
- Kroppla, B. (2005). *Beginning MapServer: Open Source GIS Development*, Apress, Berkley, CA.
- Laffey, J. T., Cox, A. P., Schmidt, L. J., Kao, M. S., and Read, Y. J. (1987). "Real-time knowledge-based systems." *AI Magazine*, 9(1), 27-45.
- Lambert, A. O. (2002). "International Report: Water losses management and techniques." *Water Science & Technology: Water Supply*, 2(4), 1-20.
- Lansley, K. E. (2006). "The Evolution of Optimizing Water Distribution System Applications." *8th Annual Water Distribution Systems Analysis Symposium*, Cincinnati, Ohio, USA.
- Lee, H.-M. (1996). "Applying fuzzy set theory to evaluate the rate of aggregative risk in software development." *Fuzzy Sets and Systems*, 79(3), 323-336.
- Lee, M., McBean, E. A., Ghazali, M., Schuster, C. J., and Huang, J. J. (2009). "Fuzzy-Logic Modeling of Risk Assessment for a Small Drinking-Water Supply System." *Journal of Water Resources Planning and Management*, 135(6), 547-552.
- Lefevre, E., Colot, O., and Vannoorenberghe, P. (2002). "Belief function combination and conflict management." *Information Fusion*, 3(2), 149-162.
- Li, H. (2007). "Hierarchical Risk Assessment of Water Supply Systems," PhD Thesis, Loughborough University, Loughborough, Leicestershire, UK.
- Li, Y., and Liao, X. (2007). "Decision support for risk analysis on dynamic alliance." *Decision Support Systems*, 42(4), 2043-2059.
- LimeSurvey. (2010). "LimeSurvey Manual." <http://www.limesurvey.org/> (accessed 20 April 2010)
-

- Liou, C. P. (1998). "Pipeline leak detection by impulse response extraction." *Journal of Fluids Engineering*, 116, 103-109.
- Liserra, T., Ugarelli, R., Di Federico, V., and Maglionico, M. (2007). "A GIS based approach to assess the vulnerability of water distribution systems." *2nd Leading Edge Conference on Strategic Asset Management (LESAM 2007)*, Lisbon, Portugal.
- Løken, E. (2007). "Use of multicriteria decision analysis methods for energy planning problems." *Renewable and Sustainable Energy Reviews*, 11(7), 1584-1595.
- Lowrance, W. W. (1976). *Of acceptable risk : Science and the determination of safety*, W. Kaufmann, Los Altos, Calif.
- Machell, J., Mounce, S. R., and Boxall, J. B. (2009). "Online modelling of water distribution systems: a UK case study." *Drink. Water Eng. Sci. Discuss.*, 2, 279-294.
- Makropoulos, C. (2003). "Spatial Decision Support for Urban Water Management," PhD Thesis, Imperial College London, London.
- Makropoulos, C. K., and Butler, D. (2006). "Spatial ordered weighted averaging: incorporating spatially variable attitude towards risk in spatial multi-criteria decision-making." *Environmental Modelling & Software*, 21(1), 69-84.
- Mansoor, M. A. M., and Vairavamoorthy, K. (2003). "Need for pressure dependent demand in analysing failure of pipe networks." *Advances in Water Supply Management*, B. M. Maksimovic, ed., Swets & Zeitlinger, Lisse, 217-225.
- Mansoor, M. A. M., Gorantiwar, S. D., and Vairavamoorthy, K. (2005). "Quantifying the performance of water distribution system as a result of failure." *Computers and Control in the Water Industry (CCWI 2005)*, Exeter, UK, 269-274.
- Marashi, S. E., Davis, J. P., and Hall, J. W. (2008). "Combination Methods and Conflict Handling in Evidential Theories." *International Journal of Uncertainty, Fuzziness and Knowledge-Based Systems*, 16(3), 337-369.
- Mashford, J., De Silva, D., Marney, D., and Burn, S. (2009). "An Approach to Leak Detection in Pipe Networks Using Analysis of Monitored Pressure Values by Support Vector Machine." *Third International Conference on Network and System Security*, Gold Coast, Queensland, Australia, 534-539.
- Mavrotas, G., and Trifillis, P. (2006). "Multicriteria decision analysis with minimum information: combining DEA with MAVT." *Computers & Operations Research*, 33(8), 2083-2098.
- Meoli, C., Leoni, G., Claudio, A., Giunchi, D., Benini, A., Caporossi, E., and Maffini, F. (2008). "Combining Criticality Analysis and Failure Rate Assessment to Plan Asset Management in the Water Supply System of the Province of Ferrara." *Proceedings of the 10th Annual Water Distribution Systems Analysis Conference WDSA2008*, Kruger National Park, South Africa, 571-583.

-
- Merrifield, T. (2005). "Automated Critical Asset Analysis (CAA)." *Computers and Control in the Water Industry (CCWI 2005)*, Exeter, UK, 241-246.
- Michaud, D., and Apostolakis, G. E. (2006). "Methodology for Ranking the Elements of Water-Supply Networks." *Journal of Infrastructure Systems*, 12(4), 230-242.
- Mikhailov, L. (2004). "Group prioritization in the AHP by fuzzy preference programming method." *Computers & Operations Research*, 31(2), 293-301.
- Misiunas, D. (2005). "Failure Monitoring and Asset Condition Assessment in Water Supply Systems," PhD Thesis, Lund University, Lund.
- Misiunas, D., Vítkovský, J., Olsson, G., Lambert, M., and Simpson, A. (2006). "Failure monitoring in water distribution networks." *Water Science & Technology*, 53(4-5), 503-511.
- Moore, R. V., and Tindall, C. I. (2005). "An overview of the open modelling interface and environment (the OpenMI)." *Environmental Science & Policy*, 8(3), 279-286.
- Morley, M. S., and Tricarico, C. (2008). "Pressure Driven Demand Extension for EPANET (EPANETpdd)." 2008/02, University of Exeter, UK, Exeter.
- Morley, M. S., Bicik, J., Vamvakeridou-Lyroudia, L. S., Kapelan, Z., and Savić, D. A. (2009). "Neptune DSS: A Decision Support System for Near-Real Time Operations Management of Water Distribution Systems." *Proceedings of the Computing and Control in the Water Industry 2009 (CCWI 2009)*, Sheffield, UK, 249-255.
- Mounce, S. R., Day, A. J., Wood, A. S., Khan, A., Widdop, P. D., and Machell, J. (2002). "A neural network approach to burst detection." *Water Science and Technology*, 45(4), 237-246.
- Mounce, S. R., Khan, A., Wood, A. S., Day, A. J., Widdop, P. D., and Machell, J. (2003). "Sensor-fusion of hydraulic data for burst detection and location in a treated water distribution system." *Information Fusion*, 4(3), 217-229.
- Mounce, S. R., and Machell, J. (2006). "Burst detection using hydraulic data from water distribution systems with artificial neural networks." *Urban Water Journal*, 3(1), 21 - 31.
- Mounce, S. R., Machell, J., and Boxall, J. B. (2006). "Development of Artificial Intelligence Systems for Analysis of Water Supply System Data." *Water Distribution Systems Analysis (WDSA 2006)*, Cincinnati, Ohio.
- Mounce, S. R., Boxall, J. B., and Machell, J. (2007). "An Artificial Neural Network/Fuzzy Logic system for DMA flow meter data analysis providing burst identification and size estimation." *Proceedings of the Water Management Challenges in Global Change (CCWI2007)*, De Montfort University, Leicester, UK.

- Mounce, S. R., Boxall, J. B., and Machell, J. (2008). "Online application of ANN and Fuzzy Logic system for burst detection." *The 10th Water Distribution System Analysis Symposium*, Kruger National Park.
- Mounce, S. R., and Boxall, J. B. (2010). "Implementation of an on-line Artificial Intelligence District Meter Area flow meter data analysis system for abnormality detection: a case study." *Water Science and Technology*, In Press.
- Mounce, S. R., Boxall, J. B., and Machell, J. (2010). "Development and Verification of an Online Artificial Intelligence System for Detection of Bursts and Other Abnormal Flows." *Journal of Water Resources Planning and Management* 136(3), 309-318.
- Murphy, C. K. (2000). "Combining belief functions when evidence conflicts." *Decision Support Systems*, 29(1), 1-9.
- Musliner, J. D., Hendler, A. J., Agrawala, K. A., Durfee, H. E., Strosnider, K. J., and Paul, C. J. (1995). "The Challenges of Real-Time AI." 28(1), 58-66.
- Nilsson, M., and Ziemke, T. (2007). "Information fusion: a decision support perspective." *Information Fusion, 2007 10th International Conference on*, 1-8.
- O'Hagan, M. (1988). "Aggregating template rule antecedents in real time expert systems with fuzzy logic sets." *Proc. 22nd Ann. IEEE Asilomar Conf. On signals, Systems and Computers*, Pacific Grove, CA., 681-689.
- OFWAT. (2008). "June return 2008 reporting requirements." http://www.ofwat.gov.uk/regulating/junereturn/prs_web_jrreportingreg (accessed 4 May 2010)
- OFWAT. (2009). "Metered and unmetered household numbers for water 2009-10." http://www.ofwat.gov.uk/regulating/reporting/custchgs2009-10/rpt_tar_2009-10householddata (accessed 4 May 2010)
- Ordnance Survey. (2010). "OS MasterMap." <http://www.ordnancesurvey.co.uk/oswebsite/products/osmastermap/> (accessed 20 April 2010)
- Orponen, P. (1990). "Dempster's Rule of Combination is #P-Complete." *Artificial Intelligence*, 44(1-2), 245-253.
- Ostfeld, A. (2001). "Reliability analysis of regional water distribution systems." *Urban Water*, 3(4), 253-260.
- Ostfeld, A., Kogan, D., and Shamir, U. (2002). "Reliability simulation of water distribution systems - single and multiquality." *Urban Water*, 4(1), 53-61.
- Oukhellou, L., Debiolles, A., Denoeux, T., and Aknin, P. (2010). "Fault diagnosis in railway track circuits using Dempster-Shafer classifier fusion." *Engineering Applications of Artificial Intelligence*, 23(1), 117-128.

- Ozger, S. S., and Mays, L. W. (2003). "A Semi-Pressure-Driven Approach To Reliability Assessment Of Water Distribution Networks." *XXX IAHR Congress*, Thessaloniki, Greece.
- Polikar, R. (2006). "Ensemble Based Systems in Decision Making." *IEEE Circuits and Systems Magazine*, 6(3), 21-45.
- Pollard, S. J. T., Strutt, J. E., Macgillivray, B. H., Hamilton, P. D., and Hrudey, S. E. (2004). "Risk Analysis And Management In The Water Utility Sector - A Review Of Drivers, Tools And Techniques." *Process Safety and Environmental Protection*, 82(B6), 453-462.
- Poulakis, Z., Valougeorgis, D., and Papadimitriou, C. (2003). "Leakage detection in water pipe networks using a Bayesian probabilistic framework." *Probabilistic Engineering Mechanics*, 18(4), 315-327.
- Preis, A., Whittle, A., and Ostfeld, A. (2009). "Online Hydraulic State Prediction for Water Distribution Systems." Kansas City, Missouri, 32-32.
- Pudar, R. S., and Liggett, J. A. (1992). "Leaks in Pipe Networks." *Journal of Hydraulic Engineering*, 118(7), 1031-1046.
- Puust, R., Kapelan, Z., Savić, D. A., and Koppel, T. (2006). "Probabilistic Leak Detection in Pipe Networks Using the SCEM-UA Algorithm." *8th Annual Water Distribution Systems Analysis Symposium*, Cincinnati, Ohio, USA.
- Puust, R., Kapelan, Z., Savić, D. A., and Koppel, T. (2010). "A review of methods for leakage management in pipe networks." *Urban Water Journal*, 7(1), 25-45.
- Race Technology. (2010). "DL1 Data Logger." http://www.race-technology.com/upload/DL1_Dsheet.pdf (accessed 6 June 2010)
- Ragot, J., and Maquin, D. (2006). "Fault measurement detection in an urban water supply network." *Journal of Process Control*, 16(9), 887-902.
- Rahman, S., Vanier, D. J., and Newton, L. (2005). "Social Cost Considerations for Municipal Infrastructure Management." *Report no. B-5123.8*, Institute for Research in Construction, National Research Council Canada, Ottawa.
- Rajani, B., and Kleiner, Y. (2002). "Towards pro-active rehabilitation planning of water supply systems." *International Conference on Computer Rehabilitation of Water Networks CARE-W*, Dresden, Germany, 29-38.
- Rakar, A., Juricic, D., and Balle, P. (1999). "Transferable belief model in fault diagnosis." *Engineering Applications of Artificial Intelligence*, 12(5), 555-567.
- Rance, J. P., Coulbeck, B., Kosov, S., Bounds, P. L. M., and Ulanicki, B. (2001). "FINESSE - a comprehensive software package for water network modelling and optimization." *The 6th Computing and Control for the Water Industry (CCWI2001)*, De Montfort University, Leicester, 381-394.

- Reddy, L. S., and Elango, K. (1989). "Analysis of water distribution networks with head-dependent outlets." *Civil Engineering and Environmental Systems*, 6(3), 102-110.
- Refractions Research. (2009). "PostGIS 1.3.6 Manual." <http://postgis.refractions.net/download/postgis-1.3.6.pdf> (accessed 5 May 2010)
- Romano, M., Kapelan, Z., and Savić, D. A. (2009). "Bayesian-based online burst detection in water distribution systems." *The 10th International Conference on Computing and Control for the Water Industry, CCWI 2009 - "Integrating Water Systems"*, Sheffield, UK, 331-337.
- Rossman, L. A. (2000). "EPANET 2 Users Manual." U.S. Environmental Protection Agency, Cincinnati, Ohio.
- Rossman, L. A. (2007). "Discussion of "Solution for Water Distribution Systems under Pressure-Deficient Conditions" by Wah Khim Ang and Paul W. Jowitt." *Journal of Water Resources Planning and Management*, 133(6), 566-567.
- Rowe, W. D. (1977). *An anatomy of risk*, Wiley, London.
- Saaty, T. L. (1980). *The Analytic Hierarchy Process*, MCGraw Hill Int., New York.
- Saaty, T. L., and Vargas, L. G. (1984). "Comparison of eigenvalue, logarithmic least squares and least squares methods in estimating ratios." *Mathematical Modelling*, 5(5), 309-324.
- Sadiq, R., Kleiner, Y., and Rajani, B. (2004a). "Aggregative risk analysis for water quality failure in distribution networks." *Water Supply Research and Technology : Aqua*, 53(4), 241-261.
- Sadiq, R., Rajani, B., and Kleiner, Y. (2004b). "Probabilistic risk analysis of corrosion associated failures in cast iron water mains." *Reliability Engineering & System Safety*, 86(1), 1-10.
- Sadiq, R., Kleiner, Y., and Rajani, B. (2005). "An Evidential Reasoning Approach to Evaluate Intrusion Vulnerability in Distribution Networks." *Computers and Control in the Water Industry (CCWI 2005)*, Exeter, UK.
- Sadiq, R., and Rodriguez, M. J. (2005). "Interpreting drinking water quality in the distribution system using Dempster-Shafer theory of evidence." *Chemosphere*, 59(2), 177-188.
- Sadiq, R., Kleiner, Y., and Rajani, B. (2006). "Estimating risk of contaminant intrusion in water distribution networks using Dempster-Shafer theory of evidence." *Civil Engineering and Environmental Systems*, 23(3), 129-141.
- Sadiq, R., Kleiner, Y., and Rajani, B. (2007). "Water Quality Failures in Distribution Networks - Risk Analysis Using Fuzzy Logic and Evidential Reasoning." *Risk Analysis*, 27(5), 1381-1394.

- Sadiq, R., Saint-Martin, E., and Kleiner, Y. (2008). "Predicting risk of water quality failures in distribution networks under uncertainties using fault-tree analysis." *Urban Water Journal*, 5(4), 287-304.
- Safranek, R. J., Gottschlich, S., and Kak, A. C. (1990). "Evidence Accumulation Using Binary Frames of Discernment for Verification Vision." *IEEE Transactions on Robotics and Automation*, 6(4), 405 - 417.
- Salomons, E., Goryashko, A., Shamir, U., Rao, Z., and Alvisi, S. (2007). "Optimizing the operation of the Haifa-A water-distribution network." *Journal of Hydroinformatics*, 9(1), 51-64.
- Savić, D. A., and Walters, G. A. (1997). "Genetic Algorithms for Least-Cost Design of Water Distribution Networks." *Journal of Water Resources Planning and Management*, 123(2), 67-77.
- Savić, D. A., Boxall, J. B., Ulanicki, B., Kapelan, Z., Makropoulos, C., Fenner, R., Soga, K., Marshall, I. W., Maksimovic, C., Postlethwaite, I., Ashley, R., and Graham, N. (2008). "Project Neptune: Improved Operation of Water Distribution Networks." *Proceedings of the 10th Annual Water Distribution Systems Analysis Conference (WDSA2008)*, Kruger National Park, South Africa, 543-558.
- Sayers, P. B., Gouldby, B. P., Simm, J. D., Meadowcroft, I., and Hall, J. (2003). "Risk, Performance and Uncertainty in Flood and Coastal Defence - A Review." DEFRA/Environment Agency - Flood and Coastal Defence R&D Programme, Wallingford.
- SensorsOne. (2010). "IMP - Industrial Pressure Transmitter." <http://www.sensorone.co.uk/pdf16301/IMP%20data%20sheet.pdf> (accessed 6 June 2010)
- Sentz, K., and Ferson, S. (2002). "Combination of Evidence in Dempster-Shafer Theory." SAND 2002-0835, Sandia National Laboratories.
- Shafer, G. A. (1976). *A mathematical theory of evidence*, Princeton University Press, London.
- Shamir, U., and Howard, C. D. D. (1968). "Water distribution systems analysis." *Journal of the Hydraulic Division, ASCE*, 94(HY1), 219-234.
- Shamir, U., and Salomons, E. (2008). "Optimal Real-Time Operation of Urban Water Distribution Systems Using Reduced Models." *Journal of Water Resources Planning and Management*, 134(2), 181-185.
- Shannon, C. E. (1948). "A mathematical theory of communications, I and II." *Bell System Technical Journal*, 27, 379-423.
- Shinozuka, M., Liang, J., and Feng, M. Q. (2005). "Use of Supervisory Control and Data Acquisition for Damage Location of Water Delivery Systems." *Journal of Engineering Mechanics*, 131(3), 225-230.

-
- Simon, H. A. (1977). *The New Science of Management Decision*, Prentice Hall PTR.
- Skipworth, P. J., Engelhardt, M. O., Cashman, A., Savić, D. A., Saul, A. J., and Walters, G. A. (2002). *Whole life costing for water distribution network management*, Thomas Telford Publishing, London.
- Smarandache, F., and Dezert, J. (2006). *Advances and Applications of DSMT for Information Fusion II (Collected Works)*, American Research Press, Rehoboth.
- Smets, P. (1990). "The Combination of Evidence in the Transferable Belief Model." *IEEE Trans. Pattern Anal. Mach. Intell.*, 12(5), 447-458.
- Smets, P., and Kennes, R. (1994). "The transferable belief model." *Artificial Intelligence*, 66(2), 191-234.
- Srdjevic, B. (2005). "Combining different prioritization methods in the analytic hierarchy process synthesis." *Computers & Operations Research*, 32(7), 1897-1919.
- Sterling, M. J. H., and Bargiela, A. (1984). "Minimum norm state estimation for computer control of water distribution systems." *Control Theory and Applications, IEE Proceedings D*, 131(2), 57-63.
- Stoianov, I., Karney, B., Covas, D., Maksimovic, C., and Graham, N. (2001). "Wavelet processing of transient signals for pipeline leak location and quantification." *International conference on computing and control for the water industry (CCWI 2001)*, Leicester, UK, 65-76.
- Tanaka, K., and Klir, G. J. (1999). "A design condition for incorporating human judgement into monitoring systems." *Reliability Engineering & System Safety*, 65(3), 251-258.
- Tanyimboh, T. T., and Tabesh, M. (1997). "Discussion: Comparison of Methods for Predicting Deficient-Network Performance." *Journal of Water Resources Planning and Management*, 123(6), 369-370.
- Tanyimboh, T. T., Tabesh, M., and Burrows, R. (2001). "Appraisal of Source Head Methods for Calculating Reliability of Water Distribution Networks." *Journal of Water Resources Planning and Management*, 127(4), 206-213.
- Technolog. (2010). "Cello - A Universal Solution for Remote Monitoring of Networks." <http://www.technolog.com/UserFiles/Datasheets/DS589003.pdf> (accessed 6 June 2010)
- Tessem, B. (1993). "Approximations for efficient computation in the theory of evidence." *Artificial Intelligence*, 61(2), 315-329.
- Thorne, O. M., and Fenner, R. A. (2009). "Risk-based climate-change impact assessment for the water industry." *Water Science and Technology*, 59(3), 443-451.

- Todini, E., and Pilati, S. (1988). "A gradient algorithm for the analysis of pipe networks." *Computer applications in water supply: vol. 1---systems analysis and simulation*, Research Studies Press Ltd., 1-20.
- Todini, E. (2000). "Looped water distribution networks design using a resilience index based heuristic approach." *Urban Water*, 2(2), 115-122.
- Todini, E. (2003). "A more realistic approach to the "extended period simulation" of water distribution networks." *Advances in Water Supply Management (CCWI 2003)*, London, UK, 173-183.
- Trietsch, E. A., and Mesman, G. A. M. (2006). "Effect of Valve Failures on Network Reliability." *8th Annual Water Distribution System Analysis Symposium (WDSA 2006)*, Cincinnati, Ohio, USA.
- Tucciarelli, T., Criminisi, A., and Termini, D. (1999). "Leak Analysis in Pipeline Systems by Means of Optimal Valve Regulation." *Journal of Hydraulic Engineering*, 125(3), 277-285.
- Tuhovcak, L., Rucka, J., and Juhanak, T. (2006). "Risk Analysis of Water Distribution Systems." *Security of Water Supply Systems: from Source to Tap*, 169-182.
- Tuhovcak, L., and Rucka, J. (2007). "Hazard identification and risk analysis of water supply systems." *2nd Leading Edge Conference on Strategic Asset Management*, Lisbon, Portugal.
- Turban, E. (1995). *Decision support and expert systems : management support systems*, Prentice-Hall, Englewood Cliffs [N.J.].
- Turner, M. (1986). "Real time experts." *Systems International*, 14(1), 55-57.
- Tynemarch Systems Engineering Ltd. (2007). "Structural Mains Rehabilitation Policy: Burst Rate Models." *J0631\GD\001\01*, Dorking, UK.
- Vamvakeridou-Lyroudia, L. S., Savić, D. A., and Walters, G. A. (2006). "Fuzzy hierarchical decision support system for water distribution network optimization." *Civil Engineering and Environmental Systems*, 23(3), 237-261.
- Vamvakeridou-Lyroudia, L. S., Bicik, J., Awad, H., Savić, D. A., and Kapelan, Z. (2009). "Developing and implementing a real-time intervention management model for water distribution systems." *Proceedings of the Computing and Control in the Water Industry 2009 (CCWI 2009)*, Sheffield, UK, 339-345.
- van Zyl, J. E., and Clayton, C. R. I. (2005). "The Effect of Pressure on Leakage in Water Distribution Systems." *Computing and Control in the Water Industry (CCWI 2005)*, Exeter, UK, 131-136.
- van Zyl, J. E., and Clayton, C. R. I. (2007). "The effect of pressure on leakage in water distribution systems." *Proceedings of ICE, Water Management*, 160(WM2), 109-114.

- Verde, C. (2001). "Multi-leak detection and isolation in fluid pipelines." *Control Engineering Practice*, 9(6), 673-682.
- Vesely, W. E., Goldberg, F. F., Roberts, N. H., and Haasl, D. F. (1981). "Fault Tree Handbook (NUREG-0492)." U.S. Nuclear Regulatory Commission, Washington, DC.
- Vitkovsky, J. P., Simpson, A. R., and Lambert, M. F. (2000). "Leak Detection and Calibration Using Transients and Genetic Algorithms." *Journal of Water Resources Planning and Management*, 126(4), 262-265.
- Vreeburg, I. J. H. G., and Boxall, D. J. B. (2007). "Discolouration in potable water distribution systems: A review." *Water Research*, 41(3), 519-529.
- Vrugt, J. A., Gupta, H. V., Bouten, W., and Sorooshian, S. (2003). "A Shuffled Complex Evolution Metropolis algorithm for optimization and uncertainty assessment of hydrologic model parameters." *Water Resources Research*, 39(8), 1201.
- Wagner, J. M., Shamir, U., and Marks, D. H. (1988a). "Water Distribution Reliability: Analytical Methods." *Journal of Water Resources Planning and Management*, 114(3), 253-275.
- Wagner, J. M., Shamir, U., and Marks, D. H. (1988b). "Water Distribution Reliability: Simulation Methods." *Journal of Water Resources Planning and Management*, 114(3), 276-294.
- Walski, T. M. (1987). "Discussion of "Quantitative Approaches to Reliability Assessment in Pipe Networks" by I. C. Goulter and A. V. Coals." *Journal of Transport Engineering*, 113(5), 585-587.
- Walski, T. M. (1993). "Water distribution valve topology for reliability analysis." *Reliability Engineering & System Safety*, 42(1), 21-27.
- Walski, T. M., Chase, D. V., Savić, D. A., Grayman, W., Beckwith, S., and Koelle, E. (2003). *Advanced water distribution modeling and management* Haestad Press, Waterbury, Connecticut.
- Wang, X.-J., Lambert, M. F., Simpson, A. R., Liggett, J. A., and Vitkovsky, J. P. (2002). "Leak Detection in Pipelines using the Damping of Fluid Transients." *Journal of Hydraulic Engineering*, 128(7), 697-711.
- Wiggert, D. C. (1968). "Unsteady Flows in Lines with Distributed Leakage." *Journal of the Hydraulics Division*, 94(1), 143-162.
- Willet, A. H. (1901). *The Economic Theory of Risk and Insurance*, The Columbia University Press, New York.
- Worsley, J. C., and Drake, J. D. (2002). *Practical PostgreSQL*, O'Reilly Media, U.S.A.

-
- Wu, Z. I., Wang, R. H., Walski, T. M., Yang, S. Y., Bowdler, D., and Baggett, C. C. (2006). "Efficient Pressure Dependent Demand Model For Large Water Distribution System Analysis." *8th Annual Water Distribution Systems Analysis Symposium*, Cincinnati, Ohio, USA.
- Wu, Z. Y., and Sage, P. (2006). "Water Loss Detection Via Genetic Algorithm Optimization-Based Model Calibration." *8th Annual Water Distribution Systems Analysis Symposium*, Cincinnati, Ohio, USA.
- Wu, Z. Y. (2007). "Discussion of "Solution for Water Distribution Systems under Pressure-Deficient Conditions" by Wah Khim Ang and Paul W. Jowitt." *Journal of Water Resources Planning and Management*, 133(6), 567-568.
- Wu, Z. Y., Sage, P., Turtle, D., Wheeler, M., Hayuti, M., Velickov, S., Gomez, C., and Hartshorn, J. (2008). "Leak Detection Case Study by Means of Optimizing Emitter Locations and Flows." *10th Annual Water Distribution Systems Analysis Conference (WDSA2008)*, Kruger National Park, South Africa.
- Wu, Z. Y. (2009). "Unified parameter optimisation approach for leakage detection and extended-period simulation model calibration." *Urban Water Journal*, 6(1), 53-67.
- Wu, Z. Y., Sage, P., and Turtle, D. (2010). "Pressure-Dependent Leak Detection Model and Its Application to a District Water System." *Journal of Water Resources Planning and Management*, 136(1), 116-128.
- Xu, C., and Goulter, I. C. (1999). "Reliability-Based Optimal Design of Water Distribution Networks." *Journal of Water Resources Planning and Management*, 125(6), 352-362.
- Xu, H., and Kennes, R. (1994). "Steps toward efficient implementation of Dempster-Shafer theory." *Advances in the Dempster-Shafer theory of evidence*, R. R. Yager, M. Fedrizzi, and J. Kacprzyk, eds., John Wiley & Sons, Inc., New York, 597.
- Yager, R. R. (1983). "Entropy and Specificity in a Mathematical Theory of Evidence." *International Journal of General Systems*, 9(4), 249 - 260.
- Yager, R. R. (1987). "On the Dempster-Shafer framework and new combination rules." *Information Sciences*, 41(2), 93-137.
- Yager, R. R. (1988). "On ordered weighted averaging aggregation operators in multicriteria decisionmaking." *IEEE Trans. Syst. Man Cybern.*, 18(1), 183-190.
- Yager, R. R. (2004). "On the determination of strength of belief for decision support under uncertainty--Part II: fusing strengths of belief." *Fuzzy Sets and Systems*, 142(1), 129-142.
- Zadeh, L. A. (1975). "The concept of a linguistic variable and its application to approximate reasoning--I." *Information Sciences*, 8(3), 199-249.

- Zadeh, L. A. (1984). "A mathematical theory of evidence (book review)." *AI Magazine*, 5(3), 81-83.
- Zeleny, M. (1973). "Compromise Programming." *Multiple Criteria Decision Making*, J. L. Cochrane and M. Zeleny, eds., University of South Carolina Press, Columbia, 262-301.
- Zongxue, X., Jinno, K., Kawamura, A., Takesaki, S., and Ito, K. (1998). "Performance Risk Analysis for Fukuoka Water Supply System." *Water Resources Management*, 12(1), 13-30.